2020-7

Bioavailability and Modes of Action of Novel Metal Based Phenanthroline Drugs

Tadhg O'Leary
Technological University Dublin

Bioavailability and modes of action of novel metal based phenanthroline drugs

Thesis submitted to the Technological University Dublin in fulfilment of the requirements for PhD examination.

School of Biological and Health Sciences Technological University Dublin, City Campus, Grangegorman, Dublin 7.

July 2020

Tadhg O'Leary, B.Sc. (Hons.)

Supervisors:

Dr. Steve Meaney

Prof. Michael Devereux

Abstract

Metal-based compounds have been utilised as chemotherapeutic agents for the last four decades due to their well-documented and clinically relevant anti-tumour properties. Acquired resistance is a challenge for the clinical use of these compounds and there is a continuing need to search for potential new therapeutic agents. Herein, the potential of two metal-based compounds containing chelated 1,10-phenanthroline (1,10-Phen), one manganese-based (CMPD 73) and one copper-based (CMPD 74), to act as novel therapeutic agents is explored.

CMPD 73 displayed high micromolar (IC_{50} >100μM) cytotoxic properties against various cell systems but interestingly displayed increased cytotoxicity against ovarian (A2780), lung (A549) and cisplatin resistant mesothelioma cells (IC_{50} 40-50 μM). CMPD 74 was equally cytotoxic against all cell lines tested (IC_{50} <6μM), with this activity also preserved in the face of cisplatin resistance. In a cellular context, each compound was capable of generating reactive oxygen species (ROS) and through the use of small molecule ROS specific scavengers, superoxide was identified as the key mediator of compound cytotoxicity in both compounds. Several different modes of cell death were investigated for these compounds, with the apoptotic cell death pathway identified as the primary mechanism of cytotoxicity. Interestingly, evidence was uncovered of a direct involvement of superoxide in the effects of 1,10-Phen.

Nuclease mimetic activity is common in 1,10-Phen based compounds, with DNA assumed as a primary target. Excellent nuclease mimetic activity against both DNA and RNA were observed for both studied compounds. However, no significant enhancement of cytotoxic action was observed following co-treatment with compounds known to enhance accessibility of genomic DNA. RNAse mimetic effects were visible under both *in vitro* and *in cellulo* conditions, where we explored a number of different PCR-based approaches to capture impacts

on RNA expression and integrity under sub-toxic conditions. The novel compounds also appear to activate ER-stress response pathways to a modest degree. Taken together these data are consistent with an impact of the compounds on cellular RNA, which – via the ER stress pathway - may represent a critical initiating factor in the cell death process.

This work thus provides important insights into the potential molecular targets of metal-based compounds incorporating 1,10-phen, uncovers potential novel mechanisms of action and provides evidence that the observed effects are likely mediated by a broad ensemble of cytotoxic effects rather than direct intracellular targets.

Declaration

I certify that this thesis which I now submit for examination for the award of PhD, is entirely my own work and has not been taken from the work of others, save and to the extent that such work has been cited and acknowledged within the text of my work. This thesis was prepared according to the regulations for graduate study by research of the Technological University Dublin (TU Dublin) and has not been submitted in whole or in part for another award in any other third level institution. The work reported on in this thesis conforms to the principles and requirements of the TU Dublin's guidelines for ethics in research.

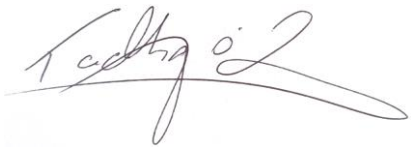

Signature_____ _____ Date: 28/07/20_____

Tadhg O'Leary

Acknowledgments

I would like to thank first and foremost my supervisor Dr. Steve Meaney without which none of this work would have been possible. For his constant patience and indispensable guidance throughout the whole of my thesis which allowed me to develop into the confident and independent researcher I am today.

I would also like to thank my second supervisor Prof. Michael Devereux and also Dr. Pauraic McCarron for providing me with the compounds necessary for my work, and always being at hand to answer any questions which arose.

I would also like to thank all the lecturing and technical staff in both Kevin Street and Grangegorman for all their help over the years and providing me with a great environment in which to conduct my research. I particularly would like to thank Dr. Paul Corcoran for his patience and knowledge in the initial stages of my PhD without which my first years would not have run anywhere near as smoothly as they did.

I would also like to thank the Trialect corporation, the University of Torino and Prof. Chiara Riganti for allowing me to work in her lab to help develop the many skills which I learnt while in Turin. In particular I would like to thank Dr. Iris Salaroglio for her patience and time in training me over the course of my 6weeks there, and also to Preeta Ananthanarayanan and Ahmad Mando for making my stay so much fun.

To my fellow Dr's to be Jamie, Brian, Rory, Conor, Fiacra, old Megan, young Megan, TJ, Aaron, Kate, and to all the others who have finished such as Alex, Shuai-shuai, Ash, Damien, Ola and many more, thanks for all the memories (and lack thereof) over the years. Whether

serving as an ear to listen to my rants about work, pints, words of advice, pints, helping with experiments and keeping cells alive (particularly TJ and old Megan), pints, and over all antics and pints, my years in TU Dublin would have been far harder and boring, but also possibly a lot healthier.

I would also like to thank my family for all their support over the years and words of encouragement. Last but not least I would like to thank my girlfriend Lauren for her unending patience and support over the course of my thesis, for dealing with cancelled plans, distant thoughts and general exhaustion particularly over this last year, but always maintaining her support and understanding.

Table of Contents

ABSTRACT ..... **I**

DECLARATION ..... **III**

ACKNOWLEDGMENTS ..... **IV**

TABLE OF CONTENTS ..... **VI**

TABLE OF FIGURES ..... **XII**

TABLE OF TABLES ..... **XVIII**

1. CHAPTER 1 ..... **1**

1.1. GENERAL INTRODUCTION 1

1.1.1. Global Rates of cancer *1*

1.1.2. Risk factors contributing to cancer development *4*

1.1.3. Hallmarks of cancer *6*

1.2. CHEMOTHERAPY 14

1.2.1. Biochemistry of cisplatin – the canonical metal-based chemotherapeutic *15*

1.2.2. Mechanisms of Cancer resistance *17*

1.2.3. The use of transition metals in anti-cancer treatments: *23*

1.2.4. Cellular redox homeostasis *24*

1.2.5. Hydrogen Peroxide (H_2O_2) *26*

1.2.6. Hydroxyl radical *27*

1.2.7. Superoxide $O_2^{\bullet-}$ radical *28*

1.2.8. Singlet oxygen ($^1O_2$) *29*

1.2.9. Nitric oxide ($NO^{\bullet}$) *30*

1.2.10. Peroxynitrite ($OONO^-$) *31*

1.2.11. Iron homeostasis and applications in cancer therapy *32*

1.2.12. Copper homeostasis and applications in cancer therapy *35*

1.2.13. Manganese homeostasis and applications in cancer therapy *37*

1.2.14. Current and novel metal-based drugs as chemotherapeutic agents *40*

1.3. HYPOTHESIS: 47

1.4. AIMS 47

2. EVALUATION OF THE CYTOTOXICITY PROFILES OF NOVEL COMPOUNDS 48
2.1. INTRODUCTION 48
2.1.1. Apoptosis: *48*
2.1.2. ROS signalling apoptosis: *54*
2.1.3. Necrosis/necroptosis: *56*
2.1.4. ROS signalling and necrosis/necroptosis: *60*
2.2. DYSREGULATION OF CELL DEATH MECHANISMS AND CANCER: 61
2.2.1. Apoptosis and Cancer: *61*
2.2.2. Necroptosis and cancer: *63*
2.3. AIMS: 65
2.4. MATERIALS 65
2.5. METHODS 67
2.5.1. Cell Viability Assay *67*
2.5.2. Cell cytotoxicity assay *68*
2.5.3. Statistical analysis *69*
2.6. RESULTS: 70
2.6.1. Cytotoxic effects of metal-based drugs *70*
2.6.2. Membrane Integrity- LDH assay *77*
2.6.3. Mode of cell death – Annexin/PI flow cytometry staining *79*
2.7. DISCUSSION: 84

3. EPIGENETIC CHEMO-SENSITISATION STRATEGIES 91
3.1. EPIGENETICS 91
3.1.1. Histone Lysine Acetylation/De-acetylation: *94*
3.1.2. Cancer Epigenetics *95*
3.1.3. Dysregulation of Histone modifications: *96*
3.1.4. Small molecule epigenetic regulators: *98*
3.2. AIMS 102
3.3. METHODS 103

3.3.1. Combinatorial treatments of HDACi and metal-phen compounds *103*

3.3.2. Western Blot *104*

3.3.3. Statistical analysis *106*

3.4. RESULTS: 107

3.4.1. Treatment with CMPD 19 and epigenetic regulators: *107*

3.4.2. Treatment with CMPD 73 and epigenetic regulators *108*

3.4.3. Treatment with CMPD74 and epigenetic regulators *109*

3.4.4. Treatment with 1,10-Phen and VPA *111*

3.4.5. Treatment with cisplatin and HDACi *111*

3.4.6. Western blot analysis of H4K16ac expression in response to HDACi *112*

3.5. DISCUSSION 114

4. INVESTIGATION OF ROS 119

4.1. OXIDATIVE STRESS AND CANCER 119

4.1.1. Mesothelioma: *123*

4.1.2. ROS and chemotherapeutics: *127*

4.1.3. Metal-based drugs and redox homeostasis *128*

4.2. AIMS: 129

4.3. METHODS: 129

4.3.1. Fluorescent staining of intracellular ROS generation *129*

4.3.2. Fluorescent staining of mitochondrial hydrogen peroxide: *131*

4.3.3. Selective inhibition of cellular antioxidant pathways: *131*

4.3.4. Selective inhibition of compound cytotoxicity using ROS scavengers *133*

4.3.5. Statistical analysis *134*

4.4. RESULTS 135

4.4.1. Fluorescent staining of intracellular ROS generation using flow cytometry *135*

4.4.2. Fluorescent staining of intracellular ROS generation using fluorescent spectrophotometry *139*

4.4.3. Fluorescent staining of mitochondrial hydrogen peroxide *142*

4.4.4. Selective inhibition of cellular antioxidant pathways: *144*

4.4.5. Selective inhibition of compound cytotoxicity using ROS scavengers *154*

4.5. DISCUSSION: 159

5. INVESTIGATING FERROPTOSIS AS A MECHANISM OF CELL DEATH 168

5.1. INTRODUCTION 168

5.1.1. Lipid peroxides *168*

5.1.2. Ferroptosis *171*

5.2. AIMS 175

5.3. METHODS 176

5.3.1. Indirect measurement of Ferroptosis using Ferroptosis inhibitors *176*

5.3.2. Detection of red cell haemolysis *176*

5.4. RESULTS 178

5.4.1. Indirect measurement of Ferroptosis using Ferroptosis inhibitors *178*

5.4.2. Detection of red cell haemolysis *182*

5.5. DISCUSSION 184

6. INVESTIGATING THE CHEMICAL NUCLEASE POTENTIAL OF 1,10-PHEN AND NOVEL METAL PHEN COMPOUNDS. 187

6.1. INTRODUCTION 187

6.1.1. Oxidative Processes in nucleotide synthesis *187*

6.1.2. Oxidative Processes in the Response to DNA damage *188*

6.1.3. Oxidative processes in DNA damage *191*

6.1.4. Attack on sugar phosphate backbone *191*

6.2. MECHANISMS OF DNA NUCLEOTIDE OXIDATION 193

6.2.1. Formation of abasic sites *193*

6.2.2. Deamination *194*

6.2.3. Oxidation of nucleotide bases *195*

6.2.4. Intra- and Inter Strand DNA crosslinks *196*

6.2.5. RNA oxidation: *198*

6.2.6. Investigation of nuclease mimetics *200*

6.2.7. Agarose gel evaluation of nuclease activity ex cellulo *200*

6.2.8. qPCR-based evaluation of nuclease activity in cellulo *202*

6.3. AIMS 204

6.4. METHODS: 204

6.4.1. Agarose gel evaluation of nuclease activity ex cellulo *204*

6.4.2. RT-qPCR evaluation of nuclease activity in cellulo *207*

6.5. RESULTS 213

6.5.1. Nuclease mimetic activity of CMPD73 and CMPD74 ..... *213*

6.5.2. Ribonuclease activity in response to ROS and RNS specific scavengers *217*

6.5.3. qPCR analysis of RNA damage *220*

6.5.4. 3':5' RT-qPCR assay *223*

6.5.1. ..... *224*

6.5.2. ..... *224*

6.5.3. ..... *224*

6.5.4. ..... *224*

6.5.5. Differential amplicon size assay *224*

6.6. DISCUSSION: 226

7. POTENTIAL INTERACTIONS BETWEEN METAL-BASED DRUGS AND ER STRESS 237

7.1. INTRODUCTION 237

7.2. AIMS 245

7.3. METHODS 246

7.3.1. Selective induction of the UPR pathway using UPR inducing compounds *246*

7.3.2. Statistical analysis: *246*

7.4. RESULTS 247

7.5. DISCUSSION: 255

8. OVERALL DISCUSSION 259

9. FUTURE PERSPECTIVES 268

10. APPENDIX 273

11. REFERENCES 276

Table of Figures

Figure 1.1 Global incidence, mortality and 5-year survival rates per continental population…….. 2

Figure 1.2-The structure of Cisplatin and Transplatin. 15

Figure 1.3-Activation of cisplatin. 17

Figure 1.4-Schematic of $^1O_2$ generation from other sources of ROS or RNS 30

Figure 1.5- Synthesis of Nitric oxide 31

Figure 1.6 - Chemical structure of 1,10-phenanthroline 41

Figure 1.7- Chemical structure of trioxaundecanedioic acid 45

Figure 1.8- Chemical structures of CMPD 73 and 74 46

Figure 2.1-Characteristic apoptotic cells as seen under holographic, fluorescent (using AnnexinV PI staining) and contrast microscopy. 49

Figure 2.2-Activation of pro-apoptotic signalling cascade in response to initiating stimuli and the subsequent activation of apoptotic caspases. 50

Figure 2.3-Extrinsic Death receptor apoptotic pathway. 52

Figure 2.4-Intrinsic mitochondrial apoptotic pathway. 54

Figure 2.5-Necroptotic cell death pathways. 59

Figure 2.6 Cytotoxic effects of Cisplatin, CMPDs 73 and 74 against CS Meso (A) and CR Meso (B) cells following 72hr incubation. 73

Figure 2.7 Cytotoxic profiles of CMPD 73, and its constituent components 74

Figure 2.8 Cytotoxic profiles of CMPD 74, and its constituent components 76

Figure 2.9 Inhibition of LDH activity in A549 cell supernatant by CMPD73. Visualization of LDH enzyme inhibition with increasing concentration of CMPD 73 as seen by loss of colour change of LDH assay reagent, when compared to triton control and EDTA control preserving LDH activity. 78

Figure 2.10 Inhibition of LDH activity in A549 cells by CMPD74. 79
Figure 2.11-Representative data (of three independent experiments) of Annexin-FITC/PI staining of A2780 cells to doxorubicin (0.3µM and 3µM) and CMPDs 73 (45µM), 74 (3µM) and 1,10-Phen (200µM). 82
Figure 2.12-Expression of non-apoptotic, apoptotic, late apoptotic and necrotic markers following flow cytometric analysis of A2780 cells 83
Figure 2.13 Proposed model of pathways of action of metal-phen compounds in cell systems. 90
Figure 3.1 Overview of chromatin dynamics. 93
Figure 3.2 Chemical structures of SAHA, VPA and SPB 99
Figure 3.3 Treatment protocols for novel metal-based drugs and cisplatin with HDACi epigenetic regulators 104
Figure 3.4-Increased expression levels of acetylated H4K16 in response to treatment with HDACi 113
Figure 3.5-(A) western blot of purified histones from A549 cells treated with SAHA and VPA 113
Figure 4.1 Pathways for the elimination of key ROS species in cells 129
Figure 4.2 Treatment protocols for novel metal-based drugs with inhibitors of GSH and Catalase antioxidant pathways 133
Figure 4.3 -Treatment protocols for novel metal-based drugs in the presence of ROS scavengers 134
Figure 4.4- A549 cells stained with 5µM DCFDA and exposed to 100µM CMPD 73, 74, 1,10-Phen and H_2O_2 control 136
Figure 4.5- A549 cells stained with 5µM DCFDA and exposed to 100µM CMPD 73, 74, 1,10-Phen and H_2O_2 control 137

Figure 4.6- A2780 cells stained with 5µM DCFDA and exposed to 100µM CMPD 73, 74, 1,10-Phen and H_2O_2 control 138
Figure 4.7- A2780 cells stained with 5µM DCFDA and exposed to 100µM CMPD 73, 74, 1,10-Phen and H_2O_2 control 139
Figure 4.8- A549 cells stained with 10µM DCFDA and exposed to A) CMPD 73 and B) CMPD 74.....140
Figure 4.9-A2780 cells stained with 10µM DCFDA and exposed to A) CMPD 73 and B) CMPD 74 142
Figure 4.10-MitoPY1 staining of A549 cells exposed to 100µM CMPD 73, 74 and H_2O_2 control 143
Figure 4.11- Selective inhibition of GSH synthesis pathway using BSO and the catalase H_2O_2 detoxification pathway by AT. 144
Figure 4.12 Chemical blockage of cellular antioxidant defences enhances susceptibility to H_2O_2 exposure in A549 cells. 145
Figure 4.13 Effect of CMPD73 on A549 cells pre-treated with BSO and AT. 146
Figure 4.14 Effect of CMPD74 on A549 cells pre-treated with BSO and AT. 147
Figure 4.15 Effect of 1,10-Phen on A549 cells pre-treated with BSO. 148
Figure 4.16-Effect of CMPD73 on CS meso cells pre-treated with BSO and AT. 149
Figure 4.17-Effect of CMPD74 on CS meso cells pre-treated with BSO and AT. 150
Figure 4.18-Effect of CMPD73 on CR meso cells pre-treated with BSO and AT. 151
Figure 4.19-Effect of CMPD74 on CR meso cells pre-treated with BSO and AT. 152
Figure 4.20-Effect of CMPD73 on A2780 cells pre-treated with AT. 153
Figure 4.21-Effect of CMPD74 on A2780 cells pre-treated with AT. 154
Figure 4.22-Chemical scavenging of H_2O_2 and superoxide decreases the susceptibility to H_2O_2 exposure in A2780 cells. 155

Figure 4.23-Effect of CMPD73 on A2780 cells pre-treated with NaPy (iH_2O_2) and Tiron (iSuperox). 156
Figure 4.24-Effect of CMPD74 on A2780 cells pre-treated with NaPy (iH_2O_2) and Tiron (iSuperox). 157
Figure 4.25-Effect of 1,10-Phen on A2780 cells pre-treated with NaPy (iH_2O_2) and Tiron (iSuperox). 158
Figure 4.26- Extracted data from Kellet *et. al* (2011) re. ROS production of analogous compounds. 162
Figure 5.1-Initiation and propagation of lipid radicals and generation of lipid peroxides 169
Figure 5.2-Mechanisms of Ferroptotic cell death. 174
Figure 5.3-CMPD 74 in response to titrations of ferroptosis inhibitors. 180
Figure 5.4-CMPD 73 and 1,10-Phen in response to ferroptosis inhibitors. 182
Figure 6.1-Various structural forms of plasmid DNA 201
Figure 6.2-2% Agarose gel electrophoresis of total cellular RNA. 202
Figure 6.3-Principle of the 3':5' assay. 203
Figure 6.4-Location of primers for the 3':5' assay from Primer 3. 209
Figure 6.5- Primer locations for differential amplicon assay form Primer 3. 211
Figure 6.6- DNAse activity of CMPD73 and CMPD74 in the presence of added ascorbate as a reductant for 0.5, 4, and 24hrs at 100μM. 213
Figure 6.7-DNAse activity of CMPD73 and CMPD74 in the absence of added ascorbate as a reductant for 24hrs at 100μM. 214
Figure 6.8 RNAse activity of CMPD73 and its precursors. 215
Figure 6.9 RNAse activity of CMPD74 and its precursors. 216
Figure 6.10 Kinetics of RNA degradation by 1μM CMPD74 and 10μM 1,10-Phen in the presence of ascorbate. 217

Figure 6.11- ROS inhibitor profiling of RNA degradation.....219
Figure 6.12- Gene expression analysis of *GAPDH, 18S, PPIA* and *PGK1* HKGs isolated from A2780 cells, in response to treatment of IC_{10} and IC_{25} values of CMPD 73 for 24hrs. 221
Figure 6.13- Gene expression analysis of *GAPDH, 18S, PPIA* and *PGK1* HKGs isolated from A2780 cells, in response to treatment of IC_{10} and IC_{25} values of 1,10-Phen for 24hrs. 223
Figure 6.14- 3':5' ratio of *PGK1* HKG isolated from A2780 cells in response to treatment of IC_{10} and IC_{25} values of CMPD 74 for 24hrs. 224
Figure 6.15- Differential amplicon size assay of *PGK1* HKG mRNA isolated from A2780 cells treated with of IC_{10} and IC_{25} concentrations of CMPD 74 for 24hrs. 225
Figure 6.16- Reduction of copper in the presence of AA and the generation of ROS (Zhou, Zhang *et al.*, 2016) 229
Figure 7.1-Activation of the UPR signalling pathway.....241
Figure 7.2-Potential crosstalk between UPR signalling and inherent metal-phen activity....243
Figure 7.3-Timeline of Anisomycin and Tunicamycin incubation regimes. 246
Figure 7.4-A549 cells pre-treated with 100nM Anisomycin for 24hrs followed by treatment with CMPD 73 for a further 24hrs. 247
Figure 7.5-A549 cells pre-treated with 100nM Anisomycin for 24hrs followed by treatment with CMPD 74 for a further 24hrs. 248
Figure 7.6-A549 cells pre-treated with 100nM Anisomycin for 24hrs followed by treatment with 1,10-Phen for a further 24hrs. 248
Figure 7.7-A2780 cells pre-treated with 100nM Anisomycin for 24hrs followed by treatment with CMPD 73 for a further 24hrs. 249
Figure 7.8-A2780 cells pre-treated with 100nM Anisomycin for 24hrs followed by treatment with CMPD 74 for a further 24hrs. 250

Figure 7.9-A2780 cells pre-treated with 100nM Anisomycin for 24hrs followed by treatment with 1,10-Phen for a further 24hrs. 250
Figure 7.10-A549 cells pre-treated with 5nM Tunicamycin for 8hrs followed by treatment with CMPD 73 for a further 24hrs. 251
Figure 7.11-A549 cells pre-treated with 5nM Tunicamycin for 8hrs followed by treatment with CMPD 74 for a further 24hrs 252
Figure 7.12- A549 cells pre-treated with 5nM Tunicamycin for 8hrs followed by treatment with 1,10-Phen for a further 24hrs. 252
Figure 7.13-A2780 cells pre-treated with 5nM Tunicamycin for 8hrs followed by treatment with CMPD 73 for a further 24hrs. 253
Figure 7.14-A2780 cells pre-treated with 5nM Tunicamycin for 8hrs followed by treatment with CMPD 74 for a further 24hrs. 254
Figure 7.15-A2780 cells pre-treated with 5nM Tunicamycin for 8hrs followed by treatment with 1, 10-Phen for a further 24hrs. 254
Figure 8.1- Chemical structures of CMPD 73 and 74 260
Figure 8.2- Model of forms of cell death associated with metal-phen compounds. 267
Figure 10.1- An example image of Multiple T-Test analysis from GraphPad Prism 8 testing statistical significance of each concentration of the intact CMPD 73 vs 1,10-Phen at the same concentration to generate a P value 274
Figure 10.2- An example image of Multiple T-Test analysis from GraphPad Prism 8 testing statistical significance of each concentration of the intact CMPD 74 vs 1,10-Phen at the same concentration to generate a P value. 274
Figure 10.3- Isolated RNA exposed to CMPD 74 and DMSO at various pre-incubation times. 275

Table of tables

Table 1.1-Top 10 cancers of 18.1 million new incidences 1

Table 1.2-Global incidence, mortality and 5-year prevalence rates of cancer of both sexes 3

Table 1.3-Cancer statistics for the island of Ireland (2016-2018) 4

Table 2.1-Alternate forms of cell death 60

Table 2.2 Cytotoxic effect of novel compounds and 1,10-Phen on cultured human cancer cells following 24 hrs. 71

Table 2.3-Effectiveness of CMPD 73 and CMPD 74 is not impacted by the presence of cisplatin resistance following 72 hr incubation 72

Table 2.4-P Values of manganese and phen components and combinations compared to CMPD 73 at each concentration tested. 75

Table 2.5-P Values of copper and phen components and combinations compared to CMPD 74 at each concentration tested 76

Table 3.1 Association of class I and II HDACs overexpressed in different cancers. 97

Table 3.2 Estimated IC_{50} Values for CMPD19 combined with HDACi with 24h treatment 107

Table 3.3 Estimated IC_{50} Values for CMPD 73 combined with HDACi with 24h treatment108

Table 3.4 Estimated IC_{50} Values for CMPD74 combined with HDACi with 24h treatment.109

Table 3.5 Estimated IC_{50} Values for CMPD74 combined with SAHA with 8h treatment. SAHA reduced cell viability by 8% in both cell lines. 110

Table 3.6 Estimated IC_{50} Values for cisplatin combined with HDACi following 72h treatment 111

Table 5.1- Percent haemolysis of RBC incubated with Triton X control, CMPDs 73 and 74, and 1,10-Phen for 16hrs. 183

Table 6.1- DNA damaging chemotherapy drugs and their corresponding types of DNA damage and cancers they treat. 187

Table 6.2-DDR pathways specific to DNA damage repair.....190

Table 6.3-ROS and RNS specific scavengers and their corresponding ROS/RNS targets and working 206

Table 6.4-Cycling conditions for qPCR assays 207

Table 6.5-Forward and Reverse primers for HKGs.....208

Table 6.6-Primer sequences used for the 3':5' assay.....210

Table 6.7-Primer sets for differential amplicon assay 211

1. Chapter 1

1.1.General introduction

1.1.1. Global Rates of cancer

Fundamentally cancer is a disease which is a result of uncontrolled division of abnormal cells in a part of the body (Stratton, Campbell and Futreal, 2009). It affects millions of people globally and is one of the most intensely studied diseases of the modern age (Bray *et al.*, 2018). The Global Cancer Incidence, Mortality and Prevalence study (GLOBOCAN) estimated that in 2018, 9.6 million people died and 18.1 million new cases of cancer were diagnosed (*ibid.*). This number is expected to increase by 11.4 million new cases by 2040 to 29.5 million (International Agency for Research on Cancer, 2019). The World Health Organisation estimates that 1 in 8 men and 1 in 11 women will die due to the disease (WHO, 2018). Of the 18.1 million new cases, a list of the ten most diagnosed cancers can be seen in Table 1.1, with lung, colorectal, and breast most prevalent. Of the 9.6 million global fatalities recorded in 2018, lung cancer will be responsible for 1.8 million deaths (18.4%), colorectal cancer 881,000 deaths (9.2%), and breast cancer 627,000 deaths (6.6%)(WHO, 2018).

Table 1.1-Top 10 cancers of 18.1 million new incidences (International Agency for Research on Cancer, 2019)

Cancer type:	New cases (millions)
Lung	2
Breast	2
Colorectal	1.8
Prostate	1.3
Stomach	1
Liver	0.84
Oesophagus	0.57
Cervical/Uterine	0.57
Thyroid	0.57
Bladder	0.54

As highlighted in Table 1.2 and Figure 1.1, global cancer incidence and mortality vary significantly between developed and developing areas of the world. Much of this variation

is explained by the population per region and, as a result of specific cultural and lifestyle practices, the prevalence of specific cancers, and the availability of sufficient treatment.

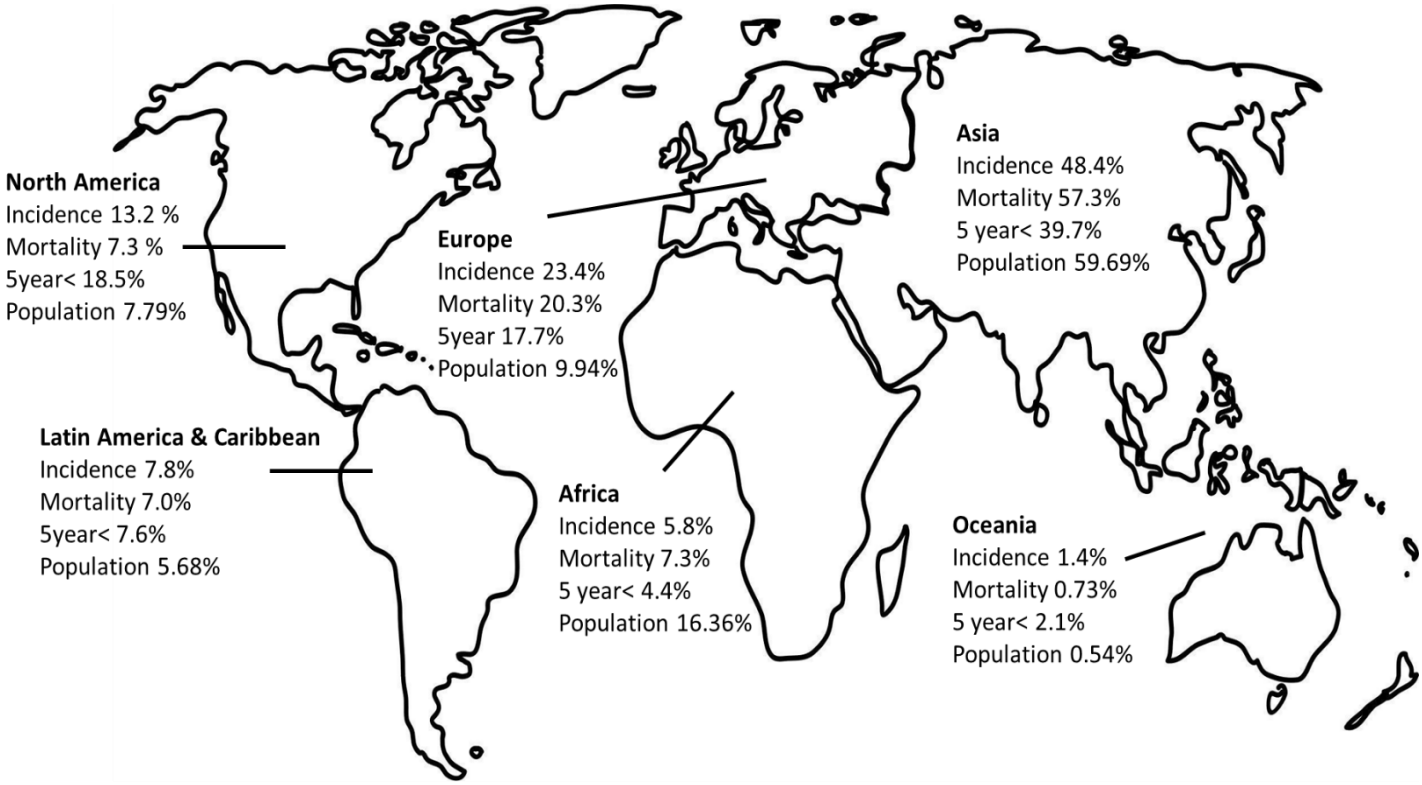

5year< 5 year survival

Figure 1.1 Global incidence, mortality and 5-year survival rates per continental population. Self-generated figure using data from (European Commission, 2018; GLOBOCAN-WHO, 2018b) and images widely available online.

Despite only containing 9% of the global population, Europe accounts for 23.4% of cancer incidences and 20.3% global mortality (European Commission, 2018; GLOBOCAN-WHO, 2018b). This is likely a result of sedentary lifestyle and poorer diet associated with western cultures (Deepa, 2016; Eschke *et al.*, 2019).

Table 1.2-Global incidence, mortality and 5-year prevalence rates of cancer of both sexes

Global incidence and mortality (%) of cancers				
Region	Incidence	Mortality	5-year Survival	% of global population
Europe	23.4	20.3	17.7	9.94
North America	13.2	7.3	18.5	7.79
LAC*	7.8	7.0	7.6	5.68
Asia	48.4	57.3	39.7	59.69
Africa	5.8	7.3	4.4	16.36
Oceania	1.4	0.73	2.1	0.54

(*Latina America and Caribbean) (Ferlay *et al.*, 2019)

However the mortality rates among European countries are much lower when compared to more developing regions such as Asia or Africa, both of which have higher mortality rates compared to incidence. This is believed to be a result of higher rates of detection among European countries, compared to the frequency of cancers with poorer prognosis and limited access to cancer appropriate healthcare in developing regions of the world such as Africa and Asia (WHO, 2018).

In Ireland, 30% of deaths (some 9,000 annually) are caused by cancer, with over 30,272 new cases reported in 2018. Ireland thus ranks third on the global scale of cancer with 373.7 per 100,000, with men also ranking third for global cancer rates at 430.8 per 100,000, and women ranking seventh at 322.9 per 100,000 (*Cancer statistics | Irish Cancer Society*, 2018). The most common cancers diagnosed in both Ireland and in women and men are shown in Table 1.3, with skin cancers the most prevalent cancer diagnosed among the Irish population.

Table 1.3-Cancer statistics for the island of Ireland (2016-2018)

Most common cancers in Ireland (2016-2018)		
Cancer Type	Cases	Deaths
Skin	10,816	228
Prostate	3,550	533
Breast	3,244	659
Bowel	2,767	942
Lung	2,561	1,693
Most common cancers in Irish Women		
Skin (Non-melanoma)	4,632	26
Breast	3,215	649
Gynaecological	1,321	502
Lung	1,170	716
Skin (melanoma)	581	60
Most common cancers in Irish Men		
Skin (Non-melanoma)	6,184	57
Prostate	4,976	585
Bowel	1,752	535
Lung	1,391	911
Skin (melanoma)	529	85

(*Cancer statistics | Irish Cancer Society*, 2018; GLOBOCAN-WHO, 2018a; HSE.ie, 2018).

1.1.2. Risk factors contributing to cancer development

The loss of cell cycle control in response to oncogenic mutations is the main cause of cancer and can arise from various different stimuli, such as genetic predisposition and family history, infection, environmental factors and age (Blackadar, 2016; Aunan, Cho and Søreide, 2017). Certain people can be born with various familial mutations that confer a predisposition to develop different cancers. A prime example is colon cancer linked with Adenomatous polyposis coli (*APC*) mutation. *APC* is a gene whose mutation is associated with a rare, hereditary form of colorectal cancer known as familial adenomatous polyposis (Schell *et al.*, 2016).

Age is one of the most significant factors for increasing the risk of developing cancer. Age and longevity increase the exposure time of a person to many of the carcinogenic factors described above, increasing the risk of DNA damage and mutations within the cell (Aunan,

Cho and Søreide, 2017). Further to this, the ends of chromosomes possess strands of DNA known as telomeres, which serve to protect from deterioration and fusion with neighbouring chromosomes and which are known to shorten after each cell division (Mcnally, Luncsford and Armanios, 2019). The progressive shortening of telomeres can result in loss of genomic integrity and chromosome instability, resulting in chromosomal fusions, translocations and mutations. As such age-associated telomere shortening has been associated as one of the primary risk factors for the development of oncogenesis and neoplasia (Jafri *et al.*, 2016).

Many different infectious agents are responsible for the development of cancers. Two of the best known are *Helicobacter pylori* (*H. pylori*) and Human Papilloma Virus (HPV). *Helicobacter pylori*, a gastric bacterial pathogen, is the strongest known risk for gastric cancer. *H. pylori* causes gastric ulcers stimulating chronic inflammation (Wroblewski, Peek and Wilson, 2010). Chronic inflammation has been identified as a major cause of cancer and metastatic cancer development (Todoric, Antonucci and Karin, 2016). Another form of carcinogenic infection is infection by HPV and the generation of cervical cancers (Brianti, De Flammineis and Mercuri, 2017). HPV infection has been strongly associated with the development of squamous cell carcinomas of the cervix (Chan *et al.*, 2019).

A multitude of environmental factors have been associated with the prevalence of cancer via the chronic entry, ingestion, or inhalation of carcinogenic agents into the body, as well as exposure to high levels of radiation e.g. UV radiation from the sun (Parsa, 2012). Many are associated with poor lifestyle choices, such as colorectal cancer and its link to poor diet and low physical activity (Thanikachalam and Khan, 2019). Poor diet and low levels of exercise are also strongly associated with obesity, with obesity being identified as a significant risk of developing many different cancers (e.g. colorectal, breast, and oesophageal cancers)

(Stone, McPherson and Gail Darlington, 2018). Further to this the link between smoking and lung cancer (O'Keeffe *et al.*, 2018), and high alcohol consumption and liver cancer (Testino, Leone and Borro, 2014) has been known for decades.

Other environmental factors include occupational exposure to carcinogens such as asbestos in the development of mesothelioma in construction workers (discussed in detail in Chapter 4 page 123) (Matsuzaki *et al.*, 2012) or exposure to dichlorodiphenyltrichloroethane (DDT) in pesticides and the development of breast cancer (Alavanja and Bonner, 2012). Exposure to high levels of UV radiation is a well-established risk factor for a variety of different skin cancers (Narayanan, Saladi and Fox, 2010).

These various genetic, pathogenic, environmental and age-related factors described will result in the accumulation of multiple mutagenic alterations capable of changing normal cell processes and initiating cancer development. These alterations are known as the hallmarks of cancer.

1.1.3. Hallmarks of cancer

The primary hallmarks of cancer are genetic and epigenetic reprogramming to facilitate sustained proliferative signalling and enabling replicative immortality; evasion of growth suppressors and resisting cell death; induction of angiogenesis and metastasis; metabolic reprogramming and alteration of the surrounding microenvironment; and evading the host immune system (Hanahan and Weinberg, 2011; Fouad and Aanei, 2017).

Cells maintain homeostasis by tightly regulating and coordinating the expression and release of growth promoting signals and the expression and release of regulatory proteins controlling

cell proliferation(reviewed by Lee & Young, 2013). It has been established that oncogenic cells alter these regulatory pathways through accumulation of somatic mutations, causing hyper activation of growth promoting signals and silencing of regulatory networks, allowing dysregulated and uncontrolled growth outside the confines of homeostasis (Sanchez-Vega *et al.*, 2018).

A classic example of this form of gene dysregulation is seen in the over activation of the oncogene coding for the Ras GTPase family (*HRas, KRas, NRas*) , which serves as a signalling protein to activate downstream mitogen-activated protein kinases (MAPK) and phosphoinositide-3 kinase (PI3K) pathways, regulating genes involved in cell growth, differentiation and survival (Fernández-Medarde and Santos, 2011). The Ras protein has been shown to be chronically active in 30% of cancers, due to an activating mutation in the Ras coding sequence or a deactivating mutation in its suppressive protein NF1 (Csermely, Korcsmáros and Nussinov, 2016). MAPK and PI3K pathways have also been seen to be dysregulated in many cancers as a result of a somatic mutation (see review Zenonos, 2013). Cancer cells also hijack Telomerase enzymes to become immortalised and replicate endlessly (Jafri *et al.*, 2016). Telomerase activity is almost non-existent in non-immortalised cells but is significantly upregulated in almost 90% of human tumours. The increase in the expression of telomerases liberates cancer cells from the confines of regulation mediated by telomere length (reviewed Hanahan & Weinberg, 2011).

To maintain this sustained growth signalling, inhibition of tumour suppressor proteins which regulate oncogenes and cell proliferation is required to maintain sustained pro-growth signalling (Wang *et al.*, 2019). Commonly inactivated TSPs include the Retinoblastoma (*RB1*) protein, *APC* and Tumour Protein 53 (*TP53*) (Sun and Yang, 2010). *RB1* inhibits the

transcription of mitotic genes by forming inhibitory complexes with transcription factors such as E2F, which positively regulates cyclins and cyclin-dependent kinases promoting G1-S phase transitions (Burke, Hura and Rubin, 2012). Inactive *RB1* leads to uncontrolled expression of cell cycle activating genes ultimately leading to the development of retinoblastoma, a rare form of hereditary eye cancer predominantly diagnosed in children (Pandey, 2014).

The APC protein negatively regulates the Wnt signalling pathway which is responsible for cell proliferation and differentiation in the gastrointestinal tract (Flanagan *et al.*, 2018). Wnt signalling causes downstream transcriptional expression of cyclin D1 and the oncogenic Myc proteins and aberrant regulation of the Wnt signalling pathway can result in increased mitotic activity and neoplasia (reviewed by Zhang & Shay, 2017). Similar to *RB1* inactivation, inactivation of the *APC* gene by germline mutation is responsible for hereditary APC, while somatic mutations of the gene are found in more than 80% of sporadic colorectal cancers.

TP53, also known as the guardian of the genome, has been seen to be mutated or altered in almost 50% of all tumours (Ozaki and Nakagawara, 2011). The p53 protein acts as a master TSP by regulating dozens of target genes responsible for regulating DNA repair such as GADD45 (Salvador, Brown-Clay and Fornace, 2013), cell cycle arrest via p21 and apoptosis by upregulating the expression of pro-apoptotic proteins such as Bax, Apaf1, PUMA and Noxa (Aubrey *et al.*, 2018). As p53 is so intrinsically linked with maintaining cell growth and apoptotic homeostasis, its inactivation via deletion or overexpression of regulatory inhibitors such as MDM2, would naturally lead to dysregulated cell growth and reduced regulatory mechanisms (Lozano, 2019). Conversely, cancer cells can increase the expression

of anti-apoptotic proteins, reducing the capacity of apoptotic control over the cell, favouring growth and division (Timucin, Basaga and Kutuk, 2019).

Epigenetic reprogramming refers to the chemical signature found on genes and their associated histones which can rapidly regulate gene expression. This is a process heavily implicated in cancer initiation, progression, and development of chemotherapy resistance, and is discussed in further detail in Chapter 3.

In addition, for cancer cell subpopulations to continue growing and proliferate, cells must develop new vascular networks to facilitate the continually growing mass of cells, a process known as angiogenesis (Rajabi and Mousa, 2017). Angiogenesis is regulated by oxygen sensitive angiogenic factors which are harnessed by cancer cells to drive the formation of new endothelial cells from existing vasculature to support the growth of the tumour (Fraisl *et al.*, 2009). One of the predominant pro-angiogenic signalling pathways is regulated by the hypoxia-inducible transcription factor (HIF) family (Krock, Skuli and Simon, 2011). The tumour microenvironment (TME) is generally hypoxic in nature as a result numerous cancer cells forming a thick three-dimensional tumour structure (Watnick, 2012). HIF proteins are normally activated by hypoxic conditions to maintain homeostasis in the wound healing process, however the hypoxic conditions of the TME can also trigger its activation. This then triggers the transcription of pro-angiogenic factors such a Vascular Endothelial Growth Factor (VEGF) and genes involved in cell survival, metabolism and inflammation (Hashimoto and Shibasaki, 2015). VEGF has been identified as the most potent factor initiating angiogenesis, and is overexpressed in most metastatic tumours (Carmeliet, 2005). VEGF stimulates angiogenesis by promoting proliferation and survival of nearby endothelial cells, increasing the permeability of surrounding blood vessels and recruiting vascular

precursor cells form the bone marrow (Yang, Yan and Liu, 2018). Permeable or ‘’leaky’’ blood vessels are capable of irrigating solid tumour cells promoting survival (Azzi, Hebda and Gavard, 2013), as well as promoting metastasis by providing an accessible framework for the entry of metastatic cells into the blood stream (Bielenberg and Zetter, 2015).

The ability of cancer to metastasise and invade surrounding tissue, forming secondary sites of growth, is a defining feature of malignancy. Metastatic disease is responsible for over 90% of cancer associated deaths (Seyfried and Huysentruyt, 2013). To metastasise cancer cells must first penetrate the extracellular matrix (ECM) of surrounding tissue, intravasate tumour vasculature, extravasate the blood vessels of distant organs and tissues, and sufficiently proliferate and grow to form new tumour colonies and reform the TME (Seyfried and Huysentruyt, 2013).

For immotile and tightly adherent epithelial and carcinoma cells to escape the ECM, they must undergo the Epithelial-Mesenchymal Transition (EMT). This entails the transition of an epithelial like cell into that of a mesenchymal cell by replacing epithelial associated proteins such as the cell surface protein E-Cadherin for mesenchymal N-Cadherin resulting in detachment of the cell from the basal membrane (Mallini *et al.*, 2014). In addition, the expression of matrix metalloproteases (MMPs), which are increased in almost all cancers, facilitates the degradation of the ECM and allows metastatic cells to escape from their site of origin into blood vessels (Gialeli, Theocharis and Karamanos, 2011).

Extravasation of cells from the circulation into tissue(s) requires reversal of the EMT process which permits re-expression of the proteins needed to anchor the tumour cells to the new tissue site (Cominetti, Altei and Selistre-De-araujo, 2019). Some organs such as the liver or

bone marrow possess highly permeable vessels, and as such may explain the high rates of metastatic cancer that migrates to these tissues (Lorusso and Rüegg, 2012). Once the invading tumour cells have colonised a foreign tissue, they either enter a state of quiescence to allow adaptation to their new environment or initiate angiogenesis to facilitate growth and survival and establish a new TME (Fouad and Aanei, 2017).

To facilitate the high-energy requirements that these hallmarks demand, cancer cells rewire their metabolic and epigenetic programming to quickly adapt to multiple new stimuli and provide a selective advantage during the initiation and progression of oncogenesis. Much of these metabolic changes are a result of selective pressure by the relatively harsh TME and hypoxia (Pavlova and Thompson, 2016). Cancer cell metabolism is adapted to the specific tumour microenvironment and a broad number of metabolic alterations have been described (Pinheiro *et al.*, 2015; Liberti and Locasale, 2016; Camara *et al.*, 2017; Waldhart *et al.*, 2017). However, reliance on aerobic glycolysis is a commonly encountered feature of cancer cells, and is known as the Warburg effect (DeBerardinis and Chandel, 2016). The Warburg effect, first proposed by Otto Warburg in the 1920's, is the effect whereby cancer cells alter their metabolic state to favour anaerobic glycolysis as its main source of ATP production over that of oxidative phosphorylation and the Tricarboxylic Acid Cycle (TCA), despite the presence of available oxygen (Epstein, Gatenby and Brown, 2017).

Altered metabolic pathways in cancer cells can also generate what are known as oncometabolites, metabolic intermediates which further oncogenic processes. An example of this is the production of 2-hydroxyglutarate (2HG) via a mutation in Succinate Dehydrogenase (SDH) (Wong, Qian and Yu, 2017). 2HG is a competitive inhibitor of many α-Keto Glutarate (α-KG) dependent enzymes. α-KG is an essential co-factor for DNA

demethylases, epigenetic enzymes involved in the removal of gene silencing methyl modifications on DNA and gene promoters (Tran, Lowman and Kong, 2017). The loss of demethylase activity results in hypermethylated gene promoters, with hyper methylation of TSP gene promoters seen as a hallmark of epigenetic cancer progression (Lewandowska and Bartoszek, 2011).

Metabolic reprogramming can also influence the survival of surrounding cells in the TME as well as cancer cells themselves (Sun *et al.*, 2018). The TME is both a consequence and driver of oncogenesis, with both acting in regulatory loops influencing the other (Ribeiro Franco *et al.*, 2020). As previously noted, a hallmark of the TME for solid tumours is hypoxia and the initiation of HIF and VEGF mediated angiogenesis (Carmeliet, 2005; Krock, Skuli and Simon, 2011). Fluctuating hypoxic conditions can also stimulate oxidative stress, which may induce further genetic mutations in cancer cell DNA, facilitating further oncogenic transformations (Wang, Zhang and Chen, 2019).

The TME consists of tumour cells, non-tumour cells such as cancer associated fibroblasts CAFs), endothelial cells and pericytes (contractile capillary associated cells), immune and inflammatory cells, bone marrow derived cells, and the ECM (Belli *et al.*, 2018). The interactions between the cells of the TME contribute to oncogenesis through the release of paracrine signals such as growth factors, chemokines, cytokines and matrix remodelling enzymes, facilitating the initiation, propagation and progression of cancer cells (Balkwill, Capasso and Hagemann, 2012). For further reviews on the TME, see Peltanova, Raudenska, & Masarik, (2019), Balkwill *et al.*, (2012), and Belli *et al*., (2018).

Finally in order to ensure the survival of tumour cells, the evasion of the host immune system is required (Nicolini *et al.*, 2018). The innate and the adaptive immune systems can recognise and eradicate developing tumour cells in response to the expression of certain extracellular markers or induction of functional apoptotic signalling (Swann and Smyth, 2007). Circulating cancer cells which have metastasised are particularly susceptible to immune surveillance and clearance (Leone, Poggiana and Zamarchi, 2018). However constant immune surveillance can confer selective pressure on tumour cells and generate subpopulations capable of immune evasion, a process termed cancer immune-editing (Mittal *et al.*, 2014). Cancer immune-editing allows cancer cells to escape immunosurveillance by reducing the expression of antigenic receptors required for T-cell recognition, resistance to cell death, and induction of immuno-tolerance via expression and secretion of immunosuppressive cytokines by tumour cells themselves, or stromal cells from the surrounding TME (Fouad and Aanei, 2017).

Macrophages recruited into the TME are known as Tumour Associated Macrophages (TAMs) (Dehne *et al.*, 2017). TAMs favour tumour growth by further suppression of the immune system via cytokine release and through the promotion of angiogenesis via VEGF secretion (Ostuni *et al.*, 2015). High levels of TAMs in the TME have been associated with poor prognosis and survival rates in breast cancer (Zhao *et al.*, 2017). For further reading on tumour immune evasion, see reviews by Chen *et al.*, 2019, Hinshaw and Shevde, 2019, Lin, Xu and Lan, 2019, and Zhang *et al.*, 2019.

1.2.Chemotherapy

To combat the vast numbers of different cancers, clinicians have developed multiple treatment regimens targeting various oncogenic pathways, using chemical, radiological and immunological strategies.

One of the most effective chemotherapeutic drugs identified to date is cis-dichloro-diammineplatinum (II), commonly known as cisplatin (reviewed by McKeage, Higgins and Kelland, 1991). Cisplatin was first synthesised in 1844 by the Italian chemist Michele Peyrone, however its potential as an anti-bacterial and anti-cancer agent would not be realised for another 120 years (Peyrone, 1844; Rosenberg, Van Camp and Krigas, 1965; Desoize and Madoulet, 2002).

In 1965 it was first identified as an antibacterial agent by Barnett Rosenberg who inadvertently discovered that cisplatin as a complex was generated by electrolysis of platinum electrodes and that it was capable of inhibiting cell division in *Escherichia coli* bacteria (Rosenberg, Van Camp and Krigas, 1965; Rosenberg *et al.*, 1967). Rosenberg then hypothesised that cisplatin would have similar effects in cancer cells. This was indeed the case with cisplatin demonstrating anti-tumour activity against sarcoma and leukaemia tumours generated in mice (Rosenberg *et al.*, 1969; Rosenberg, 1971).

Cisplatin showed great success in the treatment of testicular cancer, which until then had extremely limited treatment options (Einhorn and Donohue, 1977). Following approval by the Food and Drug Administration (FDA) in 1978, it was quickly deployed as a cancer therapy (reviewed by Kelland, 2007). In 1979 cisplatin was granted approval in the UK and several other EU countries (Ghosh, 2019). Following initial clinical success cisplatin was

granted further FDA approval to be used in the treatment of advanced ovarian and bladder cancer (Higby *et al.*, 1974; Carter, 1984; Lambert and Berry, 1985). In contemporary clinical practice, cisplatin remains effective as a frontline chemotherapeutic against a broad spectrum of cancers, including head and neck, colorectal, lymphomas, ovarian, mesothelioma and lung cancers (reviewed by Galluzzi *et al.*, 2014). Until the discovery of cisplatin as an anti-cancer agent in 1965 most anti-cancer treatments used were organic based compounds (Rosenberg, 1971). The discovery of cisplatin prompted wide-spread investigation into other metal-containing and inorganic compounds as potential anti-cancer drugs (Makovec and Makovec, 2019).

1.2.1. Biochemistry of cisplatin – the canonical metal-based chemotherapeutic

Cisplatin is a metallic coordination compound consisting of a doubly charged platinum core with four ligands – two cis chloride ligands and two amino ligands (Figure 1.2).

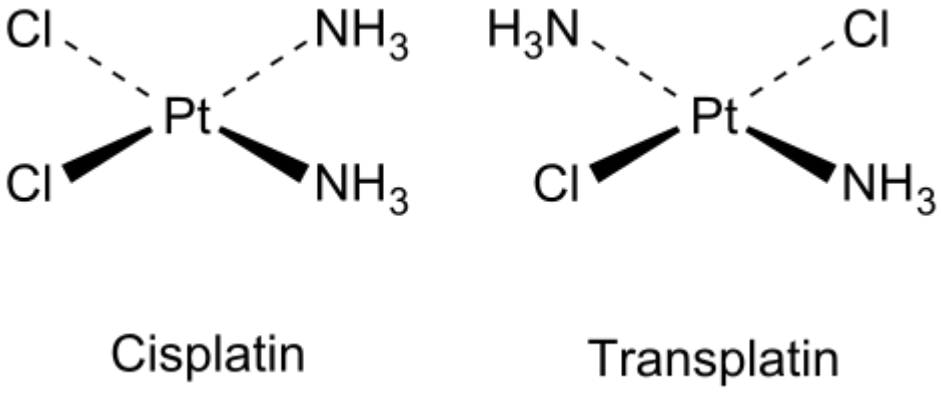

Figure 1.2-The structure of Cisplatin and Transplatin. The *cis* and *trans* configuration of the chloride ligands is evident

In the extracellular space where chloride concentration is high (100mM), the chloride ligands are considered to be stable for cisplatin chemistry (Makovec and Makovec, 2019). However,

upon entry into the cell where chloride concentration is relatively low (2-10mM), cisplatin undergoes two important steps of hydrolysis, whereby the chloride ions are sequentially replaced with two water molecules (see Figure 1.3 below)(reviewed Galluzzi *et al.*, 2014). These hydrolytic steps are important for the activation of cisplatin, as each water molecule can, in turn, be lost. This process leads to the formation of a potent electrophile which can attack various biomolecules, including the purine bases of DNA (Goodsell, 2006). Upon interaction with DNA, the formation of both intra- and inter-strand cross-links can cause double strand breaks (DSB), interfering with both cell division and transcriptional processes (reviewed Rocha, Silva, Quinet, Cabral-Neto, & Menck, 2018). DBSs induce cellular DNA damage response (DDR) pathways which ultimately culminate in the induction of apoptosis (Ghosh, 2019).

Cisplatin has also been seen to target mitochondrial DNA (mtDNA), disrupting mitochondrial integrity further capable of activating apoptosis (Yimit *et al.*, 2019). Cisplatin is thus more effective in cells that have less efficient DNA repair mechanisms (e.g. testis)(Rocha *et al.*, 2018). Although the exact mechanism of cisplatin has not been fully defined and is still actively studied, apoptosis secondary to DNA damage is thought to play a central role (Makovec and Makovec, 2019). Cisplatin has also been observed to generate reactive oxygen species which are capable of triggering apoptosis, likely further contributing to cytotoxicity (Casares *et al.*, 2012).

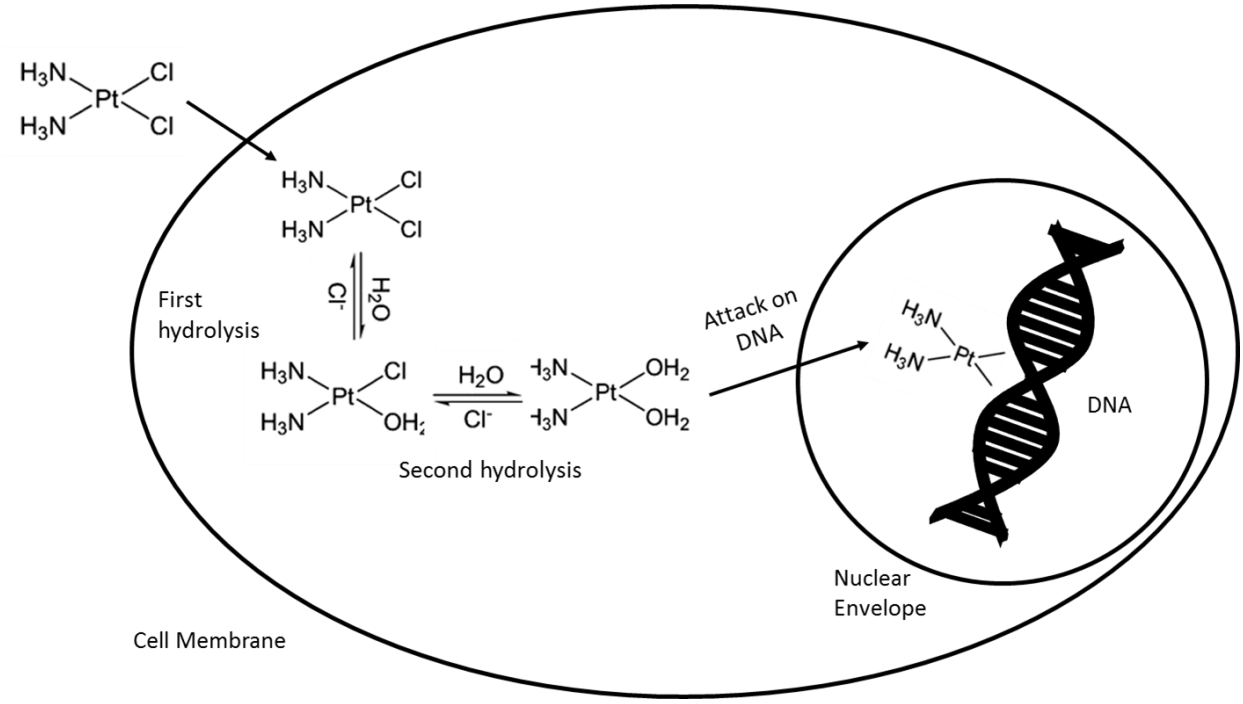

Figure 1.3-Activation of cisplatin. Stepwise hydrolysis of structural chloride ions facilitates DNA attack. Self-generated figure using Microsoft PowerPoint and images widely available online.

However, treatment with cisplatin does have its limitations - nephrotoxicity, hepatotoxicity and ototoxicity are seen in most cases. In addition, high rates of cancer relapse due to the development of acquired resistance is common (Ferreira *et al.*, 2016). Similar effects are seen with cisplatin derivatives carboplatin and oxaliplatin, which offer only limited variation in their mechanistic scope (Deo *et al.*, 2016).

1.2.2. Mechanisms of Cancer resistance

Despite many major advances in treating a multitude of cancers, the prevalence of cancer resistance and cancer relapse is still a major cause of mortality worldwide (Butow *et al.*, 2018). As such determining the mechanisms driving the development of cancer resistance has been the focus of many studies over the last few decades (Wang *et al.*, 2017). The primary hallmarks of cancer resistance are the presence of intrinsically resistant and quiescent cell populations, tumour heterogeneity, increased drug efflux, overexpression and

activation of anti-oxidant systems and drug inactivation, alteration of drug target, increased DNA repair and decreased cell death mechanisms, influence of the TME, and epigenetic alterations (Housman *et al.*, 2014; Mansoori *et al.*, 2017; Wang, Zhang and Chen, 2019).

Resistant phenotypes exist intrinsically within the tumour population or are acquired following therapy driven alterations (Wang, Zhang and Chen, 2019). Intrinsic resistance to chemotherapy is generally associated with a sub-population of tumour cells, known as Cancer Stem Cells (CSC) (Vinogradov, Wei and Thor, 2013).

CSCs are cancer cells with stem cell like features such as the capacity for self-renewal and differentiation (Shukla and Meeran, 2014). These are considered to be tumour initiating cells, feeding the generation of new tumour bulk cells for long term population and are typically intrinsically resistant to chemotherapy (Borovski *et al.*, 2011). In addition to possessing efficient DNA repair mechanisms and resistance to apoptosis, CSC appear to have slow cell cycle kinetics and thus exist in a state of quiescent dormancy. This reduces the cytotoxic capacity of chemotherapy drugs such as cisplatin which relies on cell cycle checkpoints to detect damaged DNA and initiate cell death (Chen, Huang and Chen, 2013).

The current consensus is that treatment with chemotherapeutic drugs (e.g. cisplatin) is efficient at initially killing sensitive tumour bulk cells, but the inherently resistant CSC sub-populations survive this initial treatment. This leads to an enrichment of CSC and propagates a resistant phenotype (Ayob and Ramasamy, 2018). Indeed both lung and ovarian CSCs were seen to be enriched following treatment with cisplatin, increasing overall tumour burden (Jiang *et al.*, 2013; Wang, Jin and Wang, 2014).

Tumour heterogeneity confers different degrees of drug sensitivity across the different cell populations that make up the tumour. Four levels of heterogeneity exist among tumour cells: genetic, cell type (e.g. tumour bulk cells, CSCs, TAMs), metabolic and temporal (Chen, Qian and Wu, 2015). Genetic heterogeneity is well documented in ovarian, breast and renal cell carcinoma (see reference 100, 101, 102 X. Wang *et al*., 2019). The varying degrees of drug sensitivity and resistance against chemotherapeutic agents makes killing all sub-populations of tumour cells quite difficult using a single chemotherapy agent (Baxevanis, Perez and Papamichail, 2009). As such tumour heterogeneity has prompted the development of combinatorial drug therapies to target multiple sub-populations of tumour cells (Al-Lazikani, Banerji and Workman, 2012).

The effective concentrations in which cisplatin and other chemotherapeutics are required for cytotoxicity are highly dependent on the intracellular concentrations of the drug. Both the influx and efflux of cisplatin can be altered in cisplatin resistant cells (Mansoori *et al.*, 2017). Uptake of cisplatin into the cell appears to be mediated by Copper Transporter Protein 1 (CTR1). Cisplatin resistant cells have been shown to downregulate the expression of CTR1 and so decrease cellular uptake of cisplatin (Ibrahim, Srivenugopal and Rasul, 2013).

Increased efflux of cisplatin and other chemotherapy agents via overexpression of the ATP-Binding Cassette (ABC) transmembrane transporter superfamily is another mechanism through which intracellular cisplatin concentration can be reduced (Zahreddine and Borden, 2013). The ABC family is made up of ABC transporters ranging from ABC A-G (Sodani *et al.*, 2012). Much of this superfamily has been implicated with intrinsic resistance in kidney, lung, liver, colon, rectal and ovarian cancers, while overexpression in response to acquired

cisplatin resistance has been associated with lung, breast and prostate cancers (Holohan *et al.*, 2013).

Specific members of the ABC transporter family namely the ABCB family have been termed Multi-Drug Resistant proteins (MDR). MDR1 has been shown to be responsible for removing a wide variety of anticancer agents from the cell, such as camptothecin, carboplatin, cisplatin, doxorubicin and methotrexate (Katayama, Noguchi and Sugimoto, 2014). MDRs 1, 2, 3, and 5 have specifically been implicated in the resistance towards cisplatin. MDR1 is also capable of pumping out compounds conjugated to glutathione antioxidant peptides, such as glutathione-conjugated chemotherapy agents (Chen and Tiwari, 2011). Other members of the ABC transporter family such as ABCG2 are found to be overexpressed in certain cancer cells such as breast CSCs, potentially contributing to their inherent resistance (Westover and Li, 2015).

Cancer cells may also inactivate chemotherapy drugs via increased expression of antioxidant mechanisms. Platinum compounds such as cisplatin or carboplatin have been demonstrated to have a high affinity towards thiol groups, with many antioxidant defence peptides, enzymes and metallothioneins possessing cysteine rich thiol groups (Wong and Stillman, 2018). As such platinum compounds are subject to antioxidant deactivation by glutathione, glutathione-S-transferase and metallothionein overexpression (De Luca *et al.*, 2019). As noted above, glutathione conjugated compounds are susceptible to efflux from the cell via MDR family proteins. Indeed MDR overexpression has been seen to correlate with significantly enhanced expression of glutathione and antioxidant proteins (Lopes-Rodrigues *et al.*, 2017). Antioxidant defence overexpression can also reduce the cytotoxic potential of

drugs that utilise the generation of reactive oxygen (ROS) or reactive nitrogen (RNS) species (discussed section 1.2.4).

Chemotherapy can promote the survival of cancer cells via selective pressures to increase the number of cancer cells capable of altering the intracellular drug targets. Resistance generating mutations have been seen with the use of topoisomerase inhibitors such as doxorubicin, or human epidermal growth factor receptor 2 inhibitors, such as Herceptin (Cox and Weinman, 2016; Luque-Cabal *et al.*, 2016). Following long term use, resistant cells are selected which carry structural mutations in the targets of these inhibitors or display reduced expression of the drug target to favour an alternate oncogenic pathway. This results in loss of drug target specificity and the development of resistance (Housman *et al.*, 2014).

The initiation of cancer can be a consequence of defective, or epigenetically/genetically silenced DNA repair mechanisms (Lahtz and Pfeifer, 2011). Cancer cells can increase their DNA repair capacity by increasing the expression of DNA repair enzymes (Salehan and Morse, 2013). However, following chemotherapeutic intervention, some cancer cells can induce epigenetic or genetic reversion and re-express DNA repair proteins in order to repair damage from DNA targeting chemotherapy drugs, such as cisplatin (Ashworth, 2008). Genetic reversion of *BRCA1* and *BRCA2* genes has been seen in the development of cisplatin resistant cells, which were originally cisplatin sensitive as a result of *BRCA1/2* silencing (Afghahi *et al.*, 2017). *BRCA1* overexpression has also been documented in cisplatin resistant breast and ovarian carcinoma cell lines (Gorodetska, Kozeretska and Dubrovska, 2019).

The overexpression of Nucleotide Excision Repair (NER) proteins has been associated with reduced sensitivity to cisplatin, as NER is the most efficient DNA repair system to remove cisplatin-DNA adducts and crosslinks. The mismatch repair (MMR) proteins MSH2 and MSH3 can also recognise cisplatin-DNA lesions, which if too numerous can signal apoptotic proteins to kill the cell. Thus inactivation of the MMR machinery (e.g. via mutations) has been seen in cisplatin resistance (Drummond *et al.*, 1996).

Epigenetic alterations promote cancer resistance by facilitating rapid adaptation to cytotoxic agents through dynamic alterations in gene expression (Easwaran. Hariharan, 2014). Epigenetic alterations and cancer resistance are discussed in further detail in Chapter 3.

The TME of solid tumours plays a pivotal role in mediating cisplatin and chemotherapy resistance. Primarily it acts as a physical barrier protecting the tumour initiating cells found at the core of most solid tumour masses (Son *et al.*, 2017). The vasculature surrounding the TME mediated by dysregulated angiogenesis is generally poorly differentiated and truncated in nature, delivering suboptimal concentrations of chemotherapy drugs to the tumour bulk (Narang and Varia, 2011).

Overexpression of HIF family of transcription factors, particularly HIF1α, has also been associated with cisplatin and chemotherapy resistance. HIF1α can induce mitophagy, mitochondrial degradation via autophagy to adapt to hypoxic stress (Zhang *et al.*, 2008). As the mitochondria is essential for the intrinsic apoptotic pathway, reduced mitochondrial presence results in reduced apoptotic capacity of cisplatin (*ibid*.). HIF1α-associated cisplatin resistance has been reported in ovarian and colon cancer (Lv *et al.*, 2015; Bu *et al.*, 2019).

1.2.3. The use of transition metals in anti-cancer treatments:

Metal-based drugs have been essential to chemotherapy since the development of cisplatin as a clinically effective therapeutic and the generation of its platinum analogues carboplatin and oxaliplatin (Garbutcheon-Singh *et al.*, 2011). The prevalence of cisplatin resistance and limited effectiveness of carboplatin and oxaliplatin have led to the development of novel metal-based complexes to bolster current therapies (Johnstone, Park and Lippard, 2014).

Metal complexes offer unique therapeutic potential in cancer therapy as they exhibit many advantageous characteristics, such as redox activity, variable coordination modes and reactivity towards multiple organic substrates. These attributes make metal-based drugs an attractive probe for development of novel compounds targeting specific cellular pathways, such as DNA, mitochondria and cell proliferation pathways (Ndagi, Mhlongo and Soliman, 2017). As metal homeostasis is tightly regulated detrimental effects typically occur upon disruption. As such targeting metal homeostasis using metal-based chemotherapeutics is a lucrative target.

A plethora of potential metal-based drugs have been synthesised over recent decades, many of which show promise as anti-cancer agents and have undergone clinical trials. For a full list of these novel metal compounds see Ndagi, Mhlongo and Soliman, 2017. Compounds utilising redox active transition metals such as iron have gained significant interest. However research into other redox active metals such as copper and manganese has also gained traction (Kellett *et al.*, 2011; Prisecaru *et al.*, 2012; Slator *et al.*, 2017, 2018; Zhang *et al.*, 2017; Rochford, 2018). A full understanding of the current understanding of the potential modes of action of metal-based drugs is only possible in the context of their redox activities.

1.2.4. Cellular redox homeostasis

Reactive Oxygen and Reactive Nitrogen Species (ROS, RNS) are important molecules in both physiological and pathophysiological cell processes (Ortega, Mena and Estrela, 2010). They can come in either free radical or non-radical forms and possess strong oxidising properties or the potential to generate strong oxidant properties. Free radicals are atoms or molecules with a single unpaired electron, which are highly reactive and unstable (Rahman, 2007), and can react with many biomolecules such as proteins, lipids or nucleic acids (Sharma *et al.*, 2012). Free radicals are by-products of cell metabolism in both the normal and disease states, and metabolites of xenobiotic compounds (Ray, Huang and Tsuji, 2012). Organisms utilising oxygen metabolism must, therefore, contend with the potential side effects of reactive radical species. Oxygen itself is a bi-radical and can react with various metal ions and biological molecules resulting in almost certain oxidation (Cadet and Davies, 2017).

Interaction between ROS and biomolecules found within a cell such as DNA, proteins or lipids will result in their oxidation. Such oxidation can alter molecular structure of proteins inhibiting enzymes, compromise cell integrity through lipid peroxidation of cell and organelle membranes, or lead to single or double strand lesions in DNA, potentially leading to deleterious gene mutations (Phaniendra, Jestadi and Periyasamy, 2015). Sophisticated antioxidant defence systems (including both small molecules and enzymes) are employed by cells to maintain redox homeostasis (Basria S.M.N. Mydin and Okekpa, 2019). Oxidative stress is defined as the imbalance of these two systems, resulting in cell damage, death and disease (Betteridge, 2000; Ghosh *et al.*, 2018). Indeed, oxidative stress has been implicated as a driving factor in many diseases such as cancer, diabetes, atherosclerosis, hypertension, and neurological disorders such as Parkinson's disease, dementia, and Alzheimer's disease

(Liguori *et al.*, 2018). The production of such radicals in disease can act as a double-edged sword however, as the utilisation of radical generating compounds as anti-cancer agents has been implemented for many decades (Takeshima, Kuroda and Yumura, 2019).

As noted above, sources of free radicals can be biological, generated as by-products of both normal and abnormal metabolism, immune cell generated, or exogenous agents such as xenobiotic compounds with high oxidising potential (Tiwari, Hasan and Islam, 2013). Cell-based sources of free radicals are predominantly generated by the oxidation of molecular oxygen, generating ROS and or RNS. ROS or RNS can be either radical or non-radical, with non-radical forms still possessing the potential to later form free radicals (Kehrer and Robertson, 2010). During normal cell metabolism, molecular oxygen is used by the Electron Transport Chain (ETC) to generate adenosine triphosphate (ATP), whereby oxygen is reduced into water as the end-point reaction. As the ETC does not operate with 100% efficiency small amounts of electrons can leak out of the chain where it can oxidise oxygen and form ROS (Li *et al.*, 2013). Alongside the ETC, another predominant source of ROS/RNS are the phagocytic immune cells such as neutrophils or macrophages, which generate ROS and RNS as part of a respiratory burst, to eliminate phagocytosed pathogens such as bacteria or virally infected cells (Thomas, 2017).

The forms of ROS produced in the cell that are of interest for this study are hydrogen peroxide (H_2O_2), the hydroxyl radical ($OH^{\bullet}$), the superoxide anion ($O_2^{\bullet-}$), singlet oxygen ($^1O_2$), and the peroxyl radical ($ROO^{\bullet}$) (Tiwari, Hasan and Islam, 2013). The main forms of RNS relevant to this study and are produced intracellularly are nitric oxide ($NO^{\bullet}$) and peroxynitrite ($ONOO^-$) (Adams, Franco and Estevez, 2015).

1.2.5. Hydrogen Peroxide (H_2O_2)

H_2O_2 is a diffusible non-radical form of ROS formed by the spontaneous or enzymatically catalysed dismutation of two $O_2^{\bullet-}$, that is:

$$O_2^{\bullet-} + O_2^{\bullet-} + 2H^+ \rightarrow H_2O_2 + O_2$$

It is considered to be one of the most unreactive ROS species, with little oxidative potential on its own (Valverde *et al.*, 2018). However, its longevity compared to other forms of ROS (milliseconds versus microseconds) and high diffusibility facilitates H_2O_2 to move further through the cell than other, shorter-lived ROS (Bienert, Schjoerring and Jahn, 2006). Critically in the context of metal-based drugs, upon reaction with transition metals such as copper or iron, H_2O_2 can be oxidised into the more reactive $O_2^{\bullet-}$ or the highly reactive $OH^{\bullet}$ species via the Fenton reaction (Sies, 2017):

$$Fe^{2+} + H_2O_2 \rightarrow Fe^{3+} + OH^{\bullet} + OH^-$$

$$OH^{\bullet} + H_2O_2 \rightarrow O_2^{\bullet-} + H^+ + H_2O$$

It is through these secondary processes that H_2O_2 ultimately exerts its cytotoxic effects.

At low physiological levels, H_2O_2 is utilised by the cell as a classical intracellular signalling molecule regulating kinase driven pathways involved in diverse signalling processes, such as cell proliferation (Arnold *et al.*, 2001), differentiation and survival, stem cell renewal (Goudarzi *et al.*, 2018), immune responses (Wittmann *et al.*, 2012), antioxidant defence, and autophagy. During redox signalling, H_2O_2 oxidizes the thiolate anion to sulfenic form (Cys-SOH) causing allosteric changes within the target kinase protein that alters its function (van

Bergen, Roos and De Proft, 2014). The sulfenic form can be subsequently reduced to thiolate anions by disulfide reductases (and other antioxidant proteins) restoring the protein to its original, functional state (Gough and Cotter, 2011; Schieber and Chandel, 2014). H_2O_2 also reversibly oxidises specific cysteine sulfhydryl (SH) groups in certain tyrosine kinases, causing conformational changes and activation of the enzymes (Chadwick *et al.*, 2011). Finally, a number of transcription factors are susceptible to oxidation for either their activation or inactivation, such as NF-κB, AP-1, H1F-1a, p53 and Nrf2 (all activation) and upstream stimulatory factor (USF) (inactivation) (Wang *et al.*, 2018).

In contrast, pathological levels of H_2O_2 and the initiation of oxidative stress have been implicated in the initiation of oncogenesis, due to high levels of mutations associated with DNA damage caused by oxidative injury and the prolonged activation of pro-survival transcription factors (Huang *et al.*, 1999). Furthermore, sustained activation of these pathways is associated with overall tumour cell survival and proliferation, metastasis and angiogenesis, and induction of acquired resistance (Vilema-Enríquez *et al.*, 2016).

1.2.6. Hydroxyl radical

The hydroxyl radical, $OH^{\bullet}$, is formed by the three-electron reduction of molecular oxygen and is the most reactive form of ROS, with reactivity close to the theoretical diffusion rate (10^9–10^{10} $M^{-1}.s^{-1}$). Moreover, it has essentially no target specificity and a lifespan of nanoseconds (Takeda *et al.*, 2017). It is capable of severing the sugar-phosphate backbone of DNA or RNA, causing significant increases in oxidised nucleotide bases (Dizdaroglu and Jaruga, 2012), as well as oxidising amino acids significantly altering the function of proteins (Liu *et al.*, 2017). However, the high reactivity of $OH^{\bullet}$ limits its damaging potential to within 50 molecular diameters, as a consequence of its high reactivity and thus short lifespan

(Lipinski, 2011). Due to its highly toxic nature, the $OH^{\bullet}$ is not believed to play any part in normal cell processes.

$OH^{\bullet}$ may be formed via the Fenton reaction, where H_2O_2 reacts with redox active metals such as Cu^{2+} of Fe^{2+}, producing $OH^{\bullet}$(Pham *et al.*, 2013):

$$H_2O_2 + Cu^{+}/Fe^{2+} \rightarrow OH^{\bullet} + OH^{-} + Cu^{2+}/Fe^{3+}$$

In addition, the Haber Weiβ reaction may produce $OH^{\bullet}$, via reaction of H_2O_2 with $O_2^{\bullet-}$ (Kanti Das, Wati and Fatima-Shad, 2014):

$$H_2O_2 + O_2^{\bullet-} \rightarrow OH^{\bullet} + OH^{-} + O_2$$

1.2.7. Superoxide $O_2^{\bullet-}$ radical

The $O_2^{\bullet-}$ radical is formed through the donation of a single electron to oxygen (Hayyan, Hashim and Alnashef, 2016):

$$O_2 + e^{-} \rightarrow O_2^{\bullet-}.$$

While slightly more reactive than H_2O_2 it is not considered as a strong oxidant in its own right and generally interacts with molecules close to its source of origin (Clément and Pervaiz, 2001). Although it is poorly diffusible through the plasma membrane, it can pass through via ion and chloride channels (Ramírez *et al.*, 2016).

Within the cell $O_2^{\bullet-}$ is produced as a by-product of metabolism and by specific enzymes including ETC transport chain complexes (ATP synthesis) (Murphy, 2009), xanthine oxidases (purine catabolism) (Lee *et al.*, 2014), lipoxygenases (lipid metabolism) (Zuo *et*

al., 2004), cyclooxygenases (prostaglandin synthesis) (Gao *et al.*, 2014) and NADPH oxidases (immune cell respiratory bursts) (Panday *et al.*, 2015). $O_2^{\bullet-}$ generally exerts its intracellular cytotoxic effects by dismutation into H_2O_2 via auto-dismutation or a result of Superoxide Dismutase (SOD) enzymes, where both Fenton and Haber Weiβ chemistry may produce the more reactive $OH^{\bullet}$ (Collin, 2019). $O_2^{\bullet-}$ plays a major role in phagocytic respiratory bursts and has been seen to play a role in epigenetic post-translational modifications such as DNA methylation, and histone methylation and acetylation (reviewed by Afanas'ev, 2015; Wang *et al.*, 2018). It has also been identified as the main ROS involved in the regulation of autophagy (Chen, Azad and Gibson, 2009).

1.2.8. Singlet oxygen ($^1O_2$)

Singlet oxygen ($^1O_2$) is a highly reactive and electrophilic non-radical form of ROS and is the electronically excited state of molecular oxygen (Agnez-Lima *et al.*, 2012). It possesses no unpaired electrons leaving an empty orbital to allow reaction with other molecules and has a half-life of in water of 1μs. This, however, may drop down to as low as 100ns in biological systems as a result of its ability to react with most biomolecules (Kalyanaraman, 2013). Sources of $^1O_2$ include ultraviolet radiation, endogenous enzymes (i.e. those involved in immunity or metabolic processes) or via chemical cascades secondary to the reaction of hydroperoxides and other forms of ROS with each other and/or other biomolecules (Agnez-Lima *et al.*, 2012; Kalyanaraman, 2013; Onyango, 2016; You, 2018).

UVA radiation can excite photosensitising compounds, such as porphyrins, vitamins, bilirubin, flavins, melanin and melanin precursors (found in skin), which can transfer energy to triplet oxygen ($^3O_2$) generating $^1O_2$ (Baier *et al.*, 2007; Knak *et al.*, 2014). This form of $^1O_2$ generation is exploited in Photodynamic Therapy (PDT), a combination of both chemo

and radiotherapy used in the treatment of certain cancers, such as oesophageal and non-small cell lung cancer.

The core enzymatic source of $^1O_2$ is in relation to bactericidal respiratory bursts in phagocytic cells such as neutrophils, eosinophils or macrophages (Nishinaka *et al.*, 2011). This is mediated by the enzyme myeloperoxidase (MPO) which catalyses the formation of hypochlorous acid (HOCl) from H_2O_2 (Figure 1.4 scheme 1). This in turn reacts with the hydrogen peroxide anion (HO_2^-), producing $^1O_2$ (Figure 1.4 scheme 2) (Onyango, 2016).

$^1O_2$ may also be produced as a by-product of the spontaneous dismutation of superoxide into hydrogen peroxide and the reaction of nitric oxide with superoxide or H_2O_2 (Figure 1.4, schemes 3-6) (Onyango, 2016, Agnez-Lima *et al.*, 2012).

$$H_2O_2 + Cl^- + H^+ \longrightarrow HOCl + H_2O \quad (1)$$

$$HOCl + HO_2^- \longrightarrow H_2O + Cl^- + {}^1O_2 \quad (2)$$

$$^{\bullet-}O_2 + {}^{\bullet-}O_2 + 2H^+ \longrightarrow {}^1O_2 + H_2O_2 \quad (3)$$

$$^{\bullet-}O_2 + NO^{\bullet} \longrightarrow ONOO^- \quad (4)$$

$$ONOO^- + H_2O_2 \longrightarrow ONO^- + H_2O + {}^1O_2 \quad (5)$$

$$^{\bullet-}O_2 + H_2O_2 \longrightarrow {}^1O_2 + HO^{\bullet} + HO^- \quad (6)$$

Figure 1.4-Schematic of $^1O_2$ generation from other sources of ROS or RNS (adopted from Onyango, 2016).

1.2.9. Nitric oxide ($NO^{\bullet}$)

RNS are nitrogen centred oxidants capable of both oxidising and nitrosylating the same biomolecules as oxygen centred radicals (Ozcan and Ogun, 2015). Despite its status as a free

radical gas, $NO^{\bullet}$ is an important intracellular second messenger molecule that activates the soluble guanylyl cyclase (sGC) at nanomolar concentrations and is a key modulator of smooth muscle relaxation (Adams, Franco and Estevez, 2015). It is generated by specific nitric oxide synthases (NOS)s which convert L-arginine to L-citrulline (Figure 1.5) (Phaniendra, Jestadi and Periyasamy, 2015), consisting of three isoforms: neuronal, endothelial and inducible NOS (Förstermann and Sessa, 2012).

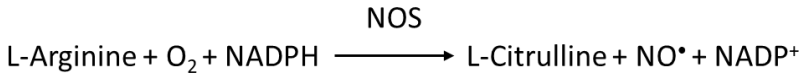

Figure 1.5- Synthesis of Nitric oxide

$NO^{\bullet}$ is both aqueous and lipid soluble and readily diffuses through the cytoplasm and across cell membranes. The estimated biological half-life and diffusion distances are on the order of 1–10 sec and 50–1,000 μm, respectively (Radi, 2018).

$NO^{\bullet}$ shares many similarities with $O_2^{\bullet-}$. High concentrations of $NO^{\bullet}$ are generated as part of the immune response in phagocytic immune cells and is free radical but is not particularly reactive on its own. Like $O_2^{\bullet-}$, it usually exerts its cytotoxic effects through generating more reactive intermediates, such as the peroxynitrite anion, which is utilised alongside H_2O_2 and $OH^{\bullet}$ to execute its bactericidal properties (Habib and Ali, 2011).

1.2.10. Peroxynitrite ($OONO^-$)

Peroxynitrite ($OONO^-$) is a highly toxic cellular oxidant with a half-life of ≈ 10 ms. It can cause direct protein oxidation, forming amino acid/nitrogen products such as nitrotyrosine and can initiate conformational changes in protein structure, thus inhibiting protein function

(Radi, 2018). DNA base oxidation and single strand breaks have also been attributed to $OONO^-$, and are thought to be a result of the generation of a "hydroxyl radical-like" oxidant ($ONOOH^\bullet$) (Kennedy *et al.*, 1997; Ozcan and Ogun, 2015). $OONO^-$ can form other highly toxic radicals as well as $ONOOH^\bullet$, resulting from its own decomposition. Decomposition can happen spontaneously and can produce the nitrogen dioxide radical ($NO_2^\bullet$) which is capable of further initiation of lipid peroxidation and nitrosylation of amino acids (Depayras *et al.*, 2018).

As it is capable of crossing cell membranes, it can exert an influence on surrounding cells within 1-2 cell diameters from its site of origin. $OONO^-$ thus appears to be an important tissue-damaging species generated at the sites of inflammation (Pacheco-Yepez *et al.*, 2014). It has been shown to be involved in various neurodegenerative disorders and several kidney diseases (Seija *et al.*, 2012; Yuste *et al.*, 2015).

1.2.11. Iron homeostasis and applications in cancer therapy

Iron is an essential trace element required for many cellular redox-dependent signalling pathways, such as oxygen transport, DNA synthesis and repair, lipid metabolism, oxidative phosphorylation and ROS signalling. Iron is highly redox active and can exist in ferrous (Fe^{2+}) or ferric (Fe^{3+}) oxidation states. The oxidation of Fe^{2+} to Fe^{3+} is capable of generating ROS, as such free state Fe^{2+} can be highly cytotoxic resulting in uncontrolled production of ROS through Fenton like chemistry and Haber Weiβ reactions (Kanti Das, Wati and Fatima-Shad, 2014). As such, iron metabolism is tightly controlled to maintain bodily and cellular homeostasis through the sequestration of iron to carrier proteins such as haem or transferrin, or in iron sulfur clusters (ISCs) (reviewed by Camaschella and Pagani, 2018).

Iron is absorbed through enterocytes in the small intestine. Once inside enterocytes iron is bound by ferritin, the iron storage protein. Ferritin stores iron in the ferric form and can store 4,500 iron atoms bound to oxygen. Ferritin can act as both an iron carrier and an intracellular source of bioavailable iron (Chiou and Connor, 2018).

Once it has been imported and bound to ferritin, iron may be transported to metabolic enzymes where it acts as an essential co-factor, such as lipoxygenases involved in lipid metabolism and heme dependent enzymes such as catalases and peroxidases (Poulos, 2014) Iron can also be sequestered in the mitochondria for haem synthesis or storage (Andreini *et al.*, 2018). The mitochondria has its own form of ferritin, known as mitochondrial ferritin, and is thought to play a protective role to deal with iron overload (Rouault, 2016). Iron can also be incorporated into ISCs in the mitochondria to be used as co-factors in iron metabolic signalling (Rouault, 2012). Iron can also be exported into the blood stream where it binds an iron transport protein called apo-transferrin forming transferrin. Approximately 75% of transferrin bound iron is transported to the bone marrow to facilitate erythropoiesis and the synthesis of haemoglobin in red blood cells (Silva and Faustino, 2015).

Iron may also exist in what are termed labile iron pools, poorly defined non-protein bound and redox active intracellular iron. The exact function of these labile iron pools is unclear. It is thought to exist as a form of readily available and exchangeable iron and is mediated by both antioxidant defence systems and protein carriers such as ferritin. However, during oxidative stress or periods of iron overload the iron buffering capacity of the cell may become overwhelmed and labile iron pools may propagate oxidative stress (reviewed Cabantchik, 2014). A form of iron and lipid mediated necrotic cell death is known as

Ferroptosis, which involves the accumulation of toxic lipid and phospholipid peroxides leading to necrotic cell death. This is discussed in detail in Chapter 5.

Due to its significant role cell signalling and maintaining cell homeostasis, iron has been implicated in tumour progression by metastasis. Tumour cells physiologically alter DNA synthetic and repair mechanisms, cell cycle regulation, and epigenetic remodelling, as well as facilitating metastasis and angiogenesis through dysregulated iron metabolism (Yafang Wang *et al.*, 2018). As such tumour cells have increased iron metabolic pathways such as pathways responsible for iron import, storage and export in order to fuel metabolic iron demands of proliferating and metastasising cells (Jung *et al.*, 2019). Iron has been recognised as an important target for chemotherapeutic intervention. Bleomycin, an antibiotic repurposed as an anti-cancer agent, is an example of a frontline chemotherapeutic which utilises iron chelation and the generation of ROS to exert anti-cancer effects (Reinert *et al.*, 2013).

Iron based chemotherapeutic strategies utilise iron chelation therapy or treatment using iron based ionophores. Several iron chelative drugs have been developed (Derasirox and Desferal®) and have entered clinical trials, however poor pharmacokinetics and serious off target side effects have severely limited their development into clinically effective drugs (Bedford *et al.*, 2013). However some progress has been made using combinatorial treatments with current chemotherapy drugs such as cisplatin, carboplatin, or doxorubicin, decreasing adverse side effects while supressing tumour growth (see references 182 and 183 Wang *et al.*, 2018).

Iron complex ionophores have also demonstrated promise as anti-cancer agents. Iron complex anti-cancer activity was first demonstrated using ferrocenium picrate and ferrocenium trichloroacetate, with cytotoxicity attributed to formation of ROS and oxidative DNA damage (Köpf-Maier, Köpf and Neuse, 1984). Research into the synthesis and development of novel iron anti-complexes as anti-cancer agents has therefore gained interest. Multinuclear complexes with variable side chains and derivatives have been designed with the aim of potentially enhancing the anti-cancer effects and increasing cancer cell specificity (reviewed Wani et al., 2016).

1.2.12. Copper homeostasis and applications in cancer therapy

Copper (Cu) is an essential trace element within the body, which plays significant roles in multiple cellular pathways (Lutsenko, 2010). As a transition metal, Cu is an essential co-factor in many redox dependant pathways, such as antioxidant defence (Cu-Zn Superoxide Dismutase), iron metabolism and transport (Ceruloplasmin), respiratory pathways (cytochrome-c oxidase, methionine synthase) and connective tissue synthesis (lysyl oxidase) (Hilton *et al.*, 2018).

Cu is highly redox active, shifting between cuprous (Cu^{+}) and cupric (Cu^{2+}) valence states facilitating its redox activity, with Cu^{2+} the most biologically relevant state. In similarity with iron, redox capabilities of Cu make it essential for life but also renders it potentially toxic. Dysregulation of Cu homeostasis has been associated with heart, liver and CNS dysfunction, as well as in inflammation, cancer and resistance to chemotherapy. As such Cu activity and availability is tightly regulated in the body (reviewed by Gaetke, Chow-Johnson, & Chow, 2014).

Cancer cells have been seen to possess elevated levels of copper, which has been seen to contribute to increased cell survival, proliferation, angiogenesis, metastasis and chemotherapy resistance, particularly in platinum-based therapies (Wang *et al.*, 2010). Patients with resistant breast, lung or colon cancers demonstrated serum copper levels of 130-160% of normal (Majumder *et al.*, 2009). As such, the potential of copper-based therapies has gained much attention in recent years. Copper can be used to target cancer cells either through the use of copper chelators to reduced essential copper levels mediating proliferative, angiogenic or metastatic processes, or through the use of copper complex ionophores (Helsel and Franz, 2015). Limited success has been reported with the implementation of copper chelators as anti-cancer agents, with cytostatic mechanisms more prevalent than cytotoxic ones. Copper chelators (such as disulfiram and trientine) have therefore been recommended to be used as a strategy to inhibit the progression of copper dependent angiogenesis and metastatic processes (reviewed by Lopez, Ramchandani, & Vahdat, 2019).

The use of copper complex ionophores has therefore seen the most promise as cytotoxic anti-cancer agents, as the high levels of copper associated with cancer signalling and resistance could predispose cancer cells to copper overload (Denoyer *et al.*, 2015). The ability of copper to bind to DNA, inducing conformational change and DNA damage indicates the chemotherapeutic potential of copper (Govindaraju *et al.*, 2013). The primary mechanisms of copper induced anti-cancer cytotoxicity documented to date are DNA interactions, ROS production, mitochondrial dysfunction, proteasome inhibition and induction of apoptosis (Denoyer *et al.*, 2015; McGivern, Afsharpour and Marmion, 2018).

Utilising copper as an anti-cancer agent may also impact iron regulation. Many regulatory proteins controlling copper (e.g. Ceruloplasmin) also regulate iron, while copper has been seen to regulate the iron sensing hormone Hepcidin (Gulec and Collins, 2014). Studies into patients suffering from Wilson's disease, a genetic disease-causing toxic accumulation of copper in the vital organs, demonstrated that patients also experience iron overload (Shiono *et al.*, 2001). As such targeting copper homeostasis in cancer cells may further disturb iron regulation increasing cytotoxic capabilities and there is likely a complex interplay between different metals under in vivo conditions.

1.2.13. Manganese homeostasis and applications in cancer therapy

Manganese, also an essential trace metal, plays a similar critical role to copper as an essential redox active co-factor to multiple cell pathways, such as mitochondrial antioxidant defence, and the metabolism of lipids, carbohydrates and amino acids to name a few (Li and Yang, 2018). Manganese has 11 potential oxidation states, ranging from Mn^{-3} to Mn^{7+}, Mn^{7+} having the highest oxidative potential, however biologically relevant oxidation states of manganese are Mn^{2+} and Mn^{3+} (O'Neal and Zheng, 2015).

Manganese shares many chemical and structural similarities with iron, sharing identical biological oxidation states, and both being transferred throughout the body bound to transferrin in the Mn^{3+} oxidation state, with Mn^{2+} primarily transported by albumin (Martinez-Finley *et al.*, 2013; Smith *et al.*, 2017). While both share redox capabilities, manganese is not thought to undergo ROS generating Fenton reactions seen in reactions involving copper or iron, as a result of its high reduction potential (Aguirre and Culotta, 2012). Manganese transport is inversely related to iron storage implying coregulatory mechanisms of each divalent cation (DeWitt, Chen and Aschner, 2013).

Intracellular manganese is found mostly in the Mn^{2+} state, where it is primarily located in the mitochondria and the nucleus (O'Neal and Zheng, 2015). The mitochondria is generally seen as the main target for manganese uptake where mitochondrial manganese is generally incorporated into Superoxide Dismutase 2 (SOD2), also known as Mn-SOD. SOD2 is a highly conserved antioxidant enzyme tasked with detoxifying superoxide anions into hydrogen peroxide as part of its antioxidant and cytoprotective role (Azadmanesh and Borgstahl, 2018). High levels of manganese have been seen to be cytotoxic, and mainly targets the brain and liver causing severe dysfunction (Harischandra *et al.*, 2019).

As the primary target of intracellular manganese is the mitochondria, Mn^{2+} mediated toxicity has been demonstrated to inactivate mitochondrial complexes I, II, III and IV, causing severe disruption to the electron transport chain and the Krebs cycle (Harischandra *et al.*, 2019). It has also been shown to increase mitochondrial superoxide, hydrogen peroxide and ROS production, further exacerbating mitochondrial dysfunction and decreasing mitochondrial membrane potential (*ibid*). The main species of manganese responsible for cytotoxicity is Mn^{2+}. While Mn^{3+} is a significantly stronger oxidising agent, it is not as readily soluble in aqueous solution as Mn^{2+}, and disproportionates into Mn^{2+} in the presence of oxygen (reviewed by Gunter, 2017). However, Mn^{3+} is the oxidation state present in SOD2 (Azadmanesh and Borgstahl, 2018).

The cytotoxic potential of Mn^{2+} has been further implicated via effects on calcium homeostasis, glutathione depletion and impairment of antioxidant processes, and oxidative stress, culminating in the activation of apoptosis and cell death (reviewed by Smith *et al.*, 2017). Mn^{2+} disrupts calcium homeostasis as it shares spherical symmetry with Ca^{2+}, and so

is capable of binding and substituting multiple Ca^{2+} binding sites involved in many biologically processes such as ATP production (see references 160 and 161 in Martinez-Finley *et al.*, 2013). Mn^{2+} can also competitively bind to Mg^{2+} and Fe^{2+} binding sites, further disrupting metal ion mediated signalling and enzymatic processes (Gunter, 2017).

In addition, manganese has been demonstrated to bind both DNA and RNA and has also been seen bound to ribosomes, resulting in disruption of transcription and translation (see references 149 and 150 Smith *et al*., 2017). The disruption of these process could result in endoplasmic reticulum (ER) stress, which can further activate apoptosis. Indeed it has been shown that manganese can trigger ER stress but it is not yet known if this directly results in ER stress mediated apoptosis or through other manganese-dependent activities (Seo, Li and Wessling-Resnick, 2013; Smith *et al.*, 2017). Stephenson *et al*., (2013) demonstrated Mn^{2+} could induce oxidative DNA damage and single strand breaks in SH-SY5Y neuroblastoma cells, a process which was attenuated by Glutathione (GSH) and N-acetyl cysteine antioxidant molecules, indicating this Mn^{2+} dependent nuclease mimetic activity was mediated by ROS. Apoptosis was confirmed as the mechanism of cell death (Stephenson *et al.*, 2013).

Despite many studies implicating manganese in DNA damage and the induction of oxidative stress, it is generally considered to have a low mutagenic or carcinogenic potential compared with other redox active metals such as copper or iron. There is no clear evidence of a link between manganese exposure and cancer (Gerber, Léonard and Hantson, 2002; Assem, Holmes and Levy, 2011; Zhang *et al.*, 2014). However, manganese associated toxicity may be a useful tool to harness in the fight against cancer. Stephenson *et al*., (2013) demonstrated the cytotoxic mechanism of manganese in neuroblastoma cells. These data were supported

by later observations made by Hernroth and collaborators which demonstrated similar apoptotic mechanisms in three different prostate cancer cells (PC3, DU145 and LNCaP) exposed to manganese (Hernroth *et al.*, 2018). This demonstrates the potential of ROS mediated, manganese dependent nuclease mimetic activity as a novel anti-cancer strategy.

1.2.14. Current and novel metal-based drugs as chemotherapeutic agents

Many novel compounds utilising many different metal ions have been developed over the last few decades (e.g. gold, silver, copper, manganese and ruthenium), with some showing potent DNA binding and anti-cancer activity (Deegan *et al.*, 2007; Tan *et al.*, 2010; Ndagi, Mhlongo and Soliman, 2017). While many variations of compounds containing these metals have been investigated, of note are compounds possessing 1,10-phenanthroline (1,10-Phen) or its derivatives as ligands.

1,10-Phen is a polycyclic aromatic hydrocarbon used for its strong chelative properties in both industrial and therapeutic synthetic processes (Natarajan, 2018). 1,10-phen has many properties which make it useful in synthetic and coordinate chemistry, including rigidity, planarity, aromaticity, basicity and the ability to chelate a variety of different metals (Accorsi *et al.*, 2009). These properties provide great versatility in binding with metal ions, allowing the synthesis of a broad range of metal-phenanthroline based compounds (Bencini and Lippolis, 2010; Bonacorso *et al.*, 2015). Echoing the discovery of cisplatin, therapeutic 1,10-Phen and associated chelates were first noted for their bacteriostatic and bactericidal proprieties (Butler *et al.*, 1969; Dwyer *et al.*, 1969).

As a result of its planar structure (Figure 1.6) 1,10-phen is an avid intercalator of DNA capable of strong DNA groove binding (Accorsi *et al.*, 2009). This ability to intercalate with

DNA coupled with its strong chelative properties are generally considered to be the key drivers of the strong cytotoxic effects against bacterial, fungal and mammalian cells seen to date (Sammes and Yahioglu, 1994; McCann *et al*., 2012). These properties of 1,10-Phen give it the potential to inhibit many other biological pathways, such as intermediate metabolism (Carver et al., 1988), transcription (Grigull et al., 2004), and a variety of metallo-enzyme dependent pathways (Abebe et al., 2018). 1,10-Phen has also been seen to sequester essential trace metals such as zinc or redox active copper or iron further adding the its cytotoxic potential (McCann et al., 2012; Viganon et al., 2017).

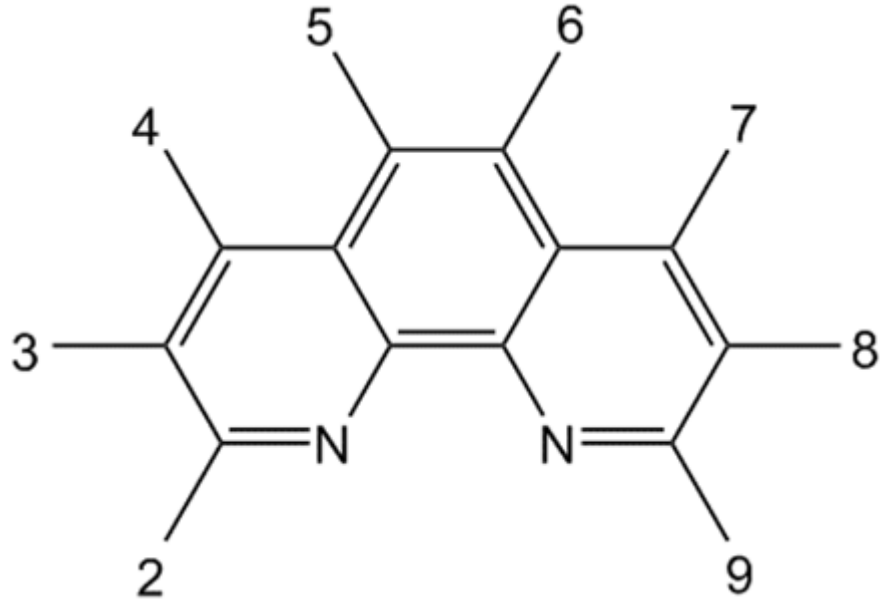

Figure 1.6 - Chemical structure of 1,10-phenanthroline with 2-9 representing numbering for substituents for coordination with other compounds (Viganor *et al.*, 2017).

Following the initial discovery of antimicrobial capabilities of 1,10-Phen, copper based phenanthroline compounds were discovered to possess synthetic chemical nuclease capabilities via oxidative cleavage of the deoxyribose sugar backbone (Sigman *et al.*, 1979). This discovery has sparked massive interest in synthesising and developing novel artificial metallo nucleases (McGivern, Afsharpour and Marmion, 2018), with copper based

phenanthroline chelates the most extensively studied to date (Kuwabara *et al.*, 1986; Murakawa *et al.*, 1989; Pitié, Boldron and Pratviel, 2006; Roy *et al.*, 2008; Anbu *et al.*, 2013; Molphy *et al.*, 2015). DNase mimetic activity is therefore considered a primary mechanism for both copper and metal-based phenanthroline compounds, and has been seen to operate via oxidative scission of deoxyribose residues or hydrolysis of the phosphodiester sugar backbone (Bonacorso *et al.*, 2015; Molphy *et al.*, 2015). Indeed, the DNase mimetic capabilities of Cu-phenanthroline based compounds can be used as a tool for DNA foot printing studies (Papavassiliou, 1995).

The use of 1,10-Phen may also further facilitate the uptake of metal-based drugs into cancer cells. Zhang *et al*., (2013) demonstrated that the uptake of 1,10-Phen ternary copper complexes into cancer cells was facilitated by the presence of 1,10-Phen compared to free copper, and that the increased Cu-Phen concentration was capable of potent proteasome inhibition and apoptosis induction in breast cancer cells. The observation of proteasome inhibition by copper-phen compounds has been further supported by recent work from Zhang *et al.* (2017).

While much attention has been given to copper-phen compounds, manganese based phenanthroline drugs have also been developed alongside copper-phen compounds demonstrating comparable potency (McCann *et al.*, 1997; Kellett *et al.*, 2011; Gandra *et al.*, 2017; Slator *et al.*, 2017). Eskandari & Suntharalingam (2019) demonstrated a Mn-Phen compound to possess significantly greater potency towards breast CSCs than cisplatin or a structurally similar Cu-Phen compound. The Mn-phen compounds was seen to produce significantly higher intracellular ROS than that of the copper-phen compound, with ROS

generation speculated to be the key cytotoxic mechanism in play (Eskandari and Suntharalingam, 2019).

A number of such derivatives, based on copper, manganese and silver have been synthesised and characterised as part of ongoing medicinal chemistry research at Technological University Dublin (Thornton *et al.*, 2016; Gandra *et al.*, 2017; Rochford, 2018). In recent years, compounds which contain multiple 1,10-phenanthroline moieties and organic carboxylic acids of various lengths have been developed. Many of these compounds, in line with previous generations, display strong DNA binding affinities, cancer cell cytotoxicity, the ability to induce reactive oxygen species (ROS) and thus oxidative stress (Kellett *et al.*, 2011).

Kellet *et al*. (2011) investigated the cytotoxicity, DNA binding/cleavage capacity, and capacity for reactive oxygen species generation of the binuclear, water soluble Cu^{2+} and Mn^{2+} bis-phenanthroline octanedioate compounds – $[Cu_2(\mu_2\text{-oda})(phen)_4](ClO_4)_2$ and $\{[Mn_2(\mu_2\text{-oda})(phen)_4(oda)_2]^{2-}[Mn2(\mu_2\text{-oda})(phen)_4(H_2O)_2]^{2+}\}$, hereafter CMPD22 and CMPD19, respectively. Both complexes displayed high affinity for binding DNA and were shown to be capable of relaxing supercoiled plasmid DNA under *in vitro* conditions. CMPD22 was also capable of DNA cleavage in the absence of O_2 and an added reductant (ascorbate), in contrast to CMPD19. In addition, CMPD22 was capable of double strand scission of plasmid DNA whereas CMPD19 was not. In studies with *in vitro* cell systems, both complexes exhibited cytotoxic properties greater than cisplatin and metal-free 1,10-phenanthroline in colorectal cancer cell lines but were significantly less toxic towards a non-cancerous HaCaT keratinocyte line. ROS production was tested using 2',7'-dichlorofluorescin diacetate (DCFDA) which demonstrated CMPD19 to be a robust ROS

generator (>25-fold increase in ROS production) at concentrations of 0.25-1 μM in HT29 colorectal cancer cells. CMPD22 displayed little activity in comparison to CMPD 19 and metal-free 1,10-Phen (Kellett *et al.*, 2011).

The mimetic SOD-like activity (dismutation of superoxide anion into hydrogen peroxide) and mimetic catalase activity (breakdown of hydrogen peroxide into H_2O and O_2) were also investigated. As noted above, SOD and catalase like activity are important catalytic reactions for the cleavage of the DNA phosphodiester backbone, as both superoxide and hydrogen peroxide (H_2O_2) can play an important role in hydroxyl radical formation via Fenton like redox chemistry involving copper and iron (Pham *et al.*, 2013). Both complexes show potent mimetic SOD activity when exposed to superoxide anions, with CMPD 19 appearing to possess exceptional activity (Kellett *et al.*, 2011). However, CMPD 19 was the only compound to display catalase like activity. CMPD 19 was further tested by (Slator *et al.*, 2017), and was found to induce autophagic cell death, apparently utilising mitochondrial superoxide generation as a key autophagic regulator to induce the intrinsic apoptotic pathway in the later stages of cytotoxicity. Double stranded breaks in cellular DNA were also detected via γH2AX and COMET assays. However, the authors attributed this damage to be a product of the natural increase in ROS production associated with both autophagic and intrinsic apoptotic cell death, as opposed to direct DNA damage caused by the compound itself.

While these compounds have seen preliminary successes, optimisation of efficacy and properties (e.g. solubility, selectivity) are required. Recently a new series of 1,10-Phen based compounds containing copper or manganese at their cores and with trioxaundecanedioic acid rather than octanedioic acid (Figure 1.7.).

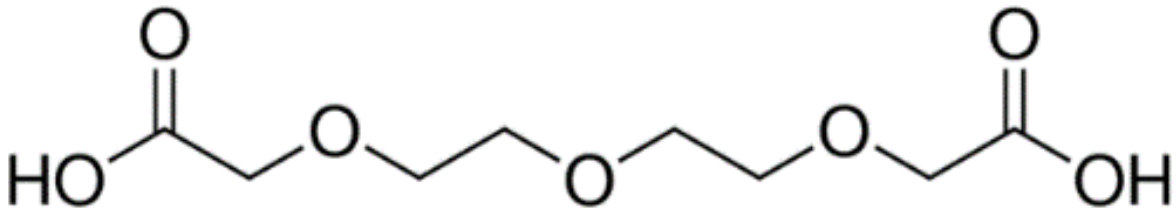

Figure 1.7- Chemical structure of trioxaundecanedioic acid

Trioxaundecanedioic acid contains three ethereal oxygens, theoretically increasing the possibilities for interaction with water leading to an anticipated enhancement of water solubility of the overall complex (McCann et al., 1997; Bartos, Hudecz and Uray, 2009). The chemical structures of Mn (CMPD 73) and Cu (CMPD 74) containing trioxaundecanedioic acid dicarboxylic acids can be seen in Figure 1.8. These compounds are analogues of CMPD19 and 22 respectively and have demonstrated potential antifungal capabilities and mammalian cell cytotoxicity to date (Gandra *et al.*, 2017).

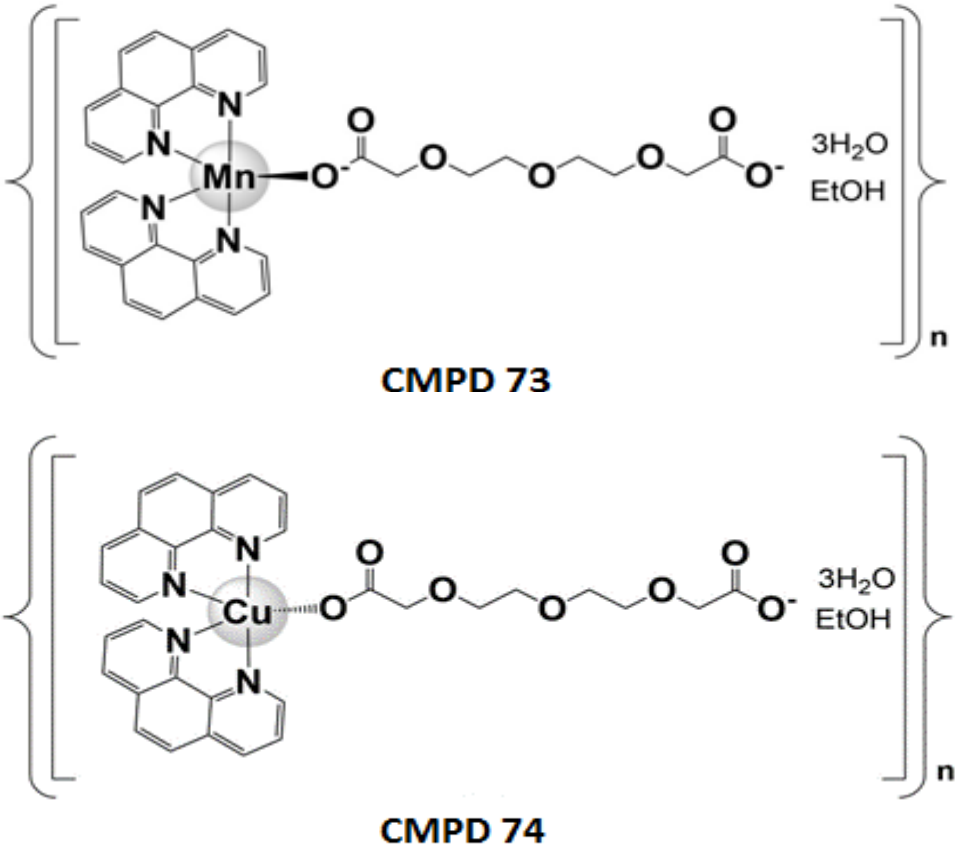

Figure 1.8- Chemical structures of CMPD 73 and 74

However, there is currently very limited data available about potential anti-cancer activity of these compounds. Both novel compounds would be expected to share many biochemical properties with compounds based on an octanedioate linked compound, i.e. ROS generation, DNA intercalation, DNA cleavage capabilities.

1.3.Hypothesis:

If novel metal-TDDA-phenanthroline compounds possess biological activities which lead to cell death, then characterisation of these activities will lead to identification of strategies to rationally enhance their activities for potential therapeutic benefit.

1.4.Aims

The general cytotoxic capacity of metal-based phenanthroline compounds is well known. The biological characteristics (e.g. cytotoxic action) or mechanism(s) of action (e.g. nucleic acid cleavage) of the novel compounds under study here are not yet known. The broad aim of this thesis is to characterise the biological action(s) of these novel compounds with a view towards identifying approaches to maximise their cytotoxic activity and revealing underlying mechanisms of action.

The specific objectives are:

-To characterise the baseline cytotoxic capacity of the compounds (Chapter 2)

-To determine if DNA compaction plays a key role compound activity (Chapter 3)

-To define the role of ROS generation in mediating the activity of the compounds (Chapter 4)

-To clarify if these compounds induce iron-mediated cell death (i.e. ferroptosis) (Chapter 5)

-To define the capacity of these compounds to cleave nucleic acids, both DNA and RNA (Chapter 6)

-To define the capacity of these compounds to induce ER stress and interact with the Unfolded Protein Response (Chapter 7)

Taken together these objectives will enable the realisation of the overall aim and identify both approaches to maximise activity as well as revealing the mechanistic basis for their action.

2. Evaluation of the cytotoxicity profiles of novel compounds

2.1. Introduction

Cytotoxicity is the quality of an agent to be toxic towards the cell. Cytotoxicity can present in many different forms, with two of the most characterised being apoptotic cell death and necrotic cell death. These differ in how they are regulated and their effects on surrounding cells and their physiological roles. Apoptosis is a highly regulated process with minimal collateral damage to the surrounding area. In contrast, necrosis has minimal regulation and causes high collateral damage to cells in the surrounding area (D'Arcy, 2019). However, despite these stark differences, crosstalk between the two pathways does exist, as will be discussed.

2.1.1. Apoptosis:

Apoptosis is a naturally occurring process involved in development and maintenance of cellular homeostasis (Gavrilescu and Denkers, 2003). Apoptosis removes old cells and cells that are stressed or injured. Apoptosis is regulated by the delicate balance of pro and anti-apoptotic signals, capable of responding to different stimuli, whereupon a threshold of pro-apoptotic signals must be reached in order to overcome anti-apoptotic pathways (reviewed Singh, Letai, & Sarosiek, 2019).

Morphological changes initiated by apoptosis are cell shrinkage where the cytoplasm and cell organelles are tightly condensed and pyknosis where chromatin becomes highly condensed and disintegration of the nuclear membrane occurs. Apoptotic cells appear round with dense nuclear fragmentation when observed microscopically (Saraste, 2000). Early and advanced apoptotic cells can be seen in Figure 2.1, taken from Balvan *et al.*, (2015).

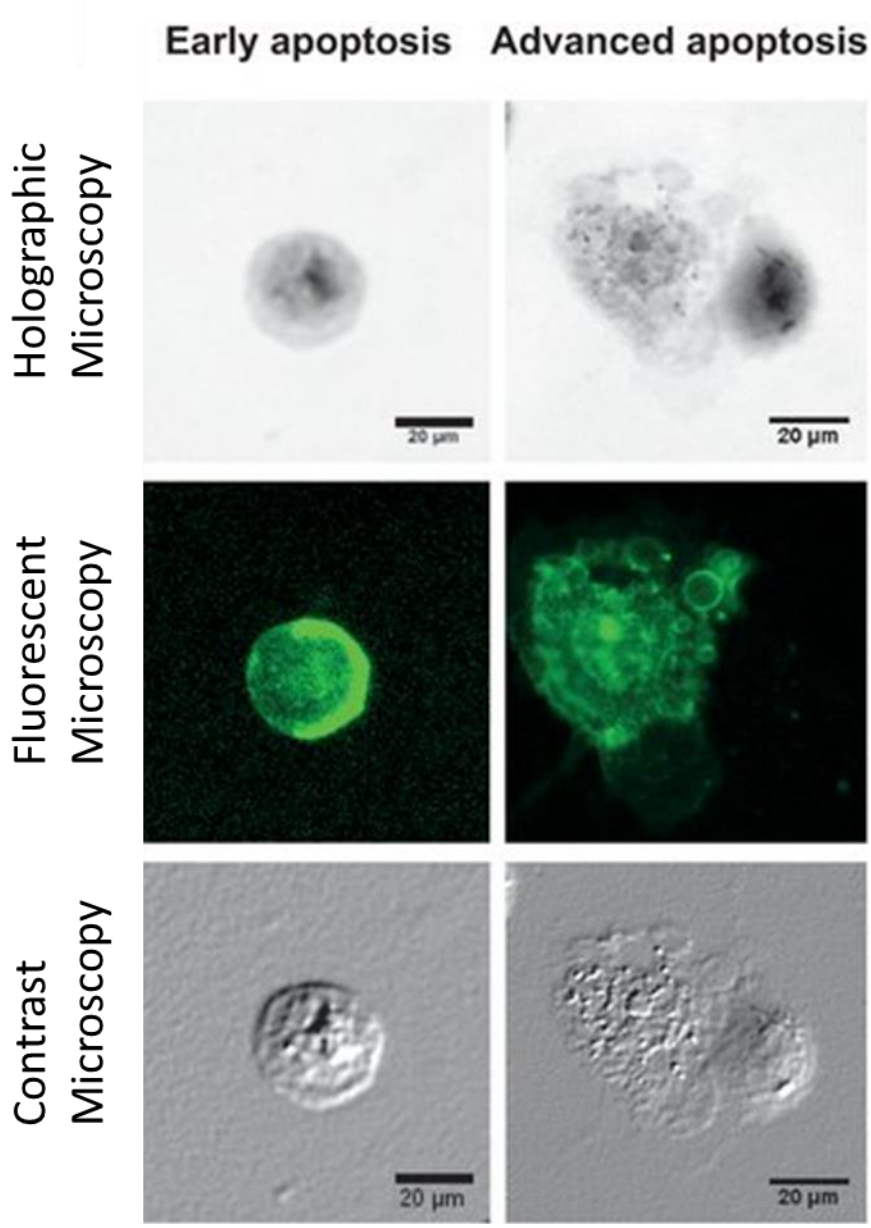

Figure 2.1-Characteristic apoptotic cells as seen under holographic, fluorescent (using AnnexinV PI staining) and contrast microscopy. Early stage apoptotic cells appear as typically round-shaped cells, which undergo extensive membrane blebbing and compartmentalisation into apoptotic bodies (Balvan *et al.*, 2015).

Extensive membrane blebbing results in the separation of cell fragments and the formation of small apoptotic bodies, which are then engulfed by phagocytic cells, with little to no inflammatory response initiated (reviewed by Elmore, 2007). The compartmentalisation of cell organelles protects surrounding cells from the release of potentially toxic metabolic

intermediates or degradative enzymes involved in intracellular recycling, such as proteasomal or lysosomal proteins (Aits and Jäättelä, 2013).

Apoptosis relies on the activation of a family of proteases called cysteine-aspartic proteases (Caspases) which, once activated, are responsible for initiating apoptosis through the degradation of DNA and cell organelles. Cells that experience sustained forms of injury or insult, generally xenobiotic compounds (such as chemotherapy agents, viral infection, oxidative stress, DNA damage, or dysfunctional organelles like the endoplasmic reticulum or mitochondria) initiate pro-apoptotic proteins which further activate executioner Caspases present within the cell, as seen in Figure 2.2 (reviewed Czabotar, Lessene, Strasser, & Adams, 2013).

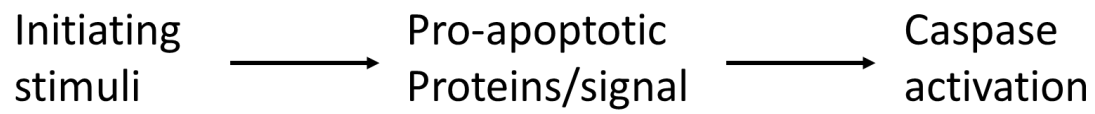

Figure 2.2-Activation of pro-apoptotic signalling cascade in response to initiating stimuli and the subsequent activation of apoptotic caspases.

Caspases can be divided into initiator (caspases 2, 8, 9, 10) and executioner (3, 6, and 7) caspases. Another category of caspases (1, 4, 5 and 12L) are involved in the inflammatory response (McIlwain, Berger and Mak, 2013). Caspases are synthesised as inactive procaspases which require either dimerization (initiator caspases) or cleavage (executioner caspases) to become activated. As such caspases exist as dormant proteins capable of rapid activation of apoptosis in response to apoptotic stimuli, bypassing the slower traditional protein transcription and translation processes (Patel *et al.*, 2015). Initiator caspases become activated in response to upstream signalling events, which in turn cause proteolytic cleavage

of executioner caspases (Shi, 2004). Caspases are responsible for the characteristic morphological changes seen in apoptotic cells, primarily cell shrinkage and membrane blebbing, nuclear fragmentation, chromatin/chromosomal condensation and fragmentation, and global mRNA decay (Parrish, Freel and Kornbluth, 2013).

Apoptotic stimulus can be either external or internal. External stimuli (e.g. immune cells detecting oncogenic extracellular membrane markers or virally infected cells) initiate the extrinsic apoptotic pathway that operates through membrane bound death receptors that initiate caspase activation. Both pathways converge through the activation of executioner caspases to carry out programmed cell death (Loreto *et al.*, 2014).

The extrinsic apoptotic pathway is regulated by death receptor ligands such as the Tumour Necrosis Factor (TNF) superfamily (e.g.TNFα) or FasL, and their corresponding death receptors, TNFR for TNF and FasR for FasL. TNFs are cytokines secreted by inflammatory cells, whereas FasL is a transmembrane protein expressed on cytotoxic T-cells (Nair *et al.*, 2014). Upon ligand binding the cognate receptors TNFR and FasR undergo homo-trimeric clustering, whereby they recruit their corresponding intracellular adapter proteins to potentiate the death signal. TNFR recruits TNFR1-associated death domain protein (TRADD) and FasR recruits Fas-associating protein with death domain (FADD) (Pobezinskaya and Liu, 2012).

Homo-trimeric death receptor binding following ligand activation allows for the formation of a multi-protein complex to form on the intracellular domain of the death receptor and is known as the Death Inducing Signal Complex (DISC). DISC functions as a molecular platform for the regulation and activation of Caspase 8 or Caspase 10 (Yang, 2015).

Activated caspase 8 can then go on to activate executioner caspases 3, 6 and 7, or pro-apoptotic proteins such as BH3 family (BH3 Interacting Death agonist (BID), Bcl-2 Agonist of cell Death (BAD) and Bcl-2 Associated X (BAX)) proteins which can in turn activate the intrinsic apoptotic pathway, demonstrating crosstalk between both pathways (Mariño *et al.*, 2014). The extrinsic apoptotic pathway is demonstrated in Figure 2.3.

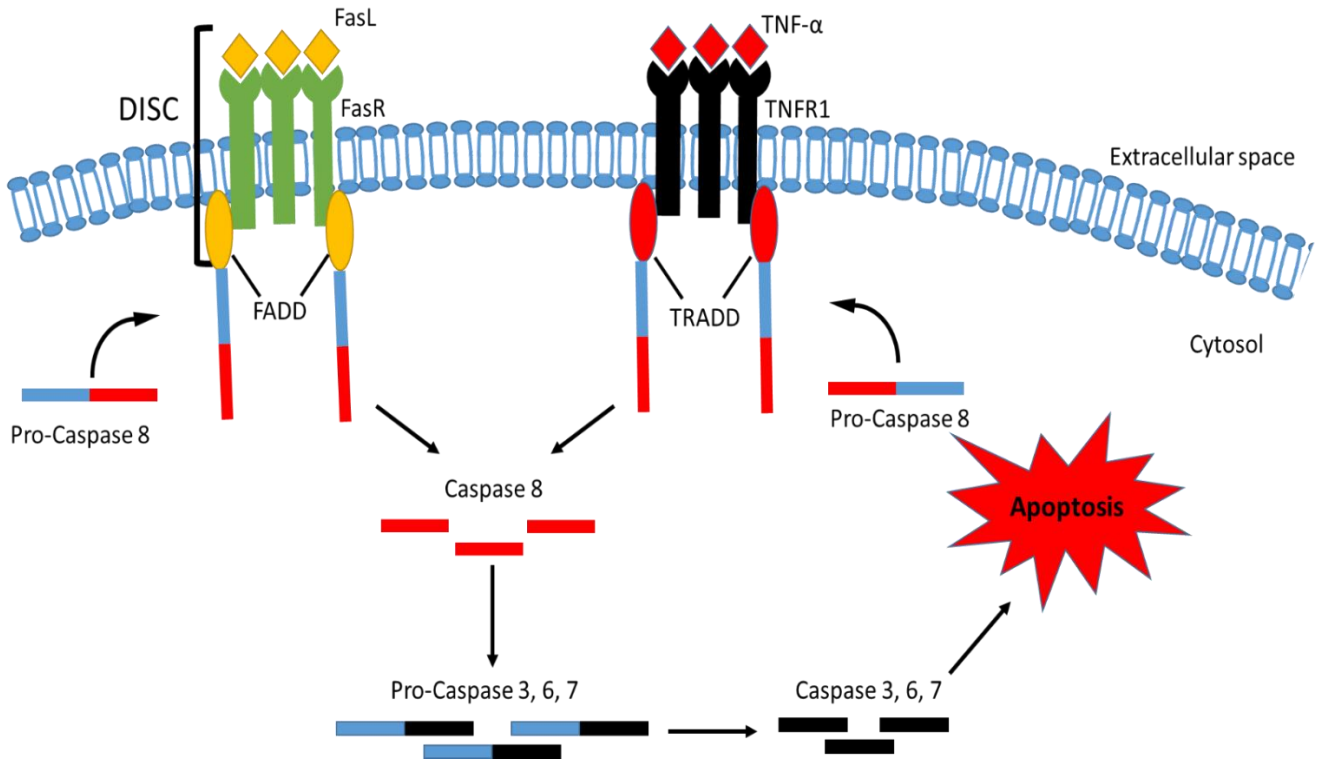

Figure 2.3-Extrinsic Death receptor apoptotic pathway. FasL and TNF-α death ligands bind FasR and TNFR1 death receptors causing homo-trimeric ligation, recruiting FADD and TRADD adaptor proteins forming the DISC complex. DISC can then catalytically cleave procaspase 8 causing its activation. This in turn can catalytically activate pro-executioner caspases (3, 6 or 7) initiating apoptosis. This figure was self-generated using Microsoft PowerPoint based on the current understanding of knowledge from a multitude of sources.

Internal stimuli (oxidative stress, DNA damage, hypoxia, growth factor deprivation or organelle dysfunction) initiate the intrinsic apoptotic pathway through activation of the pro-apoptotic family of BH3 proteins, such as BAX and BAK, and the inhibition of anti-apoptotic proteins such as the Bcl-2 family of proteins (Martin and Henry, 2013). Once the

apoptotic threshold of pro apoptotic BH3 proteins has been reached, activated BAX and BAK oligomerise and attach to the outer mitochondrial membrane. Here they simultaneously inhibit mitochondrial membrane bound anti-apoptotic Bcl-2 proteins such as Bcl-xL, and initiates Mitochondrial Outer Membrane Permeabilisation (MOMP) (Suhaili *et al.*, 2017).

MOMP results in the release of pro-apoptotic intermembrane space proteins such as cytochrome c, which once released into the cytosol, binds to and activates Apoptotic protease activating factor 1 (Apaf1). Apaf1 is an inactive cytosolic pro-apoptotic protein which is synthesised in a dormant state similar to that of procaspases (Kalkavan and Green, 2018). Activated Apaf1 then forms an oligomeric complex known as the apoptosome, a large wheel like quaternary protein assembly which serves to activate initiator caspase 9, which then goes on to cleave and activate executioner caspases 3, 6, and 7, initiating apoptosis (Shakeri, Kheirollahi and Davoodi, 2017). MOMP and activation of the intrinsic apoptotic pathway can be visualised in Figure 2.4.

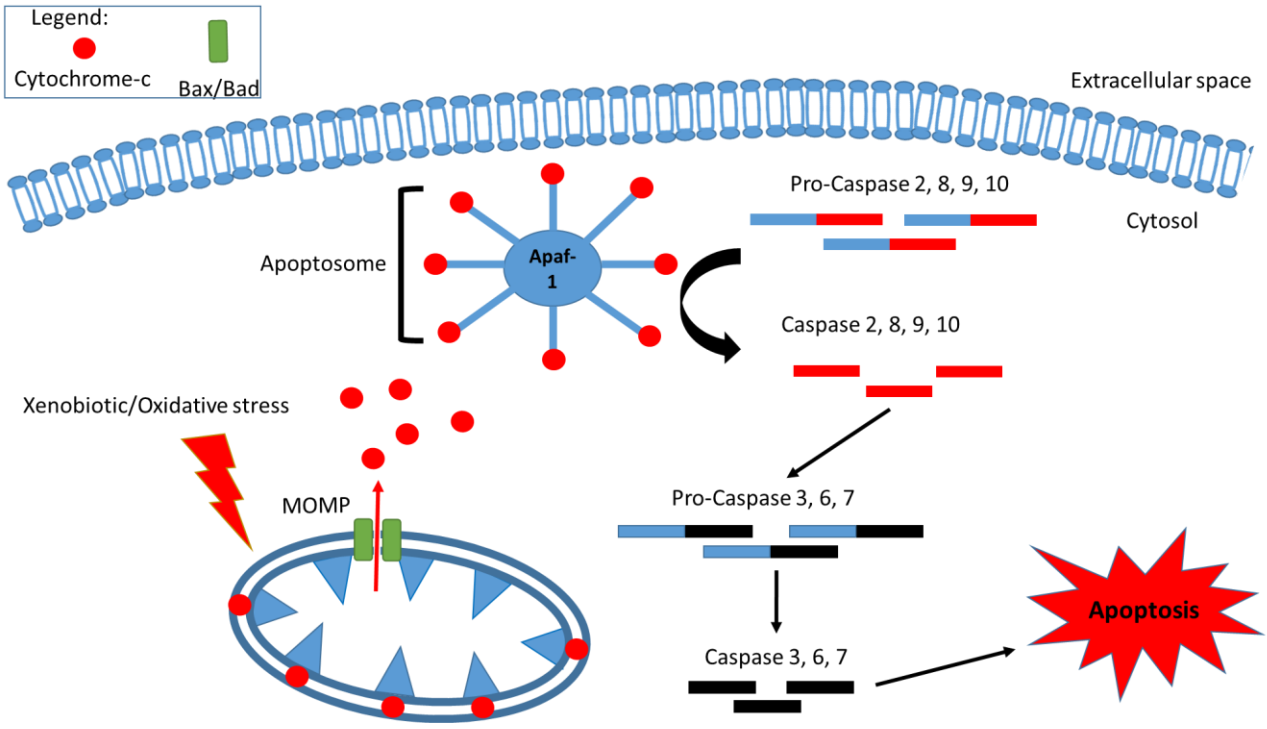

Figure 2.4-Intrinsic mitochondrial apoptotic pathway. Intracellular stress signals (xenobiotics, oxidative stress) disrupt mitochondrial signalling activating pro-apoptotic Bax and Bad forming MOMP complex and releasing mitochondrial bound cytochrome-c. Released cytochrome-c binds with Apaf-1 forming apoptosome which catalytically cleaves pro-initiator caspases (2, 8, 9, and 10) which in turn activate pro-executioner caspases (3, 6, or 7) initiating apoptosis. This figure was self-generated using Microsoft PowerPoint based on the current understanding of knowledge from a multitude of sources.

Other pro-apoptotic intermembrane space proteins released in response to MOMP are Apoptosis inducible factor (AIF) and endonuclease G (eG). AIF and eG are part of what is known as caspase independent apoptosis, as both translocate to the nuclease causing significant DNA degradation and induction of apoptosis, but are not activated by or cause the activation of caspases (Yang *et al.*, 2017).

2.1.2. ROS signalling apoptosis:

ROS has been seen to play a dual role in regulating apoptosis, serving as both an inhibitor and an inducer in a concentration dependent manner. Low levels of H_2O_2 have been seen to inhibit apoptosis through signalling cell survival pathways and activation of the tumour

suppressor p53 (Redza-Dutordoir and Averill-Bates, 2016). Low levels of oxidative stress causes p53 induced cell cycle arrest, DNA repair and senescence, allowing the cell to repair any damage and survive (He and Simon, 2013). However prolonged p53 signalling in response to high levels of ROS and oxidative stress results in p53 inhibition of anti-apoptotic Bcl-2 protein, and upstream regulation of both extrinsic and intrinsic apoptotic pathways (Aubrey *et al.*, 2018). Procaspases and caspases also possess redox sensitive cysteine residues in their active sites, facilitating redox regulation. Theses cysteine residues can become activated upon oxidation by ROS initiating the apoptotic pathway, or in some circumstances can experience inhibitory irreversible inactivation (Izeradjene *et al.*, 2005). Pro-caspases-3 and -9 are also available to undergo S-Glutathionylation, reducing the accessibility for proteolytic cleavage and activation. This process occurs during low levels of oxidative stress where antioxidant defences attempt to repair oxidative damage before apoptotic signalling kills the cell (Huang *et al.*, 2008). However if this damage is irreparable or levels of oxidative stress are increased then apoptotic mechanisms will become activated.

ROS signals the intrinsic apoptotic pathway by targeting mitochondrial DNA and RNA, and by causing disruption to the electron transport chain and ATP production, leading to the loss of mitochondrial membrane potential and MOMP formation, initiating apoptosis (Wu and Bratton, 2013). P53 activation has also been implicated as an upstream regulator of mitochondrial apoptosis by directly inhibiting Bcl-2 anti-apoptotic proteins (Bcl-2, Bcl-XL and Mcl-1) and directly activating pro-apoptotic proteins (Bax and Bak) facilitating MOMP (Pietsch *et al.*, 2008; Aubrey *et al.*, 2018).

ROS has been seen to be an activator of TNFR1, initiating the death receptor pathway through activation of DISC and caspase 8 activation (Wajant and Siegmund, 2019). Many

components of the death receptor pathway consist of redox sensitive proteins, such as Apoptosis signal-regulating kinase 1 (ASK1) and JNK. ASK1 is a downstream component of TNFR signalling, and under normal conditions is kept inactive by bound reduced Trx (Hattori *et al.*, 2009). However under high levels of oxidative stress Trx becomes oxidised releasing ASK1 which serves to activate JNK, initiating apoptosis (Soga, Matsuzawa and Ichijo, 2012). JNK itself is activated by ROS, promoting apoptosis (Shi *et al.*, 2014). Finally, FasL is seen to be both transcriptionally upregulated and catalytically activated by H_2O_2, initiating FADD translocation to the plasma membrane and caspase 8 activation (Wang and Su, 2018).

2.1.3. Necrosis/necroptosis:

In contrast to apoptosis, necrosis is generally associated with cell injury and premature death as a result of autolysis of the plasma membrane (reviewed Golstein & Kroemer, 2007). It is associated with pathologic processes such as exposure to bacterial/viral infection, toxins/venoms, and compounds capable of attacking the cell membrane (Escobar, Echeverría and Vázquez-Nin, 2015). Unlike apoptosis which is the controlled disintegration of the cell, necrosis is associated with the sudden and uncontrolled release of intracellular contents into the surrounding area (Escobar, Echeverría and Vázquez-Nin, 2015). This release is detrimental to surrounding cells, and necrosis is significantly associated with initiation of the inflammatory response, while apoptosis is seen to be significantly less inflammatory (Martin and Henry, 2013).

However while initially thought to be a form of uncontrolled cell death, necrosis has in some instances been seen to be mediated by multiple highly regulated intracellular signalling pathways (Festjens, Vanden Berghe and Vandenabeele, 2006). This form of regulated

necrosis is often referred to as necroptosis, and demonstrates shared morphological features of both necrosis and apoptosis (Dhuriya and Sharma, 2018).

Necrosis often refers to the un-programmed swelling and rupture of the cell in response to severe injury, such as physical damage, heat, or toxins (Jog and Caricchio, 2014). Necroptosis shares similar features as necrosis such release of cytoplasmic content and initiating an inflammatory response, however necroptosis is seen to be regulated by many signalling pathways in a caspase independent manner (Karch and Molkentin, 2015), and can be inhibited at the molecular level by necroptotic specific inhibitors (Hou *et al.,* 2019). Necroptosis is heavily regulated by Receptor Interacting Protein Kinase 1 and 3 (RIPK1 and RIPK3), which in turn are regulated predominantly by three signal transduction cascades, TNFR, Toll-like Receptor (TLR) and poly-(ADP-ribose) polymerase 1 (PARP1) (Berghe *et al.,* 2014), as seen in Figure 2.5. PARP1 is an enzyme involved in DNA repair such as single and double strand breaks. Its primary role is to catalyse the formation of poly ADP-ribose chains to both itself and to target proteins using NAD^+ as a cofactor to recruit further DNA repair mechanisms (Ray Chaudhuri and Nussenzweig, 2017).

Interaction of RIPK1 with activated death receptors (e.g. TNFR) leads to the activation of RIPK1 which subsequently activates RIPK3 (He *et al.*, 2009). However RIPK1 activation can only take place when caspase 8 is inactive which may occur in response to viral, bacterial or pharmacological factors (Tummers and Green, 2017). Caspase 8 thus acts as a molecular switch between apoptosis and necroptosis (Tonnus *et al.*, 2019). Activated RIPK3 in turn phosphorylates a pseudo kinase called Mixed Lineage Kinase Like (MLKL) protein. Phosphorylated MLKL then oligomerises and translocates to the plasma membrane. Here it forms a transmembrane pore, compromising membrane integrity, resulting in necrosis and

induction of the inflammatory response through the release of damage associated molecular patterns (DAMPs) (Dhuriya and Sharma, 2018).

TLR regulated necroptosis follows a similar pathway to TNFR mediated signalling. TLR 3 or TLR 4 use the adaptor molecule TIR domain-containing adapter-inducing interferon-β (TRIF), to directly activate RIPK3, which initiates the downstream necroptotic signalling cascade involving MLKL and loss of plasma membrane integrity (Kaiser *et al.*, 2013).

Following extensive DNA damage by ROS or DNA damaging agents, the DNA repair enzyme PARP1 becomes hyper activated (Shin *et al.*, 2015). PARP1 catalyses the hydrolysis of NAD^+ into nicotinamide in order to catalyse the addition of poly-ADP-ribose side chains to itself and target proteins, and so hyper activation results in a severe drop in NAD^+ and ATP levels, and induction of cell energy failure death mechanisms (Alano *et al.*, 2010). This signals the activation of RIP1K which can initiate RIPK3 mediated necrosis, or activates c-Jun N-terminal Kinase (JNK) which then translocates to the mitochondria where it induces mitochondrial membrane depolarisation, resulting in loss of membrane integrity and membrane rupture, initiating necrosis (Baines, 2010). The three main necroptotic pathways are represented in Figure 2.5.

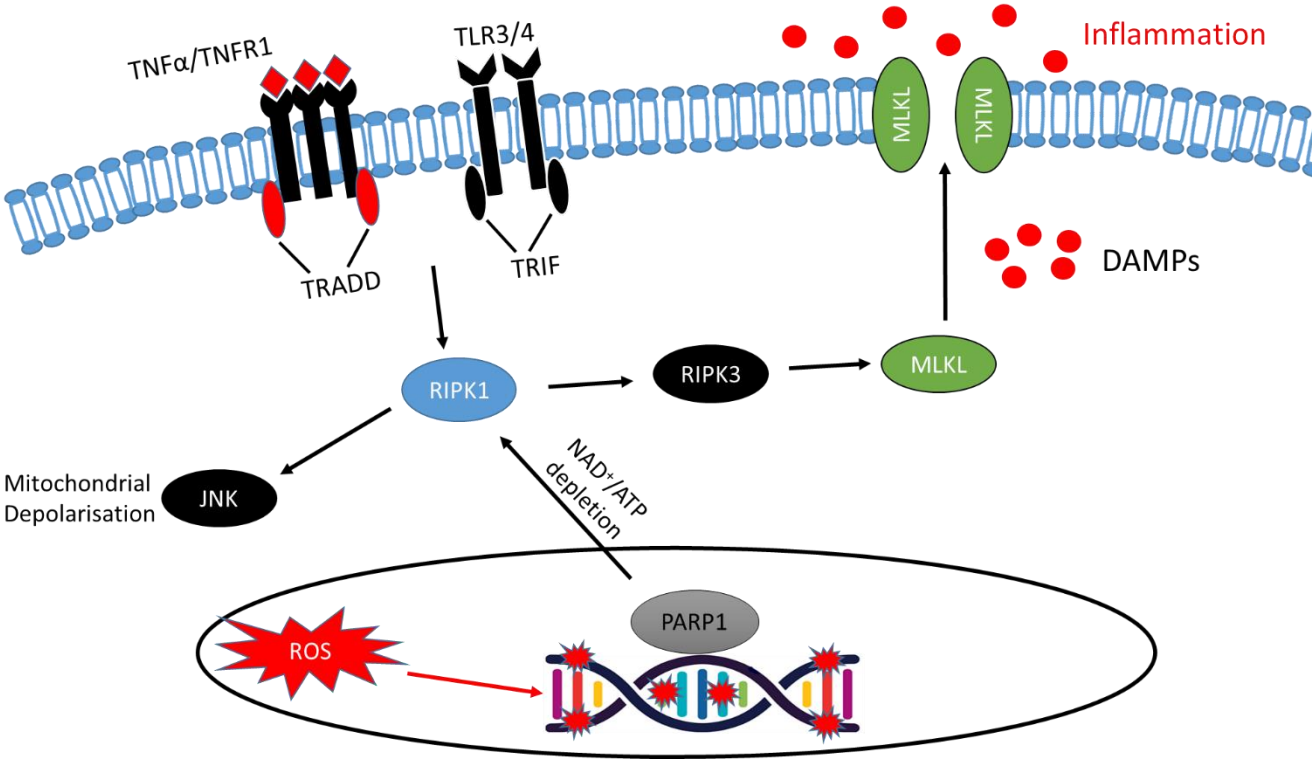

Figure 2.5-Necroptotic cell death pathways. TNFR1/TLR3 and 4 death receptor activation results in the activation of RIPK1, which in turn activates RIKP3. RIPK3 then activates MLKL which dimerizes and migrates to the cell membrane, where it forms membrane pores resulting in a loss of membrane integrity and the release of pro-inflammatory DAMPs. Intracellular ROS can induce DNA damage which activates PARP1. PARP1 hyper activation depletes the cell of NAD+ and ATP, resulting in RIPK1 activation. RIPK1 can then active the RIKP3/MLKL pathway or activate JNK which can target the mitochondria for membrane depolarisation and induction of mitochondrial necrosis. This figure was self-generated using Microsoft PowerPoint based on the current understanding of knowledge from a multitude of sources.

As well as apoptosis and necroptosis, many other distinct variations of cell death exist. Examples of these and corresponding reviews detailing these processes are shown in Table 2.1. Ferroptosis is an iron regulated form of necrotic cell death and is discussed in detail in Chapter 5: Investigation of Ferroptotic cell death.

Table 2.1-Alternate forms of cell death

Form of Cell death:	**Mechanism:**	**Review:**
Pyroptosis	Regulated osmotic swelling and necrosis of infected macrophages	(Robinson et al., 2019)
Oncosis	Non-regulated ischemic cell death	(Weerasinghe and Buja, 2012)
Entosis	Regulated invasion of a living/malignant cell into neighbouring viable cell	(Galluzzi *et al.*, 2018)
Ferroptosis	Iron regulated necrotic cell death	(Xie *et al.*, 2016)
Lysosomal cell death	Regulated release of cathepsins causing necrotic or apoptotic cell death	(Aits and Jäättelä, 2013)

2.1.4. ROS signalling and necrosis/necroptosis:

ROS can signal necrosis/necroptosis through many different pathways, for example via induction of PARP1, mediated necrosis secondary to ROS induced DNA damage. During times of sustained oxidative stress calcium homeostasis can become dysregulated. Disruption of calcium homeostasis and influx of calcium into the ER increases the activity of NOS enzymes and thus nitric oxide production and oxidative stress. Elevated nitric oxide can disrupt mitochondrial stability and thus lead to the release of ROS such as superoxide. Superoxide can react with nitric oxide forming peroxynitrite, which in turn can cause

significant levels of DNA damage therefore activating PARP1. The loss of mitochondrial integrity would significantly reduce the cells ATP producing capacity, which when coupled with energy deficiency from PARP1 activation, will initiate necroptosis. Nitric oxide has also been seen to inhibit caspases through nitrosylation, therefore reducing the apoptotic capacity of the cell, further favouring necrosis (Festjens, Vanden Berghe and Vandenabeele, 2006; Berghe *et al.*, 2014; Karch and Molkentin, 2015; Tonnus *et al.*, 2019).

2.2.Dysregulation of cell death mechanisms and cancer:

The ability of cancer cells to evade cell death has been discussed as a primary hallmark of cancer cells and the oncogenic process. As such the manipulation and dysregulation of both apoptotic and necrotic/necroptotic pathways to favour unrestrained cell growth is a primary mechanism of this hallmark.

2.2.1. Apoptosis and Cancer:

Cancer cells arise from the imbalance of regulatory mechanisms controlling the expression of cell cycle control genes and apoptotic regulatory genes. Cancer cells evade apoptotic mechanisms through the dysregulation of Bcl-2 family proteins and increased expression of Inhibitors of Apoptosis Proteins (IAPs), reduced caspase activity, defective or mutated p53 signalling, and impaired receptor signalling pathways (Hassan *et al.*, 2014). Cancer cells utilise dysregulated apoptotic protein signalling pathways to confer distinctive survival advantage and escape cell death mechanisms. This is done via downregulation of pro-apoptotic genes (Bax, Bak, Bid, Bim, Puma, and Noxa), or the overexpression of anti-apoptotic genes (Bcl-2, Bcl-xL, Mcl-1, BF-1) or IAPs (XIAP, cIAP1, cIAP-2, survivin) (Chen, Zeng and Zhou, 2018). Increased anti-apoptotic Bcl-2 proteins serve to inhibit their BH3 containing pro-apoptotic Bcl-2 counterparts by preventing them from forming MOMP

and initiating intrinsic apoptotic pathways (Campbell and Tait, 2018). IAPs are endogenous inhibitors of apoptosis which serve to inhibit caspase activity by marking them for degradation (Pluta *et al.*, 2015). The disruption of the balance between expression of pro and anti-apoptotic genes and proteins has been demonstrated in many different cancers, reducing overall survival rates and has been implicated in the prevalence of acquired resistance to chemo or radiotherapies (Wong, 2011).

Reduced caspase activity can be initiated in response to reduced signalling of pro-apoptotic signals previously mentioned or through direct downregulation of caspase genes, further reducing the apoptotic capacity of the cell (Jakubowska *et al.*, 2016). P53, referred to as the guardian of the genome and one of the most studied tumour suppressor proteins, has been seen to be mutated in almost 50% of all cancers (Rivlin *et al.*, 2011). As discussed p53 is a major regulator of apoptosis, cell cycle regulation, differentiation, DNA repair and cellular senescence. Loss of p53 signalling would result in further dampening of apoptotic signalling (Aubrey *et al.*, 2018).

Finally, many cancers have been seen to possess several abnormalities in many of their death receptor signalling pathways. Other members of the death receptor family, such as Death Receptor 3 (DR3), Death Receptor 4 (DR4), and TNF-related apoptosis-inducing ligand (TRAIL), have been seen to be altered in different cancers (Oikonomou and Pintzas, 2013). Many cancer cells have been seen to either reduce the expression of these receptors or their ligands, or impair their function through downregulation of surface receptors by generating receptors without an intracellular death domain (decoy receptors) capable of propagating the extracellular death signal from the death ligand (Shirley, Morizot and Micheau, 2011).

2.2.2. Necroptosis and cancer:

Necroptosis has been implicated in all three stages of cancer, initiation, progression and metastasis (Najafov, Chen and Yuan, 2017). However it is seen to have dual roles in whether it acts as an oncogenic factor or tumour suppressor, and does so in a cancer type specific manner (Seifert and Miller, 2017). RIPK3 has been seen to be targeted by the epigenetic machinery of cancer cells for genetic silencing through hyper methylation of its promoter region, in multiple cancers (breast, colorectal, Acute Myeloid Leukaemia (AML)) and has been associated with poor prognosis and survival rates (see references 7 and 65, Gong et al., 2019). MLKL has also been seen to be downregulated in AML, with both RIPK3 and MLKL being downregulated in T-cell Lymphomas (Höckendorf, Yabal and Jost, 2017; Van Hoecke *et al.*, 2018). As most cancer cells have escaped the control of apoptotic processes, reducing the necroptotic fail safe cells have for such an event may provide a survival advantage to certain cancer cells (Gong *et al.*, 2019).

However many cancers have been seen to have increased RIPK3 expression (glioblastoma, lung, and pancreatic adenocarcinoma) which has also been associated with poor prognosis and overall survival rates (see references 10, 72, 64 and 73, Gong et al., 2019). Much of the role necroptosis plays in promoting tumour progression and metastasis comes from its regulation of the surrounding microenvironment and immune cell suppression (Qin *et al.*, 2019). The release of pro-inflammatory cytokines and DAMPs may stimulate proliferation in surrounding cells, further promoting neoplasia through increased levels of ROS or RNS (Gong *et al.*, 2019). It has also been demonstrated that the release of certain cytokines can promote an immunosuppressive microenvironment by downregulating Tumour Associated Macrophages, a phenomena demonstrated in pancreatic adenocarcinoma cells (Seifert *et al.*, 2016).

Cancer cells appear to hijack RIPK3 and necroptotic signalling to induce necroptosis in surrounding endothelial cells in order to facilitate metastasis and extravasation in order to invade foreign tissues. This has been demonstrated by Strilic *et al*., (2016), using co cultures of human and murine endothelial and tumorigenic cells in the presence of necroptotic inhibitors, demonstrating that tumorigenic cells utilise Death Receptor 6 (DR6) expressed on endothelial cells to initiate necroptosis as part of the metastatic process (Strilic *et al.*, 2016).

As cancer cells generally possess inherent resistance towards apoptosis and with the prevalence of acquired resistance, the necroptotic pathway may be a lucrative alternative for potential chemotherapeutic intervention (Wu, Dong and Sheng, 2020).

The mechanism through which the novel compounds initiate cell death is therefore of high importance, with apoptotic induced cytotoxicity being favoured over necrosis in order to minimise inflammation and collateral damage to surrounding cells. To determine the cytotoxic capabilities of the novel phen compounds CMPD 73 and CMPD 74, a panel of different cancer cell lines, and one cell line of non-cancerous origin were exposed to both compounds for 24 hours and cell viability was measured using the Alamar Blue assay, and cell cytotoxicity using the LDH assay and the AnnexinV-FITC/PI Dead cell assay for apoptosis. As a point of comparison, known chemotherapeutic agents cisplatin and doxorubicin were also tested.

2.3.Aims:

As a first step in the characterisation of these new compounds, we evaluated their cytotoxicity in a panel of different cell lines, including several cancer lines of different origin and one of non-cancerous origin. To determine compound efficiency alongside a mainstream anti-cancer drug, cisplatin was also tested in parallel in some experiments.

2.4.Materials

Compounds 73, 74 as well as all precursors were synthesised in house according to standard procedures (McCann *et al.*, 1997; Gandra *et al.*, 2017) and dissolved in sterile water as 10mM stocks. The characterisation data for both compounds can be seen in the Appendix page 271. The following cell lines were used: A2780 (ovarian cancer), A549 (alveolar adenocarcinoma), HT-29 (colonic adenocarcinoma), PC3 (prostatic carcinoma), U373MG (glioblastoma), CS and CR P31 cells (isogenic cisplatin sensitive and cisplatin resistant mesothelioma cells, respectively). BeaS2B (SV40/adenovirus 12 transformed bronchial epithelium) were used as a non-cancer origin cell system. Cells were cultured in RPMI 1640, supplemented with 10% foetal bovine serum and 1% L-glutamine, with the exception of BeaS2B and U373MG, which were cultured in DMEM with supplements as above. Cells were incubated in a humidified atmosphere of 5% CO_2 in air at 37°C. A solution of 0.44mM Resazurin salt in PBS (pH 7.4) was prepared in house. This is equivalent to the commercial Alamar Blue reagent (O'Brien *et al.*, 2000).

The Lactate Dehydrogenase (LDH) cell cytotoxicity assay was conducted as per protocol (Chan, Moriwaki, & De Rosa, 2013). The preparation of the LDH reagent was conducted in house on the day of experimentation and was prepared as follows: 200µl of INT (2-p-iodophenyl-3-p-nitrophenyl-5-phenyl tetrazolium chloride, 3.3mg/ml stock prepared in DMSO), 200µl of PMS (N-methylphenazonium methyl sulfate, 0.9mg/ml stock

in H_2O), 98mg of Lithium Lactate (Sigma), and 17.4mg of NAD (nicotinamide adenine dinucleotide) were added to 10mls of H_2O and 5mls of 200mM Tris pH 8. Reagent was stored in the dark at four degrees until use. All reagents were purchased from Sigma Aldrich Ireland.

The Annexin V FITC/PI Dead Cell apoptosis Kit (V13242 Thermo Fisher) was prepared as per protocol on the day of experimentation.

2.5.Methods

2.5.1. Cell Viability Assay

Cells were plated in octuplet wells ($1x10^4$ cells/well in 100µL of media) of Greiner 96 well flat-bottomed, black-walled plates and allowed to acclimatise over-night before exposure to the different compounds. Following drug exposure for the specified time (typically 24 hours) cell viability was then investigated using the Resazurin reduction assay, also known as the Alamar Blue assay, described in section 2.4. 10µl of resazurin reagent was added to each well (i.e. 10% of final well volume) and incubated for optimised, cell-specific time periods (2-4 hours). The fluorescence at the end of the incubation period was detected using a Spectra Max M3 spectrophotometer (Molecular Devices) at excitation 530 nm and emission 590 nm. Cisplatin was used as a drug of comparison in A2780 cells for 24 hours and in the isogeneic mesothelioma cell lines for 72 hours, in accordance with the timescale in which cisplatin became active within the cells. Data was expressed as a percentage of the non-treated control.

A549 cells were selected as a model to investigate the cytotoxicity of compounds compared to constituent components and so were seeded at a density of 10,000 cells, allowed to attach overnight, and then exposed to test compounds. To fully map the molecular entity responsible for the biological activity, all complex components were tested individually or in combination. Pilot studies of some combinations e.g. $CuCl_2$/$MnCl_2$ combined with TDDA (0.1%) did not elicit any cytotoxic response and so were not exhaustively investigated. The highest concentration of TDDA used was 4.5mM as higher concentrations resulted in artefactual resazurin reduction, leading to false positive results (result not shown).

2.5.2. Cell cytotoxicity assay

LDH Assay: A549 cells were plated in quadruplet wells ($1x10^4$ cells/well in 100µL of media) of Greiner 96-well flat-bottomed clear plates and allowed to acclimatise over-night before exposure to the different compounds. Following drug exposure for the specified time (typically 24hours), 50µL of cell supernatant was removed from each test well and dispensed into fresh wells of the same plate. 150µL of LDH reagent was then added to each well and incubated for 45mins in the dark. Absorbance was measured at 490nm using a *MULTISKANGO* spectrophotometer (ThermoFischer) and data was expressed as a percentage of full lysis control (1% *v:v* of Triton-X 100).

Annexin V FITC PI Flow Cytometry: A2780 cells were plated at $5x10^5$ cells/well in a 6 well plate and allowed to acclimatise over-night before exposure to the different compounds. A2780 cells were used as A2780 cells were seen to be more sensitive to chemotherapeutic controls (cisplatin, doxorubicin) than A549 cells, allowing 24hr incubation periods over 72hr. Cells were then exposed to approximate IC_{50} concentrations of CMPD 73 (45µM), 74 (3µM) and 1,10-Phen (200µM) for 24hrs. Doxorubicin (3µM) was also used as a positive inducer of apoptosis, and is reported to have a very low IC_{50} value when used in A2780 cells (Altaf *et al.*, 2019). Following 24hr treatment, A2780 cells were then stained with Annexin V FITC/PI for 15mins as per protocol, and read in a BD Accuri C6 Flow cytometer, using FITC FL1 channels and PI FL3 channels. Compensation between FL1 and FL3 channels was conducted as per the BD Accuri C6 cytometer manual in order to remove spectral overlap between FITC and PI. Dead cells and cellular debris were removed by selective gating based on forward and side scatter data, and a positive response was selected by gating events with a higher fluorescent intensity than that of the non-treated control. Levels of apoptosis were determined using quadrant-based gating strategies. Lower Left (LL)

quadrants contained low FITC/PI expressing cells and were determined to be viable cells. Lower Right (LR) quadrant contained high FITC expression but low PI and were determined to be early apoptotic cells with bound AnnexinV but without membrane permeabilization. Upper Right (UR) quadrants contained cell populations expressing both high FITC and PI levels and were determined to be late stage apoptotic cells with high levels of bound AnnexinV and instances of membrane permeabilization allowing entry of PI. Upper Left (UL) quadrants were determined to be cell populations with high levels of PI but low levels of FITC and were therefore determined to be predominantly necrotic cells with high levels of membrane permeabilization.

2.5.3. Statistical analysis

All data including calculation of IC_{50} values was analysed using GraphPad Prism Version 8.3. Statistical analysis was conducted using Two-way ANOVA, multiple T-Test or students T-Test where applicable. Significant differences were expressed as a P Value < 0.05, 0.01, 0.001. Where multiple T-test analysis was used, Figure 10.1 and Figure 10.2 in the appendices provides an example of output of the comparisons made by GraphPad Prism Version 8.3.

2.6.Results:

2.6.1. Cytotoxic effects of metal-based drugs

To investigate the cytotoxic effects of metal-based drugs and identify suitable cell models for future experiments a variety of cancer cell lines were tested. Cell lines which demonstrated the highest cytotoxic effect following exposure to test compounds were investigated further. As shown in Table 2.2, CMPD73 shows cancer cell cytotoxicity against A2780 ovarian (IC_{50} 45 µM), A549 alveolar (IC_{50} 45 µM) and Cisplatin Resistant (CR Meso, IC_{50} 49 µM), but not Cisplatin Sensitive mesothelioma (CS Meso, IC_{50} 306 µM). IC_{50} values for the other cell lines ranged from 250-430 µM. CMPD 73 is seen to be comparable with cisplatin following 24hr treatment in ovarian cancer cells (IC_{50} 27 µM) and following 72hr treatment with Cisplatin Sensitive mesothelioma (Table 2.3). 1,10-Phen demonstrated a similar high micro-molar range (329-580 µM) across all cell lines. PC3 cells were not available for treatment with 1,10-Phen.

Table 2.2 Cytotoxic effect of novel compounds and 1,10-Phen on cultured human cancer cells following 24 hrs.

Cell Line	IC_{50} µM (95% CI)		
	CMPD73	**CMPD74**	**1,10-Phen**
A2780	45 (39-51)	2 (0.5-3.3)	495 (475-515)
A549	45 (37-54)	3.7 (3.5-3.9)	328.6 (275-382)
HT-29	266 (157-375)	5.6 (2.6-8.5)	580 (410-749)
CS Meso.	306 (226-386)	3 (2.6-3.5)	364 (311-417)
CR Meso.	49 (37-60)	2.6 (2.3-2.8)	534 (502-567)
PC3	422 (352-491)	6.9 (6.2-7.5)	N.A.
U373MG	378 (286-470)	2.9 (2.5-3.5)	423 (354-492)
BeaS2B	384 (278-489)	3 (2.5-3.5)	440 (400-480)

N.A- Not available

Interestingly, CMPD 73 is seen to overcome cisplatin resistance in the Resistant Mesothelioma cell line when compared to cisplatin (Table 2.3, Figure 2.6) following 72hr treatment, indicating applicability as a novel treatment for acquired chemotherapeutic resistance.

A direct comparison with the data described by Gandra *et al.*, (2017) regarding the effects of CMPD 73 against A549 cells demonstrates some variability with the results from Table 2.2. Gandra *et al.*, (2017) determined the CC_{50} of CMPD 73 to be 261.7mg/L (calculated to 356 µM) which is significantly higher than the IC_{50} value of 45µM seen in Table 2.2. However the method Gandra *et al.*, (2017) used to determine this value was the MTT assay, whereas the Alamar Blue assay was used to determine the IC_{50} values in Table 2.2. While it would be expected that both assays should provide comparable results these inconsistencies

can likely be explained by differences in sensitivity between the MTT and Alamar Blue assays (Hamid *et al.*, 2004; Damiani *et al.*, 2019), batch variability among the synthesised compounds or slight differences in the A549 cells themselves. Variability among compounds used for cancer cell screening is also a common obstacle in modern cancer research (He *et al.*, 2016).

Table 2.3-Effectiveness of CMPD 73 and CMPD 74 is not impacted by the presence of cisplatin resistance following 72 hr incubation (Data generated from two independent experiments)

Cell Line	**IC50 µM (95% CI)**		
	CMPD73	**CMPD74**	**Cisplatin**
CS Meso.	3.0 (2.6-4.0)	1.6 (0.6-2.6)	4.5 (3.3-5.6)
CR Meso.	4.1 [a] (3.6-4.6)	2.4 [a] (1.2-3.5)	59.1 [b] (43.1-75.0)

([a] Significantly different from Cisplatin control $P<0.05$, [b] Significantly different from CS Meso $P<0.05$ calculated using students t-test).

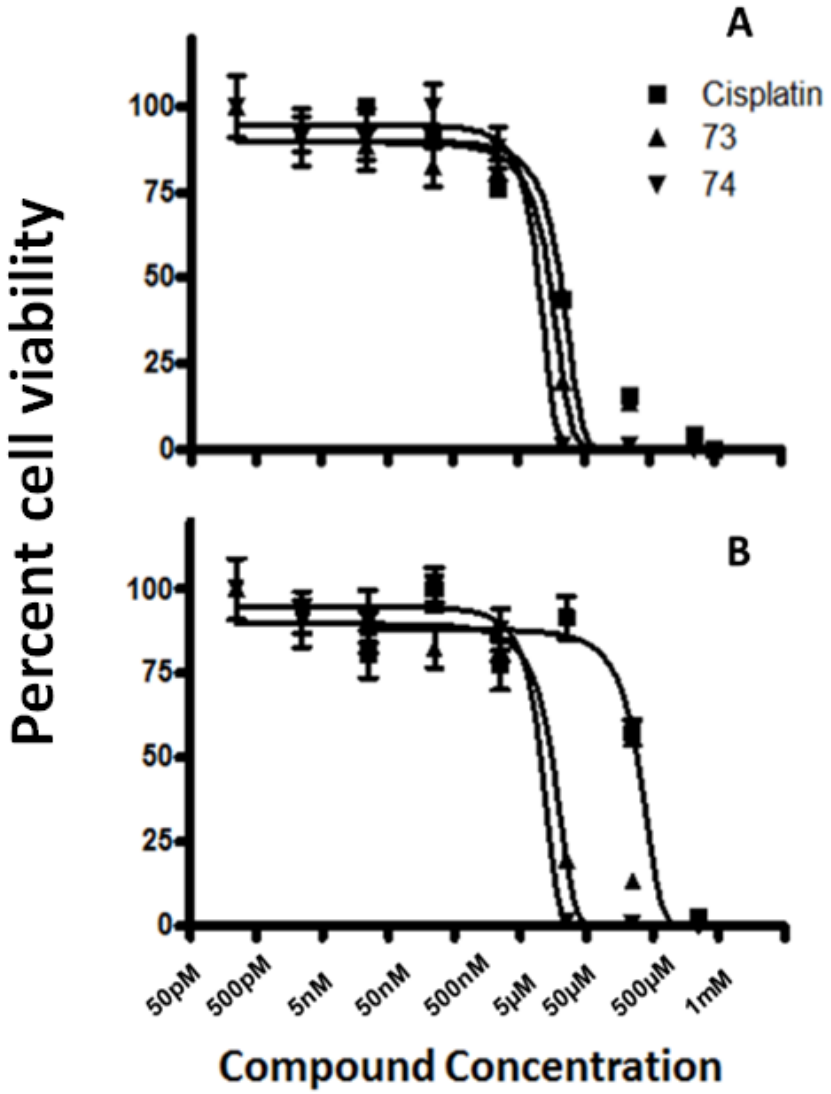

Figure 2.6 Cytotoxic effects of Cisplatin, CMPDs 73 and 74 against CS Meso (A) and CR Meso (B) cells following 72hr incubation. (± 1 Standard Deviation of two independent experiments using 8 technical replicates).

CMPD 73 and its constituent components were tested using A549 cells. As an intact compound CMPD73 is moderately more cytotoxic towards A549 cells than either 1,10-Phen or 1,10-Phen combined with free manganese (Figure 2.7). CMPD 69 (precursor to CMPD73 lacking the 1,10-Phen moiety) displayed limited activity with high micro-molar/milli-molar concentrations required. Manganese alone, TDDA or a combination of both had minimal effect.

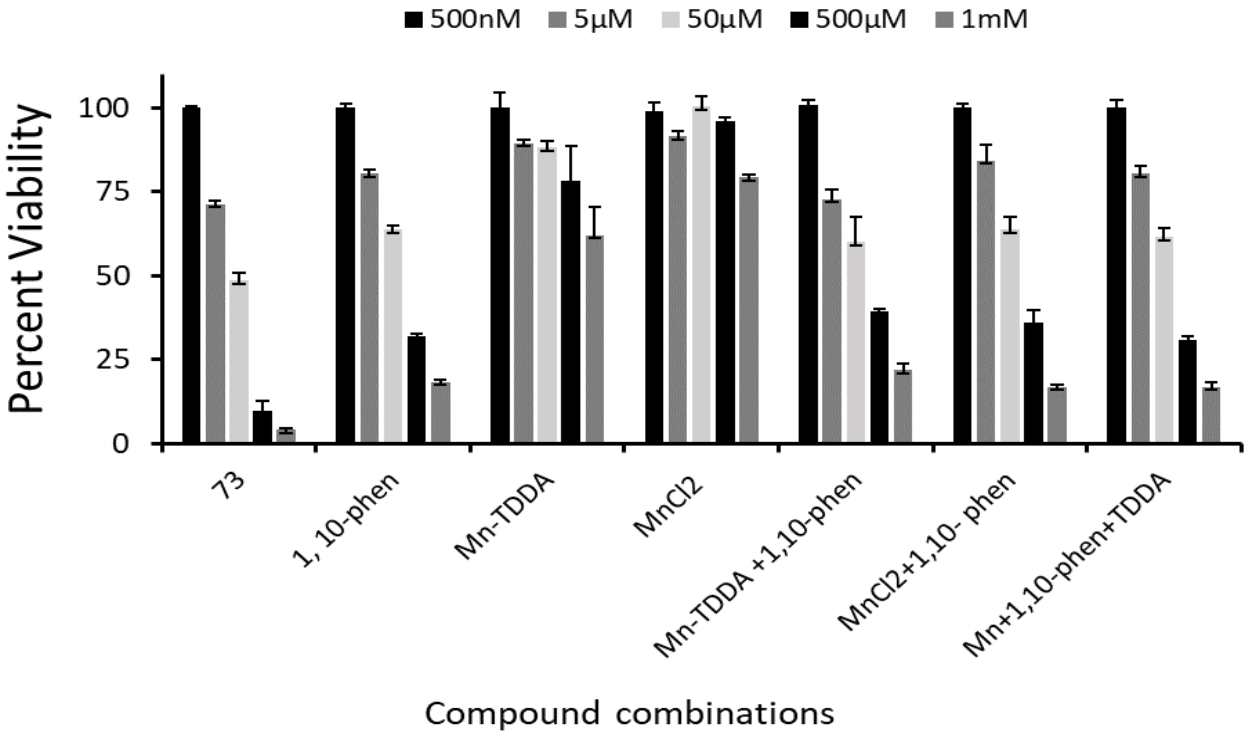

Figure 2.7 Cytotoxic profiles of CMPD 73, and its constituent components CMPD 69 (Mn-TDDA), $MnCl_2$, 1,10-Phen, and combinations of each constituent in A549 cells. (±1 Standard deviation of three independent experiments using 4 technical replicates).

Table 2.4-P Values of manganese and phen components and combinations compared to CMPD 73 at each concentration tested.

Conc.	**1,10-Phen**	**Mn-TDDA**	**$MnCl_2$**	**Mn-TDD+ 1,10-Phen**	**$MnCl_2$+1,10-Phen**	**$MnCl_2$+1,10-Phen+TDDA**
500nM	N.S	N.S	N.S	N.S	N.S	N.S
5μM	P<0.001	P<0.001	P<0.001	N.S	N.S	P<0.01
50μM	P<0.001	P<0.001	P<0.001	N.S	N.S	P<0.01
500μM	P<0.001	P<0.001	P<0.001	P<0.001	P<0.01	P<0.001
1mM	P<0.001	P<0.001	P<0.001	P<0.001	P<0.001	P<0.001

(Calculated using multiple T-Tests) (N.S= not significant)

CMPD 74 is seen to be significantly more cytotoxic than CMPD73, with IC_{50} Values in the low μM range (2-6μM, Table 2.2) However the compound did not appear to possess either cancer cell specificity or cancer cell selectivity, as it is equally as effective against all cell lines, cancerous and non-cancerous (Table 2.2). In time course studies it is observed that potent cytotoxic action of CMPD74 is readily observable in short time courses – the IC_{50} against A549 cells is 6.3μM within 6 hours and that against CS Meso. is 6.5μM within 8 hours. This is very similar to the value following 24 hours. The IC_{50} value of CMPD 74 was also seen to be comparable with the data described in Gandra *et al.*, (2017), where a value of 1.06mg/L (1.4μM) was obtained.

Compound 74 (CMPD74) and its constituent components were tested using A549 cells (Figure 2.8). These data indicate that both copper and 1,10-Phen are required to generate potent cytotoxic effects in this cell model with effects most obvious at 5μM (Figure 2.8 light grey columns). A slight additive effect of CMPD74 compared to a mix of components is

noted. No significant effect is observed under conditions lacking copper and 1,10-Phen together.

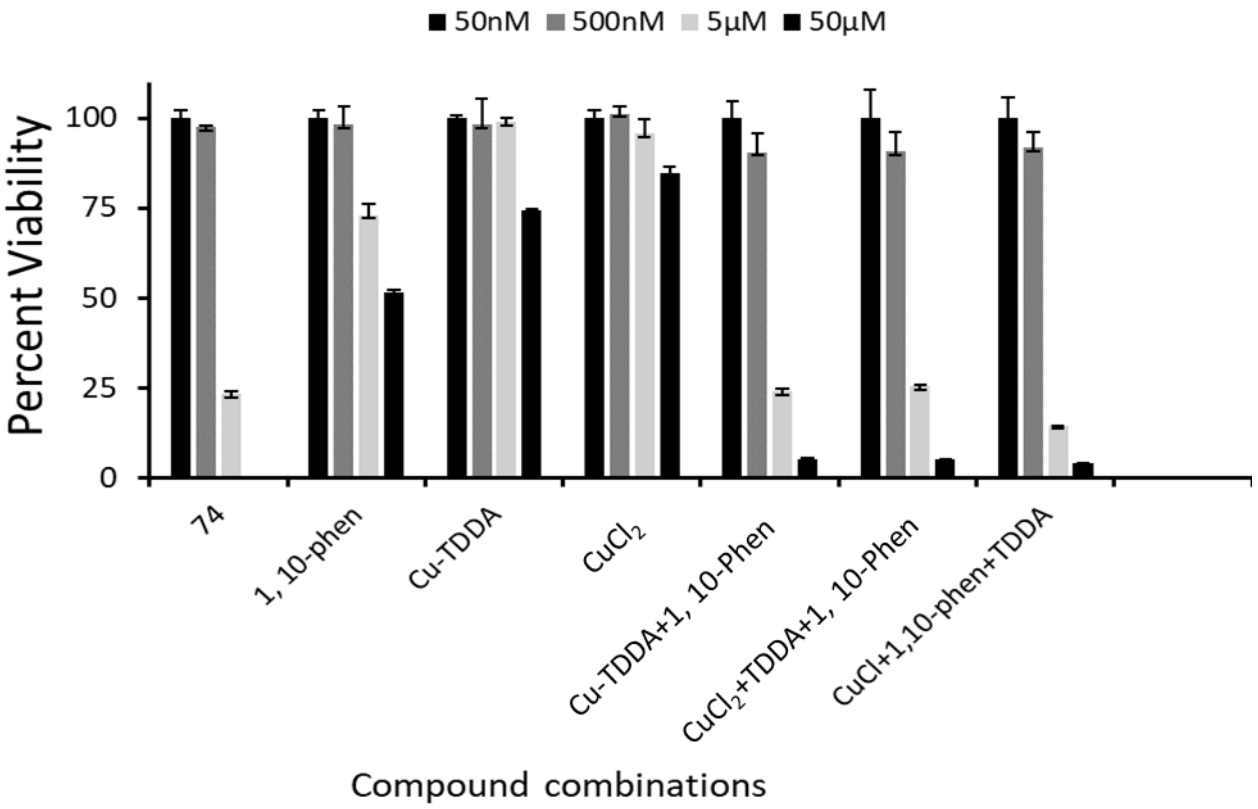

Figure 2.8 Cytotoxic profiles of CMPD 74, and its constituent components CMPD 70 (Cu-TDDA), $CuCl_2$, 1,10-Phen, and combinations of each constituent in A549 cells (±1 Standard Deviation of three independent experiments using 4 technical replicates).

Table 2.5-P Values of copper and phen components and combinations compared to CMPD 74 at each concentration tested

Concentration	**1,10-Phen**	**Cu-TDDA**	**$CuCl_2$**	**Cu-TDD+ 1,10-Phen**	**$CuCl_2$+1,10-Phen**	**$CuCl_2$+1,10-Phen+TDDA**
50nM	N.S	N.S	N.S	N.S	N.S	N.S
500nM	N.S	P<0.001	N.S	N.S	N.S	N.S
5µM	P<0.001	P<0.001	P<0.001	N.S	N.S	P<0.001
50µM	P<0.001	P<0.001	P<0.001	P<0.001	P<0.001	P<0.001

(Calculated using multiple T-Tests) (N.S= not significant)

2.6.2. Membrane Integrity- LDH assay

To examine if necrosis is the key mode of cell death, we employed the LDH assay, which is based on the release of LDH from cells which lyse during necrosis and is thus a measure of the integrity of the plasma membrane (Chan, Moriwaki and De Rosa, 2013). Surprisingly, treatment of cells with CMPD73 resulted in a paradoxical reduction in LDH activity (Figure 2.9), with measured LDH activities in the presence of higher concentrations of the compound actually less than that of the negative control. Addition of EDTA before the assay procedure eliminates the inhibitory effect on LDH activity, suggesting that free metal ions are involved in the process (compare lanes 9 and 10 in Figure 2.9). These data are consistent with findings in the literature where Cu^{2+} has been reported to markedly inhibit LDH activity in brain homogenates at a concentration of 10μM, while Mn initially induced activity and subsequently markedly decreased it (Heron *et al.*, 2001). Raw absorbance values were zero following blank subtraction compared with 1.11 absorbance values in wells where 0.1% triton was used. Treatment with EDTA in wells treated with 1mM CMPD 73 gave average absorbance units of 0.39.

Similar results were obtained for CMPD74, although the effect is not as potent (Figure 2.10). Again, EDTA eliminates the inhibitory effect. Raw absorbance values were also zero following blank subtraction, however 10μM of CMPD 74 did appear to elicit a response giving an absorbance value of 0.483, which is comparable with EDTA-treated wells using CMPD 74 at 100μM (absorbance of 0.432). 1, 10- Phen (data not shown) did not appear to affect LDH activity.

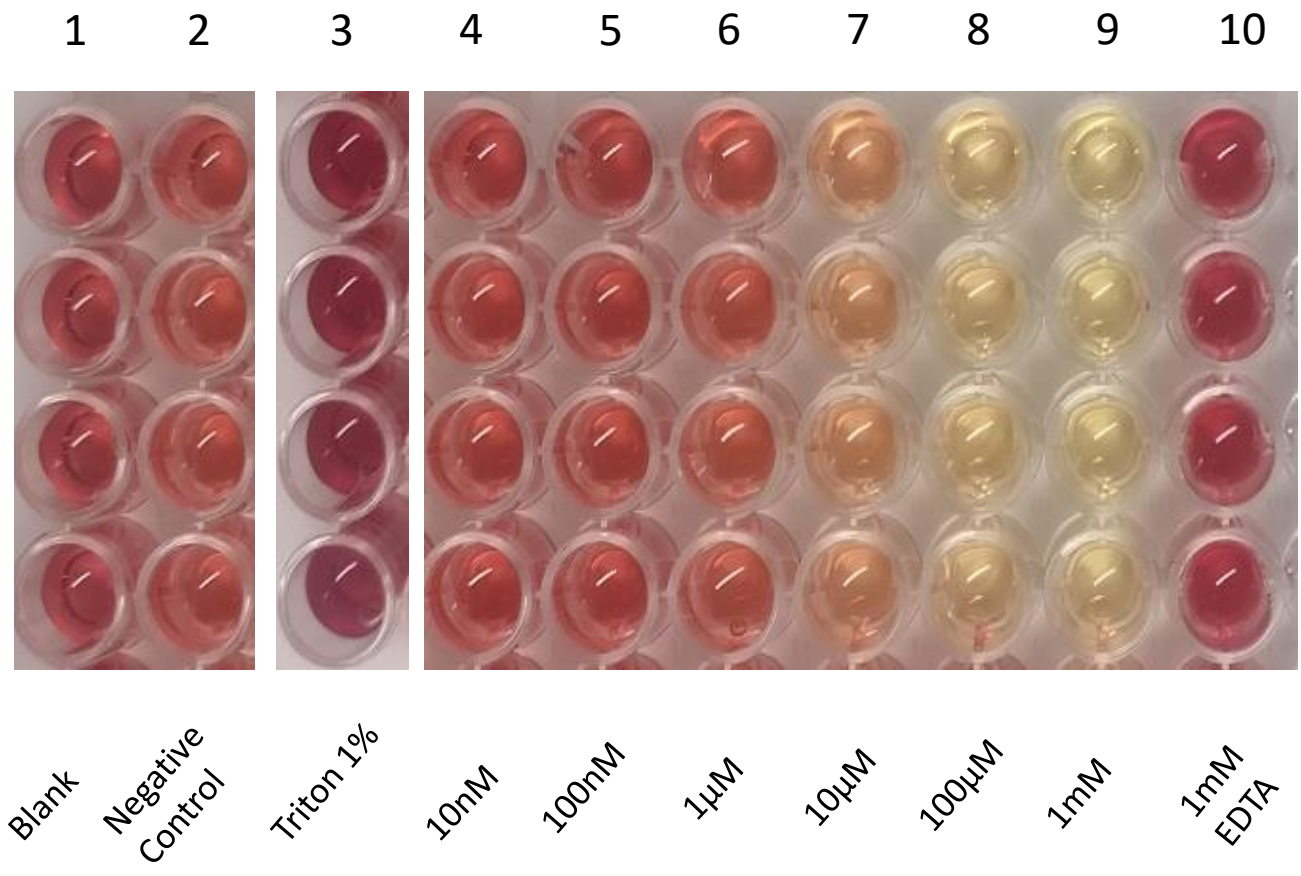

Figure 2.9 Inhibition of LDH activity in A549 cell supernatant by CMPD73. Visualization of LDH enzyme inhibition with increasing concentration of CMPD 73 as seen by loss of colour change of LDH assay reagent, when compared to triton control and EDTA control preserving LDH activity.

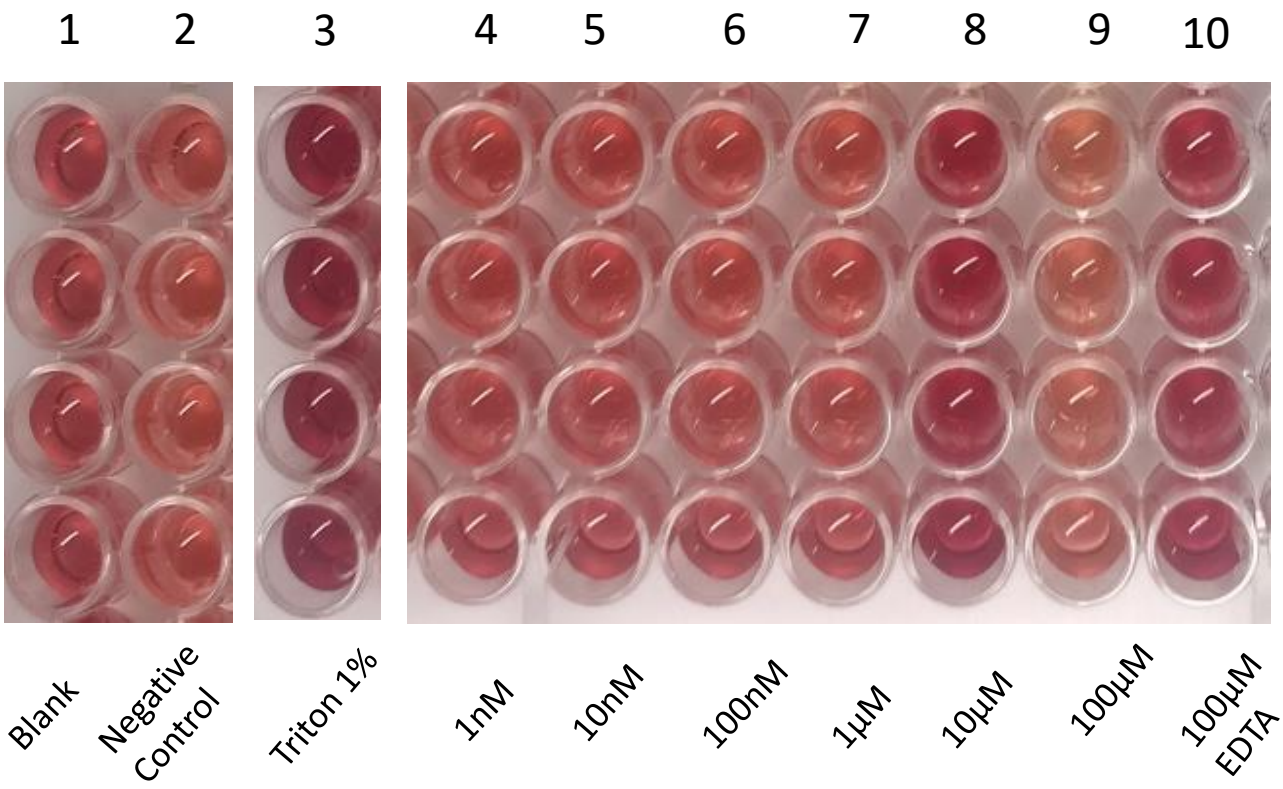

Figure 2.10 Inhibition of LDH activity in A549 cell supernatant by CMPD74.Visualization of LDH enzyme inhibition with increasing concentration of CMPD 74 as seen by loss of colour change of LDH assay reagent, when compared to triton control and EDTA control preserving LDH enzymatic activity in A549 cells.

2.6.3. Mode of cell death – Annexin/PI flow cytometry staining

To determine whether CMPD 73 and 74 were capable of initiating apoptosis as the mechanism through which they kill cancer cells, A2780 ovarian cancer cells were stained with AnnexinV-FITC and PI following 24hr treatment with IC_{50} concentrations of test compounds and Doxorubicin control. AnnexinV-FITC/PI staining utilises a FITC conjugated AnnexinV protein which has a strong affinity towards a plasma membrane phospholipid phosphatidylserine (PS). During apoptosis, PS is flipped from the cytosolic domain of the plasma membrane to the extracellular side of the plasma membrane, where it acts as a recognition marker for phagocytes to engulf apoptotic cells. FITC bound AnnexinV is therefore a useful biomarker for cells undergoing apoptosis. Counter staining with PI, a DNA intercalating fluorescent dye which can only enter the cell upon plasma membrane

permeabilization, can determine whether the cell is in late stage apoptosis where breakdown of the cell membrane is taking place if it is detected alongside AnnexinV-FITC expression. Cells expressing only PI are generally considered to be undergoing necrosis, as lysis of the plasma membrane by necrosis allows entry of PI without the expression of the apoptotic marker PS (Logue, Elgendy and Martin, 2009).

CMPD 73 is seen to significantly induce the apoptosic pathway, as seen in Figure 2.11 (D) and Figure 2.12 demonstrating an increase (22.1%) in cells expressing both AnnexinV-FITC and PI (UR quadrant). Minimal amounts of early stage apoptosis were detected (2.2% LR quadrant), likely a result of longer exposure times to the compound, with shorter exposure times possibly increasing this percentage. Low levels of necrosis were detected (9.8% UL quadrant) indicating that CMPD 73 may induce low levels of necrosis. However this may also be a result of extreme late stage apoptosis owing to the presence of highly permeable apoptotic bodies. It is likely that apoptosis is the main form of cell death through which CMPD 73 exerts its cytotoxic effects.

Similarly, CMPD 74 appears to significantly induce apoptosis over necrosis as its primary mechanism of cytotoxicity, however higher levels of necrosis were detected in CMPD 74 (19.1%) (UL quadrant) when compared to CMPD 73 (9.8%), hinting at induction of necrosis (Figure 2.11E). However, this may again be indicative of very late-stage apoptosis rather than necrosis owing to 24 hr exposure time, as significant detection of late stage apoptosis (52.3% UR quadrant) indicates a high population of apoptotic cells following treatment with CMPD 74.

1,10-Phen is demonstrated to have similar results to CMPD 73 (Figure 2.11 F, Figure 2.12) albeit with a slightly lower level of necrotic cells (4% UL quadrant). Near identical expression of late stage apoptotic cells (21% UR quadrant) is also seen compared to CMPD 73.

Surprisingly doxorubicin, used as an inducer of apoptosis demonstrated higher levels of necrosis (70% UL quadrant) than apoptosis (18% UR quadrant) in A2780 cells (Figure 2.11 C, Figure 2.12), even when used at 0.3µM (55.8% necrosis vs 17.4% late apoptosis, 1-2% apoptosis) Figure 2.11 B). This effect is also seen at concentrations of 0.5 and 1µM (data not shown), further demonstrating that doxorubicin may favour necrosis over apoptosis in the A2780 cell model.

Non-treated control cells (Figure 2.11 A, Figure 2.12) did not demonstrate any significant increases in either apoptosis or necrosis (91.5% viability as seen in LL quadrant). High levels of background fluorescence were detected in non-treated control cells regarding AnnexinV-FITC (up to 10^4 -10^5 fluorescence units), resulting in normalisation of the x-axis.

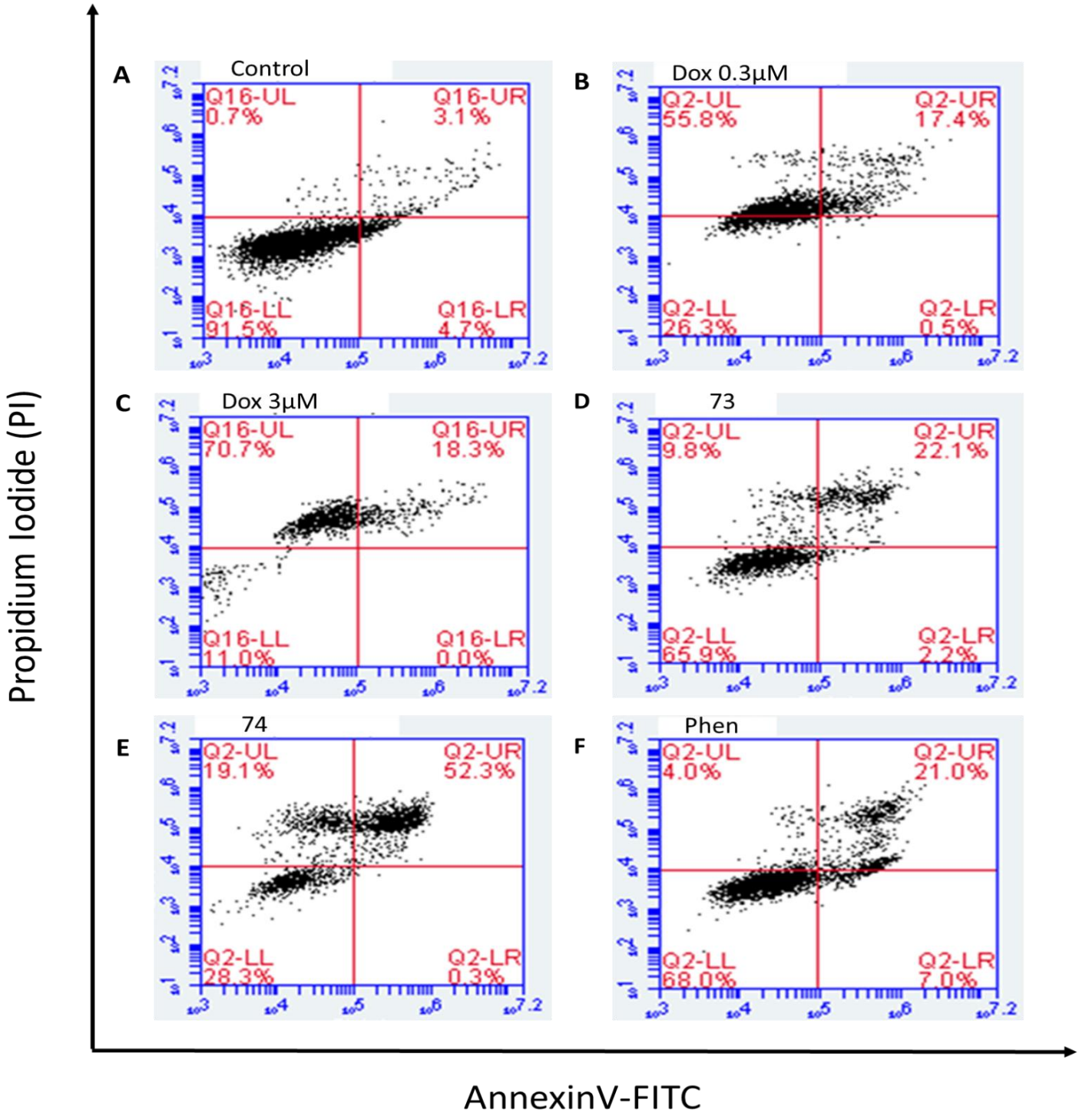

Figure 2.11-Representative data (of three independent experiments) of Annexin-FITC/PI staining of A2780 cells to doxorubicin (0.3µM and 3µM) and CMPDs 73 (45µM), 74 (3µM) and 1,10-Phen (200µM). A) Negative control cells showing no significant increase in Annexin-FITC/PI expression. B) Doxorubicin control showing an increase in expression of late apoptosis (UR quadrant) and necrosis markers (UL quadrant). C) Doxorubicin at higher concentrations showing a similar increase in late apoptosis markers and a significant increase in necrotic markers. D) CMPD 73 displaying an increase in late apoptotic and a moderate increase in necrotic markers. E) CMPD 74 displaying a significant increase in late apoptotic markers and an increase in necrotic markers. F) 1,10-Phen showing an increase in late apoptotic markers and a moderate increase in necrotic markers.

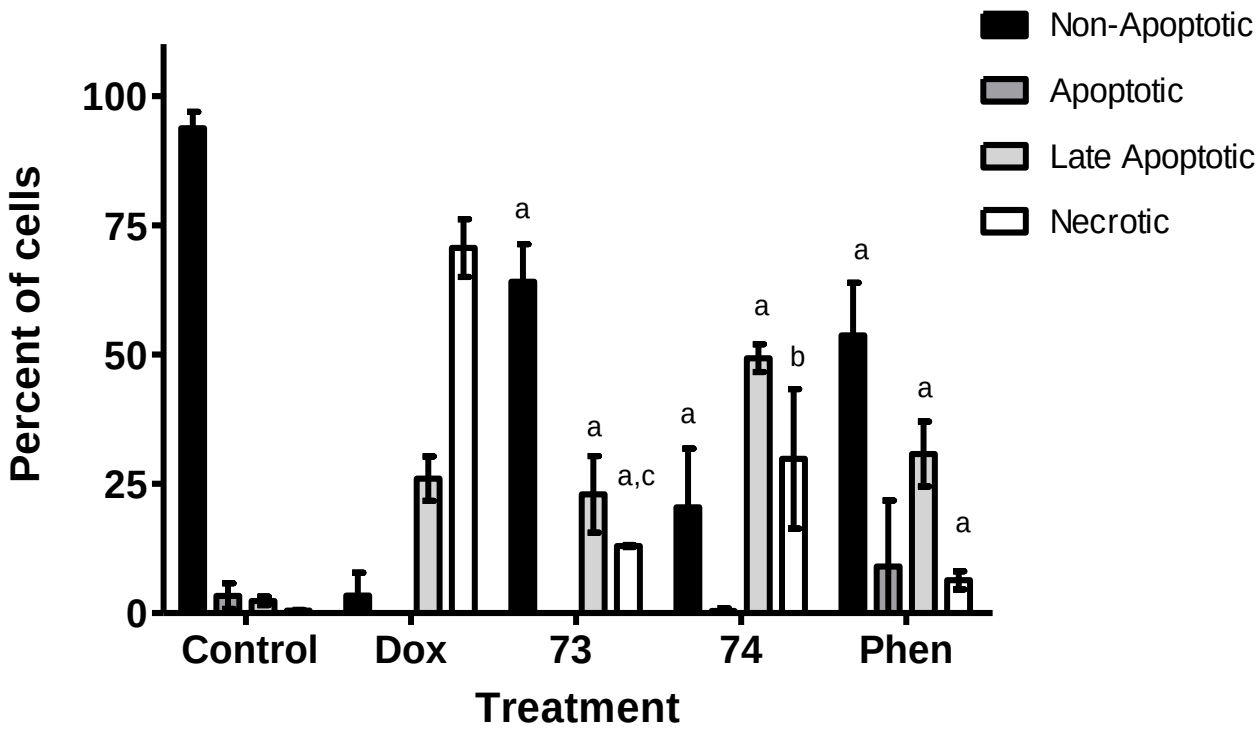

Figure 2.12-Expression of non-apoptotic, apoptotic, late apoptotic and necrotic markers following flow cytometric analysis of A2780 cells exposed to Doxorubicin (3µM), CMPD 73 (45 µM), CMPD 74 (3 µM) and 1,10-Phen (200 µM) stained with Annexin-FITC/PI. (± 1 Standard deviation of three independent experiments using duplicate technical replicates) points of significance calculated using multiple t-test (a= $P<0.01$ compared to control) (b=$P<0.05$ compared to control) (c=$P<0.01$ compared to phen)

2.7.Discussion:

The cytotoxic properties of two new coordination compounds, which incorporate a trioxaundecanedioate rather than an octanedioate acid linker to enhance aqueous solubility, were evaluated. CMPD73 incorporated manganese as a coordinating metal, while CMPD74 incorporated copper. Importantly for cell experiments, these new compounds were found to be readily water soluble, particularly the copper-based compound, in contrast to its octanedioate-based analogue, which is only partially soluble in aqueous media, even following sonication (Kellett *et al.*, 2011).

Both compounds were seen to be effective against a panel of cancer cell lines including cells with a cisplatin resistant phenotype, with CMPD 73 observed to be more active against ovarian, lung and the cisplatin resistant mesothelioma cell line than all other cell systems tested. Apoptosis was identified as the primary mechanism of cell death activated by both compounds, with evidence for compound dissociation as an active part of compound cytotoxicity also observed.

CMPD74 is observed to be significantly more active than CMPD73 in the reduction of resazurin (i.e. the Alamar Blue) assay. Estimated IC_{50} values (24-hour exposure) for CMPD74 were in the low (2-7) micro molar range across all cell types tested, while those for CMPD73 were approximately 45 µM for A2780 (ovarian) and A549 (lung epithelia) cells, and greater than 200µM for the remaining cells lines. Inclusion of HT29 (colonic) cells allowed comparison of the novel compounds described here with their saturated analogues.

The current results were comparable with data previous reported for the octanedioate analogue (Kellett *et al.*, 2011). IC_{50} values for CMPD74 were estimated at 6, 8, 24, and 72

hrs after treatment. Almost identical values for IC_{50} were obtained, indicating that its mode of action is very rapid and intracellular activation, if any, proceeds very rapidly. Use of isogenic cisplatin sensitive and resistant cells revealed an intriguing observation for CMPD73 – in cisplatin resistant cells only, the estimated IC_{50} value (49 µM with 24 hours exposure) were observed to be in the same range as the estimates for A2780 and A549 cells, significantly lower than the IC_{50} for cisplatin sensitive cells. This selectivity disappeared when these cells were exposed to the compounds for 72 hours. The reason(s) for the selectivity towards these cells during short incubations are unclear and warrant further investigation.

Using A549 cells as a model, we combinatorically evaluated the cytotoxic effects of each of the precursors of the coordination compounds. As Figure 2.7 and Figure 2.8 show, the presence of 1,10-phenanthroline is necessary to generate the cytotoxic effects. However, it did not seem to be critical if metal-trioxaundecanedioate complexes or free metals were present. Compared to the presence of free 1,10-Phen there is a modest increase in efficacy for the CMPD73, with a greater magnitude of effect as the concentration of CMPD73 increases. Similar findings were observed for CMPD74, although the increase in efficacy, and concentration effect, were more pronounced. It is interesting to note that CMPD73 is only more effective than 1,10-Phen in the three cell models noted above - A2780, A549 and cisplatin resistant mesothelioma.

Treatment with different coordination complexes has been reported to lead to cell death by a variety of different mechanisms, such as necrosis and apoptosis (Ndagi, Mhlongo and Soliman, 2017). Initial attempts to assess if necrosis is the principal mode of cell death were unsuccessful due to the impact of the compounds on the LDH assay, which assesses

membrane integrity. It has been reported that LDH activity may be reduced by various toxic compounds including menadione (a known superoxide generator), H_2O_2 and cisplatin (Kendig and Tarloff, 2007). In addition, it has been demonstrated in the literature that both copper and manganese ions are able to inhibit LDH enzyme activity (Dobryszycka and Owczarek, 1981; Xue *et al.*, 2014). If the inhibition observed in the cell systems used here is due to release of free metal ions following the dissociation of the compound, then addition of EDTA would be expected to eliminate the inhibitory effect under assay conditions. Indeed, this is the case with the addition of EDTA leading to a restoration of LDH activity, which can be attributed to the sequestration of the metal ions by EDTA (Figure 2.9 and Figure 2.10). Using a modified LDH assay method where a molar excess of EDTA is added before the start of the LDH assay post compound treatment, it appears that significant metabolic effects occur at a much lower concentration than any effects on membrane integrity. Similarly as LDH serves as an intermediate link between glycolysis and the TCA cycle LDH inhibition either by compound activity or dissociation may serve as yet another metabolic mechanism of action. However while interesting, this line of investigation is outside the scope of this thesis. This observation suggests that necrosis may not be the major mode of cell death and that other modes e.g. apoptosis are more likely explanations. Investigations using erythrocytes as model to test effects on membrane integrity are described Chapter 5.

These data are further supported by the significant induction of apoptosis by both CMPD 73 and 74 following the AnnexinV-FITC Dead Cell apoptosis assay. While some significant levels of necrosis were detected, this may be a result of long exposure times allowing accumulation of late stage apoptotic bodies rather than direct induction of necrosis, with the ratio of apoptosis to necrosis favouring apoptosis for both test compounds and 1,10-Phen.

While initially utilised as an apoptotic inducing agent, doxorubicin presented more necrotic cell death than apoptotic death.

Doxorubicin has been demonstrated to be a strong anti-tumour drug and inducer of apoptosis (Pilco-Ferreto and Calaf, 2016). However as the ratio of late stage apoptotic cells to necrotic cells favours necrosis in doxorubicin treated cells at both concentrations, it appears doxorubicin may be more indicative of necrotic rather than apoptotic cell death in the A2780 cell model. Doxorubicin has been reported to induce necrotic cell death through activation of poly-(ADP-ribose) polymerase 1 (PARP1) in HK-2 cells (Shin *et al.*, 2015) and at concentrations exceeding 1μM in A2780 cells (Demoy et al., 2000; Fong et al., 2012). As such the data described demonstrating doxorubicin's effects on necrosis rather than apoptosis will be influenced by the concentrations used. Therefore comparing metal-phen and phen compounds to doxorubicin at necrotic inducing concentrations supports metal-phen mediated apoptosis induction over necrosis, as metal-phen cell populations appear to flux through apoptosis before entering necrotic/late apoptotic stages of cell death. Given the importance of the metal ligand for the overall structure of the novel compounds tested here, examination of the potential involvement of ferroptosis (a metal dependent cell death mechanism) will be prudent to rule out its involvement in mediating the effects described here (Dixon *et al.*, 2012; Feng and Stockwell, 2018).

Comparison of CMPD 73 with 1,10-Phen supports previous observations that much of CMPD 73's cytotoxicity may be driven by the action of 1,10-Phen, with near identical apoptotic and necrotic levels following 24 hr treatment. When present at high concentrations, 1,10-Phen is known to be a protease inhibitor, due to its ability to chelate metals and it has also been widely used as a metal chelator during protein purification processes (Bencini and

Lippolis, 2010). Chelation of metals present within cells (or provided via the cell media) has been shown to lead to the formation of a mixed population of metal-Phenanthroline complexes from 1,10-phenanthroline (e.g. as reviewed McCann et al., 2012), with potential cytotoxic activities. This is supported by the similarity of the cytotoxicity profiles of 1,10-Phen alone and with addition of equimolar amounts of the copper or manganese chlorides (Figure 2.7 and Figure 2.8).

In addition, generation of free 1,10-phen due to partial dissociation of the compound may lead to chelation of free ions such as magnesium or zinc, with potentially broad impacts on metabolic pathways. Magnesium is strongly associated the regulation of multiple enzymes of the glycolytic and oxidative phosphorylation pathways (reviewed Pilchova 2017). Chelation of magnesium by 1,10-Phen has been shown to alter energy metabolism (Laughlin 1996). Many transcription factors and gene regulatory enzymes are zinc-binding proteins (Nyborg 2004). Events such as this may explain why cell viability assays (Alamar blue) detecting a disruption in cellular metabolism are more sensitive at detecting compound effects over cytotoxicity assays such as LDH.

The observed impact of EDTA on the LDH assay is further evidence that there is some increase in the concentration of free metal ions following treatment with the novel compounds. If full dissociation and chelation occur, two moles of 'alternate' metal-phen complexes could be generated for each one mole of compound, potentially doubling the concentration that the cells would be exposed to in this event. Moreover, the typical concentration of copper in A549 cells is in the order of 0.1-0.2 μmol/10^6 cells which would be of a similar order of magnitude to the highest concentration of 1,10-Phen used (González *et al.*, 1999). Intracellular copper content is also known to increase significantly following

exposure to $CuCl_2$ (Rupp *et al.*, 2017). In this context it should be noted that the concentration of iron is approximately 5-6 times higher than that of copper.

However, the greater efficacy of CMPD73 and CMPD74 compared to treatments including free 1,10-Phen support the contention that at least part of the supplied compound remains intact and functional. As 1,10-Phen is thought to contribute significantly to the overall cytotoxicity of the metal-phen compounds a greater increase in cytotoxicity would be expected from compounds containing twice the molar equivalent of 1,10-Phen than 1,10-Phen alone.

Taken together, these data are consistent with the idea that the observed action of the compounds is due to the presence of a mixture of different active agents formed in connection with the interaction of the compounds with biological fluids (Figure 2.13). While the evidence for this viewpoint is indirect, it should be noted that a very recent paper from Nunes *et al.*,(2020) presented detailed speciation data which supports the viability of this viewpoint. In that study, analogous copper-phen compounds decomposed when added mixed with cell media during experimental set-up and a variety of different metal-phen complexes were observed. This supports the proposed pathway outlined in Figure 2.13 and underscores the need to complete detailed speciation work on the current compounds.

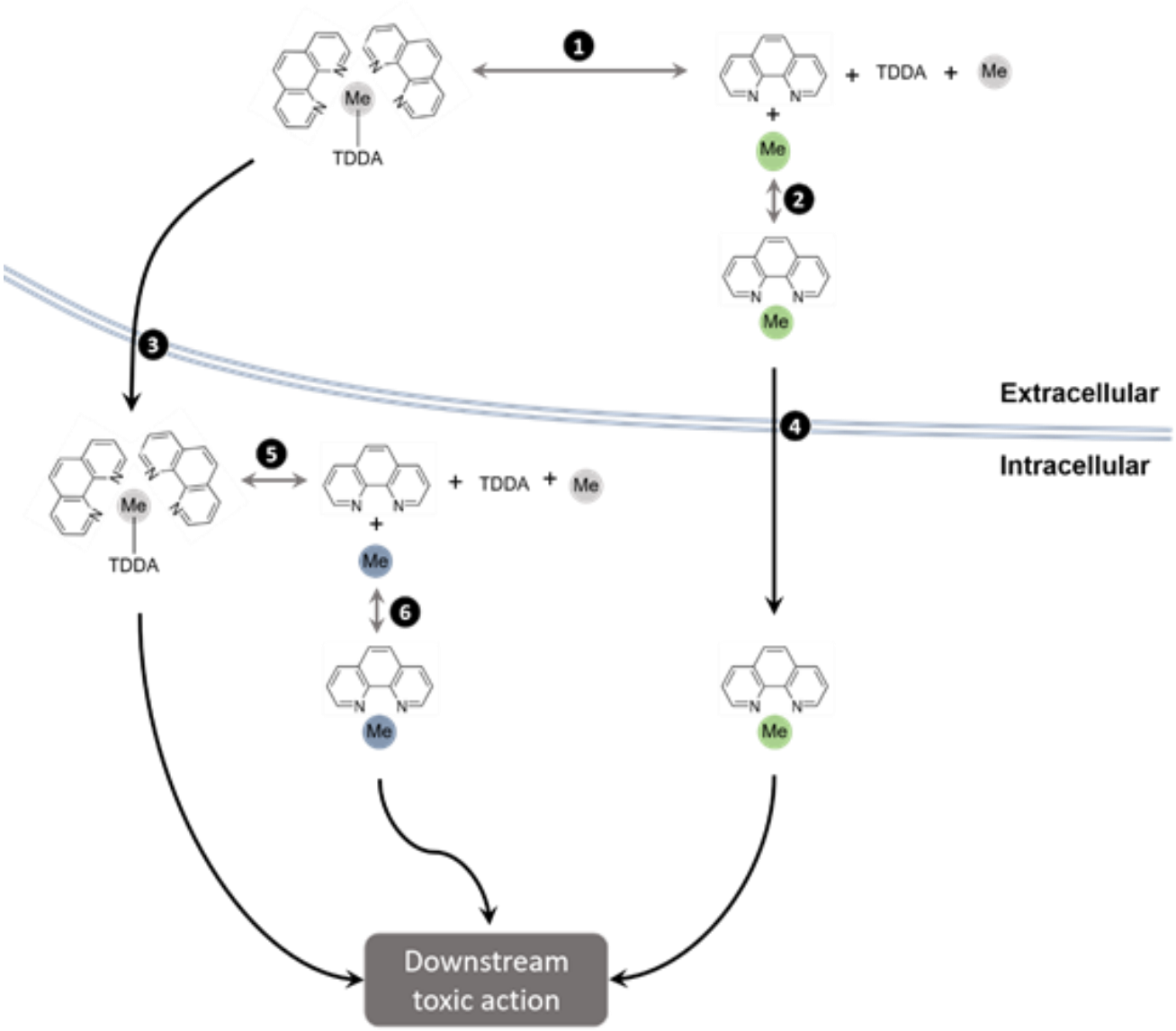

Figure 2.13 Proposed model of pathways of action of metal-phen compounds in cell systems. 1) Dissociation of compound outside of cells to produce 1,10-phen, TDDA and the metal ion, 2) Chelation of metal (either original or alternate) present in cell medium by 1,10-phen, 3) direct uptake of intact compound by cells, 4) direct uptake of 1,10-Phen-metal complex by cells, 5) Dissociation of compound inside of the cell to produce 1,10-Phen, TDDA, and the metal ion, 6) Chelation of metal (either original or alternate) present within the cell by 1,10-Phen. Overall toxic action would be via a combination of various metal-phen complexes, potentially acting via different mechanisms.

3. Epigenetic Chemo-sensitisation strategies

3.1.Epigenetics

Epigenetics is defined as heritable chemical alterations to DNA and its histone or non-histone associated proteins, capable of changing the structure of chromatin, resulting in modulation of gene expression, without changing the DNA code itself (Rivera and Bennett, 2010). It has emerged over the last decade as a key process explaining higher levels of complexity regarding gene expression by offering an extra highly dynamic layer of regulation independent from genes (Cohen *et al.*, 2011). It has been demonstrated as essential for embryonic development, maintenance of specific cell lineages, and overall homeostasis of gene expression in response to environmental changes and cell signalling pathways (Rivera and Bennett, 2010). However it has also emerged as a process deeply involved in the initiation, progression, prognosis and potential treatment for many cancers (Biswas and Rao, 2017). These discoveries have begun to push epigenetics to the forefront of cancer research, acting as a target for the development of novel therapeutics and treatment regimes.

Control of gene expression is carried out by combining the effects of altering the structural properties of packaged DNA (chromatin) and its interactions with various transcription factors through chemical modifications on either the chromatin proteins themselves or the DNA it envelopes. These signals can control mRNA production in its initial stages in response to cellular and environmental factors, and is mediated by the aforementioned processes of chromatin structure alteration, DNA modification and transcription factor binding (reviewed by Brkljacic & Grotewold, 2017).

The most well characterised modifications are (i) DNA cytosine methylation, and (ii) Post Translation Modification (PTM) of the histone octamer, primarily acetylation and

methylation of lysine or arginine residues in the N-terminal tails of histone 3 (H3) and histone 4 (H4) (Gibney and Nolan, 2010). DNA methylation and histone modifications regulate gene expression by altering chromatin between eu- and hetero- chromatin states. They act as transcription factor binding sites, serving as ‘’epigenetic tags’’ for gene activation or repression (Rodenhiser and Mann, 2006).

Initially, DNA and histone lysine methylation were associated with gene silencing, while DNA demethylation and histone lysine acetylation were associated with gene activation. However, it is now recognised that acetylation and methylation of lysine residues can act in a synergistic and context dependant manner to either contribute towards gene activation or repression, and form what has now been termed as the ‘’Histone Code’’ (Cosgrove and Wolberger, 2005). The most dynamic of epigenetic marks that make up this code are histone modifications. The ‘’Histone Code’’ is written by either epigenetic writers or erasers, being either transcriptionally active or repressive depending on their effects on chromatin structure (Morera, Lübbert and Jung, 2016). The dynamic action of the ‘’Histone Code’’ can be visualised in Figure 3.1. Of primary interest for this project is the process of histone lysine acetylation, written by Histone Acetyltransferase (HATs) and erased by Histone De-Acetylases (HDACs).

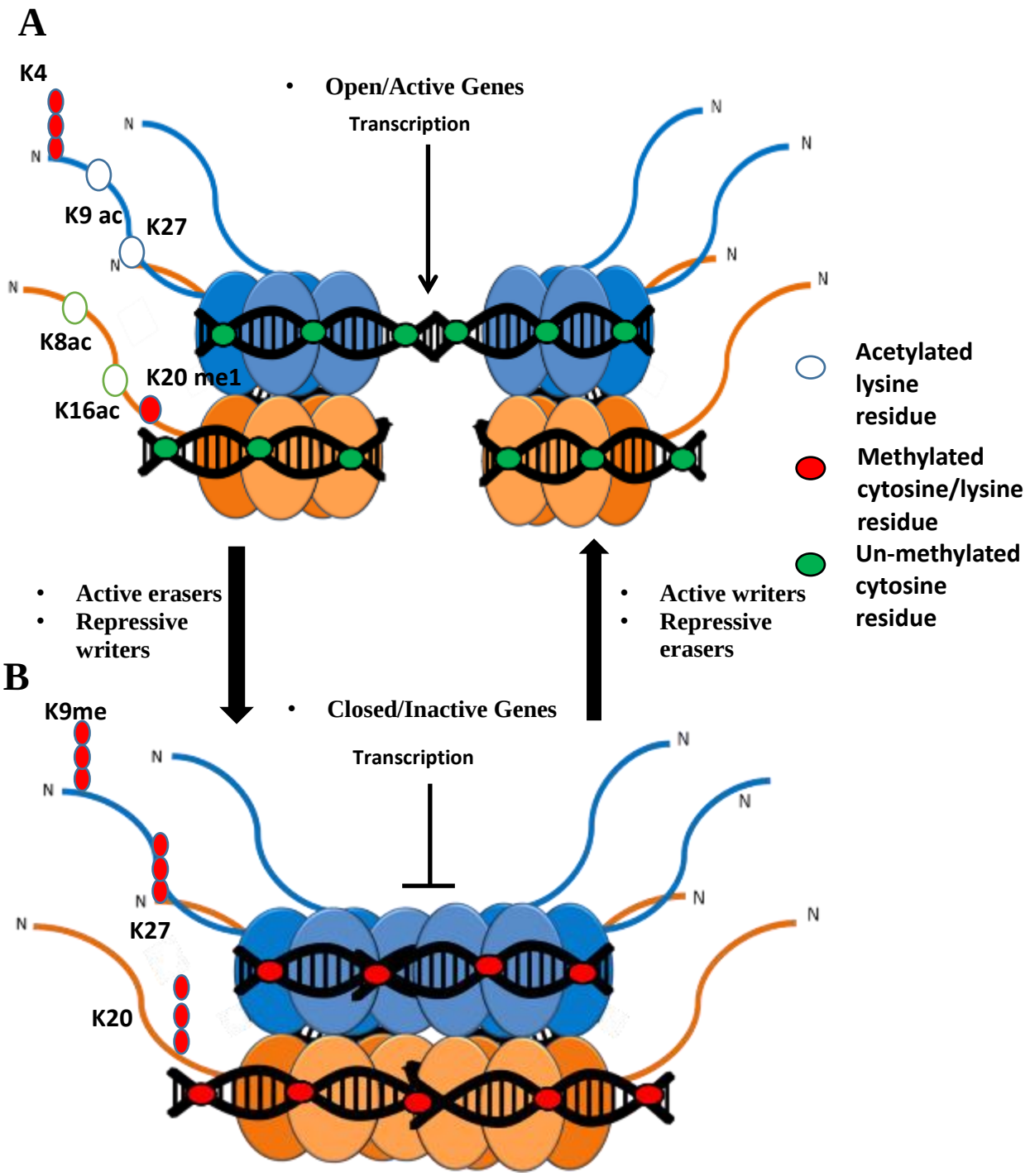

Figure 3.1 Overview of chromatin dynamics.(A) Chromatin (blue and orange circles with extending N-terminal tails) and DNA structure (in black) in an open configuration as a result of activating lysine marks laid down by transcriptionally active epigenetic writers. This specific acetyl, methyl lysine modifications along with hypomethylated DNA allow for the access and binding of transcription factors to begin transcription. (B) Closed inactive chromatin/DNA structure as a result of removal of activating acetyl- lysine modifications by Active Erasers, and the laying down of transcriptionally inactive methyl marks by repressive epigenetic Writers. The removal of acetyl groups condenses the chromatin, while specific methyl groups on specific lysines found in histone tails and cytosine bases of DNA either prevent transcription factors or bind transcriptional repressors. These combined with the closed chromatin state prevent any transcription from taking place. This figure was self-generated using Microsoft PowerPoint based on the current understanding of knowledge from a multitude of sources.

3.1.1. Histone Lysine Acetylation/De-acetylation:

Acetylation of H3 or H4 lysine residues is one of the primary drivers of histone associated gene regulation. Acetylated and de-acetylated lysine residues can rapidly switch chromatin between open and active states, and closed and repressive states, depending on how the histone code is incorporated (Dancy and Cole, 2015). HATS transfer an acetyl unit from the acetyl-coenzyme A donor to the ε-amino group of the target lysine residue, which confers an overall net negative charge to the core histone complex (Allfrey, Faulkner and Mirsky, 1964). DNA is a negatively charged molecule and so is repulsed by the negative histone, leading to the opening of the nucleosome structure into euchromatin. This allows the easy access of transcription, replication, recombination and repair factors via bromodomain containing proteins that bind acetyl-lysine (Bedford and Brindle, 2012).

The removal of an acetyl group by HDACs diminishes the net negative charge of the histone complex and DNA, and causes the nucleosome to revert to a compact and silenced heterochromatic state (Rivera and Bennett, 2010). Examples of the most characterised acetylation sites that are strongly associated with both activation and repression have already been seen in Figure 3.1. In conjunction with targeting chromatin structure, both HATs and HDACs can target non-histone protein targets (NHPTs) in the nucleus or cytoplasm. This can in turn have further up-stream or down-stream effects on gene expression and cellular homeostasis (Wapenaar and Dekker, 2016).

Four classes of HDAC's are known to exist, and can be divided into zinc dependent (Classes I, II, and IV) or NAD+ dependent (Class III) groups (Micelli and Rastelli, 2015). Class I HDACs comprise of HDACs 1, 2, 3 and 8 and are localized in the nucleus (Verdone, 2006). Class II HDACs are divided into sub-class IIa (HDACs 4,5,7 and 9) and subclass IIb

(HDACs 6 and 10) and shuttle between the nucleus and cytoplasm upon certain cellular signals and are expressed in a limited number of human tissues (Verdone, 2006).

Class IV contains only HDAC11, while Class III HDACs consist of seven enzymes known as sirtuins (Sirt1, 2, 3, 4, 5, 6 and 7) (Delcuve, Khan and Davie, 2012). As a result of their dependency on NAD+ over zinc, sirtuins are structurally and mechanistically very different from the other 3 classes of HDACs, and are involved in a broader range of cellular processes and pathways (Dang, 2014). With regards to disease initiation and progression, it is primarily the zinc dependent HDACs (class I, II, IV) which have been studied most extensively, *cf* below.

HATs can be classified into two groups, group A HATs located in the nucleus and group B HATs located in the cytoplasm. While these two families play pivotal roles in gene regulation and can themselves be a source of disease propagation, they are not a direct line of inquiry for this project, and so will not be discussed further.

3.1.2. Cancer Epigenetics

Cancer cells were originally thought to arise as a result of genetic mutations which increased the function of oncogenic genes and decreased the function of Tumour suppressor genes (TSP), resulting in loss of chromosomal stability and uncontrolled cell growth. However, it has emerged that genetic alterations to DNA alone do not account for the complexity seen in tumour cells, and so epigenetics seems to be the key explanation to this underlying problem. The spontaneous mutation rate of a cell is estimated to be 10^{-10} mutations per nucleotide base pair per division, whereas the rate for gaining or losing methylation is estimated to be 2×10^{-5} per CpG site per division (Yatabe, Tavare and Shibata, 2001). Since

DNA methylation and histone modifications are so closely linked, alteration of one pathway will have substantial effects on the other. This indicates that epigenetic dysregulation is a far more likely candidate for the initiation of cells to undergo oncogenic transformation than by acquiring genetic mutations alone, and aberrant epimutations have been implicated in the early stages of initiation and progression of a vast number of cancers (Sharma, Kelly and Jones, 2009).

These epimutations primarily manifest as global hypomethylation of gene promoters (including many oncogenic promoters) (Feinberg, 2005) and site-specific hyper methylation of other gene promoters, primarily in regulatory regions of TSP Genes (Barradas *et al.*, 2009). Over 300+ genes have been seen to be altered in various forms of cancer as a result of altered methylation patterns and DNA methylation patterns, with 5%–10% of normally un-methylated CpG promoter islands becoming abnormally methylated in various cancer genomes (Dawson and Kouzarides, 2012). Another epigenetic alteration seen in cancers is the dysregulation of histone modifying enzymes, primarily HDACs, as they interact intimately with the DNA methylation network, and result in global loss of acetylation patterns, and alterations of Histone acetylation patterns (Kanwal and Gupta, 2012).

3.1.3. Dysregulation of Histone modifications:

The hallmark changes to histone modifications seen in cancer are primarily global loss of acetylated Histone 4 lysine 16 (H4K16ac) and Histone 3 lysine 9 acetylation (H3K9ac) and an increase in H3K9 and H3K27 tri-methylation patterns, associated with aberrant gene silencing (Sharma, Kelly and Jones, 2009).

The global loss of H4K16ac and other important acetyl histone tags is primarily as a result of either HDAC over expression or increased HDAC activity, both causes of which are seen

in various cancers (Yixuan and Seto, 2016). A list of class I and class II HDACs and their associated cancers can be seen in Table 3.1.

Table 3.1 Association of class I and II HDACs overexpressed in different cancers. Data from (Yixuan and Seto, 2016).

HDAC member	**Associated cancer**
HDAC 1	Liver, colorectal, breast, ovarian, prostate, renal, bladder, Acute Lymphoblastic Leukaemia (ALL), Chronic Lymphocytic Leukaemia (CLL)
HDAC 2	Liver, pancreas, colorectal, breast, ovarian, prostate, renal, bladder, ALL, Cutaneous T-Cell Lymphoma (CTCL), Diffuse Large B-Cell Lymphoma (DLBCL)
HDAC 3	Liver, colorectal, breast, ovarian, prostate, bladder, melanoma, ALL, CTCL, DLBCL, Hodgkin's Lymphoma (HL)
HDAC 4	Acute Myelogenous Leukaemia (AML), ALL, bladder
HDAC 5	Colorectal, breast, bladder, ALL, AML
HDAC 6	Liver, pancreatic, breast, ALL, CLL, DLBCL, CTCL
HDAC 7	Pancreatic, colorectal, bladder, ALL, CLL
HDAC 8	Melanoma, bladder, ALL
HDAC 9	ALL, CLL
HDAC 10	CLL, cervical

De-acetylation of histone and non-histone proteins (e.g. certain transcription factors) results in the silencing of various genes, which are involved in the regulation of the cell cycle, apoptosis induction or repression, DNA-damage response, metastasis, angiogenesis, and other cellular processes (Yixuan and Seto, 2016). How HDACs are targeted specifically to this subset of genes is not yet known.

HDAC activity promotes cell cycle progression through G1/S phase of the cell cycle by decreasing the expression of various cell cycle regulators such as p21WAF1/CIP1, p27KIP1, and p57KIP2(Yamaguchi et al., 2010; Zupkovitz et al., 2010). HDACs regulate apoptosis through inhibiting the expression of pro-apoptotic genes such as PUMA, Bax, and Apaf-1,

while increasing the expression of anti-apoptotic such as the anti-apoptotic Bcl-2 family of proteins (Yixuan and Seto, 2016).

During the DNA damage response (DDR), HDACs facilitate chromatin remodelling and the binding of DDR proteins, such as non-homologous end joining (NHEJ) proteins, ataxia telangiectasia and Rad3-related protein (ATR), Ataxia-telangiectasia mutated (ATM) and BRCA1 (Yixuan and Seto, 2016). An increase in DDR mechanisms allows cancer cells to favour repair and survival over apoptosis through suppression of apoptotic signalling and is also implicated in the development of resistance of cancer cells towards DNA damaging chemo or radiotherapy treatments (Davalli *et al.*, 2018).

Cancer cells exploit the dynamic properties of epigenetic mechanisms such as histone acetylation or DNA cytosine methylation to quickly alter their expression profiles to generate resistant phenotypes against radio/chemotherapeutics. Examples of this would be the de-methylation of the promotor for the Multidrug Resistant Protein (MDR1) (Sharma *et al.*, 2010), the aforementioned increase in DDR by HDACs, and HDAC repression of genes responsible for maintaining cell lineage, causing de-differentiation and inducing increased resistance to chemo/radio therapies (Brown *et al.*, 2014).

3.1.4. Small molecule epigenetic regulators:

Over the last decade many small molecule inhibitors targeting either all or specific HDACs/ HDAC families have come to the forefront of cancer research, with some gaining FDA approval. The disruption of HDACs and the resulting alterations regarding acetylation levels in cancer cells have shown promising results in the treatment of various cancers, primarily haematological cancers. HDACi can be broken down into members of four classes of

compounds: (i) hydroxamic-acids (hydroxamates), (ii) aliphatic acids, (iii) benzamides and (iv) cyclic tetrapeptides (reviewed Stiborova *et al.*, 2012).

Of note for this project is suberoylanilide hydroxamic acid (SAHA), also known as vorinostat, belonging to the hydroxymate class of inhibitors, and Valproic acid (VPA), and Sodium Phenylbutyrate (SPB), which are aliphatic acids. All three are Zinc dependant HDACi, with SAHA being a pan inhibitor targeting classes I, II, and IV of HDACs, and VPA and SPB targeting class I and class IIa (Kim and Bae, 2011). The structures of SAHA, VPA, and SPB are shown in Figure 3.2.

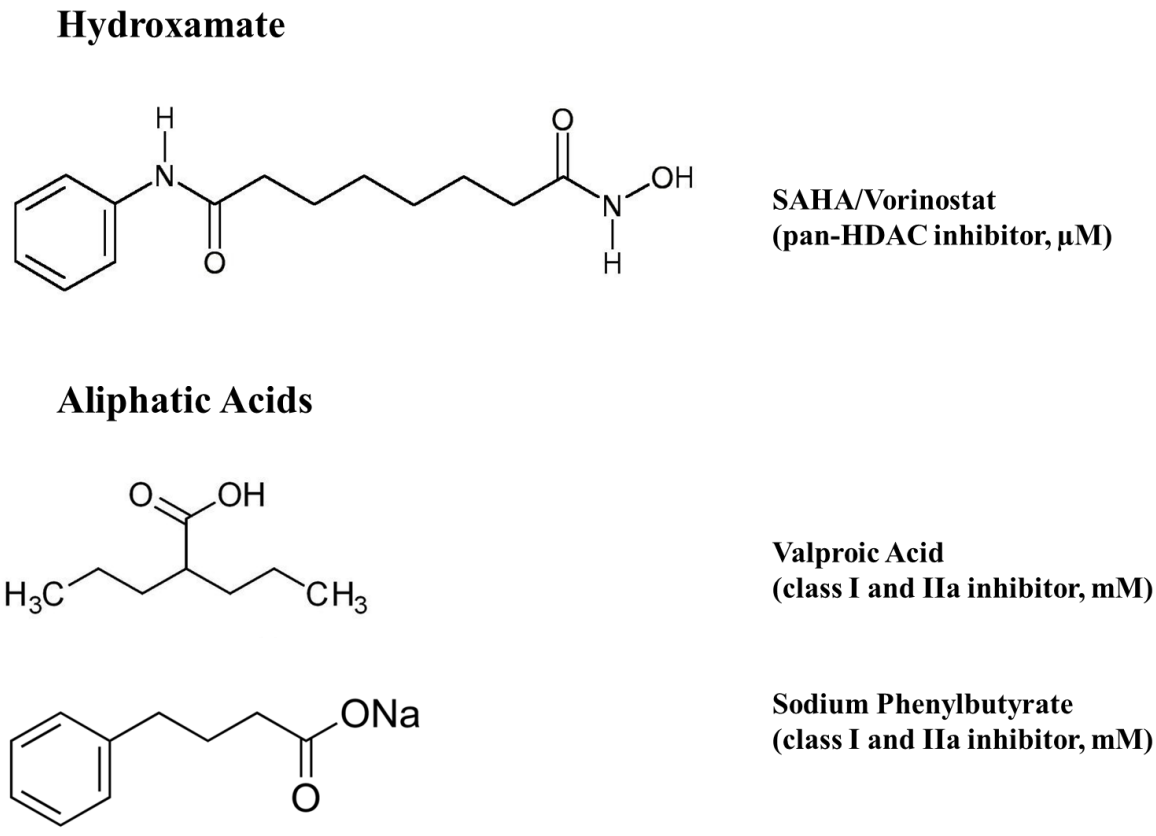

Figure 3.2 Chemical structures of SAHA, VPA and SPB with (from left to right) enzyme binding group, spacer group, and zinc chelating group (Kim and Bae, 2011).

The effects of HDACi are attributed to re-establishing normal apoptotic, cell cycle, DDR, and intracellular regulatory signalling pathways, which is usually as a result of restoration of normal NHPT acetylation status which regulate these pathways (reviewed Stiborova *et al.*, 2012). An example of this would be the acetylation and stabilisation of the TSP p53, which is then capable of increasing the expression of these target genes, as well as inhibiting anti apoptotic proteins (Reed and Quelle, 2014).

SAHA, which was FDA approved in 2006, has seen remarkable success in the treatment of cutaneous T-cell lymphoma (CTCL), and has been entered into clinical trials for the treatment of other cancers such as Acute Myeloid Leukaemia (Mann *et al.*, 2007). SAHA has been demonstrated to induce growth and cell cycle arrest in both a multitude of cancer cell lines as well as *in vivo* rodent models, primarily through transcriptional activation of cell cycle control and apoptotic genes and transcriptional repression of mitotic genes (Richon, 2006). SAHA has also been demonstrated to result in an increased production of ROS and apoptosis induction in acute myeloid leukaemia cells (Petruccelli *et al.*, 2011) as well as increased ROS production accompanied by DNA damage (Brodská and Holoubek, 2011). However SAHA has also been demonstrated to induce the expression of the antioxidant Nrf2 pathway, indicating that cell type specific effects are likely present (Xu *et al.*, 2018).

Despite initial pre-clinical success in both *in vitro* and animal models however, data from clinical trials using SAHA to treat breast, colorectal, non-small cell lung and other various other solid tumours have met with little to no success (Kim and Bae, 2011). This has led to the investigation of poly-therapies using SAHA and chemotherapeutic agents as potential avenues of treatment for solid tumours.

It was demonstrated that treatment with HDACi significantly increased the cytotoxic effects of all the anti-cancer agents used, with no added effect seen in non-cancerous cells. This demonstrated the potential for combining HDACi with mainstream chemotherapy for targeted treatment of cancer cells (Kim *et al.*, 2003).

VPA, FDA approved in 2008 for the treatment of epilepsy, induces differentiation, growth arrest, and apoptosis in a broad spectrum of transformed cells through HDAC inhibition (Vandermeers *et al.*, 2009). VPA when combined with cisplatin was capable of increasing cytotoxicity on both cisplatin sensitive and resistant ovarian cancer cell lines, through upregulation of TSP PTEN, DNA repair and apoptotic signaller ATM, and through accumulation of ROS (Lin *et al.*, 2008). The re-sensitisation of an otherwise resistant cell line to chemotherapy offers HDACi combination therapy as a strong candidate for the treatment of chemotherapy resistant tumours. As well as inhibiting HDACs, VPA can act as an inhibitor of voltage gated sodium channels and can affect metabolic enzymes and processes such as the tricarboxylic acid cycle (Ghodke-Puranik *et al.*, 2013).

Sodium phenylbutyrate, while not yet having FDA approval, has been seen to demonstrate very similar results to VPA due to shared structural similarities. SPB as a monotherapy has been demonstrated to suppress both proinflammatory molecules and ROS as well possessing HDACi properties (Roy *et al.*, 2012). A study conducted that used both *in vitro* and *in vivo* models investigating interaction between SPB and cisplatin, found that combined treatment increased cisplatin's cytotoxic effect in HeLa cells, and increased the survival of albino mice transfected with Ehrlich ascites tumour. SPB treatment was also seen to cause hyper acetylation of H4 in regions of heterochromatin, and was associated with the reactivation of apoptotic control genes (Koprinarova *et al.*, 2010).

The value of combined epigenetic therapies as novel cancer treatments has been clearly demonstrated by almost a decade of experimentation. However acquired resistance to chemotherapy persists, despite the progress of some epigenetic combinatorial treatments. As highlighted previously the ability of cytotoxic metal-based drugs to mediate cell death in cisplatin resistant cell systems supports the notion that novel metal-based drugs can circumvent mechanisms of resistance. Combinatorial treatment with such drugs and epigenetic regulators may provide a novel mechanism to potentiate drug efficacy. This is the subject of the current work.

3.2.Aims

This chapter reports the results of experiments that aim to investigate whether the metal-phen compounds of interest are available for epigenetic chemosensitisation with three different HDACis SAHA, VPA and SPB. As these compounds are hypothesised to target DNA as a primary mechanism of action it would be expected that chromatin relaxing agents such as HDACi would sensitise cells to DNA damaging drugs by allowing greater access to the DNA target.

3.3.Methods

3.3.1. Combinatorial treatments of HDACi and metal-phen compounds

To determine the presence of potential epigenetic enhancing effects in combination with novel metal-based anti-cancer drugs, cell viability assays were used to screen epigenetic regulators and novel metal-based drugs against CS and CR mesothelioma cells. HDACi have been demonstrated to reverse chemo-resistant phenotypes to sensitive states (Vandermeers *et al.*, 2009; Diyabalanage, Granda and Hooker, 2013) and as such these isogeneic cells offered an extra point of comparison regarding novel metal-based compound efficacy against resistant cancer cells. A2780 (ovarian) and A549 (lung) cancer cells lines were also used in certain circumstances to further investigate epigenetic effects in different cell lines.

HDACi which appeared to enhance test compound cytotoxicity were then the focus of further investigation. Optimised resazurin reduction assays, as described in section 2.5.1 above were used to estimate the IC_{50} for compounds in the presence and absence of various epigenetic modulators (SAHA, SPB, VPA). Fold change in IC_{50} value was used to evaluate impact of treatment.

The treatment protocol for each experiment can be seen in Figure 3.3. Screening of HDACi was conducted as both co-treatments and pre-treatments (4hrs) with CMPD 73, 74, and CMPD 19 (described in Chapter 1 and by (Kellett *et al.*, 2011; Slator *et al.*, 2017). Control experiments utilising cisplatin and HDACi were conducted over a 72hr timescale, in accordance with the timescale cisplatin was seen to become active in mesothelioma cell lines (mentioned in section 2.6.1).

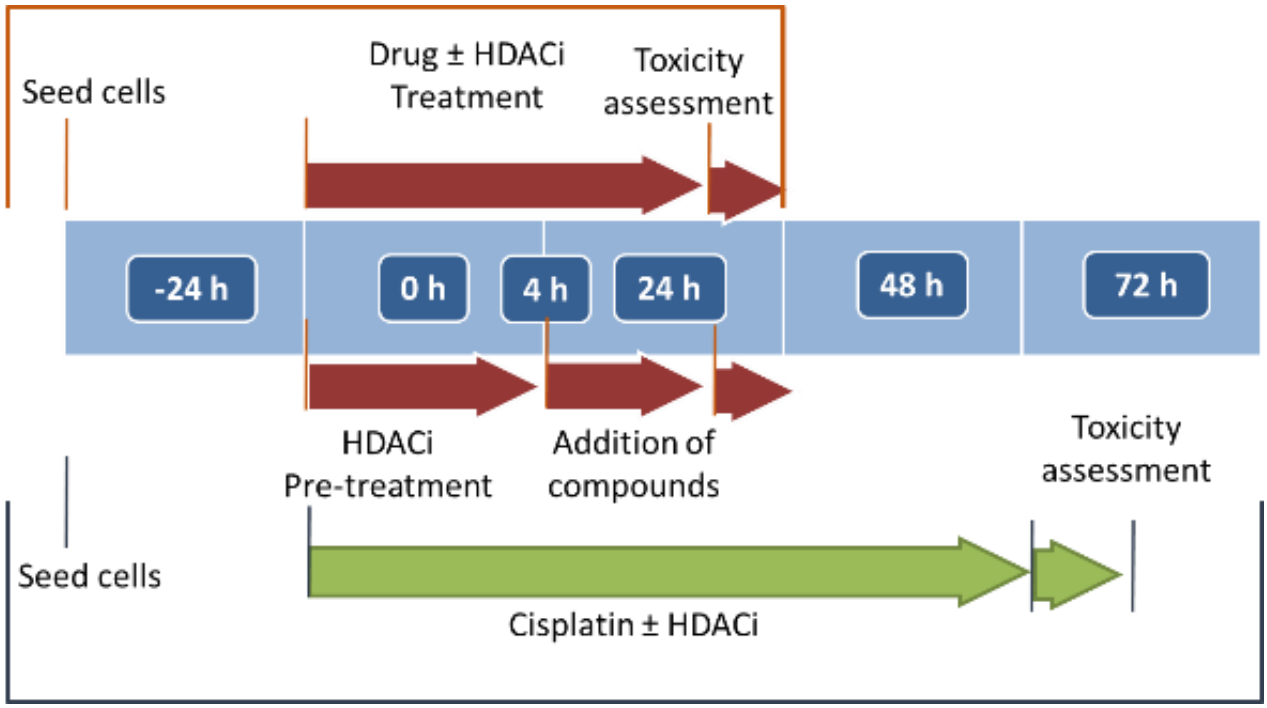

Figure 3.3 Treatment protocols for novel metal-based drugs and cisplatin with HDACi epigenetic regulators

3.3.2. Western Blot

To determine that HDAC inhibition had taken place in response to specific inhibitors, western blot analysis on purified histones from cells treated with SAHA and VPA was conducted. Due to the government restrictions in response to the Coronavirus outbreak and university closures investigating SPB using western blot was no longer possible. Histone 4 Lysine 16 acetylation (H4K16ac) levels were used as a biomarker for HDAC inhibition, as increased levels of H4K16ac have been associated with open chromatin states and increased gene expression (Shogren-Knaak *et al.*, 2006).

Briefly A549 cells were plated in duplicate in 6well plates and treated with SAHA (5µM) and VPA (5mM) for 24hrs. Cells were then lysed, and histones purified by acid extraction

as per protocol from Shechter *et al.*, (2007). Histone concentration was then determined using the Bradford assay.

20µg of histones were then loaded in triplicate wells of a 15% SDS gel and electrophoresed at 130V for 90mins and transferred onto nitrocellulose membrane (BioRad, 0.45µm) using a BioRad Turbo Blot semi-dry transfer system (25V, 7mins). The membrane was then blocked for 1hrs using 5% Non-Fat dry milk (NFDM). Membrane was washed once following blocking with TBST and incubated with Rabbit Anti- H4K16ac antibody (Merck-Millipore 07-329) 1:10,000 dilution in 2.5% NFDM overnight at 4°C under constant rotation.

The membrane was washed for 10mins (x3) with TBST and incubated with anti-rabbit goat secondary antibody (Sigma) 1:5000 in 2.5% NFDM for 1hr under constant rotation. The membrane was washed for 10mins (x3) with TBST, and then incubated with ECL buffer for 3mins and chemi-luminescence was analysed.

Histone loading concentration was optimised before experimentation to ensure optimal image output and prevent over saturation of the membrane blot. Total Protein Normalisation (TPN) was done using SDS-PAGE bromophenol blue staining of the SDS gel post transfer and calculated using ImageJ software. TPN using the PonceauS stain was conducted however was not used for normalisation due to issues with sensitivity. Combined signal of histones H3, H2B, H2A and H4 bands were used for TPN.

Briefly, background signal was subtracted from the combined signal intensities of H3, H2A, H2B and H4 for each lane. These were then normalised according the highest signal intensity

to determine differences in protein loading onto the SDS gel. Signal intensity for bands apparent in western blot images were subjected to the same background subtraction methodology as histone bands from SDS gel images. Each western blot band was then normalised to its corresponding SDS histone bands, which were then averaged to calculate the average change in acetylation levels relative to conditions.

3.3.3. Statistical analysis

All data was analysed using GraphPad Prism Version 5.0.0. and Microsoft excel. Statistical analysis was conducted using students T-Tests and expressed as a P Value < 0.05, 0.01, 0.001. Statistical analysis was conducted on mean IC_{50} values of biological replicates identified.

3.4.Results:

3.4.1. Treatment with CMPD 19 and epigenetic regulators:

CS meso and CR meso, A549 alveolar and A2780 ovarian cancer cells were exposed to CMPD19 with or without the addition of SAHA (5μM), VPA (5mM) or SPB (5mM) for 24hrs to generate IC_{50} values (Table 3.2). SAHA reduced cell viability by 11% in CS Meso. cells and by 27% in CR. Meso cells. VPA increased cell viability by 7% in both cell lines, with SPB increasing viability by 24% also in both cell lines.

Table 3.2 Estimated IC_{50} Values for CMPD19 combined with HDACi with 24h treatment

Compound	**Mean IC_{50} μM (95% CI)**	
	CS Meso.	CR Meso.
CMPD19	60 (46-75)	28 (18-38)
CMPD19+ SAHA	50 (38-65)	42 (36-48)
CMPD19 + VPA	35* (26-44)	38 (29-46)
CMPD19 + SPB	57 (42-72)	39 (31-47)

* Significantly different from compound control, $P<0.05$.

Co-treatment with SAHA or SPB had no effect in any of the cell systems tested, indicating that there is no obvious complementary effect between CMPD19 and these HDACi compounds under the conditions used. There is a modest but statistically significant ($P<0.05$) decrease in IC_{50} value in the presence of 5mM VPA, which may indicate a possible relationship between CMPD 19 and VPA. Treatment with SAHA in A549 lung adenocarcinoma cells also failed to yield an effect, as did VPA treatment in A2780 cells. In some experiments, a four-hour pre-treatment of SAHA and VPA was carried out in CS meso. and CR meso cells, with little or no additional effect on IC_{50} values (results not shown).

3.4.2. Treatment with CMPD 73 and epigenetic regulators

In similarity with the conditions noted in 3.4.1 above, CS meso and CR meso, A549 alveolar and A2780 ovarian cancer cells were exposed to CMPD73 with or without the addition of SAHA (5μM), VPA (5mM) or SPB (5mM) for 24hrs to generate IC_{50} values (Table 3.3). SAHA reduced cell viability by 11% in CS Meso. cells and by 27% in CR. Meso cells. VPA increased cell viability by 7% in both cell lines, with SPB increasing viability by 24% also in both cell lines.

Table 3.3 Estimated IC_{50} Values for CMPD 73 combined with HDACi with 24h treatment

Compound	**Mean IC_{50} μM (95% CI)**	
	CS Meso.	CR Meso.
CMPD73	300 (244-402)	48 (37-58)
CMPD73+ SAHA	240 (111-356)	58 (43-73)
CMPD73 + VPA	42* (32-52)	52 (43-60)
CMPD73 + SPB	55* (43-68)	42 (27-57)

* Significantly different from control, $P<0.01$.

No significant change in IC_{50} values is observed following treatment of any cell system with SAHA. However, significant decreases (approximately one order of magnitude) in IC_{50} were noted in CS Meso. cells following treatment with the aliphatic acids VPA (5mM) or SPB (5mM) and CMPD73. In contrast, there is no effect in CR Meso. cells which suggests a mechanistic link between mechanisms of cisplatin resistance and sensitivity to HDACi chemo sensitisation. Treatment with SAHA in A549 lung adenocarcinoma cells also failed to yield an effect, as did VPA treatment in A2780 cells. These data suggest that CMPD73 may be a candidate for epigenetic chemo sensitisation approaches.

3.4.3. Treatment with CMPD74 and epigenetic regulators

In similarity with the conditions noted in 3.4.1 above, CS meso and CR meso and A549 alveolar cancer cells were exposed to CMPD74 with or without the addition of SAHA (5μM), VPA (5mM) or SPB (5mM) for 24hrs to generate dose response curves and IC_{50} values (Table 3.4). SAHA reduced cell viability by 11% in CS Meso. cells and by 27% in CR. Meso cells. VPA increased cell viability by 7% in both cell lines, with SPB increasing viability by 24% also in both cell lines.

Table 3.4 Estimated IC_{50} Values for CMPD74 combined with HDACi with 24h treatment.

Compound	**Mean IC_{50} μM (95% CI)**	
	CS Meso.	CR Meso.
CMPD74	3.0 (2.5-3.3)	2.6 (2.3-2.8)
CMPD74+ SAHA	3 (2.4-3.3)	2.7 (2.4-3.1)
CMPD74 + VPA	4.3 (4.0-4.6)	3.7 (3.4-3.8)
CMPD74 + SPB	5.0 (4.5-5.4)	4.0 (3.8-4.2)

No significant change in IC_{50} values is observed following treatment of any cell system with any of the HDACi compounds. This may be explained by the already low IC_{50} for CMPD74. In some experiments, a shorter eight-hour treatment was carried out in CS meso. and CR meso cells (Table 3.5) There is no enhancement of cytotoxicity under these conditions. Treatment with SAHA in A549 lung adenocarcinoma cells also failed to yield an effect.

Table 3.5 Estimated IC_{50} Values for CMPD74 combined with SAHA with 8h treatment. SAHA reduced cell viability by 8% in both cell lines.

Compound	**Mean IC_{50} μM (95% CI)**	
	CS Meso.	CR Meso.
CMPD74	6.7 (5.6-7.6)	4.0 (3.8-4.2)
CMPD74 +SAHA	6.5 (6.0-6.8)	3.9 (3.6-4.2)

Taken together these data suggests that CMPD74, while highly active, does not appear to be suitable for epigenetic chemo sensitisation using HDACi. This may be due to an already highly effective cytotoxic action.

3.4.4. Treatment with 1,10-Phen and VPA

Given the data described above CS Meso. cells were exposed to 1,10-phen in combination with VPA (5mM) for 24hrs to investigate potential increases in cytotoxicity. CS cells and VPA were chosen due to previous responses with VPA in this cell line using CMPD19 and CMPD73. No significant alteration in the IC_{50} values were observed following treatment with 1,10-Phen (IC_{50} 276μM) or 1,10-phen with VPA (304μM), indicating that VPA does not potentiate the action of one of the component parts of CMPD19 or CMPD73.

3.4.5. Treatment with cisplatin and HDACi

CS and CR mesothelioma cells were exposed to Cisplatin with or without SAHA (2.5μM) and VPA (5mM) for 72 hrs. In some experiments, A2870 cells were exposed to cisplatin and HDACi for 48 hrs. SAHA reduced cell viability by 11% in CS Meso. cells and by 20% in CR. Meso cells. VPA had no effect on cell viability in CS Meso. cells and reduced viability by 17% in CR cells.

Table 3.6 Estimated IC_{50} Values for cisplatin combined with HDACi following 72h treatment

Compound	**Mean IC_{50} μM (95% CI)**	
	CS Meso.	CR Meso.
Cisplatin	4.5 (3.3-5.6)	59.1 (43.1-75)
Cisplatin + SAHA	4.7 (3.8-5.6)	31.4* (25.0-37.8)
Cisplatin + VPA	1.5* (0.7-2.3)	5.5* (5.1-6.0)

* Significantly different from control, P<0.05

A modest, but significant, reduction in IC_{50} values is observed in CS Meso. cells following treatment with VPA but not with SAHA. In contrast, the IC_{50} for CR Meso. cells were

moderately influenced by SAHA (approximately two-fold reduction) while the impact of VPA is much greater (approximately ten-fold reduction). Intriguingly, the IC_{50} value obtained for CR Meso. cells treated with cisplatin and VPA is almost identical to that for CS Meso cells only treated with cisplatin (Table 3.6). These data suggest that VPA may be able to sensitise the CR Meso. cells to cisplatin, via mechanisms which involve epigenetic regulation. A2780 cells displayed modest (approximately two-fold decreases) in IC_{50} when co-treated with either SAHA (IC_{50} 2.7μM) or VPA (IC_{50} 3.1μM) when compared to cisplatin control (IC_{50} 6.6μM).

3.4.6. Western blot analysis of H4K16ac expression in response to HDACi

Purified histones from A549 cells treated with SAHA (5μM) and VPA (5mM) for 24hrs were assayed using Western Blot staining with the global histone acetylation marker H4K16ac antibody to detect increased acetylation levels in response to HDAC inhibition. Figure 3.4 and Figure 3.5 (A) demonstrates a significant increase in acetylated histone levels in response to SAHA (≈ 9-fold increase) and VPA (≈ 6.5-fold increase) treatments, compared to purified histones isolated from non-treated controls. Figure 3.5 (B) also displays SDS gel stained post-transfer, showing stained purified histones H3, H2B, H2A and H4, which were used for TPN.

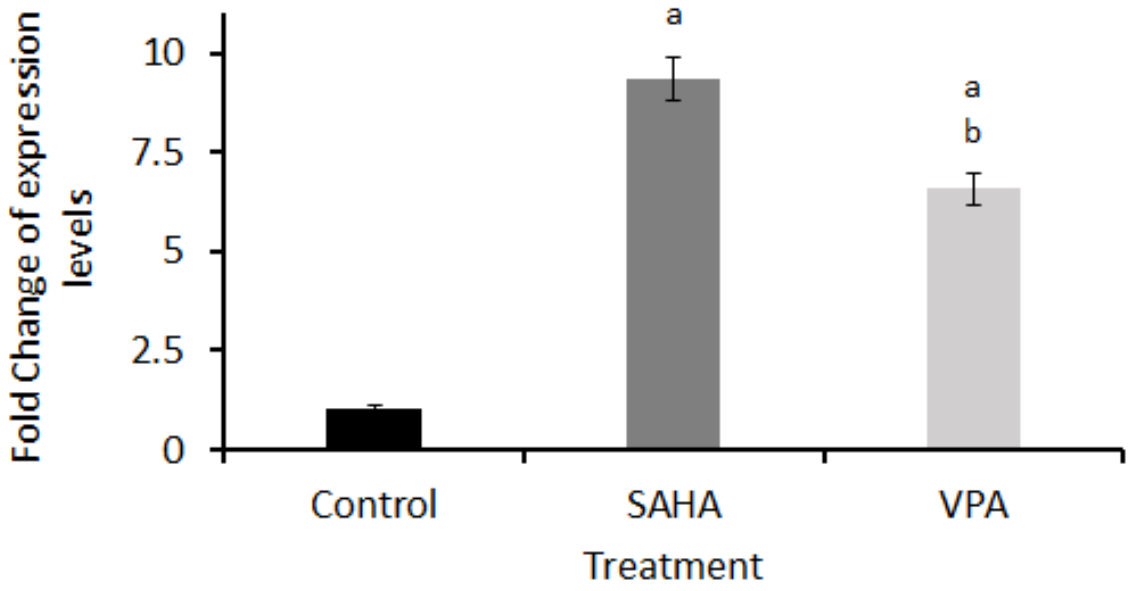

Figure 3.4-Increased expression levels of acetylated H4K16 in response to treatment with HDACi SAHA and VPA compared to non-treated controls (Results expressed as relative fold increases ± 1 standard deviation of a representative sample) (a P<0.001 compared to control, b P<0.001 compared to SAHA).

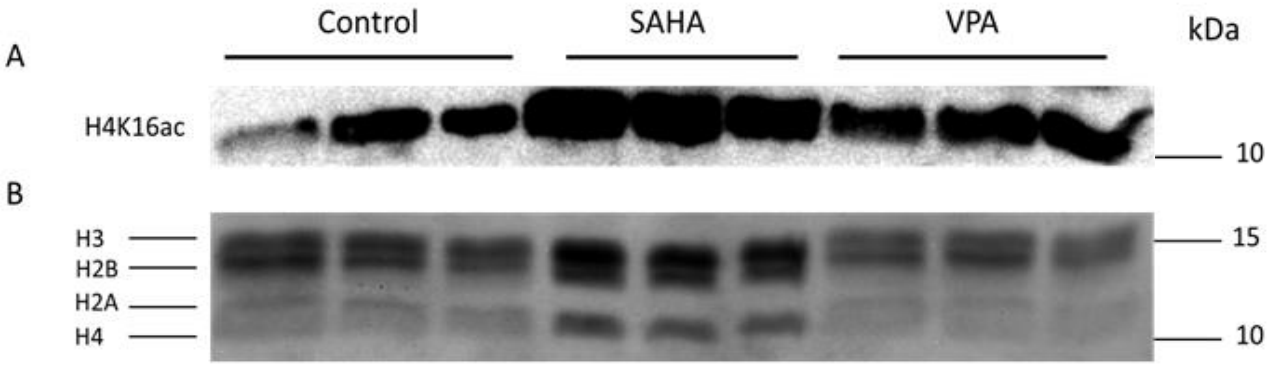

Figure 3.5-(A) western blot of purified histones from A549 cells treated with SAHA and VPA demonstrating an increase in H4K16 acetylation in response to treatment with HDACi. (B) SDS gel of purified histones stained post-transfer displaying histones H3, H2B, H2A and H4 which were used for TPN.

3.5.Discussion

The mixed results of the novel metal phen compounds with HDACi can likely be attributed to their inherent mechanisms of action and the effects of the HDACi used. As reported by Kellet *et.al* (2011) and as will be seen in Chapter 6 of this thesis, CMPD19, CMPD73 and particularly CMPD74 all display nuclease capabilities and so would have been expected that some form of epigenetic enhancement would have been seen, particularly when compared to increased cytotoxicity using cisplatin as a positive control for HDACi therapy.

However CMPD 74 was not seen to interact with any HDACi used, while the manganese containing CMPD 19 and CMPD 73 appeared to experience an increase in cytotoxicity following treatment with aliphatic acids VPA and SPB. Following western blot analysis however this interaction between Mn-phen compounds and the aliphatic acid HDACi was determined to likely be a result of alternate cellular HDACi targets rather than their effects on DNA. As such it is speculated that DNA may not be a primary target of the metal-phen compounds in question.

Although generally reacting in a weak to modest fashion, and with the exception of SAHA in CS mesothelioma cells, cisplatin did react with HDACi SAHA and VPA to increase the cytotoxic effects of the drug in sensitive and resistant cancer cells. This can be attributed to cisplatins' known DNA damaging capabilities, combining with chromatin relaxation in response to HDACi treatment, and so supports the hypothesis that cancer cells can be epigenetically sensitised to DNA damaging drugs. Differences in reactivity between anticancer drugs and HDACi can be attributed to cell type specificity and may be an explanation for cisplatin's lack of response with SAHA in CS cells.

However contrary to our original hypothesis, it may be the case that the mechanism of cytotoxicity is not exclusively by direct DNA damage. The subtle differences between how cisplatin and the novel metal-phen compounds react with the HDACi may be telling of the intra-cellular targets on which they act.

The inability to observe an effect between SAHA and any of the compounds may be the most suggestive result to support this. The mechanism through which SAHA primarily exerts its effects is attributed to HDACi and the effect this has on chromatin compaction and increased acetylation status of cellular proteins (Richon, 2006). Indeed SAHA generated the strongest increase in acetylated histones when investigated using western blot. The inability of these compounds to react at all with a potent HDACi further supports the contention that cellular DNA is not the primary target of the drugs.

It would certainly seem that in the case of CMPD 74, its rapid levels of cytotoxicity may suggest that it is not available for epigenetic enhancement, as it may already begin degrading DNA and killing the cells before the HDACi can fully take effect. If CMPD 74 were to target cellular DNA, it would outpace the effects of HDACi, which are reported to take effect up to 4hrs during treatment. 4hr pre-treatment (data not shown) and 8hr co-treatment with SAHA and CMPD 74 were conducted to identify any potential rapid responses. However, no such response was observed. If CMPD 74 were to act so rapidly on cellular DNA, it would have been expected that either pre-treatment or a narrower exposure time would show this. It is may be however that despite significant nuclease capabilities, CMPD 74 exerts its effects elsewhere from cellular DNA and that it may have other nucleic acid targets. Again, this is further supported by a lack of interaction with SAHA despite being observed as the strongest HDACi demonstrated by western blot. SAHA has also been demonstrated to

increase the expression of Nrf2 the cells master genetic regulator of the antioxidant defence system (Xu *et al.*, 2018). This class of compounds are typically found to be redox active as such upregulation of the antioxidant defence system may counter act the primary cytotoxic mechanism of the metal-phen compounds. Details on the investigation of the redox properties of these compounds are described in the next chapter.

Regarding positive effects seen with VPA and CMPDs 19 and 73, this could be attributed to more 'off target' and unintended interactions of VPA with the compounds, other than epigenetic related effects. VPAs primary use is as an anticonvulsant treatment for epilepsy and is also used to treat bi-polar disorder and migraine headaches, among many other neurological disorders. As well as inhibiting HDACs, it can act as an inhibitor of voltage gated sodium channels and can affect metabolic enzymes and processes such as the tricarboxylic acid cycle (Ghodke-Puranik *et al.*, 2013). It may be that the increased cytotoxic effect induced by CMPD 19 and in particular CMPD 73 are a result of interactions with one of the many altered pathways induced by VPA treatment, and not primarily a result of HDAC inhibition as originally hypothesised.

Specifically it has been reported that VPA, particularly in mesothelioma cells, is capable of producing ROS as one if its primary mechanisms of cell death when combined with cisplatin or pemetrexed (Vandermeers *et al.*, 2009). As reported by Kellet 2011 and as will be demonstrated later in this thesis, both CMPD 19 and 73 exhibit ROS production as a key mechanistic event. It could be the case that it is a crossover between ROS production and not HDAC inhibition which is the driving force behind the increase in cytotoxicity seen between VPA and the manganese-based compounds. Manganese cytotoxicity has been

reported to be a result of GSH depletion, and so the addition of ROS-producing VPA may explain the increase in cytotoxicity.

This could further be supported by the lack of response seen in CS cells treated with 1,10-Phen and VPA. It would have been expected that 1,10-Phen, a known DNA intercalator, would experience an increased effect in response to VPA. However, the inability to observe an effect using this combination may hint that many of VPAs effects are in fact not driven by its HDACi capabilities. However, this may also indicate that while possessing DNA intercalative capabilities, 1,10-Phen may also not act on cellular DNA as its primary mechanism of action.

Furthermore, despite sharing structural similarities and belonging to the same family of aliphatic acid HDACi, SPB did not elicit the same response as VPA with either CMPD 19 or 73. This again may play into the mechanism of ROS generation reported by VPA. In contrast to VPA, SPB has been reported to suppress the generation of ROS in murine models (Roy *et al.*, 2012), and so it could be a loss of target specificity that explains why SPB did not affect the cytotoxicity of the manganese compounds. This again supports the notion that it may be the generation of ROS and not HDACi that enhances the effect of the manganese phen compounds when combined with VPA. However, CMPD 73 did appear to experience a significant increase in cytotoxicity with SPB in CS mesothelioma cells, but not in CR cells.

The increase in cytotoxic action seen between CMPD 73 and SPB in CS meso cells may therefore be a result of HDACi, since there have been no reports of ROS generation by SPB to date. While western blot analysis of SPB treated cells was unavailable to fully determine increased levels of histone acetylation, its shared structural similarities with VPA and

positive effects on cell viability, which have been reported in literature indicate the presence of cellular effects. SPB has been seen to prematurely push the cell from the G1 stage of the cell cycle into S phase before cell cycle checkpoints such as DNA damage surveillance have been completed. This allows the progression of damaged DNA which is later detected in G2 phase and initiates apoptosis (Koprinarova *et al.*, 2010; Kusaczuk *et al.*, 2016). These effects have been attributed to the synergy observed between SPB and DNA damaging drugs such as cisplatin (Koprinarova *et al.*, 2010), and may explain as to why both mesothelioma cell lines experienced an increase in viability in the absence of a DNA damaging agent, as both cell lines may experience a premature push through the cell cycle but lack sufficient DNA damage to undergo apoptosis.

While a relaxed chromatin state may be responsible for these effects it is likely previously discussed "off target" effects which are being targeted by SPB, again supported by no observable effect with SAHA. SPB has been demonstrated to positively interact with cell cycle control and apoptotic pathways that may be responsible for the increased effects with CMPD 73 which has been demonstrated to initiate apoptosis (Digiuseppe *et al.*, 1999; Witzig *et al.*, 2000). Increased levels of apoptotic signalling can easily synergise with a vast number of different cellular injuries, such as oxidative stress, a common feature of these compounds.

As it is becoming more likely that these novel metal phen compounds do not appear to primarily affect cellular DNA, pursuing the potential additive or synergistic effects of CMPD 73 and SPB are likely beyond the scope of this investigation, which is primarily focused on a relaxed chromatin state interacting with DNA damaging drugs.

4. Investigation of ROS

The lack of interaction between metal-phen compounds and HDACis is indicative of an alternate mechanism of action as previously hypothesised. As both CMPD 73 and 74 are presumed to be redox active, identifying their potential ROS generating capabilities, and which species may be involved is likely to prove a fruitful avenue of investigation.

4.1. Oxidative stress and cancer

While oxidative stress can be cytotoxic to the cell, it is the mutagenic potential of oxidised DNA that has detrimental effects regarding the initiation of oncogenesis. High levels of either chronic inflammation or chronic exposure to sub-lethal oxidants (cigarette smoke, UV radiation, industrial pollutants) have been implicated in the somatic mutation of many genes and transcription factors responsible for controlling cell growth and division (Yang *et al.*, 2018). Either the overexpression or silencing of these transcription factors can result in the initiation of oncogenic transformation. Aberrant cell signalling in response to ROS and oxidative stress has been implicated in a vast number of cancers, such as prostatic, pancreatic, breast, liver, colon and ovarian cancers (reviewed Afanas'ev, 2011). Oxidative stress has been demonstrated to interact with all three stages of the cancer process: initiation, promotion and progression (Reuter *et al.*, 2010). Overexpression of antioxidant defence genes has also been implicated in facilitating cancer cell survival and progression (Sznarkowska *et al.*, 2017).

During the initiation stage, a high oxidant environment can trigger mutations within genes responsible for balancing the cell control mechanisms. This can lead to the promotion of oncogenesis through abnormal cell signalling such as alterations to second messengers, increased levels of cell cycle proteins and decreased levels of apoptosis (Reuter *et al.*, 2010; Sosa *et al.*, 2013; Galadari *et al.*, 2017). Oxidative stress can further promote oncogenesis

through dysfunctional redox signalling as well as by initiating mutagenesis within specific gene promotor regions (Hegedűs *et al.*, 2018), as will be discussed using H_2O_2 as a primary model.

As noted previously in Chapter 1, H_2O_2 has already been discussed as the primary ROS implicated in normal cell signalling processes, owing to its stability and low reactivity with biomolecules. Therefore, under elevated levels of oxidative stress, increased concentrations of H_2O_2 can also contribute to the dysfunction of normal intracellular signalling processes. H_2O_2 has been seen to play a dual role in oncogenic activation. It has been demonstrated to induce activating mutations in the human Ras oncogene, while also being implicated in mutagenic inactivation of the tumour suppressor p53 (Xu, Trepel and Neckers, 2011; He and Simon, 2013). H_2O_2 can induce Ras signalling by oxidising the cysteine thiol groups of the tumour suppressor and regulator of Ras PTEN, causing its inactivation (Brewer *et al.*, 2015). Activation of Ras can then initiate the activation of the PI3K, Akt, mTOR, MAPK/ERK (phosphatidylinositol 3-kinase, Akt, mammalian target of rapamycin, mitogen protein activated kinase/extracellular signal regulated kinase) signal transduction pathway responsible for growth factor signalling (Zenonos, 2013). This in turn can propagate further ROS production, as Ras activation has been seen to increase ROS levels, and p53 inactivation has been linked with an increase in cytokine production capable of adding to inflammation and oxidative stress (Galadari *et al.*, 2017). The implication of oxidative regulation of Ras and its potential contribution towards oncogenesis have been demonstrated by the inhibition of its mitogenic activity by chemical antioxidants (Reuter *et al.*, 2010 reference 222).

ROS induced silencing of PTEN can further aid cancer cell survival by causing the increased expression of Akt. Akt serves to facilitate tumorigenesis by stabilising cell cycle proteins such as cyclin D1 and c-Myc while destabilising and causing the degradation of cell cycle control proteins such as cyclin-dependent kinase inhibitor protein p27Kip1 (Prasad *et al.*, 2015). Akt also serves to negatively regulate and inactivate pro-apoptotic proteins such as caspase 9, Bad, and BH3 (Sangawa *et al.*, 2014).

Finally, high levels of H_2O_2 are capable of degrading IκBα, the suppressive regulator of the transcription factor NF-κB, responsible for cytokine production and cell survival (Hoesel and Schmid, 2013). Nitrosative stress has also been implicated alongside oxidative stress to play a role in oncogenic initiation, with both oxidative insults capable of activating Activator Protein 1 (AP-1), a redox-sensitive transcription factor involved in cell proliferation and transformation (see references 139 and 162 Reuter *et al.*, 2010). S-nitrosylation can also cause premature activation of Ras in response to high levels of RNS (Ortega, Mena and Estrela, 2010). ROS plays a role in cancer progression by facilitating further mutagenesis to allow rapid response to adaptive pressures, and to allow cancer cells to metastasise or undergo angiogenesis (Reuter *et al.*, 2010).

To survive in high ROS environments, cancer cells implement a new redox balance between higher levels of ROS and antioxidant systems (Sosa *et al.*, 2013). This allows the cells to maintain higher levels of ROS and oxidation than normal cells to maintain both oncogenic signalling and mutagenesis required for growth and adaptation, while still being afforded the protection from detrimentally high levels of ROS which would be cytotoxic (Gill, Piskounova and Morrison, 2016). One of the main antioxidant defence pathways seen to be upregulated in oncogenic cells is the Nuclear factor erythroid 2-related factor 2 (Nrf2), also

known as nuclear factor erythroid-derived 2-like 2 (Nguyen, Nioi and Pickett, 2009). Nrf2 is a cytosolic transcription factor that in humans is encoded by the *NFE2L2* gene and is a master regulator of the cellular antioxidant response, controlling the expression of genes that counteract oxidative and electrophilic stresses, alleviating oxidative stress (Dodson, Castro-Portuguez and Zhang, 2019). Under normal conditions, Nrf2 is kept in the cytoplasm by its associated regulatory protein Kelch like-ECH-associated protein 1 (Keap1). Keap-1 is a ubiquitin ligase, ubiquitinating Nrf2 causing its degradation. Under homeostatic conditions Nrf2 has a half-life of only 20 minutes (Kobayashi *et al.*, 2004). However, as Keap-1 is a cysteine rich protein (27 cysteine residues in humans), it is sensitive to high oxidant environments (Kansanen *et al.*, 2013).

When a cell experiences oxidative stress, the high ROS environment oxidises Keap-1, inducing conformational change and releasing Nrf2. Nrf2 is then translocated to the nucleus, where it recognises specific promoter sequences known as Antioxidant Response Elements (ARE), within specific genes responsible for the antioxidant response (Jaramillo and Zhang, 2013). Examples of genes possessing an ARE are Glutathione-S Transferase (GST), glutamate-cysteine ligase (GCL, required for GSH synthesis), Glutathione Peroxidases (GPx), Heme oxygenase-1 (HMOX1) responsible for controlling iron metabolism, genes responsible for NADPH regeneration, thioredoxins, and multi-drug resistance proteins (MDR) responsible for efflux of GSH conjugated xenobiotics, such as cisplatin (Ma and He, 2012; Tonelli, Chio and Tuveson, 2018).

As the master regulator of the antioxidant defence systems Nrf2 overexpression confers a distinct survival advantage to cancer cells to prevent lethal amounts of oxidative damage (Zimta *et al.*, 2019). Overexpression of Nrf2 is generally a result of either somatic mutation

of the Nrf2 gene or an inactivating mutation/methylation within the promoter of Nrf2s inhibitory regulator Keap-1 (Kitamura and Motohashi, 2018). Nrf2 expression can also be positively regulated by c-myc and Ras signalling, as well as resulting from PTEN inactivation (as described) (Rojo *et al.*, 2014; Panieri and Saso, 2019). In conjunction with its role in maintaining transformed cancer cells, Nrf2 also plays a significant role in the development of acquired resistance towards chemotherapy.

The upregulation of the antioxidant defence system allows cancer cells to adapt to oxidative stress induced by xenobiotic compounds such as ROS generating chemotherapy agents (cisplatin, carboplatin, oxaliplatin, and doxorubicin) (Yang *et al.*, 2018). Detoxification of these compounds and repair of oxidative damage is a key mechanism through which Nrf2 overexpression and signalling is used by cancer cells to acquire chemo resistant mechanisms to survive treatment with various chemotherapeutics (Kitamura and Motohashi, 2018). For example, GCL the rate limiting enzyme required for GSH synthesis, possesses an ARE within its promoter (Mani *et al.*, 2013) therefore increasing the intracellular pool of GSH available to detoxify ROS generating compounds (Bansal and Celeste Simon, 2018). Enzymatic inactivation of drugs such as cisplatin by GST enzymes has also been seen to contribute significantly to drug-resistance (Allocati *et al.*, 2018).

4.1.1. Mesothelioma:

Malignant Mesothelioma (MM) is an example of a rare and highly aggressive form of cancer whose initiation has been directly attributed to a high ROS environment and chronic inflammation (Matsuzaki *et al.*, 2012). MM is a cancer of the mesothelial cells lining the pleura of the lung, and is predominantly caused by the inhalation of carcinogenic asbestos fibres (Tipu, Ahmed and Ishtiaq, 2013). Asbestos is a term referring to six fibrous silicate

minerals naturally found in rocks and soil, which was used extensively in building and industrial processes as a fire retardant and insulator up until the 1970s when its hazardous effects became apparent (Nynäs *et al.*, 2017). When handled asbestos fibres are easily inhaled and become trapped within the smallest bronchial tubes and alveoli, where it is a source of major irritation and can cause MM (Nishimura *et al.*, 2013).

MM generally has a dire prognosis, with median survival rates of just a year from diagnosis. It is estimated to kill 43,000 people worldwide each year, with 3,000 deaths occurring in the U.S. and 5,000 in Western Europe (Boyer *et al.*, 2018). The world Health Organisation (WHO) has recognised asbestos as one of the most important occupational carcinogens and declared asbestos-related diseases to be eliminated (Galateau-Salle *et al.*, 2015). The development of MM can be a very slow process taking years to manifest, with the interval between exposure to asbestos fibres and the diagnosis of MM between 30-40 years (Røe and Stella, 2015). Therefore the global mortality rate of MM is expected to rise, as generations born in the 1940's and 50's who have been exposed to asbestos before tight governmental regulations were implemented will reach the peak age for MM incidence and mortality (La Vecchia *et al.*, 2000). Many cases are expected to arise in developing countries, such as India, where the regulation of asbestos in construction is either not tightly controlled or is non-existent (Cavone *et al.*, 2019).

The WHO estimates that up to 125 million people worldwide are still exposed to asbestos in their homes or workplace (Stayner, Welch and Lemen, 2013). MM is also notoriously hard to diagnose requiring expertise in specific histochemical staining to distinguish it from other lung cancers such as adenocarcinomas (Bianco *et al.*, 2018). Both the long latency period and difficulty in diagnosis significantly contributes to MMs high mortality rate, with poor

treatment responses and limited treatment options further contributing (Tomasson *et al.*, 2016).

Asbestos can initiate oncogenesis of pleural mesothelial cells both directly and indirectly, both of which are facilitated by chronic oxidative stress and inflammation (Afaghi *et al.*, 2015). Insoluble asbestos fibres are engulfed by mesothelial cells causing chronic irritation and initiating lung fibrosis (Norbet *et al.*, 2015). Asbestos fibres possess a high iron content, and so could significantly increase ROS production (H_2O_2, $O_2^{\bullet-}$, $OH^{\bullet}$) through Fenton-like chemistry following ingestion. Asbestos has also been seen to induce the expression and activity of nitric oxide synthase (NOS) in alveolar macrophages and mesothelial cells. High NOS activity would result in higher levels of RNS production, which alongside ROS, could cause mutagenic alterations in genomic DNA resulting in the initiation of oncogenesis (reviewed by Benedetti, Nuvoli, Catalani, & Galati, 2015). DNA damage and genotoxicity may also be caused by direct interference of asbestos fibres with DNA, particularly during chromosome segregation during mitosis (Carbone and Yang, 2012).

The irritation caused by asbestos fibres also serves to recruit immune cells (such as nearby alveolar macrophages) in order to try and remove both the foreign body fibres and the mesothelial cells which have engulfed them (Maeda *et al.*, 2010). The presence of immune cells and resulting inflammation further contributes to the high oxidant environment capable of initiating mutagenesis (Hasselbalch, 2013). However immune cells, particularly phagocytic cells, are unable to break down the insoluble asbestos fibres, causing immune cell death via necrosis and the release of inflammatory cytokines, such as Tumour Necrosis Factor α (TNFα), Tumour Necrosis Factor β (TNFβ) and Interleukins 1β, 6 and 8 (IL-1β, IL-6, IL-8) (Hillegass *et al.*, 2010). The release of inflammatory cytokines, ROS, and un-

degraded asbestos fibres are then able to react with neighbouring cells further propagating chronic oxidation and inflammation, further contributing towards DNA damage, mutations, and oncogenic transformation (Benedetti *et al.,* 2015).

Like all cancers, prolonged exposure to DNA damaging agents such as ROS and chronic inflammatory responses will result in the activation of various oncogenes and the inactivation of tumour suppressor genes. Many of the cell signalling pathways dysregulated in MM have already been discussed, as initiation of neoplasia in MM is attributed to ROS signalling. The PI3K/Akt/mTOR (Wilson *et al.,* 2008) and MAPK signalling pathways (Hylebos *et al.,* 2016), as well as NfkB, have all been demonstrated to be activated in MM (Nishikawa *et al.,* 2014). Increased signalling through activated receptor tyrosine kinases has also been documented (Zhou *et al.,* 2014). MMP expression has also been seen to be upregulated in MM, contributing to metastasis (Yoon *et al.,* 2002). One of the hallmarks of MM is the inactivation of the tumour suppressor's $p16^{INK4a}$ and $p14^{ARF}$ which are inactivated in ≈ 70% of MM, owing to homozygous deletions or missense/nonsense mutations within their genes (Hylebos *et al.,* 2016). Both $p16^{INK4a}$ and $p14^{ARF}$ are cell cycle regulators and interact with p53 tumour suppressor pathways, meaning their loss of activity would significantly influence oncogenic transformation (Ohtani *et al.,* 2004; Ko, Han and Song, 2016).

Current treatments for MM are very limited. The most successful treatment is surgical removal of the tumour, however since most MM is diagnosed at advanced stages, most cases of MM are unresectable, and therefore radiotherapy or chemotherapy is implemented (Carbone and Yang, 2012). First line treatment for MM is usually a combination of cisplatin and pemetrexed, which can increase median survival rates by ≈ 3-4 months (Vogelzang *et*

al., 2003). However in most cases MM has a rate of high recurrence with a high prevalence of multi drug resistant phenotype (Vandermeers *et al.*, 2009). Contributing factors towards acquired resistance have been attributed to MM cells displaying increased expression of the antioxidant Mn-SOD and catalase enzymes capable of detoxifying further oxidative insult from ROS generating cisplatin (Kahlos *et al.*, 1998). As discussed in previous sections high ROS environments can act to signal an increase in antioxidant defence systems to mitigate potential cytotoxic levels of ROS. Another factor is the prevalence of Cancer Stem Cell (CSC) populations within MM tumours, which possess inherent chemo resistant properties and are capable of repopulating a depleted tumour population following what appears to be a successful round of chemotherapy (Cortes-Dericks *et al.*, 2014). The current limitations of treatment options and prevalence of resistance demonstrates the need for novel therapies capable of improving the poor survival rate associated with MM.

4.1.2. ROS and chemotherapeutics:

Despite resetting the landscape of redox homeostasis to their own advantage, cancer cells exist in a state of high ROS sensitivity (Liu and Wang, 2015). Increased antioxidant defence systems may facilitate higher levels of oxidative stress to allow oncogenesis, but certain thresholds exist within the cell regarding how much oxidative stress they can tolerate (Ogundele *et al.*, 2017). This phenomenon has formed the basis for many chemotherapeutics in order to target cancer cells (Moloney and Cotter, 2018). As discussed in previous sections, ROS generating chemotherapeutics (cisplatin, carboplatin, and doxorubicin) are implemented in the treatment of many cancers. However the prevalence of acquired resistance to these compounds is significant. To combat this, many novel redox active metal compounds are also in development in order to exploit these processes and are designed with

the hopes of overwhelming antioxidant defence systems of both chemo sensitive and chemo resistant cancer cells.

4.1.3. Metal-based drugs and redox homeostasis

Many metal-phen compounds are able to generate ROS, with the formation of various ROS typically linked with the mechanism of action of the compound(s). As CMPD 73 and 74 are next generation analogues of CMPDs 19 and 22, which have already been demonstrated as potential ROS generating compounds (Kellett *et al.*, 2011), it is likely that the current compounds will demonstrate analogous biochemical behaviour.

The generation of ROS following treatment of cells with CMPD 73 and CMPD 74 is anticipated to be a likely mechanistic event in their cytotoxic effect. Whether ROS generation is a key mechanistic event utilised to cleave cellular DNA or whether DNA damage results indirectly by ROS produced elsewhere in other organelles of the cells, is yet to be determined. It may be the case that these compounds have other targets than DNA within the cell and utilise ROS to target these, as highlighted in Chapter 3. Figure 4.1 displays core pathways involved in the clearance of cytotoxic ROS from the cell, and highlights pathways which would leave the cell vulnerable to oxidative stress if inhibited.

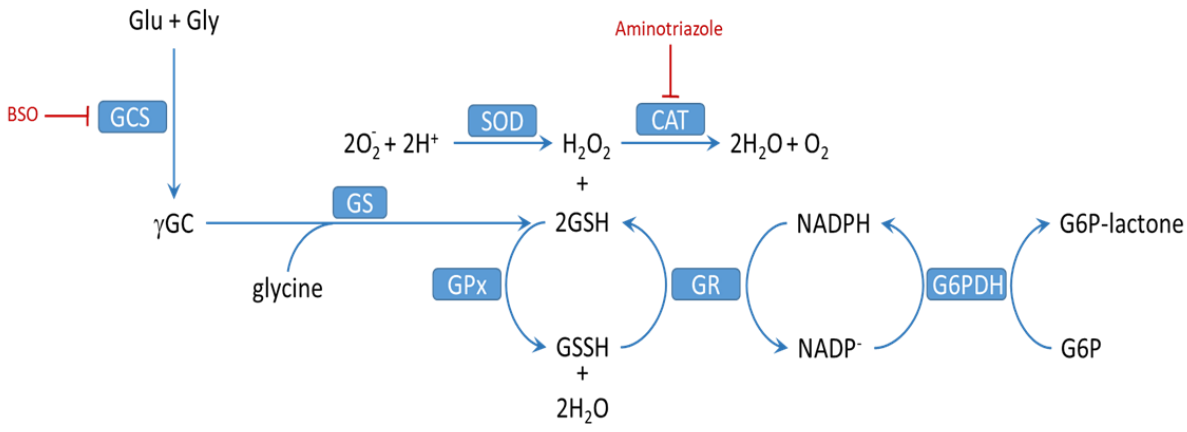

Figure 4.1 Pathways for the elimination of key ROS species in cells, highlighting inhibitors of GSH and Catalase pathways. This figure was self-generated using Microsoft PowerPoint based on the current understanding of knowledge from numerous sources. (SOD, superoxide dismutase; CAT, catalase, GSH, reduced glutathione; GSSG, oxidised glutathione; GPx, glutathione peroxidase; GR, glutathione reductase; GS, glutathione synthetase; GCS, glutamate–cysteine ligase, G6PDH, gluscose-6 phosphate dehydrogenase).

In order to confirm this, spatiotemporal dynamics of ROS production in cells was investigated using CMPDs 73 and 74 in A549 and A2780 cells. This was carried out using ROS-specific organelle dyes and inhibitors of intracellular antioxidant pathways as well as chemical scavengers of specific ROS.

4.2.Aims:

This chapter describes the results that were aimed at clarifying potential ROS generating capabilities of CMPD 73 and 74 using ROS-sensitive intracellular chemical fluorescent probes, and also the use of both targeted inhibitors of the cells antioxidant pathways and ROS specific scavengers to determine the species of ROS generated and if that species is biologically relevant to the cell death process observed in Chapter 2.

4.3.Methods:

4.3.1. Fluorescent staining of intracellular ROS generation

To investigate whether CMPD 73 and CMPD 74 can cause an increase in intracellular ROS levels, A2780 and A549 cells were stained with 2', 7′-Dichlorofluorescin Diacetate (DCFDA). CS and CR meso. cells were not included in this study as their primary use was to investigate responses to epigenetic therapies with metal-phen compounds. DCFDA can be assayed using both flow cytometry and fluorescent microplate reader and as such both techniques were implemented.

For analysis using flow cytometry $2.5x10^6$ cells (A2780, A549) were stained with 5µM DCFDA in PBS for 30mins at 37°C, washed thrice with PBS and exposed to 100µM concentrations of CMPD 73, 74 and 1,10-Phen for 40mins again at 37°C. 100µM H_2O_2 was used as a positive control. 100µM concentrations were used to ensure that any changes in fluorescence were not overlooked as a result of low fluorescent signals from low concentrations. Fluorescence was then read in a Beckman Coulter Cytoflex flow cytometer, using FL1/FITC channels. Dead cells and cellular debris were removed by selective gating based on forward and side scatter data, and a positive response was selected by gating events with a higher fluorescent intensity than that of the non-treated control. Data was analysed using CytExpert software, and histogram plots were generated using FlowJo version 10.6.1.

Analysis using a fluorescent microplate reader cells were plated in sextuplet wells of a black 96 well plate at a density of $2x10^4$cells/well and allowed to attach for 24hours. Cells were then stained with DCFDA (1µM) in PBS for 40mins at 37°C. Cells were then washed thrice with PBS, and exposed to CMPDs 73, 74 and 1,10-Phen at concentrations of 10nM, 100nM and 1µM and incubated at 37°C. The use of these specific concentrations was to ensure a broad spectrum of potential compound activity could be detected. H_2O_2 was used as a positive control at matched concentrations. Fluorescence was measured at 15min intervals for a total of 90mins using a fluorescent spectrophotometer at 485nm excitation/535nm emission. Results are expressed as fold changes compared to non-treated control cells with comparisons made to increases higher than that of the positive control H_2O_2.

4.3.2. Fluorescent staining of mitochondrial hydrogen peroxide:

To investigate this A549 cells were stained with MitoPY1 (as per protocol (Dickinson, Lin and Chang, 2013)) and exposed to CMPDs 73 and 74. Cells were plated in duplicate in 6 well plates at a density of $5x10^5$ cells/well and allowed to attach for 24hours. Cells were then stained with MitoPY1 (5mM) in PBS for 90mins at 37°C. Cells were then washed thrice with PBS, detached using citric saline solution and transferred to a 1.5ml Eppendorf tube. Cells were then exposed to ROS generating compounds for 45mins at 37°C, with 100µM H_2O_2 being used as a positive control. CMPDs 73 and 74 were used at a concentration of 100 µM. Concentrations of 100µM were used as per Dickinson and colleagues (2013) as an effective concentration of H_2O_2 in order to generate a robust response. As such CMPD 73 and 74 were used at identical concentrations as a point of comparison to the positive control and to ensure sensitivity towards low compound concentration was not an issue.

Following incubation cells were again washed 3 times with PBS and read in a Beckman Coulter Cytoflex flow cytometer, using FITC channels. Dead cells and cellular debris were removed by selective gating based on forward and side scatter data, and a positive response was selected by gating events with a higher fluorescent intensity than that of the non-treated control. Due to difficulties in sourcing commercial material, MitoPY1 was no longer available for use with A2780 cells and so this cell line was not investigated.

4.3.3. Selective inhibition of cellular antioxidant pathways:

Indirect profiling of intracellular ROS generation was detected using a potent glutamate cysteine ligase (rate limiting enzyme in glutathione synthesis) inhibitor, Butathione Sulfoximide (BSO) (Sigma), and a catalase inhibitor, 3-Amino-1, 2, 4-Triazol (A.T.) (Sigma). BSO has been demonstrated primarily to sensitise cells to oxidative insult and has

been tested in combination with many ROS generating chemotherapeutics (Rocha *et al.*, 2014; Tagde *et al.*, 2014). A.T. has been demonstrated to inhibit heme synthesis as well as catalase enzymes and has also been implicated in effecting metabolic processes (Bayliak *et al.*, 2008; Nunes-Souza *et al.*, 2020).

Suspected ROS-generating compounds present in antioxidant deficient cells should experience an increase in cytotoxic potential as a result of unchallenged ROS generation. An increase in cell cytotoxicity in response to antioxidant deficiency demonstrates generation of ROS by the compounds of interest. Multiple cell lines were used for this study to minimise cell type specific variables and to highlight possible differences or sensitivities between CS mesothelioma and CR mesothelioma cell lines.

Isogeneic mesothelioma and A549 cells were pre-treated with 1mM of BSO and 1mM of A.T. for 24hrs and exposed to concentrations of CMPDs 73, 74, and H_2O_2 control in the same co-treatment methodologies as described in methods Chapter 2 page 68, Alamar blue assay, and displayed in Figure 4.2. Isogenic mesothelioma cells were included in this particular study to fully determine effects of both BSO and A.T. across multiple cell lines. A2780 cells were also treated with 1mM of A.T. for 24hrs and exposed to concentrations of CMPDs 73 and 74, and H_2O_2 control. The molar concentrations (1mM) and pre-incubation times (24hrs) for both BSO and A.T. were determined to be the optimal conditions to observe an effect as determine by previous optimisation studies.

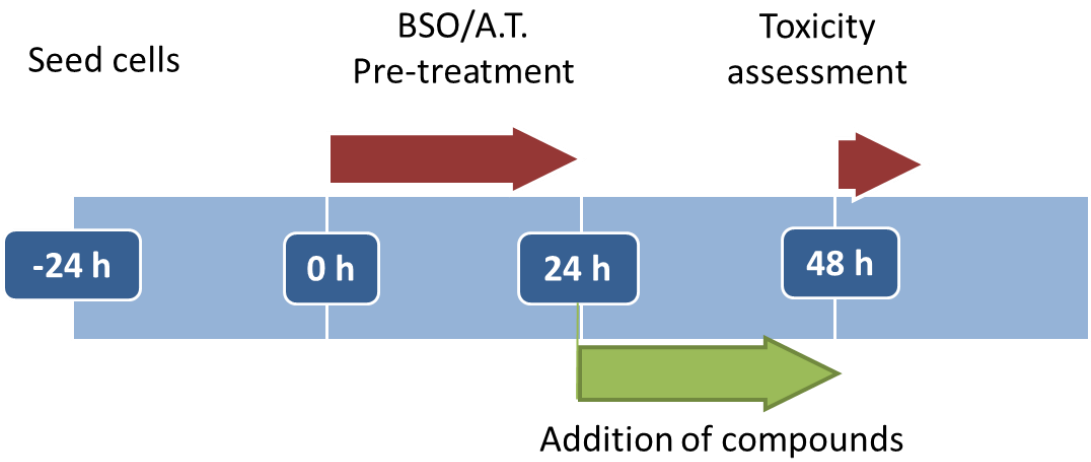

Figure 4.2 Treatment protocols for novel metal-based drugs with inhibitors of GSH and Catalase antioxidant pathways

4.3.4. Selective inhibition of compound cytotoxicity using ROS scavengers

Intracellular profiling of reactive species responsible for cytotoxic action of CMPD 73 and 74 was detected using a H_2O_2 specific scavenger Sodium Pyruvate (NaPy) (Sigma) and a superoxide specific scavenger Tiron (Sigma). Suspected ROS produced by metal-phen compounds should cause a decrease in cytotoxic potential of CMPD 73 and 74 when scavenged by their corresponding scavenger compounds. A decrease in cytotoxicity in response to ROS scavengers demonstrates the generation of the specific ROS by the compounds of interest.

A2780 ovarian cancer cells were pre-treated for 1hr with 10mM of either NaPy or Tiron, and then were exposed to concentrations of CMPDs 73 and 74, 1,10-Phen and H_2O_2 control in the same co-treatment methodologies as described in methods Chapter 2 page 68, Alamar blue assay, similar to those displayed in Figure 4.3. A2780 cells were seen to be more sensitive to ROS generation as determined using DCFDA fluorescent staining than A549 cells, and so were chosen on this basis for experimentation using ROS scavengers.

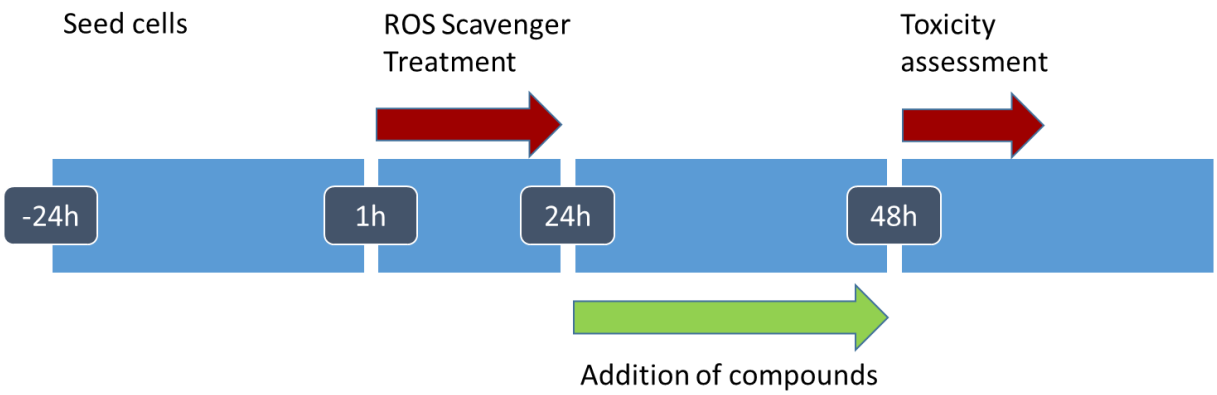

Figure 4.3 -Treatment protocols for novel metal-based drugs in the presence of ROS scavengers

4.3.5. Statistical analysis

All data was analysed using GraphPad Prism Version 8.3.0. or Microsoft Excel. Statistical analysis was conducted using Students T-Test or multiple T-Tests where applicable and expressed as a P Value < 0.05, 0.01, 0.001. Where multiple comparisons were made using the students T-test the Holm-Bonferroni correction was used.

4.4.Results

4.4.1. Fluorescent staining of intracellular ROS generation using flow cytometry

Figure 4.4 and Figure 4.5 displays DCFDA staining using A549 cells exposed to 100µM concentrations of test compounds for 40mins. CMPD 73 displays significant ROS generating capabilities (≈5-fold increase) compared to both control conditions and H_2O_2 (≈1.3-fold increase). CMPD 74 increased ROS production by (≈ 1.6-fold) compared to control conditions with 1,10-Phen showing higher ROS production (≈ 3.9-fold increase). H_2O_2 did not appear to be notably different compared to control cells however control conditions did demonstrate high levels of background DCFDA fluorescence relative to control conditions using the A2780 cell model (Figure 4.6). Initial analysis of this data demonstrated CMPD 73 to be statistically different compared to control values (non-treated and positive controls) and compared to CMPD 74 (significant values for all analysis $P<0.05$). However following Holm-Bonferroni correction for multiple comparisons the data fell short of the corrected significance threshold ($P<0.01$). Despite the lack of statistical significance these notable increases in ROS detected are still apparent for the compounds of interest. These data indicate both CMPD 73 and 74 as well as 1,10-Phen as ROS generating compounds as detected by DCFDA fluorescence.

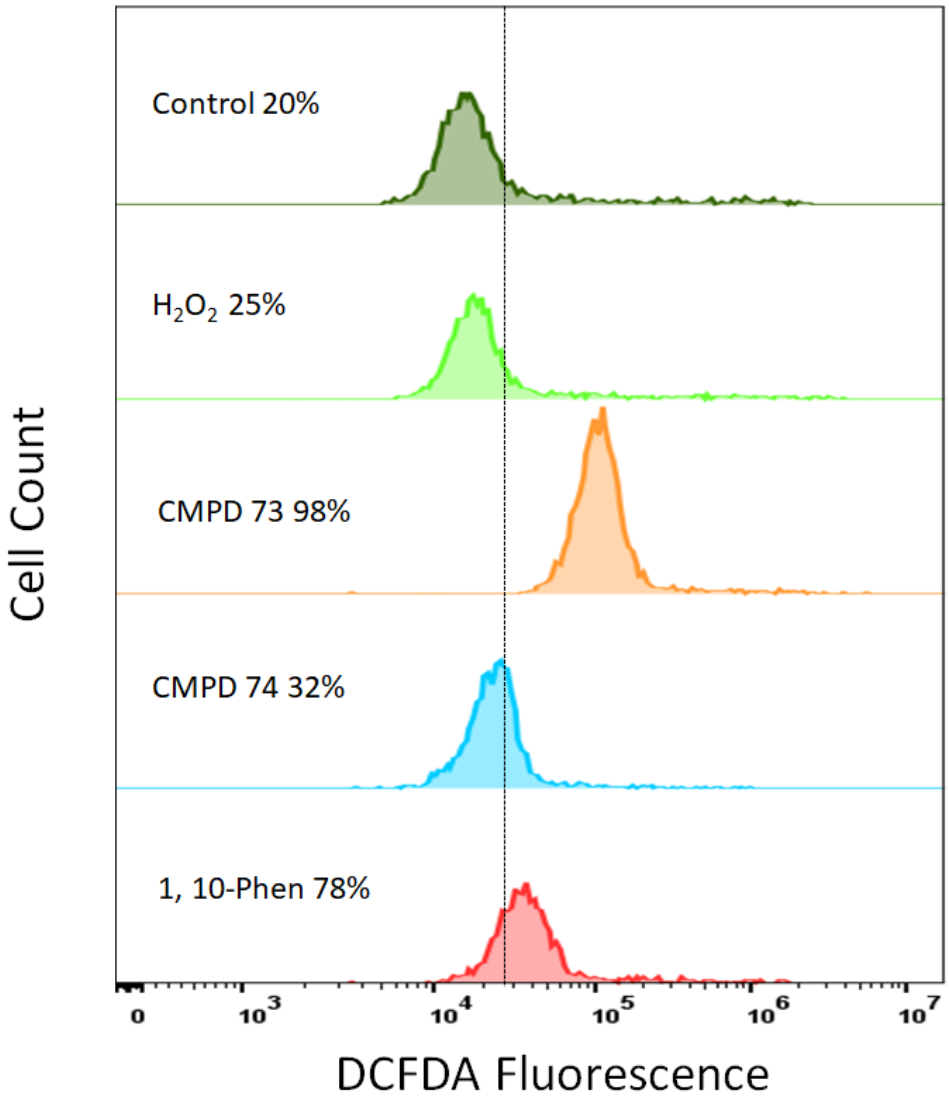

Figure 4.4- A549 cells stained with 5µM DCFDA and exposed to 100µM CMPD 73, 74, 1,10-Phen and H_2O_2 control for 40mins. Representative data of two independent experiments using duplicate technical replicates. Dashed line represents gated events indicating increases in fluorescent signal relative to control conditions.

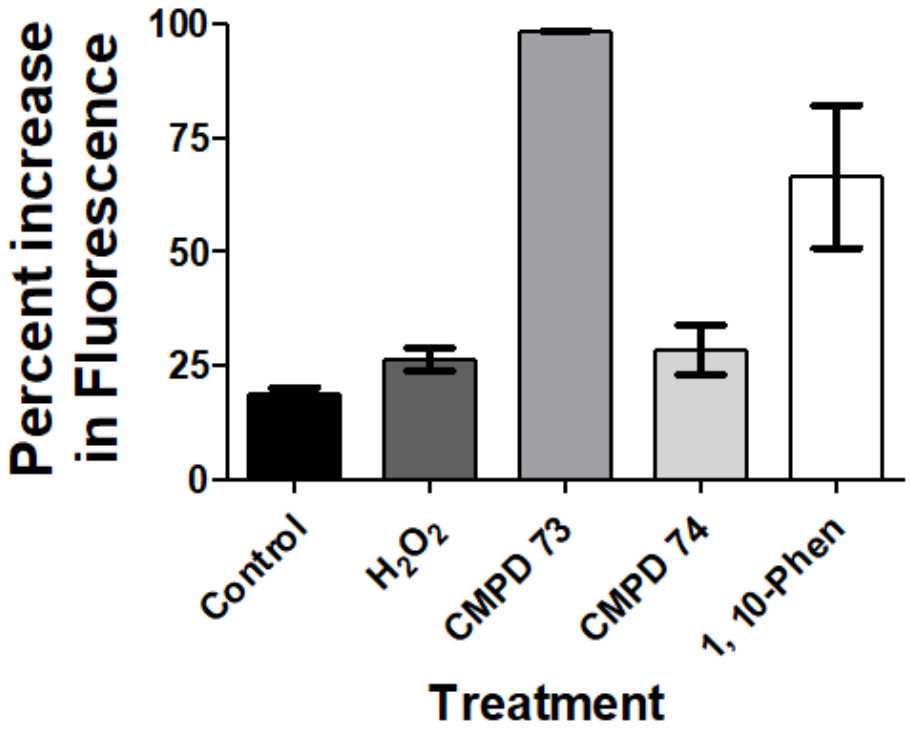

Figure 4.5- A549 cells stained with 5µM DCFDA and exposed to 100µM CMPD 73, 74, 1,10-Phen and H_2O_2 control for 40mins. Results are expressed as mean percent increase in fluorescent intensity of DCFDA compared to control conditions (± 1 Standard deviation of two independent experiments).

Figure 4.6 and Figure 4.7 displays DCFDA staining using A2780 cells exposed to 100µM concentrations of test compounds for 40mins. As seen in A549 cells, CMPD 73 displays highly notable ROS generating capabilities (≈ 33-fold increase) further indicating it is an exceptional ROS catalyst. CMPD 74 appeared to be observably more active in A2780 cells than in A549 cells (27-fold vs 1.6-fold). 1,10-Phen appeared to react in a similar fashion regardless of cell line used as seen with near identical results in A2780 cells compared to A549 cells.

As discussed with regards to A549 cells initial analysis of this data demonstrated CMPD 73, 74 and 1,10-Phen to be statistically different compared to control values and following inter-compound comparisons (significant values for all analysis $P<0.05$). However following

Holm-Bonferroni correction for multiple comparisons the data fell short of the corrected significance threshold ($P<0.01$). Significant differences were not detected using comparisons to the positive control before corrections were made with all compounds. Despite this the notable increases in ROS detected are still apparent. These data suggest A2780 cells are a more sensitive cell model to use in further ROS studies.

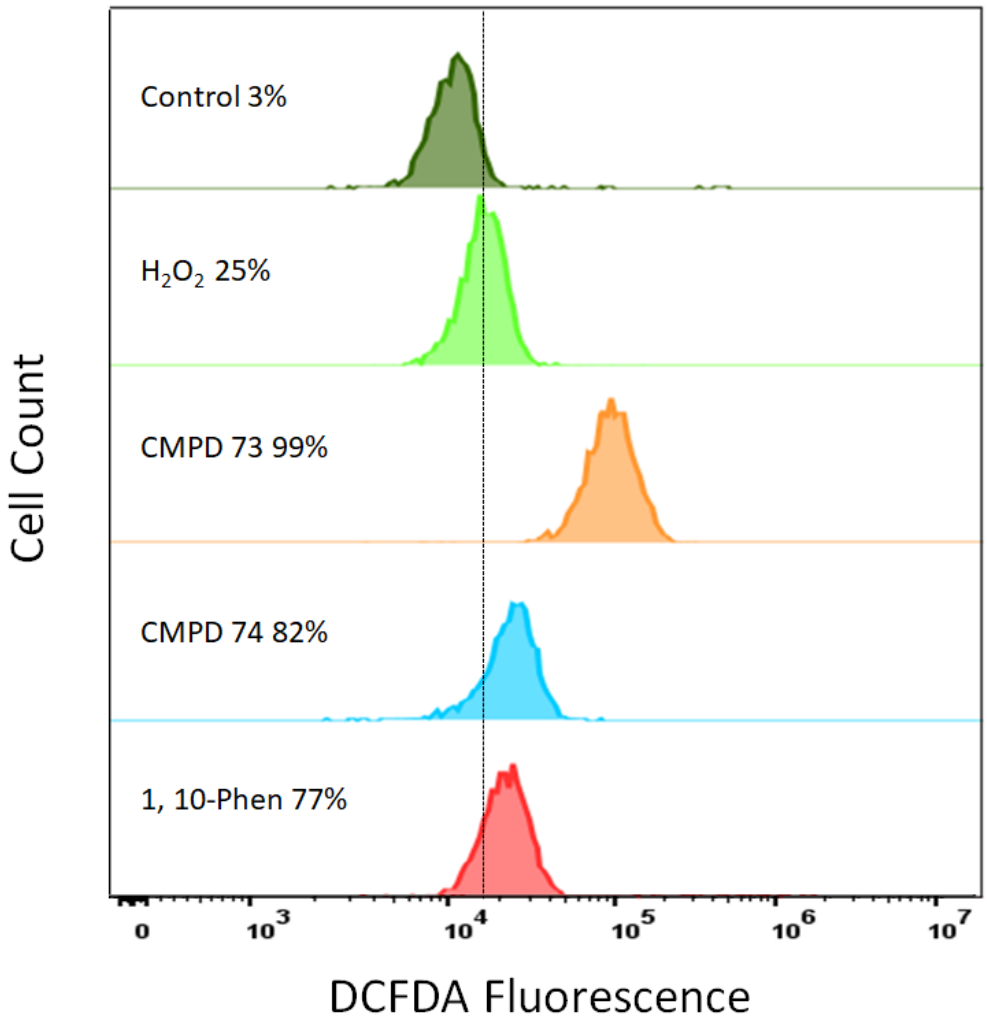

Figure 4.6- A2780 cells stained with 5µM DCFDA and exposed to 100µM CMPD 73, 74, 1,10-Phen and H_2O_2 control for 40mins. Representative data of two independent experiments using duplicate technical replicates. Dashed line represents gated events indicating increases in fluorescent signal relative to control conditions.

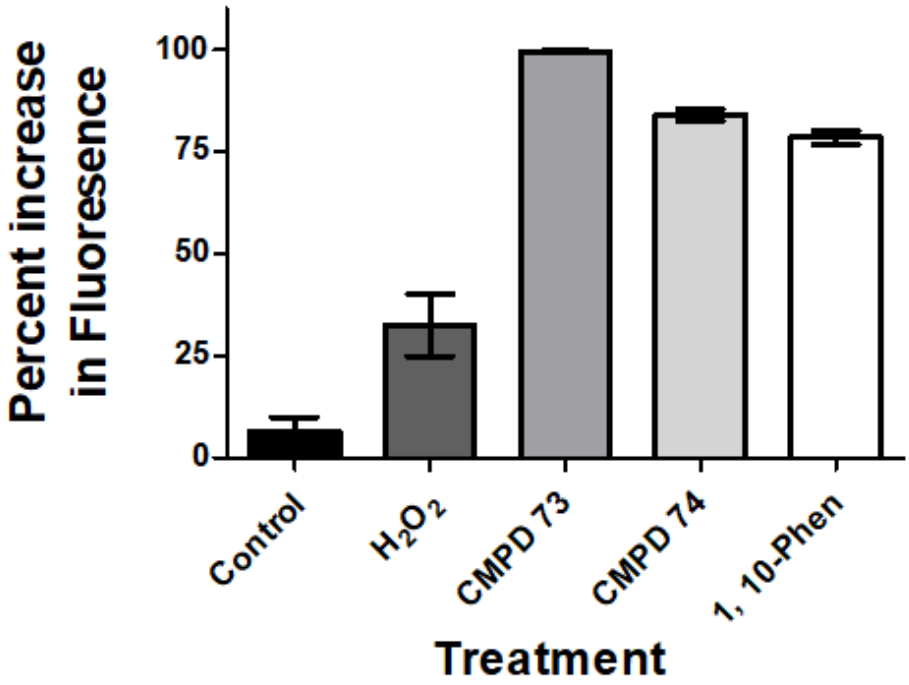

Figure 4.7- A2780 cells stained with 5µM DCFDA and exposed to 100µM CMPD 73, 74, 1,10-Phen and H_2O_2 control for 40mins. Results are expressed as mean percent increase in fluorescent intensity of DCFDA compared to control conditions (± 1 Standard deviation of two independent experiments).

4.4.2. Fluorescent staining of intracellular ROS generation using fluorescent spectrophotometry

Figure 4.8 displays DCFDA fluorescence in response to metal phen treatment in A549 cells. H_2O_2 control demonstrated little to no increase in DCFDA fluorescence even after 90mins at higher concentrations compared to non-treated control cells. As seen in Figure 4.8 (A) CMPD 73 displays potent increases in ROS production as seen by maximum ≈10fold increases in 100nM (significantly higher than H_2O_2) concentrations and exceptionally high ≈ 40-fold increases in 1µM concentrations after 60mins (significantly higher than H_2O_2 and 100nM), which appears to become saturated after 90mins as no fold increases were observed. No change is seen in cells treated with 10nM concentrations of CMPD 73 at any time point compared to either H_2O_2 control or non-treated control.

By comparison CMPD 74 is not seen to be as potent as ROS generator as CMPD 73 (Figure 4.8 (B)). CMPD 74 displayed moderate ≈2-fold increases at 10nM and 100nM concentrations and modest ≈5-fold increases with 1µM concentrations (as seen more clearly using a smaller scale of fold change), indicating significant levels of ROS production compared to H_2O_2 and 100nM treated cells but not as pronounced as CMPD 73. 1,10-Phen produced very low levels intracellular ROS under these conditions but did not exceed the low levels of fluorescence compared to H_2O_2 control and so were not included in Figure 4.8.

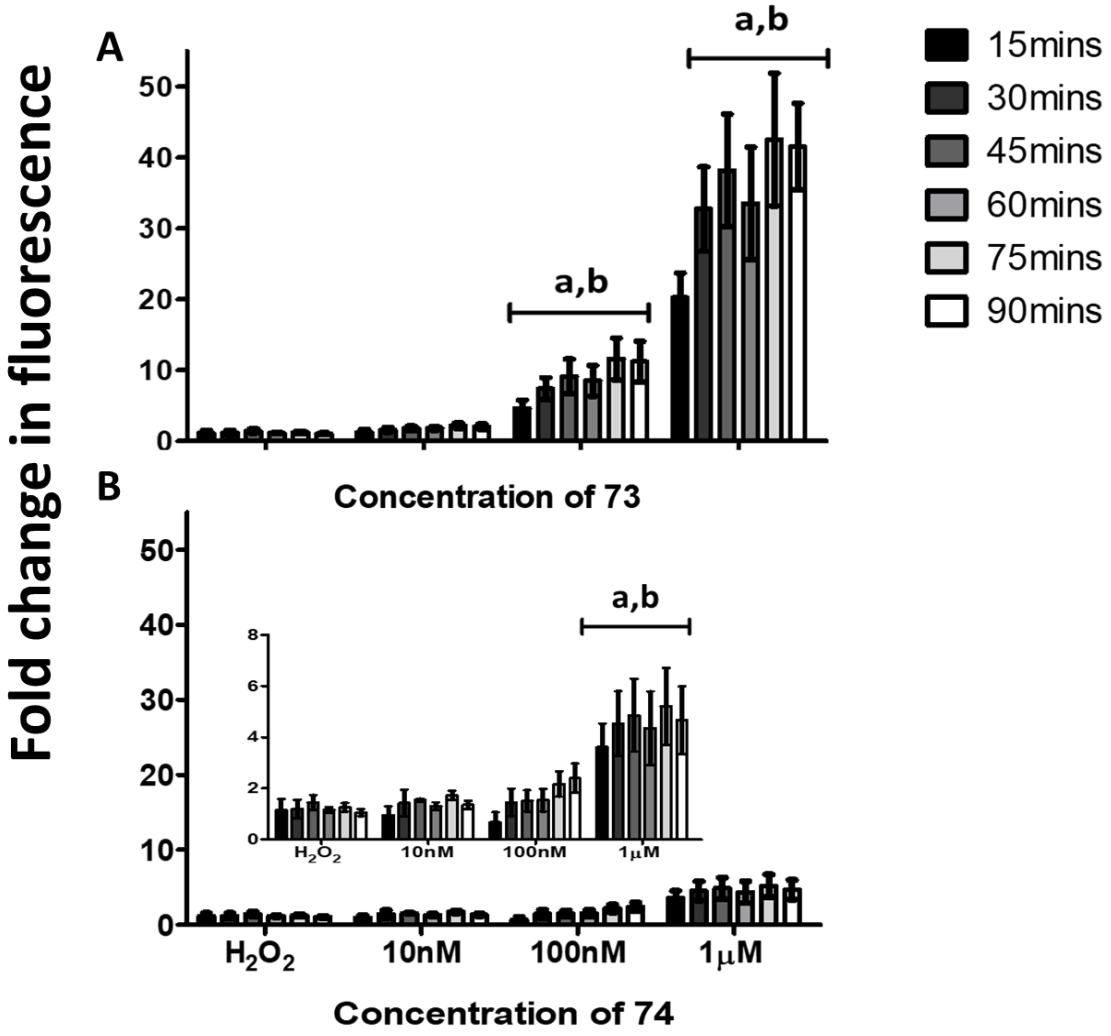

Figure 4.8- A549 cells stained with 10µM DCFDA and exposed to A) CMPD 73 and B) CMPD 74 for 15-90mins. Results are expressed as mean fold increase in fluorescent intensity ±1 Standard deviation of two independent experiments. (a= P<0.001 compared to 100nM or 10nM concentration, b= P<0.001 compared to H_2O_2 control). Inset shows the data for CMPD 74 with enlarged scale.

Figure 4.9 displays DCFDA fluorescence in response to metal phen treatment in A2780 cells. In contrast to A549 cells H_2O_2 produced a ≈5-fold increases in fluorescence compared to control cells in the A2780 cell line. Similar to A549 cells CMPD 73 demonstrated a ≈20fold increase in fluorescence at 100nM concentrations and ≈40-fold increase following 60 and 90min treatments at 1µM compared to non-treated control cells (Figure 4.9 A). No change is seen in cells treated with 10nM concentrations of CMPD 73 at any time point. Initial analysis of this data demonstrated CMPD 73 to significantly produce ROS in a concentration and time dependent manner and compared to H_2O control ($P<0.05$ for all comparisons). However following Holm-Bonferroni correction for multiple comparisons the data fell short of the corrected significance threshold ($P<0.01$). Despite this the notable increases in ROS detected are still apparent. Taken with similar results in A549 cells these data indicate CMPD 73 is a robust ROS catalyst.

CMPD 74 demonstrated immediate and potent ROS production at 10nM and 100nM concentrations (≈3-5-fold increases in fluorescence) in A2780 cells, an event not seen in A549 cells at the same concentrations. However while these increases in fluorescence were higher than in A549 cells (Figure 4.9 B) they did not exceed the maximum fold increases observed by H_2O_2 control at the same concentrations. CMPD 74 at 1µM increased DCFDA fluorescence ≈6-7 fold in A2780 cells, slightly higher than in A549 cells. This increase is not statistically significant compared to H_2O_2 however it is significantly higher than the previous 10nM and 100nM concentration. Similar to A549 cells 1,10-Phen did appear to produce intracellular ROS but again did not exceed the low levels of ROS detected by the H_2O_2 control and again were not included in Figure 4.9.

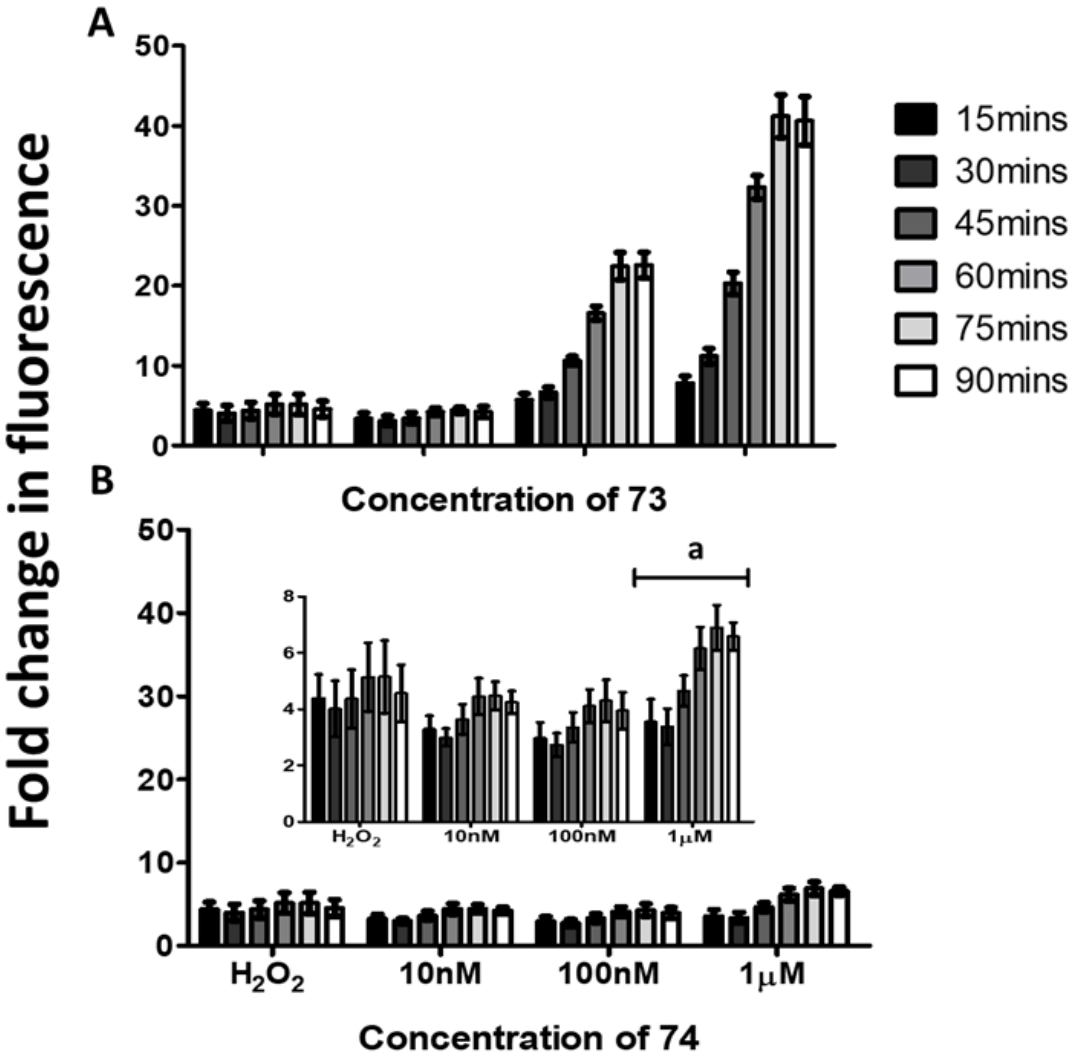

Figure 4.9-A2780 cells stained with 10μM DCFDA and exposed to A) CMPD 73 and B) CMPD 74 for 15-90mins. Results are expressed as mean fold change in fluorescent intensity ±1 Standard deviation of two independent experiments (a= P<0.001 compared to 100nM or 10nM concentration). Inset shows the data for CMPD 74 with enlarged scale.

4.4.3. Fluorescent staining of mitochondrial hydrogen peroxide

Addition of 100μM CMPD 73 or CMPD 74 to MitoPY1 treated A549 cells did not lead to the generation of significant amounts of mitochondrial H_2O_2 above that of the negative control (Figure 4.10). It has previously been reported (Kellett *et al.*, 2011) that treatment with analogous compounds lacking the ethereal bridge structure results in a 1.2-fold increase

in ROS generation following treatment of cells for 30 minutes and a 4-fold in ROS generation after 60 minutes. The current data, when expressed in a similar manner is comparable to these data – 45-minute treatment with CMPD74 led to ≈ 2-fold increase in mitochondrial-specific H_2O_2. Treatment with CMPD73 did not result in any increase in mitochondrial-specific H_2O_2 when compared to the non-treated control.

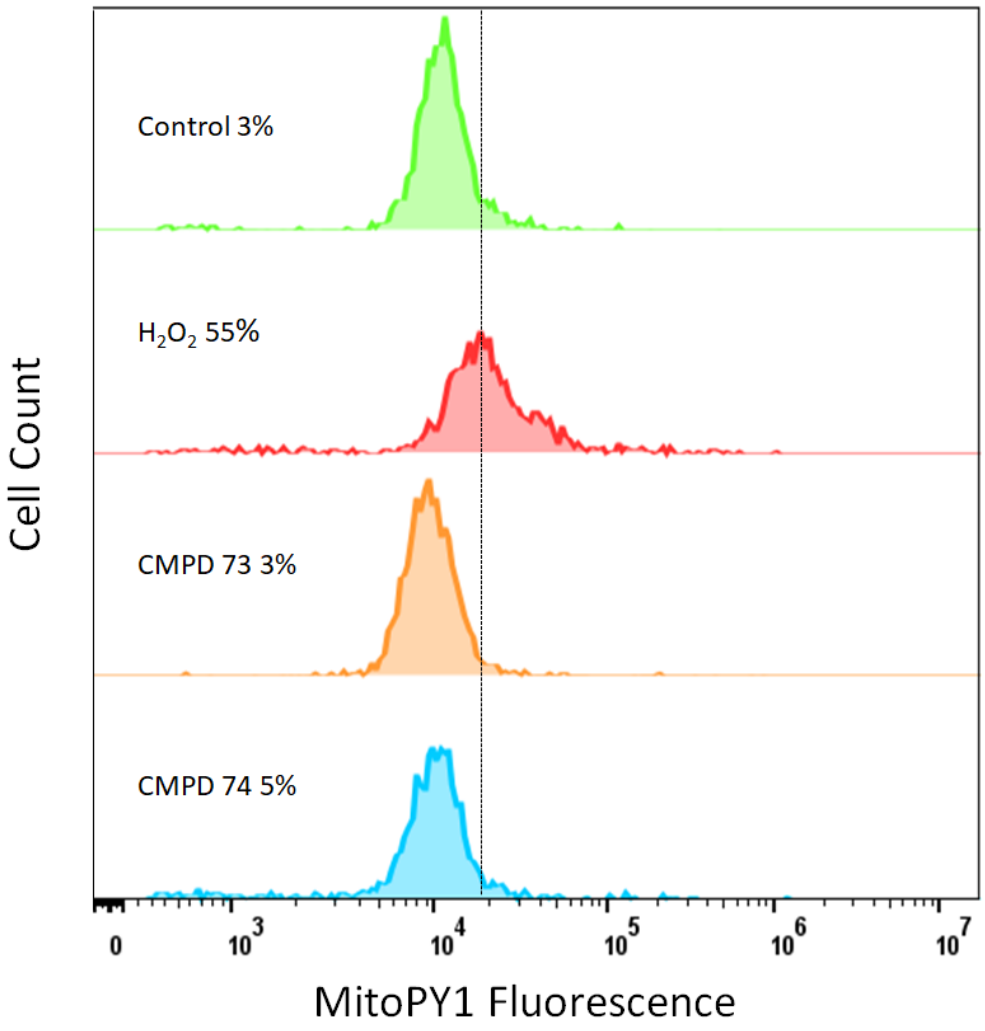

Figure 4.10-MitoPY1 staining of A549 cells exposed to 100µM CMPD 73, 74 and H_2O_2 control for 45mins. Representative data of two independent experiments using duplicate technical replicates. Dashed line represents gated events indicating increases in fluorescent signal relative to control conditions.

4.4.4. Selective inhibition of cellular antioxidant pathways:

H_2O_2 was used a model compound to evaluate the efficacy of the inhibitors in modifying treatment-dependent cytotoxicity, with a 24-hour treatment period. BSO and AT are expected to lead to a reduction of intracellular capacity to metabolise ROS and H_2O_2 and thus enhance its ability to cause cell death (Figure 4.11). As predicted, there were significant effects on the efficacy of H_2O_2 to act as a cytotoxic agent, with cell death essentially complete in the presence 50µM H_2O_2 and BSO or AT (Figure 4.12). Individually BSO and AT had no effect on cell viability. These results validate the use of BSO and AT as tools to interrogate the importance of H_2O_2 removal/deactivation mechanisms in cells treated with metal-phen compounds.

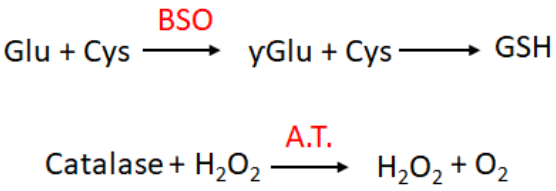

Figure 4.11- Selective inhibition of GSH synthesis pathway using BSO and the catalase H_2O_2 detoxification pathway by AT.

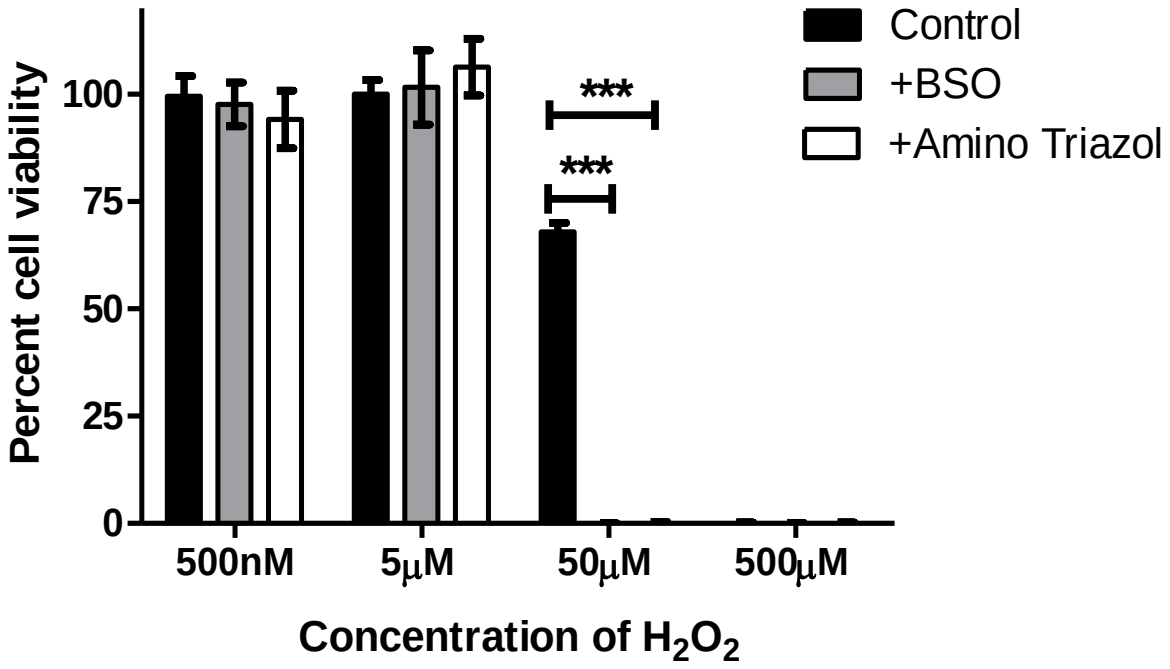

Figure 4.12 Chemical blockage of cellular antioxidant defences enhances susceptibility to H_2O_2 exposure in A549 cells. Results are expressed as mean percent viability ± 1 Standard deviation of two independent experiments (*** P<0.001 compared to control concentration). BSO and AT had no effect on cell viability.

Pre-treatment of A549 cells with BSO or AT for 24 hours before treatment with CMPD73 resulted in a modest, but significant, enhancement of efficacy with BSO more potent than AT (Figure 4.13). This effect is lost at higher concentrations of CMPD73, possibly due to a more generalised toxic effect on the cells.

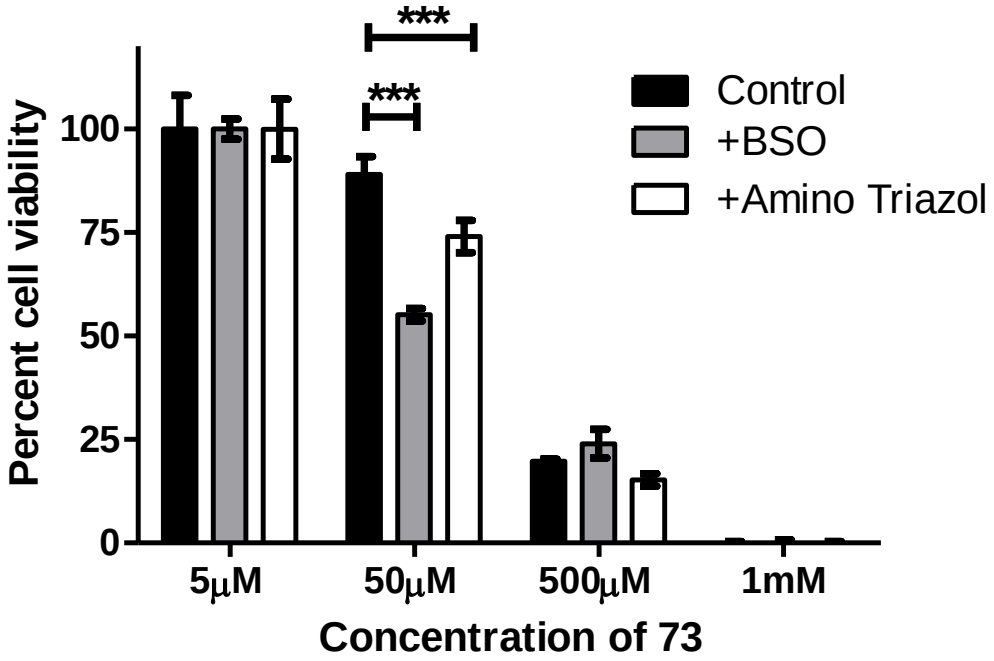

Figure 4.13 Effect of CMPD73 on A549 cells pre-treated with BSO and AT. Results are expressed as mean percent viability ±1 Standard deviation of four independent experiments. (*** P<0.001 compared to concentrations of compound control). BSO and AT had no effect on cell viability.

In a parallel experiment with CMPD74, there is a similar potentiation of the action of the compound, albeit at much lower concentration (Figure 4.14). There is essentially complete loss of cell viability at 5μM (P<0.001), a concentration which had no observable impact with CMPD73. There is only a modest decrease in viability for CMPD74 following addition of BSO. Intriguingly, there is no significant impact following AT treatment, in contrast to the analogous situation with CMPD73. In fact, there is an apparent slight increase in viability following AT treatment compared to the control.

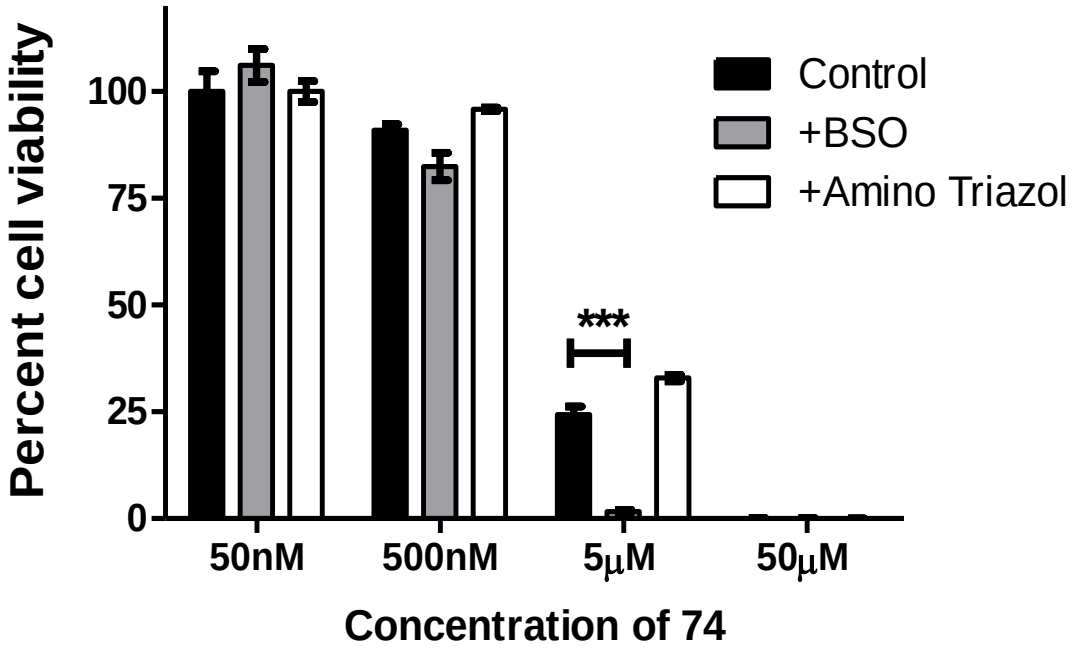

Figure 4.14 Effect of CMPD74 on A549 cells pre-treated with BSO and AT. Results are expressed as mean percent viability ±1 Standard deviation of four independent experiments. (*** P<0.001 compared to concentrations of compound control). BSO and AT had no effect on cell viability.

A549 cells pre-treated with BSO and exposed to concentrations of 1,10-Phen showed modest yet significant decreases in cytotoxicity following treatment with 10μM 1, 10-Phen (Figure 4.15), indicating that 1,10-Phen can kill cells via the production of ROS.

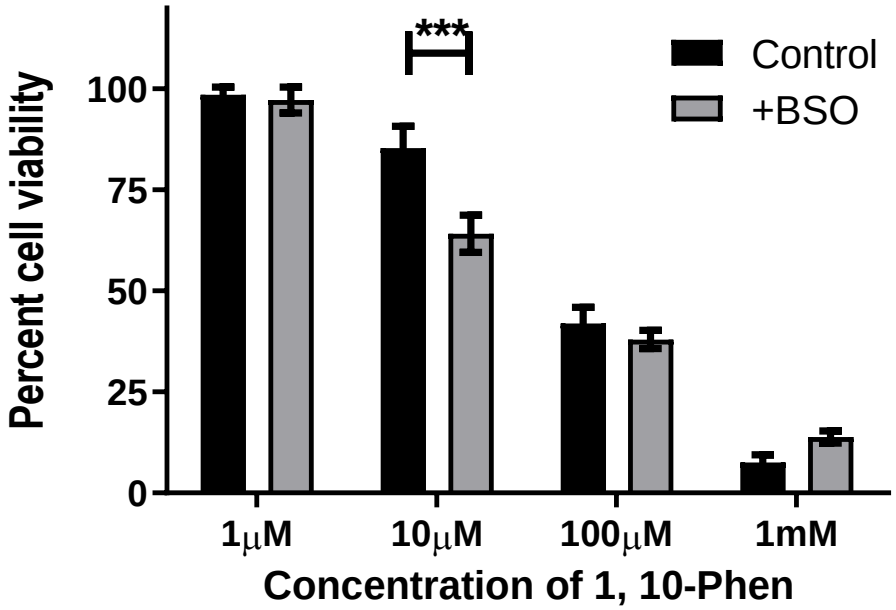

Figure 4.15 Effect of 1,10-Phen on A549 cells pre-treated with BSO. Results are expressed as mean percent viability ±1 Standard deviation of two independent experiments. (*** P<0.001 compared to concentrations of compound control). BSO and AT had no effect on cell viability.

Pre-treatment of CS mesothelioma cells with BSO or AT for 24 hours before treatment with CMPD73 resulted in a modest, but significant, enhancement of efficacy with BSO (Figure 4.16). No enhancement of efficacy is seen in treatments using AT, in contrast to effects noted in A549 cells with concentrations of 50μM experiencing a modest but significant enhancement of activity. This difference may be a result of cell type specificity and expression levels of antioxidant enzymes. In further contrast to A549 cells, the effect of BSO mediated enhancement continued significantly at higher concentrations of CMPD73, as CS cells are less sensitive to CMPD 73 than A549 cells.

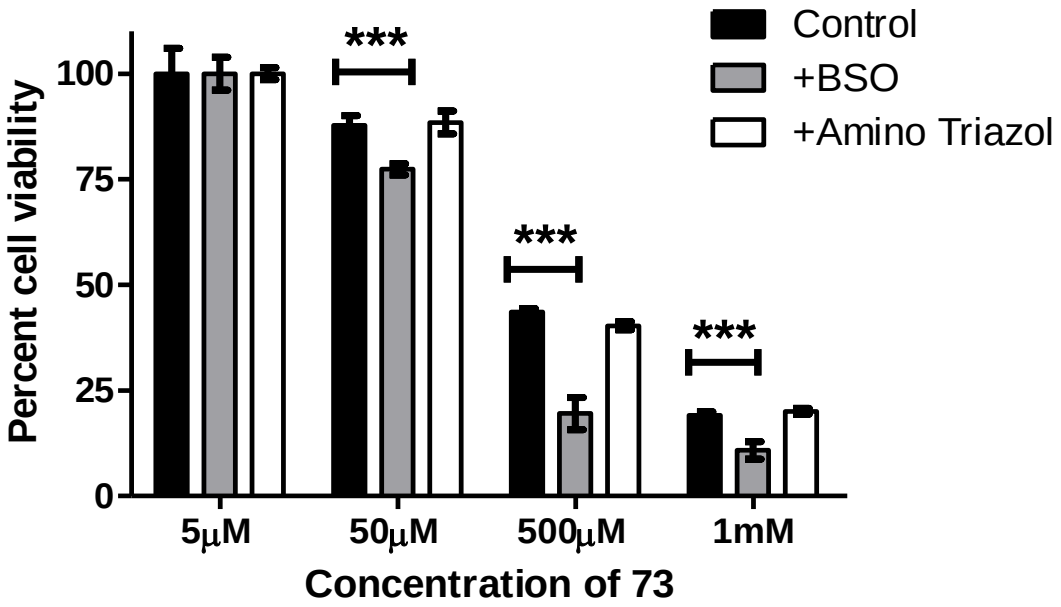

Figure 4.16-Effect of CMPD73 on CS meso cells pre-treated with BSO and AT. Results are expressed as mean percent viability ±1 Standard deviation of four independent experiments. (*** P<0.001 compared to concentrations of compound control). BSO and AT had no effect on cell viability.

CMPD74 displayed a similar response in CS meso cells as it did in A549 cells (Figure 4.17), with significant reduction in cell viability at 5μM (P<0.001). A similar comparison can be made between CMPD 73 and 74 as in A549 cells, in that potentiation of the CMPD 74 happens at a much lower concentration than CMPD 73. Similar to CMPD 73, there is no significant impact following AT treatment seen with CMPD 74. This result is also similar to AT treatment in A549 cells exposed to CMPD 74.

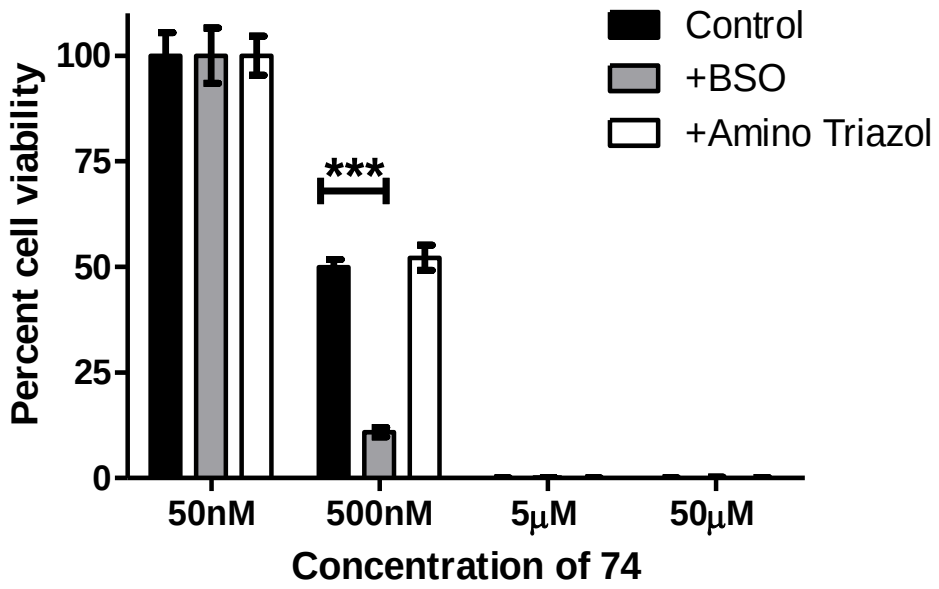

Figure 4.17-Effect of CMPD74 on CS meso cells pre-treated with BSO and AT. Results are expressed as mean percent viability ±1 Standard deviation of four independent experiments. (*** P<0.001 compared to concentrations of compound control). BSO and AT had no effect on cell viability.

Pre-treatment of CR mesothelioma cells with BSO or AT for 24 hours before treatment with CMPD73 resulted in a near identical result as CS meso cells treated in similar fashion (Figure 4.18). No increase in enhancement is seen in cells pre-treated with AT, with significant modest increases in enhancement in response to BSO pre-treatment. As CR meso cells are more sensitive to CMPD 73 than CS meso cells, this effect is lost at higher concentrations.

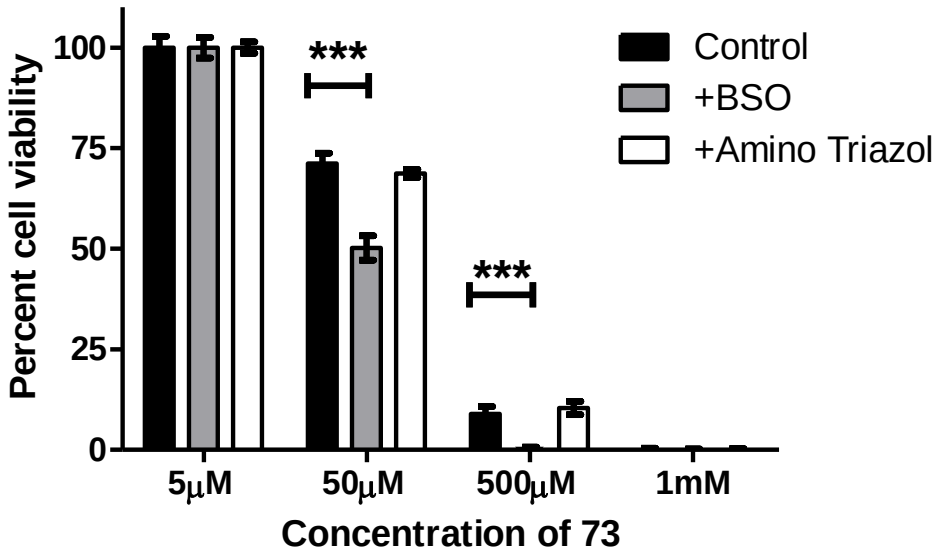

Figure 4.18-Effect of CMPD73 on CR meso cells pre-treated with BSO and AT. Results are expressed as mean percent viability ±1 Standard deviation of four independent experiments. (*** P<0.001 compared to concentrations of compound control). BSO and AT had no effect on cell viability.

Pre-treatment of CR mesothelioma cells with BSO or AT for 24 hours before treatment with CMPD74, as seen with CMPD 73, resulted in a near identical result as CS meso cells treated in similar fashion (Figure 4.19). No increase in enhancement is seen in cells pre-treated with AT, with significant increases in enhancement in response to BSO pre-treatment. As CMPD 74 does not distinguish between CS and CR meso cells near identical results were expected.

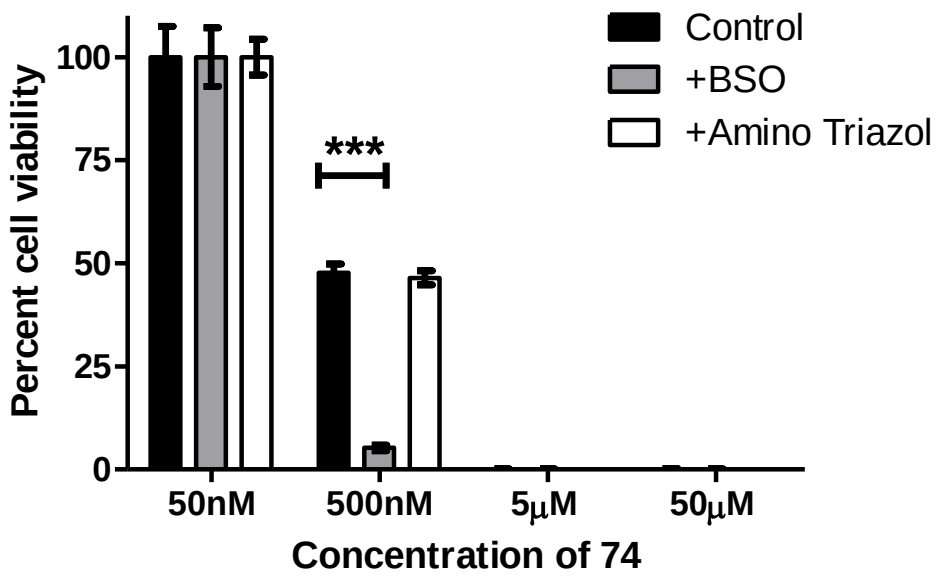

Figure 4.19-Effect of CMPD74 on CR meso cells pre-treated with BSO and AT. Results are expressed as mean percent viability ±1 Standard deviation of four independent experiments. (*** P<0.001 compared to concentrations of compound control). BSO and AT had no effect on cell viability.

A2780 cells were pre-treated with 1mM AT in order to determine whether limited enhancement of compound activity is a result of cell type specificity (Figure 4.20). CMPD 73 experienced no enhancement of efficacy in A2780 cells pre-treated with AT. It would appear A549 cells only can be sensitised to AT treatment regarding CMPD 73, albeit modestly only at 50μM.

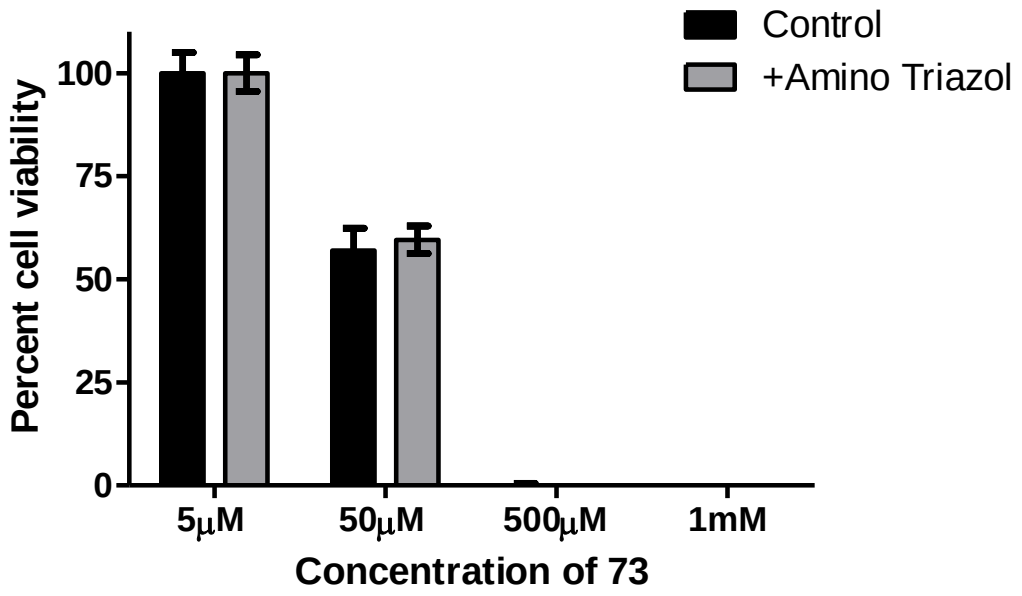

Figure 4.20-Effect of CMPD73 on A2780 cells pre-treated with AT. Results are expressed as mean percent viability ±1 Standard deviation of two independent experiments. AT had no effect on cell viability.

Pre-treatment of A2780 cells with AT and CMPD 74 did show very modest but significant increases in specificity at both 500nM and 50μM concentrations ($P<0.01$) (Figure 4.21). This is in contrast to the three other cell lines used where no enhancing effect is seen between CMPD 74 and AT.

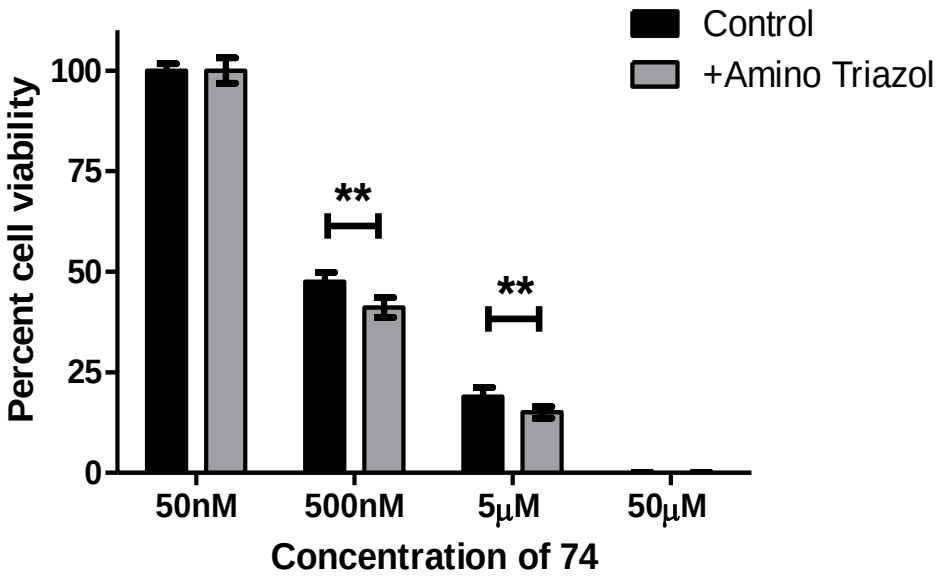

Figure 4.21-Effect of CMPD74 on A2780 cells pre-treated with AT. Results are expressed as mean percent viability ±1 Standard deviation of two independent experiments. (** P<0.01 compared to concentrations of compound control). AT had no effect on cell viability.

After extensive testing using multiple cell lines in can be determined that pre-treating cells with BSO significantly increases the cytotoxicity of both CMPD 73 and 74, indicating that the GSH antioxidant pathway is involved in compound detoxification. This supports previous observations using ROS detecting probes (DCFDA) that ROS generation is a key mechanistic event for these compounds. As inhibition of catalase using A.T. did not significantly increase the cytotoxic effects of either novel compound, catalase is not implicated in the detoxification of these compounds and likely excludes H_2O_2 generation as a key mechanistic event.

4.4.5. Selective inhibition of compound cytotoxicity using ROS scavengers

H_2O_2 was used a model compound to evaluate the efficacy of ROS scavengers in modifying treatment dependent cytotoxicity, with a 24-hour treatment period. NaPy and Tiron are expected to lead to increases in cell viability in response to treatment with H_2O_2 and thus

decreasing its ability to cause cell death. As predicted, there were significant effects on the efficacy of H_2O_2 to act as a cytotoxic agent, with cell death essentially reversed in the presence 50μM H_2O_2 and NaPy, and significantly reduced in the presence of Tiron (Figure 4.22). Individually NaPy had no effect on cell viability, while Tiron reduced cell viability by 25-30%. These results validate the use of NaPy and Tiron as tools to interrogate the scavenging capabilities of generated ROS in cells treated with metal-phen compounds.

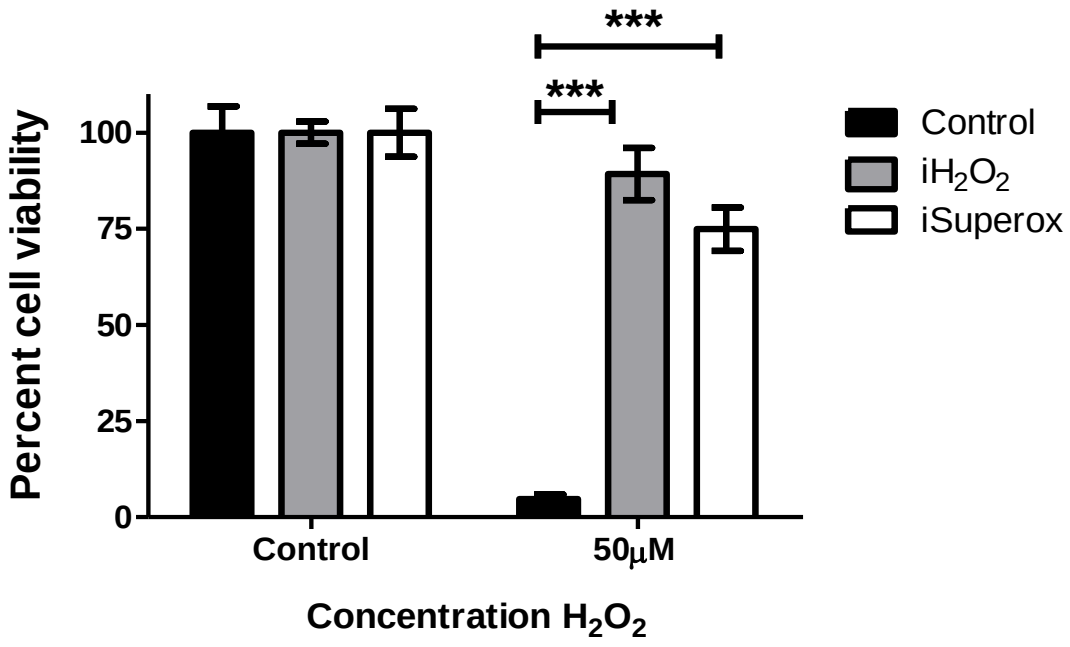

Figure 4.22-Chemical scavenging of H_2O_2 and superoxide decreases the susceptibility to H_2O_2 exposure in A2780 cells. Results are mean expressed as percent viability ±1 Standard deviation of two independent experiments. (*** P<0.001 compared to concentrations of compound control). NaPy had no effect on cell viability, while Tiron reduced cell viability by 25-30%.

Pre-treatment of A2780 cells with NaPy or Tiron for 1 hour before treatment with CMPD73 resulted in a significant increase in cell viability in response to Tiron (iSuperox), but not NaPy (H_2O_2) (Figure 4.23). This effect is lost at higher concentrations of CMPD73 and is likely a result of extreme levels of cytotoxicity overcoming scavenger effects.

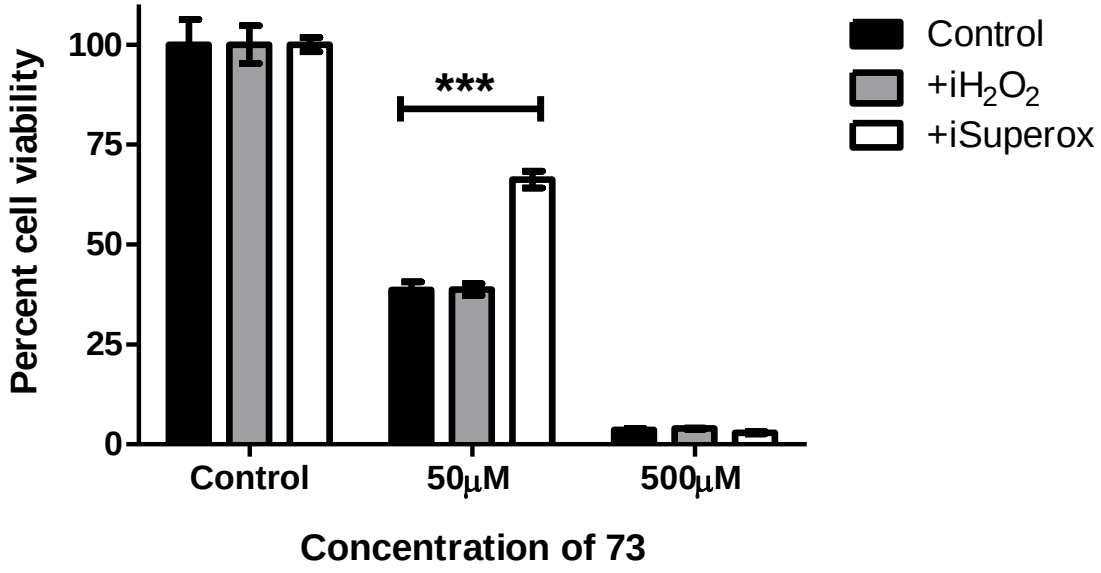

Figure 4.23-Effect of CMPD73 on A2780 cells pre-treated with NaPy (iH_2O_2) and Tiron (iSuperox). Results are expressed as mean percent viability ±1 Standard deviation of three independent experiments (*** P<0.001 compared to concentrations of compound control). NaPy had no effect on cell viability, while Tiron reduced cell viability by 25-30%.

In a parallel experiments with CMPD74, there is essentially a complete rescuing of cells from CMPD 74 cytotoxicity seen at 500nM (P<0.001) when cells were incubated with Tiron, compared to a 50% drop in viability in control conditions using CMPD 74 (Figure 4.24). A significant increase in viability is also seen at 5μM (P<0.001) to almost 75%, compared with near total cytotoxicity in control conditions. CMPD 74 is also seen to be significantly more susceptible to inhibition by Tiron than CMPD 73. NaPy had a more moderate but significant increase in cell viability when compared to CMPD 74 control conditions at both concentrations used.

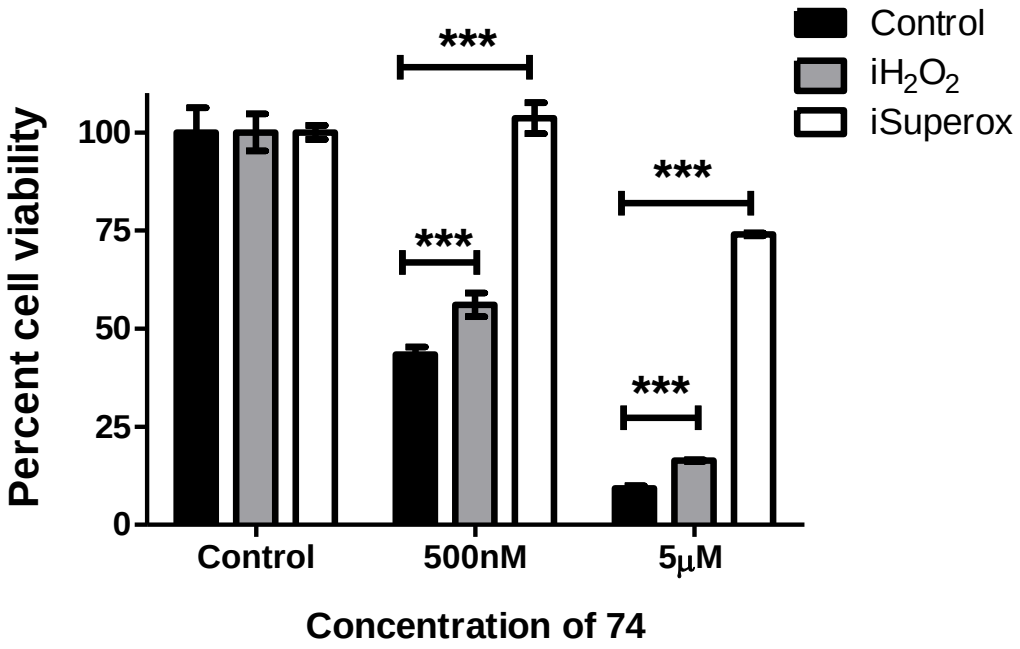

Figure 4.24-Effect of CMPD74 on A2780 cells pre-treated with NaPy (iH_2O_2) and Tiron (iSuperox).Results are expressed as mean percent viability ±1 Standard deviation of three independent experiments.(*** $P<0.001$ compared to concentrations of compound control). NaPy had no effect on cell viability, while Tiron reduced cell viability by 25-30%.

1,10-Phen displayed an almost identical ROS scavenging profile as CMPD 73 (Figure 4.25). No interaction is seen when NaPy is used. However, there is a significantly more pronounced, near total rescuing effect seen in response to treatment with Tiron, when compared to the same conditions and concentration using CMPD 73.

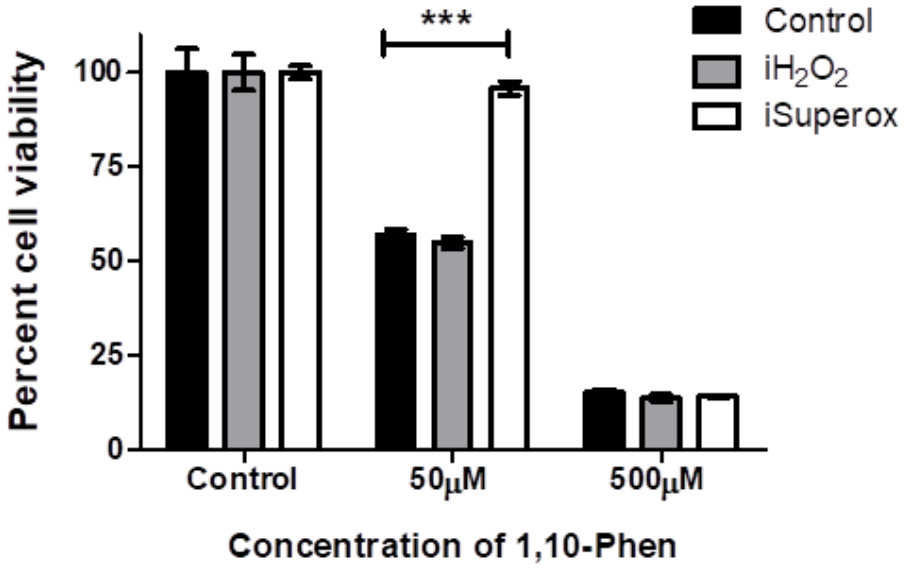

Figure 4.25-Effect of 1,10-Phen on A2780 cells pre-treated with NaPy (iH_2O_2) and Tiron (iSuperox). Results are expressed as mean percent viability ±1 Standard deviation of three independent experiments (*** $P<0.001$ compared to concentrations of compound control). NaPy had no effect on cell viability, while Tiron reduced cell viability by 25-30%.

4.5.Discussion:

Metal-phen compounds are often redox active and the generation of ROS is typically associated with the cytotoxic action of these compounds. So far both CMPD 73 and 74 have been demonstrated to possess potent cytotoxic effects towards cancer cell lines with an as of yet undefined cytotoxic mechanism. The data obtained from studies involving epigenetic chemo sensitisation strategies (Chapter 3) has highlighted potential crossovers between ‘’off target’’ effects of HDACi with suspected ROS generating capabilities of both test compounds and as such the production of ROS by these compounds has been investigated. Both compounds as well as 1, 10-Phen itself were demonstrated to generate ROS, with superoxide generation identified as the primary mediator of compound cytotoxicity.

The fluorescent probe DCFDA was used to investigate ROS generating potential of CMPDs 73 and 74 in A549 adenocarcinoma cells and A2780 ovarian cancer cells, with both cell lines indicating notable ROS production by both compounds comparable or comparably higher than both H_2O_2 and analogous CMPD 19 and 22. Following the use of appropriate statistical corrections (Holm-Bonferroni correction) to account for Type 1 errors, data which was initially statistically significant (flow cytometric analysis of compounds in both cell lines, CMPD 73 in microplate setting using A2780 cells) no longer appears to be statistically significant. However, the observed impacts of both compounds are comparable between cell lines and is interpreted as an authentic biological effect. Biochemical probing for the generation of ROS is demonstrated to produce statistically significant results supporting the observations made using fluorescent DCFDA staining. As such the loss of significance using DCFDA staining to detect ROS generation by metal-phen compounds may be a result of strict significant thresholds associated with Bonferroni/Holm-Bonferroni corrections coupled with a degree of variability among biological replicates.

Interestingly 1,10-Phen is also demonstrated to produce significant amounts of ROS when examined using flow cytometry, an event which is not detected using DCFDA in a fluorescent spectrophotometric setting. This may possibly be a result of the lower concentrations of test compounds which are generally used for fluorescent spectrophotometric assays to avoid saturation of the detecting instrument. This data suggests that the hypothesis for both CMPD 73 and 74 operating through a redox active mechanism of cytotoxicity is correct and that ROS generation can be conducted by either the compounds, 1,10-Phen or any potential alternate compounds that may arise following compound disassociation. However, it should be noted that caution must be taken when examining results provided by the DCFDA probe as can be seen when careful examination of CMPD 19 and 73 is undertaken. CMPD 73 is seen to follow a similar trend to CMPD 19, with significant, rapid, and potent generation of ROS even more so than that of CMPD 19. This apparent rapid generation of ROS as detected by DCFDA staining however may be an artefactual effect rather than a biological one.

Previous studies using the analogous compounds lacking the ethereal oxygens revealed that they may be capable of leading to the production of ROS within the cell (Kellett *et al.*, 2011). Careful examination of the data related to ROS revealed that the copper containing compound (CMPD22, dark grey circles in Figure 4.26) did not promote the formation of a greater amount of ROS compared to 1,10-phen alone (average across all concentrations of 2.2-fold increase in ROS for both CPMD22 and 1,10-phen). In contrast, the manganese containing CMPD 19 is reported to induce significant production of cellular ROS with a 20-fold increase in DCF fluorescence at 1μM (Figure 4.26).

CMPD 19 has also been reported to have significant superoxide dismutase and catalase mimetic activities. It has been described that DCFDA generates a radical intermediate (DCF•−) which is capable of reacting extremely rapidly with O_2 to generate superoxide (Wrona and Wardman, 2006). The SOD mimetic activity of CMPD 19 would lead to the generation of H_2O_2 from this superoxide in a concentration dependent manner which can, in the presence of iron, react with the DCFH2 to generate the DCF•− intermediate. This process creates a potential amplification loop for the generation of intracellular ROS, once the SOD activity increases sufficiently. Indeed a reanalysis of the data from Kellet *et al* (2011) reveals that up to 500nM of CMPD 19 the increase in ROS almost perfectly follows the expected pattern for exponential growth (Figure 4.26, black circles) which is consistent with the hypothesis described above. A possible explanation for the decrease observed at the highest concentration (1μM) is that the catalase mimetic activity of the compound may become sufficient to degrade the H_2O_2 and block this cycle. Since CMPD 73 is also manganese containing with further potential for SOD-mimetic activity the same artefactual reaction described for CMPD 19 may explain the rapid increase in apparent ROS production detected by DCFDA in both flow cytometric and spectrophotometric settings.

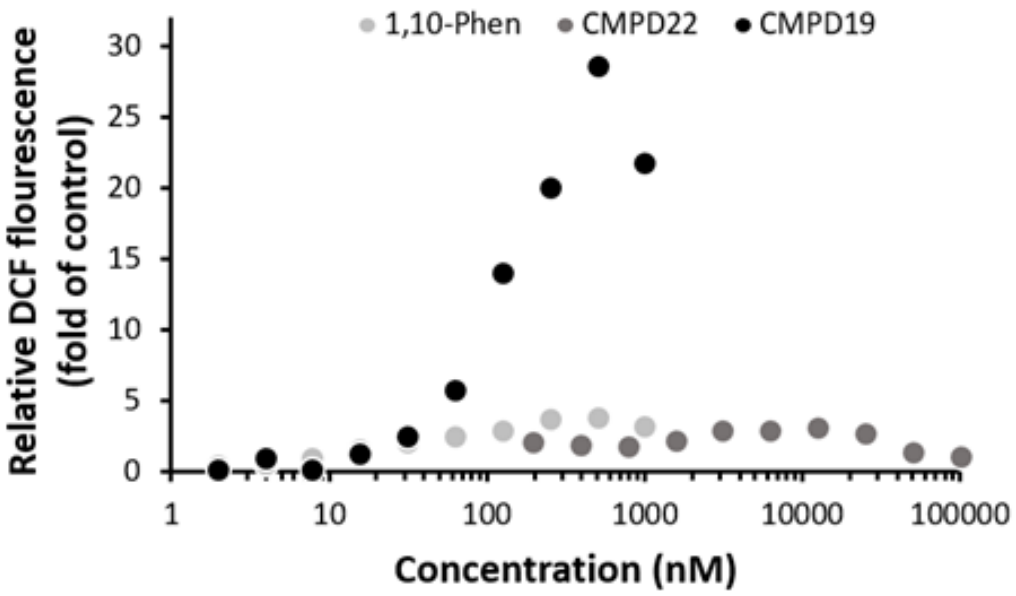

Figure 4.26- Extracted data from Kellet *et al* (2011) re. ROS production of analogous compounds. CMPD 22 is the analogous copper compound, while CMPD19 is the analogous manganese compound.

As such the apparent potency of ROS generation by manganese-phen compounds may be a caveat when using DCFDA staining resulting from potential SOD-mimetic activity, rather than that of significant intracellular ROS generation. While the use of DCFDA staining is suggestive of ROS production by both CMPD 73 and 74, DCFDA staining may not be the most reliable method for ROS detection at least with regards to manganese containing compounds. As such other methods are required to overcome these limitations, such as ROS specific fluorescent probes that do not undergo artefactual feedback loops. Other limitations of DCFDA staining are that only generic ROS generation is detected rather than exact reactive species and as such further investigation using ROS specific probes and scavengers as well as inhibitors of antioxidant pathways is warranted. The lack of the apparent artefactual SOD mimetic activity seen with CMPD 74 and free 1,10-Phen potentially validates data obtained for these compounds by DCFDA staining; however speciation of ROS detected is required.

Using a chemically distinct mitochondrial specific H_2O_2 probe, MitoPY1, only a very minor increase in mitochondrial H_2O_2 is observed. This is observed in A549 as well as isogenic mesothelioma cells (data not shown). The increase is considered to be within the margin of error for the method rather than a reflection of intra-mitochondrial production of H_2O_2.

Although it is not possible to resolve significant changes in mitochondrial ROS concentrations following treatment with CMPD73 and CMPD74, pre-treatment of cells with BSO or AT (in the case of CMPD 73) significantly enhanced the cytotoxic capacity of the compounds. There is no impact of either BSO or AT on the cell viability alone. These data indicate that adequate GSH levels and catalase activity are required to limit cell death, consistent with an elevation in cellular ROS levels.

In the A549 cell model a greater enhancement in cytotoxic activity is observed following BSO treatment than AT, particularly with regards to CMPD74. These data suggest that the GSH pathway may be more critical for the elimination of intracellular ROS generated as a result of the (direct or indirect) action of the metal-phen compounds. Treatment of CS or CR mesothelioma cell lines with CMPD73 under conditions where catalase is inhibited did not reveal any enhancement in cytotoxicity. This may be due to the development of mesothelioma in a high ROS environment (e.g. asbestos exposure) which promotes high level expression of SOD, catalase and other redox defence enzymes and may explain in part why the isogenic CS mesothelioma cell line is more tolerant to CMPD 73 than the A549 cells. Indeed it has been reported that this is in fact the case in malignant mesothelioma (Kahlos *et al.*, 1998). This can further be supported by the modest yet significant enhancement of CMPD 74 by AT in A2780 cells, indicating that CMPD 74 may indeed interact with the catalase pathway, albeit to a very low degree in a cell type specific context.

The possibility that CMPD73 has inherent catalase mimetic activity similar to that of CMPD 19 may also be a reason for the less pronounced effect of AT in the various model systems tested. If catalase mimetic activity is taking place, then it would remove H_2O_2 through its inherent biochemical mimetic activity and would therefore not rely on H_2O_2 production for biological activity.

Comparing both CMPD 73 and free 1,10-Phen in A549 cells in response to knockdown of GSH (indirectly confirmed by increased cytotoxicity of H_2O_2 assay control) may again demonstrate that compound efficacy is predominantly driven by the action of 1,10-Phen rather than the compound as a whole. Both CMPD 73 and Phen appear to respond to GSH synthesis inhibition only within the 10-100μM range, before the effect experiences a plateau at higher concentrations. These similarities further support these previous observations. Inhibition of the GSH pathway also supports the notion that the exceptionally high levels of apparent ROS generation detected by DCFDA fluorescent staining were likely a result of the artefactual reaction described regarding CMPD 73. While highly significant, the levels of enhanced cytotoxicity mediated by CMPD 73 in BSO treated cells is much lower than would be expected for a compound with the exceptional ROS generating potential demonstrated by DCFDA staining. While DCFDA staining is still indicative of ROS generation by CMPD 73 despite artefactual reactions further experimentation using biochemical probes and genetically encoded ROS sensors will be required to validate observations made with the current fluorescent probes.

Comparing both BSO/AT treatments with results obtained from ROS scavenging studies sheds further light on intracellular redox status induced by both CMPD 73 and 74, in the

context of A2780 ovarian cancer cells. The use of NaPy to scavenge H_2O_2 again demonstrates cell type specificity regarding intracellular H_2O_2 production, as results from AT-treated A2780 cells reflects those of NaPy-treated cells. While H_2O_2 can vary between cell types, it does not appear to be a key reactive species in ROS-mediated cytotoxicity of either compound. The limited detection of H_2O_2 may be a result of indirect generation in response to the dismutation (randomly by diffusion or by SOD activity) of the large quantity of superoxide produced by both compounds. H_2O_2 may therefore not be as far reaching throughout the cell as superoxide appears to be, if produced significantly at all. These data also indicate the use of H_2O_2 scavengers over the inhibition of H_2O_2 detoxifying enzymes for accurately determining the role of intracellular H_2O_2.

The identification of the superoxide anion as the major species of ROS required for metal-phen cytotoxicity can serve as a possible link between the modes of cell death already established in Chapter 2 for each compound. Superoxide has been implicated as a mediator of both mitochondrial and ER induced cell death (Inoue and Suzuki-Karasaki, 2013), as well as been implicated as a master regulator of autophagy and therefore autophagic cell death (Chen, Azad and Gibson, 2009).

Both CMPD 73 and 74 have been demonstrated to interact significantly with the apoptotic pathway, and so superoxide may be the signalling molecule responsible for its activation. This may particularly be the case regarding CMPD 74 owing to is apparent high level of dependency on superoxide production to mediate cytotoxicity (≈65% increase in viability compared to control compound). However, where superoxide is targeting e.g. the mitochondria is yet to be determined and doing so should shed light on the exact mechanism through which both CMPD 73 and 74 exert their cytotoxic effects. Redox sensitive

fluorescent probes such as MitoSOX red, which specifically stains mitochondria and fluoresces upon activation by superoxide would likely shed light on the intracellular targets of metal-phen generated superoxide, particularly when used in combination with apoptotic markers to determine a causal link between the two, as assayed by Mukhopadhyay *et al*., (2007) using flow cytometry-based methods.

Upon further comparison between CMPD 73 to metal-free 1,10-Phen, a very similar ROS profile emerges with a key difference being the sensitivity in which Tiron scavenging of superoxide protects A2780 cells from either compound, with test cells experiencing near total protection from 1,10-Phen, and significant but a slightly less degree of protection from CMPD 73. The reasons to this are yet unknown however it could be speculated that the higher molar equivalents 1,10-Phen delivered by CMPD 73 are overwhelming the cytoprotective effects of Tiron and lower concentrations of CMPD 73 may show similar effects (discussed Chapter 2 page 88-89). As such this line of study warrants further investigation. As 1,10-Phen is the major contributor to CMPD 73 cytotoxicity, (discussed in Chapter 2), shared ROS profiling further supports this hypothesis. The generation of superoxide by 1,10-Phen may occur indirectly as a result of SOD1 and 2 inhibition mediated by 1,10-Phen chelation. Evidence of 1,10-Phen-associated superoxide generation is presented later in this thesis.

An attempt to use DMSO, a hydroxyl radical scavenger, was conducted in order to determine whether hydroxyl radical inhibition could have potential cytoprotective effects on the cells in response to metal-phen treatments. However, pilot studies using both 1% and 10% DMSO in RNA degradation studies determined that only 10% DMSO is capable of hydroxyl radical

inhibition. DMSO at 10% concentration is seen to be highly cytotoxic itself and was unsuitable for this investigation.

SOD mimetic activity of metal-phen compounds has been a point of investigation for many previous analogues, CMPDs 19 and 22 from Kellet (2011) a prime example. However the data described may be telling that SOD mimetic activity, at least regarding CMPD 73 or 74, may not be as biologically relevant as originally hypothesised. SOD mimetic activity has not yet been directly determined for CMPD 73 or 74, however the data obtained from DCFDA staining are highly suggestive of SOD mimetic activity regarding CMPD 73. This coupled with the larger effect of the superoxide scavenger compared to H_2O_2 scavenger (none for 73 and minimal for 74, Figures 4.21 and 4.22) indicate superoxide is quite likely not being dismutated by either compound, at least at a level of any biological significance. Taking this into account SOD mimetic activity may not be a fruitful avenue for probing potential cytotoxic mechanisms and may only be relevant as a caveat when using fluorescent ROS probes as discussed above. Catalase mimetics have also been demonstrated for previous analogues (CMPD 19 and 22 respectively Kellet *et.al* 2011). However the low reliance on H_2O_2 production for cytotoxicity again likely renders this avenue of investigation redundant.

Taken together these data provide significant evidence to the ROS-dependent cytotoxic nature of both CMPD 73 and 74 metal-phen based compounds, and that superoxide generation is the ROS critical for these toxic effects. Further studies will be required to fully determine the intracellular targets of generated superoxide, and if it is the key mediator of previously determined apoptotic cell death pathways induced by both compounds.

5. Investigating Ferroptosis as a mechanism of cell death

5.1. Introduction

As discussed in Chapter 4 cell injury as a result of oxidative stress can manifest in many different forms. One potential route for metal-phen compounds, and in particular CMPD 74, to target cells via oxidative stress is through the generation of peroxyl radicals and toxic lipid peroxides. As the main component of cellular membranes, lipids have an indispensable role in maintaining the structural integrity of cells, as well as acting as signalling molecules (Fahy *et al.*, 2011). Lipid peroxidation is defined as the oxidative degeneration of lipids, and so extensive peroxidation alters the physical properties of cellular membranes and can cause covalent modification of proteins and nucleic acids (Gaschler and Stockwell, 2017).

5.1.1. Lipid peroxides

Lipid peroxides are formed by the oxidation of lipids containing carbon-carbon double bonds, in particular polyunsaturated fatty acids (PUFAs) (Newcomer and Brash, 2015). Lipid peroxidation consists of three distinct steps, initiation, propagation, and termination. In the initiation step, pro-oxidant molecules such as the hydroxly radical ($OH^{\bullet}$), peroxyl radical ($ROO^{\bullet}$), singlet oxygen ($^1O_2$), or peroxynitrite ($ONOO^-$) extract allylic hydrogen forming a carbon-centred radical forming a lipid radical ($L^{\bullet}$). In the propagation step, $L^{\bullet}$ reacts with oxygen forming lipo-peroxyl radicals ($LOO^{\bullet}$), which can in turn extract another hydrogen from its neighbouring lipid molecule, yielding another $L^{\bullet}$ and a lipid hydroperoxide (LOOH). This will manifest as a cascade of continuing oxidation of neighbouring lipid molecules within the membrane (reviewed Ayala, Muñoz, & Argüelles, 2014). The propagation step will continue until terminated by chain breaking antioxidants such as lipid soluble Vitamin E, found within cell membranes (Niki, 2015). The steps of initiation, propagation and termination can be seen in Figure 5.1.

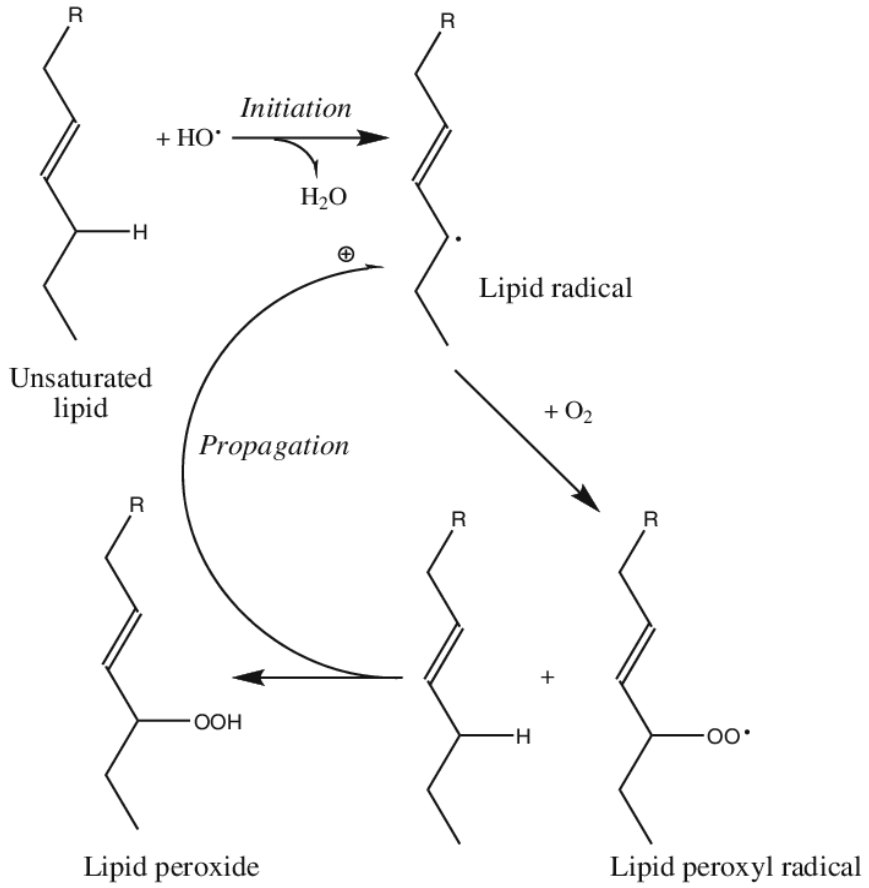

Figure 5.1-Initiation and propagation of lipid radicals and generation of lipid peroxides (Freinbichler *et al.*, 2011).

Lipid peroxides, non-radical intermediates of lipid oxidation, are moderately more stable in contrast to highly reactive lipid radicals ($L^{\bullet}$, $LOO^{\bullet}$) (Shahidi and Zhong, 2010). As a hydroperoxide, lipid peroxides behave similarly to H_2O_2, with their relative stability allowing them to transverse cell membranes and permeate the cell much further from their point of origin than other peroxidation products (Girotti, 1998). They are also vulnerable to further reduction by Fenton like chemistry by free iron or copper, as well as by other lipid radicals breaking down into more reactive intermediates, predominantly aldehydes such as hexanal, 4-hydroxynonenal (HNE) or malonaldehyde (MDA) (Barrera, 2012). HNE is the most intensively studied aldehyde produced by lipid peroxide reduction, as it is known as a second messenger of free radicals and is a major biomarker for lipid peroxidation (Ayala,

Muñoz and Argüelles, 2014). MDA is also an important lipid metabolite as it can form covalent adducts with deoxyguanine and deoxyadenine in DNA (Marnett, 1999), adding another layer of potential oxidative damage attributed to lipid peroxidation.

Lipid peroxides are known to be produced in an iron-dependent manner within cells, either enzymatically or non-enzymatically (Kristinova *et al.*, 2014). Non-enzymatic peroxidation occurs in response to oxidative stress via the Fenton reaction in response to increased iron and the production of free radicals such as $OH^{\bullet}$ (Carlsen, Møller and Skibsted, 2005). Other non-enzymatic oxidation can result from lipid photo-oxidation as a result of high energy radicals produced by UVA light (sunlight), such as $^1O_2$, or by spontaneous auto-oxidation resulting from the reaction of oxygen with traces of transition metals (iron)and PUFAs (Sun *et al.*, 2011).

Enzymatic lipid oxidation is carried out by a family of iron-dependent Lipoxygenases (LOX), which catalyse the dioxygenation of long chain PUFAs containing 2-6 double carbon bonds, such as linoleic, arachidonic, and docosahexaenoic acids (Gaschler and Stockwell, 2017). They are non-heme containing, iron-dependent oxygenases heavily involved in cell signalling via production of eicosanoids such as prostaglandins (Mashima and Okuyama, 2015), and the inflammatory response by producing leukotrienes (pro-inflammatory molecules), or lipoxins (anti-inflammatory molecules) (Chandrasekharan and Sharma-Wali, 2015). Lipoxygenases are classified as 5-, 8-, 12, and 15-lipoxygenases according to their selectivity to oxygenate specific carbons found within fatty acids (Wisastra and Dekker, 2014).

The deleterious effects of cytotoxic lipid peroxides (loss of membrane integrity, DNA damage) if left unresolved will result in induction of either apoptotic, autophagic or necrotic cell death pathways (Su *et al.*, 2019). However, in recent years it has been shown that another form of iron regulated programmed cell death, known as ferroptosis, can occur in response to lipid peroxidation (Dixon *et al.*, 2012).

5.1.2. Ferroptosis

Ferroptosis is defined as an iron-dependent regulated form of necrotic cell death, characterised by the accumulation of lethal lipid peroxides (Dixon *et al.*, 2012). It is mechanistically distinct from other regulated forms of cell death such as apoptosis or autophagy (Gaschler and Stockwell, 2017). In ferroptosis, release of cellular pools of iron from degraded ferritin via autophagy (termed ferritinophagy) results in uncontrolled production of lipid ROS, which in turn initiates the generation of toxic lipid peroxides, which can either disrupt membrane integrity or become incorporated incorrectly into membrane lipid bi-layers, disrupting homeostatic function and membrane protein signalling, causing membrane disruption, loss of function of membrane bound organelles and cell death (Latunde-Dada, 2017). Ferroptosis is distinct from apoptosis in that it is not caspase dependent and does not exhibit the same structural changes such as chromatin condensation or membrane blebbing. Ferroptotic cells tend to present as rounded and detached, with shrunken mitochondria devoid of cristae (Xie *et al.*, 2016).

The cause of ferroptosis is primarily dependent on the repletion and depletion of iron and GSH within the cells causing uncontrolled production of lipid peroxides. This can be triggered via oxidative stress from exogenous or endogenous agents, resulting in the inhibition of both GSH synthesis and the GSH dependent enzyme Glutathione Peroxidase 4

(GPx4) (Su *et al.*, 2019). GPx4 has been identified as the primary enzymatic antioxidant responsible for detoxification and removal of lipid peroxides from the cell (Ighodaro 2018). The role that iron plays in ferroptosis is two-fold, either through ferritinophagy in response to cysteine deprivation, or acting as a co-factor in the iron-dependent LOX family of enzymes (Newcomer and Brash, 2015; Lei, Bai and Sun, 2019). High levels of free iron are available to degrade H_2O_2 via Fenton like reactions to produce the hydroxyl and peroxyl radicals, which in turn can oxidise membrane PUFAs and either initiate or propagate lipid peroxide production. LOX enzymes experience an increase in activity in response to elevated levels of cellular free iron, uncontrollably generating higher levels of lipid peroxides within the cell (Gao and Jiang, 2018). The primary species of PUFA identified as the main ferroptotic death signals are phosphatidylethanolamines (PE) containing both arachidonoyl (AA) and adrenoyl (AdA) fatty acyls. Bis-allylic PEs containing these fatty acyls are subject to oxidation by 15-LOX to generate lipid hydroperoxides, which then initiate ferroptosis (Feng and Stockwell, 2018).

Lipid peroxidation can also result from the inactivity or inhibition of GPX4, either by direct inhibition by an exogenous agent, or indirect inhibition resulting from reduced synthesis of GSH, the critical co-factor for GPX4 activity. GPX4, a phospholipid hyrdroperoxidase, is the primary antioxidant enzyme tasked with detoxifying lipid peroxides and maintaining membrane fluidity and integrity. It exists in 3 isoforms, cytosolic, mitochondrial and nuclear forms. GPX4 uses reduced GSH as a cofactor to reduce oxidised PUFAs, preventing further propagation of lipid oxidation. The resulting oxidised GSSG disulphide is then reduced by GSH reductase (reviewed Seibt, Proneth, & Conrad, 2019).

GSH synthesis is dependent on System X_c^-, a plasma membrane bound cystine/glutamate antiporter responsible for importing cystine, the oxidised form of cysteine required for GSH synthesis (Dixon *et al.*, 2014). Cysteine and glutamate are then incorporated into the active GSH molecule by glutamate cysteine ligase (GCL). Both the importation of cysteine and the subsequent GSH synthesis are two of the most vulnerable sites within the ferroptosis pathway which are subject to inhibition by ferroptosis inducing drugs (Zou *et al.*, 2019). Erastin and BSO target System Xc- and GCL to cause a decrease in GSH synthesis and availability, while RSL3 and RSL5 directly targets GPX4 activity essential for ferroptosis induction, with Erastin-mediated inhibition further capable of activating ferritonphagy releasing iron from ferritin increasing cellular labile iron pools (Wang *et al.*, 2018; Lu *et al.*, 2018; Sato *et al.*, 2018). Therefore, it is generally seen that it is the downregulation of GSH and GPX4 activity that is the primary mechanism mediating ferroptotic cell death, and that labile iron pools are a downstream factor responsible for the final execution of the process (Dixon, 2017).

Inhibitors of ferroptosis tend to be lipid antioxidants capable of terminating iron or lipid oxidation reactions (e.g. Ferrostatin-1 chelates iron, Liproxstatin-1 and α-tocopherol scavenge lipid ROS) (Skouta *et al.*, 2014). Ferrostatin-1 and Liproxstatin-1 are lipophilic amines/imines that are thought to accumulate within the cell at high concentrations, and furthermore in acidic intracellular compartments such as lysosomes and peroxisomes (Stoyanovsky *et al.*, 2019). Trolox, a water-soluble form of Vitamin E, has also been implicated as an inhibitor of ferroptosis, as it acts as a chain-breaking antioxidant for lipid peroxide generation (Cao and Dixon, 2016). The ferroptotic pathway, its inducers and its inhibitors can be seen in Figure 5.2.

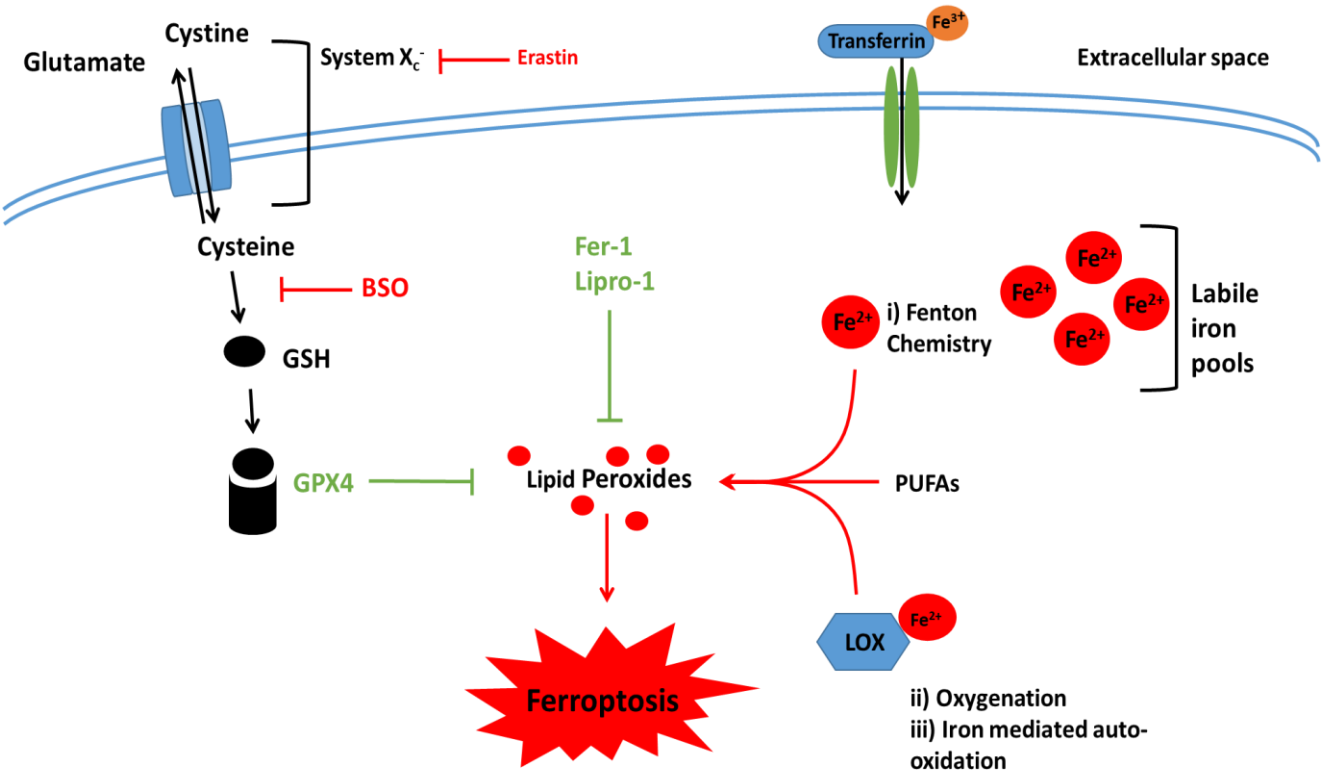

Figure 5.2-Mechanisms of Ferroptotic cell death. Inducers of ferroptosis are represented in red (arrows, inhibitory bars) while inhibitors of ferroptosis are represented in green (inhibitory bars). Inhibition of system X_c^- by Erastin or BSO prevents GSH synthesis and reduces GPX4 activity. Excess importation of transferrin-associated iron increases labile iron pools which serve to increase LOX activity and Fenton like chemistry to generate lipid peroxides capable of inducing ferroptosis. Ferroptosis can be inhibited by GPX4 and Fer-1 or Lipro-1 which prevent accumulation of lipid peroxides. This figure was self-generated using Microsoft PowerPoint based on the current understanding of knowledge from a multitude of sources.

Ferroptosis has been implicated in numerous human pathologies (neurodegenerative diseases, ischemic perfusion injury), but a normal physiological function for ferroptosis has not been identified (Feng and Stockwell, 2018). However, ferroptosis has recently been investigated as a novel target for potential chemotherapeutic agents (Xu *et al.*, 2019). Cancer cells, as a result of metabolic reprogramming, are often more sensitive to ferroptosis than that of their non-cancerous counterparts (Friedmann Angeli, Krysko and Conrad, 2019). The activation of Ras-mitogen-activated protein kinase (MEK) signalling in certain cancers has been seen to be responsible for increasing iron abundance in activated cancer cells, by increasing the expression of both the transferrin receptor and ferritin (Mou *et al.*, 2019).

One such example is the state of chronic inflammation that cancer cells tend to exist in, as well as relying on inflammation for oncogenic transformation to begin with. Cancer cells in an environment of chronic inflammation have been shown to depend on GPX 4 activity to regulate the activity of LOX and other eicosanoid synthesising enzymes (cyclooxygenases) to tip the balance in favour of sustaining cell growth (Pang, Hurst and Argyle, 2016; Zou *et al.*, 2019).

Metal-phen compounds, particularly copper based CMPD 74, may be available to induce ferroptosis. As copper is capable of initiating Fenton-like chemistry in similar fashion to iron, it is plausible hydroxyl radical production may be capable of producing large quantities of lipid peroxides. The significant increases in cytotoxicity demonstrated by both compounds support this proposal. While CMPD 73 and free 1,10-Phen may not be available to partake in Fenton-like chemistry, their potential to induce oxidative stress and therefore cause GSH depletion, may sensitise the cells to undergo ferroptosis, and so further investigation is warranted.

5.2.Aims

This chapter describes the results of experiments that were aimed at clarifying if these compounds interact with iron-mediated ferroptotic cell death in response to treatment with ROS-generating CMPD 73 and 74. Multiple ferroptosis inhibitors will be used to investigate this pathway as a potential mechanism of cell death, particularly regarding copper-based CMPD 74.

5.3.Methods

5.3.1. Indirect measurement of Ferroptosis using Ferroptosis inhibitors

A549 alveolar carcinoma cells were incubated with both Ferrostatin-1 (Sigma), Liproxstatin-1 (sigma) and Trolox (sigma), a water-soluble form of vitamin E/α-tocopherol between 4-8 hours, and then treated with metal-phen compounds for 24hrs. Where 24hr pre-treatment was used, cells were exposed to ferrostatic agents during plating, allowed to attach for 24hrs, and then exposed to both metal-phen and ferrostatic agents. $FeCl_2$ was used as a potential positive control for iron overload, alongside BSO, a suspected inducer of ferroptosis (Feng and Stockwell, 2018). All pre-treatments and incubations were conducted at 37°C. Following 24hr incubation with suspected ferroptosis-inducing agents, cell viability was assessed using the Resazurin based Alamar Blue assay, as stated in previous sections. Where 24hr pre-treatment with BSO was also used, it again was added to the cells during cell plating. A positive result would present as an increase in cell viability as Ferroptotic cell death is inhibited.

5.3.2. Detection of red cell haemolysis

Loss of membrane integrity in response to lipid peroxidation, ferroptotic or otherwise, was investigated as a potential mechanism of cell death for CMPD 73, 74, and free 1,10-Phen. Red Blood Cells (RBC) offer a unique model as they are inherently delicate to both mechanical and chemical stress, but also lack many cell organelles otherwise found in human cells. e.g. nucleus, mitochondria, Golgi apparatus, lysosomes and the smooth and rough endoplasmic reticulum (Moras, Lefevre and Ostuni, 2017). A such, they offer a model for determining cytotoxic mechanisms of novel compounds, as loss of target organelles such as DNA/RNA or mitochondria may manifest as an absence of toxic effect. On the other hand,

the delicacy of these cells means that if haemolysis occurs, it could easily be attributed to a membrane attack mechanism causing haemolysis, ferroptotic or necrotic.

The lysis of intact RBC can be detected via the absorbance of released free oxyhaemoglobin (Hb) at 540nm. Agents capable of causing haemolysis should cause an increase in absorbance at this wavelength over time as Hb is released into the extracellular space.

Briefly, 250µl of 25% (v/v) horse blood (Cruinn) (diluted with 0.9% saline) was plated into a clear flat-bottomed 96-well plate and incubated with CMPD 73, 74, free 1,10-Phen, and 1% Triton-X (total lysis control) at 37°C for 0, 1, 2, and 16hrs. At each incubation time, the plate was spun at 300rpm for 5mins, and 50µl of supernatant was sampled and read at an absorbance spectrum ranging from 500-600nm, recorded at 10nm intervals. Haemolysis was then expressed as a percent of Triton-X control at 540nm. 25% total horse blood was determined to be the optimal concentration of total blood that gave the highest absorbance reading without saturating the spectrophotometer and was determined in previous optimisation steps.

5.4.Results

5.4.1. Indirect measurement of Ferroptosis using Ferroptosis inhibitors

Known inhibitors of ferroptosis were utilised in both mono and combinatorial therapies against $FeCl_2$, metal-phen and free 1,10-Phen compounds, in order to investigate ferroptosis as a potential mechanism of cell death in A549 cells. As a Cu^{2+} containing compound, CMPD 74 is predicted to interact with the ferroptotic pathway and experience inhibited activity in response to cytoprotective inhibitors. Surprisingly this is not the case, as demonstrated in Figure 5.3 A-D.

$FeCl_2$ was employed as a potential positive control as iron overload has been suggested to initiate ferroptosis (Dixon *et al.*, 2012). $FeCl_2$ did not appear to be cytotoxic towards the cells at any concentration used (nM, µM or mM) and therefore did not interact with ferroptosis inhibitors (data not shown). However, assays employing both a combination of Ferrostatin and Liproxstatin and 24hr pre-treatment of both inhibitors demonstrated a significant reduction in A549 cell viability when compared to $FeCl_2$-only control (data not shown).

A549 cells pre-treated for 8hrs with increasing concentrations of Trolox (Vitamin E) demonstrated no change in cell viability after the addition of CMPD 74 (Figure 5.3 A). As Trolox is known to inhibit ferroptosis by scavenging lipid radicals within lipid membranes, this indicates that lipid peroxidation is likely not a key process in CMPD 74s initiation of cell death. Figure 5.3 B-D, showing both mono and combinatorial, and co and pre-treatment therapies utilising Ferrostatin and Liproxstatin -1 displayed near identical results, and further indicate that ferroptosis is not the likely mechanism of cell death for CMPD 74, as previously hypothesised.

Pre-treatment assays using both BSO and Ferrostatin/Liproxstatin inhibitors were also pursued, in order to investigate whether ferroptotic inhibitors could prevent BSO sensitisation of cells to CMPD 74. No difference is seen between CMPD 74/BSO treatments and the same treatments employing ferroptotic inhibitors (data not shown). This extensive testing demonstrates that CMPD 74 does not interact with the ferroptosis pathway, and that increased cytotoxic effects seen in response to BSO treatments are a result of lowered antioxidant defence as opposed to the induction of ferroptotic-driven cell death.

A

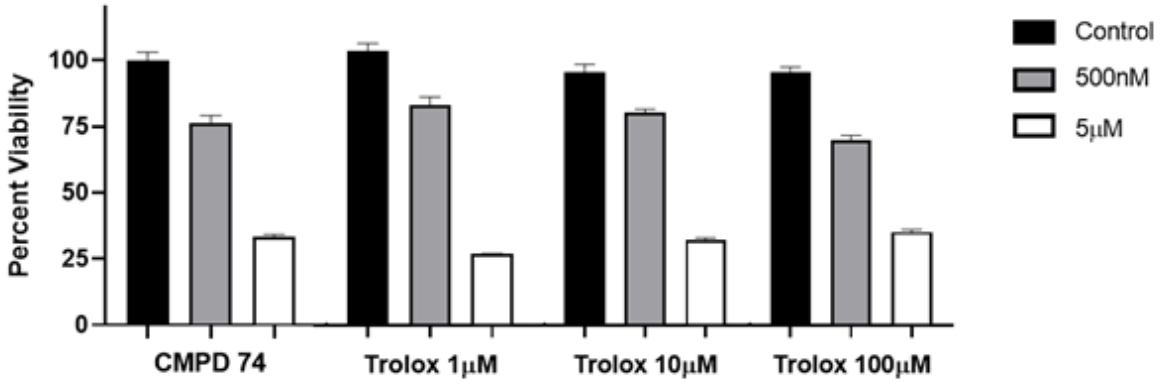

B

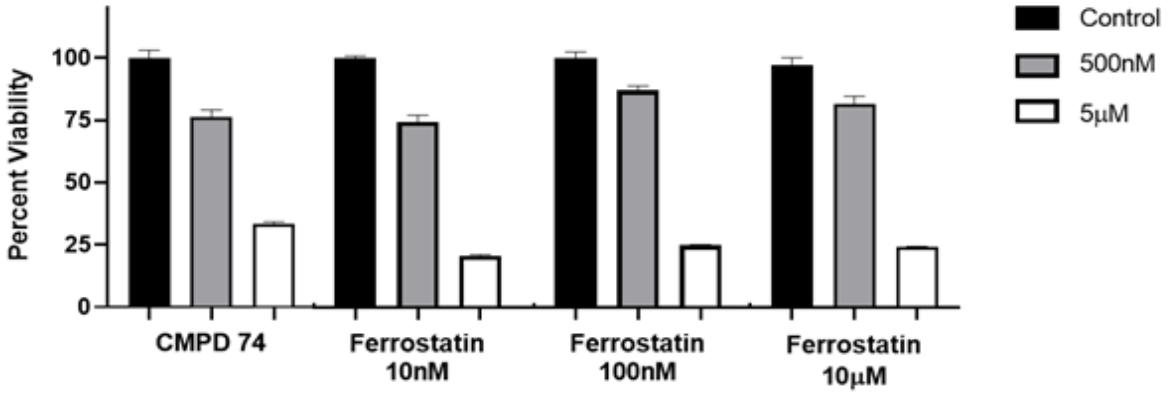

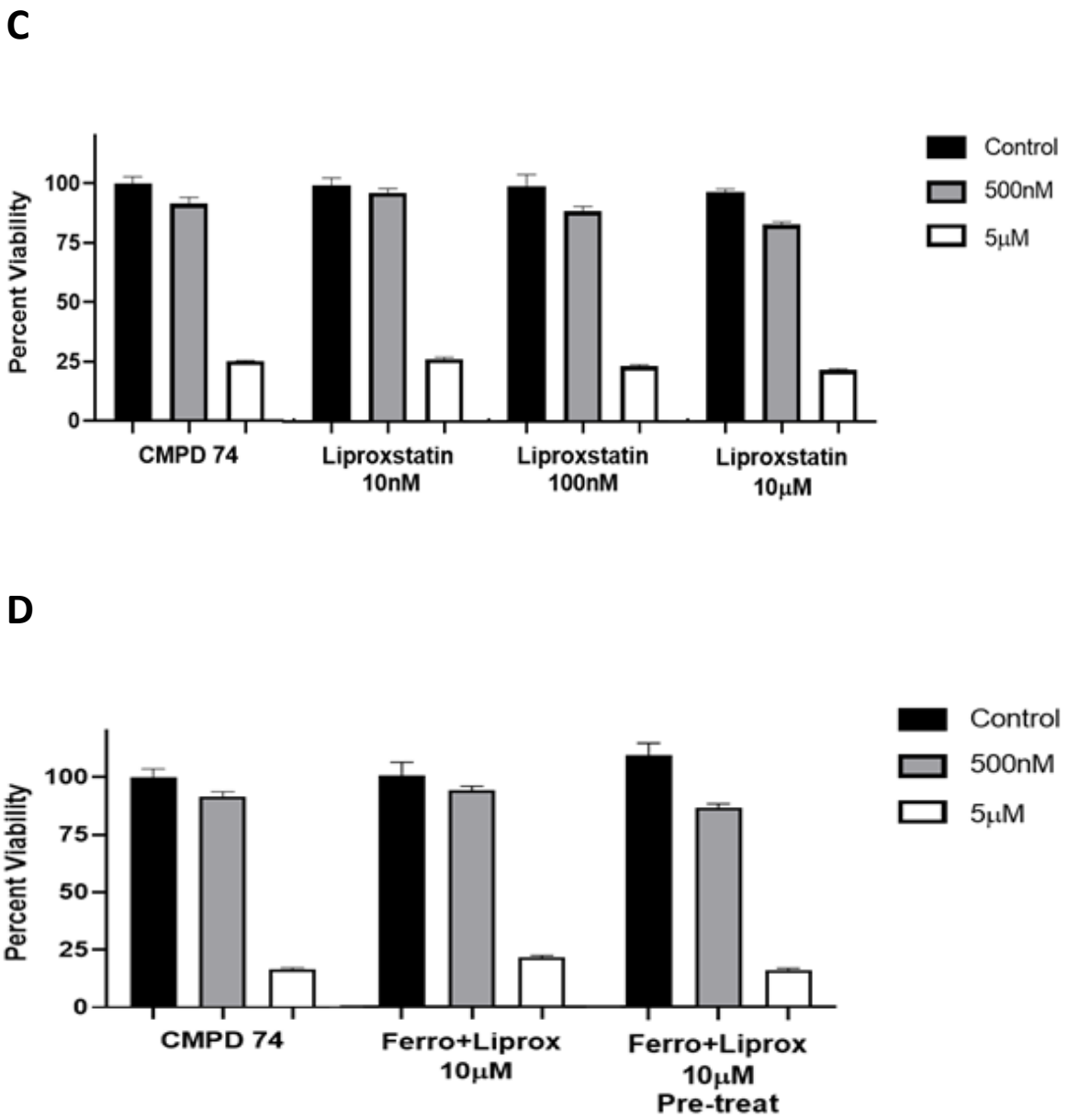

Figure 5.3-CMPD 74 in response to titrations of ferroptosis inhibitors. A) Trolox B) Ferrostatin-1, C) Liproxstatin-1, and D) combinations of Ferro- and Liprox-statins, co-treated or pre-treated for 24hrs (± 1 Standard deviation of two independent experiments). Trolox caused a reduction of 2-8% A549 cell viability. Ferrostatin and Liproxstatin reduced cell vaibilty 10-15%. Ferrostatin and Liproxstatin combined reduced cell viability by 40%.

Ferroptotic mechanisms were also investigated for CMPD 73 and free 1,10-Phen, as both compounds demonstrated modest increases in cytotoxicity in response to GSH inhibition by BSO. Although likely lacking Fenton like capabilities of copper or iron, it may be plausible that both compounds can initiate ferroptosis through an indirect method such as increased

oxidative stress or GSH depletion, as opposed to direct activation of lipid peroxides seen with iron. Further to lacking Fenton-like abilities, it is assumed that direct production of lipid peroxides is not within the capabilities of either compound and so treatments using Trolox were not employed.

Similar to CMPD 74, neither CMPD 73 nor 1,10-Phen demonstrated any increases in cytotoxicity in the presence of ferroptosis inhibitors, indicating no interaction with the pathway. However, both compounds did appear to undergo a similar enhanced cytotoxic effect as $FeCl_2$ when a combination of Ferro and Liproxstatin were employed as a 24hr pre-treatment (Figure 5.4 A&B).

Both Ferrostatin and Liproxstatin inhibited cell growth between 10-15% in A549 cells, while a combination of both is capable of causing up to 40% reduction in cell viability, particularly following 24hr pre-treatment. Pre-treatment with combinations of Ferrostatin and Liproxstatin above 10µM proved to be lethal to the cells. Pre-treatment with Trolox had minimal effect on A549 cell viability (2-8% reduction).

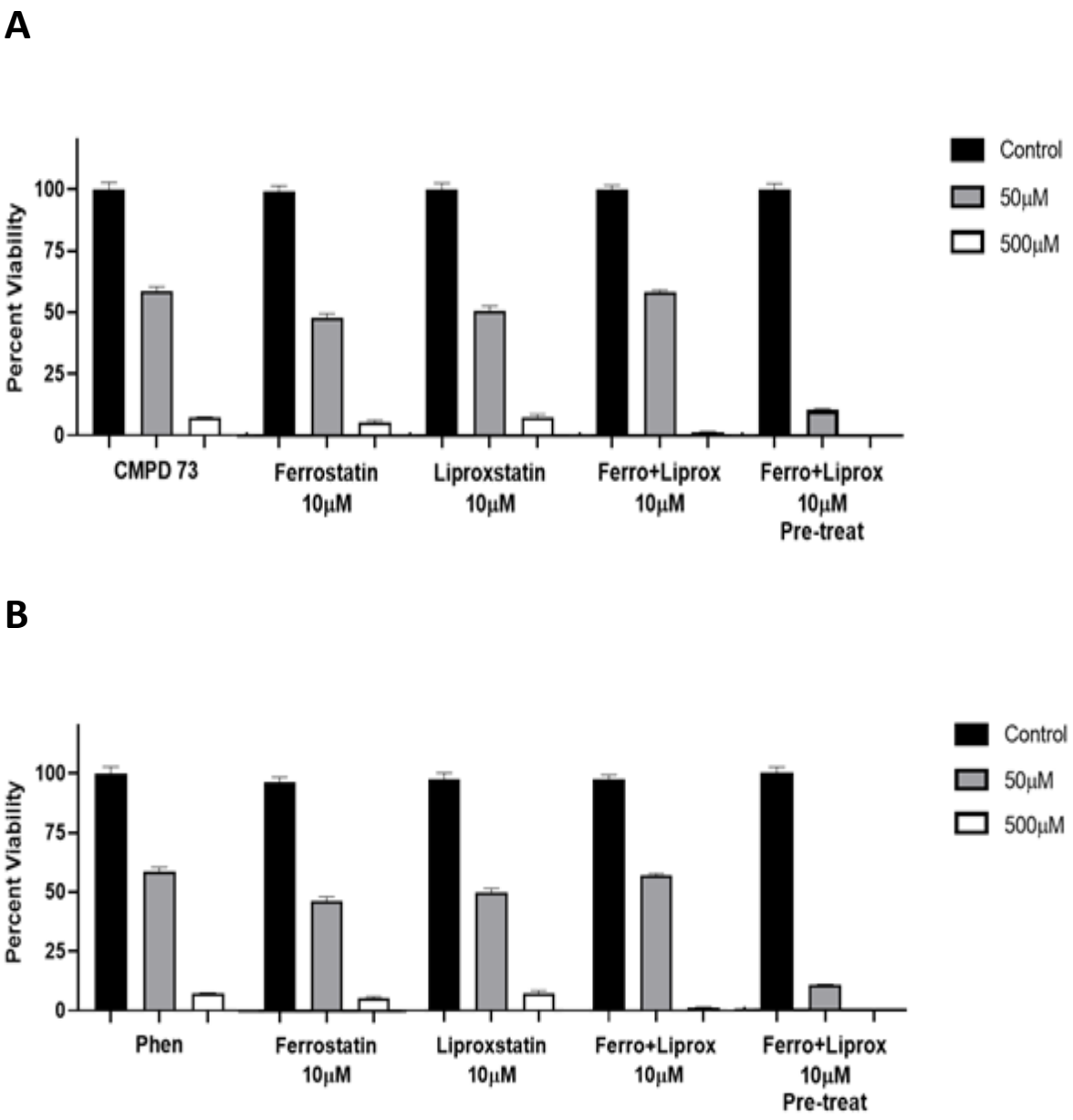

Figure 5.4-CMPD 73 and 1,10-Phen in response to ferroptosis inhibitors. A) CMPD 73 in response to ferroptosis inhibitors Ferrostatin-1 and Liproxstatin-1, alone and in combinations of Ferro- and Liprox-statins, co-treated or pre-treated for 24hrs. B) 1,10-Phen in response to ferroptosis inhibitors Ferrostatin-1 and Liproxstatin-1, alone and in combinations of Ferro- and Liprox-statins, co-treated or pre-treated for 24hr. (± 1 Standard deviation of two independent experiments). Ferrostatin and Liproxstatin reduced cell vaibilty 10-15%. Ferrostatin and Liproxstatin combined reduced cell viability by 40%.

5.4.2. Detection of red cell haemolysis

Table 5.1 displays the results of RBC lysis assay measuring the release of free Hb in response to treatment with metal phen compounds after 16hrs incubation. None of the metal-phen or

free phen compounds caused any significant increase haemolysis, compared to the Triton-X control. A small percent of haemolysis is detected for both CMPD 73 and 1,10-Phen at 1mM concentrations (2-3%) however this is likely resulting from disruption of the RBC pellet following centrifugation and contamination of supernatant with RBCs. As such the detected haemolysis is likely artefactual.

This supports the previous observation that lipid radicals and loss of membrane integrity are not key features of metal-phen cytotoxicity. Interestingly, these results may shed light on which cell organelles these compounds are targeting. The lack of haemolysis in response to metal and free phen compounds indicates that a loss of target specificity has occurred, and focus should now be turned towards investigating these subcellular organelles as candidates required for cytotoxic action.

Table 5.1- Percent haemolysis of RBC incubated with Triton X control, CMPDs 73 and 74, and 1,10-Phen for 16hrs (± 1 Standard deviation of a single experiment). Absorbance read at 540nm.

Concentration (μM)	Haemolysis (%)		
	CMPD 73	CMPD 74	1, 10-Phen
0	0 (± 0)	0 (± 0)	0 (± 0)
10	0 (± 0)	0 (± 0)	0 (± 0)
250	0 (± 0)	0 (± 0)	1 (± 0.02)
500	0 (± 0)	0 (± 0)	1 (± 0.01)
1000	2 (± 0.04)	0 (± 0)	3 (± 0.05)
Triton-X (1%)	100 (± 0.05)	100 (± 0.05)	100 (± 0.05)

5.5.Discussion

Through extensive testing utilising 3 different inhibitors of ferroptosis it can be determined conclusively that neither of the novel metal-phen compounds nor free 1,10-Phen itself can interact with the ferroptotic cell death pathway. The data described is somewhat surprising as copper and iron share some mechanistic similarities, as both can undergo Fenton like chemistry capable of producing the hydroxyl radical to induce lipid peroxidation. However upon further investigation, it has been reported that copper, while mimicking iron in Fenton like chemistry, does not appear to sensitise cells to ferroptosis which have been further sensitised with Erastin, a ferroptosis inducer (Dixon *et al.*, 2012). This disparity has since been attributed to the regulated nature of ferroptotic cell death and the role of iron-dependent LOX enzymes (Shintoku *et al.*, 2017).

The high reactivity and non-specific nature of hydroxyl radicals (copper or iron produced) do not fit within the confines of a highly regulated process such as ferroptosis, and as such the high levels of oxidative stress are not thought to be a driving factor of the process. Coinciding with this Percival *et al.*, 1992 demonstrated that 5- LOX is sensitive to inhibition by low micromolar levels of H_2O_2 and appears to undergo irreversible inhibition by even lower levels of Cu^{2+}. This likely supports previous observations that compound dissociation may be occurring, as seen when the LDH cytotoxicity assay is employed (Chapter 2 pages 77-78). It is thought instead that the iron-dependence of LOX enzymes inducing lipid peroxidation is the predominant factor (Yang and Stockwell, 2016).

It is interesting to note however that $FeCl_2$, an assumed positive inducer of ferroptosis (data not shown), demonstrated a significant drop in viability in response to ferrostatic compounds, as opposed to $FeCl_2$ on its own, displaying no effect on cell viability. While no

change in effect could be explained in a similar fashion to CMPD 74 i.e. a reliance on LOX enzymes rather than ROS produced by redox metals themselves, drastically increasing the cytotoxic effect of an otherwise non-toxic compound is completely unprecedented.

This however may be explained by the nature of both Ferrostatin and Liproxstatin-1. Zilka *et al.*, (2017) have described both inhibitors as radical-trapping antioxidants (RTAs), preventing the propagation of lipid peroxidation. This phenomenon only occurred when both inhibitors were added together as a pre-treatment before the addition of $FeCl_2$, and so it may be the case that the combination of both RTAs at higher concentrations is causing them to adopt a pro-oxidant role as opposed to antioxidant one.

This process has been seen with other antioxidant molecules e.g. ascorbic acid when used at high concentrations (Chen *et al.*, 2008). Indeed, studies from later chapters have shown ascorbic acid to be essential for the chemical nuclease capabilities of all compounds under investigation, when used at high enough concentrations. Experiments conducted in this lab attempting to utilise ascorbic acid as an antioxidant to protect cells from metal-phen compounds were unsuccessful as even concentrations in the low micromolar range were enough to kill all test cells before ROS-inducing agents were added.

CMPD 73 and free 1,10-Phen equally do not interact with the ferroptotic pathway similar to CMPD 74. However, they did appear to undergo a similar enhancing effect as $FeCl_2$ control at higher concentrations, particularly CMPD 73 at 50 and 500 µM. This again may be due to high concentrations of antioxidant molecules switching to pro-oxidant roles. While intriguing, this phenomenon of pro-oxidant reversal is beyond the scope of this investigation and is therefore deemed to be an artefactual event.

Analysis of both lipid peroxide inhibition (Trolox) and RBC integrity assays demonstrated that none of the compounds operated through lipid peroxide generation, and that plasma membrane autolysis/haemolysis is not a direct mechanism of action for the compounds. This supports previous observations from Chapter 2 that necrotic mechanisms of action are likely not present. However, this result indicates that both metal-phen and free 1,10-Phen operate through alternate mechanisms targeting intracellular organelles as opposed to nonspecific necrotic autolysis of the cell membrane.

6. Investigating the Chemical nuclease potential of 1,10-Phen and novel metal phen compounds.

6.1.Introduction

Oxidative cellular processes are important for multiple nucleic acid pathways, such as synthesis, repair, regulation of transcription factors and epigenetic control of gene expression (Luo *et al.*, 2010). As abundant molecules within the cell, nucleic acids are also targets for oxidative attack by ROS and lead to the formation of many different mutagenic products.

Despite many cancers arising due to DNA damage and formation of mutagenic products, induction of DNA damage has been the target of a variety of chemotherapeutics to date (Povirk, 2012; Jekimovs *et al.*, 2014). A list of DNA damaging chemotherapeutics, the DNA damage they induce, and the cancers they treat can be seen in Table 6.1.

Table 6.1- DNA damaging chemotherapy drugs and their corresponding types of DNA damage and cancers they treat. (Adapted from Woods & Turchi, 2013). (NSCL Non-Small Cell Lung Cancer, SCLC Small Cell Lung Cancer).

Chemotherapy Agent	Type of Damage	Cancers treated
Cisplatin	Intra and inter strand Crosslinks	Testicular, NSCL, Mesothelioma
Carboplatin	SSB	Ovarian, Lung
Oxaliplatin	DSB	Colon
Doxorubicin	Topoisomerase-DNA Adducts	Breast
Etoposide	DSB	SCLC
Bleomycin	SSB	Testicular
	DSB	
	Oxidised bases	

6.1.1. Oxidative Processes in nucleotide synthesis

Several enzymes involved in nucleotide synthesis depend on redox catalytic strategies to carry out their biochemical function. Ribonucleotide reductase (RNR) catalyses the *de novo* synthesis of deoxyribonucleotides (dNTPs) from ribonucleotides, which are required for

DNA synthesis. RNR is thus an essential enzyme conserved across all forms of life (Chen *et al.*, 2019). RNR employs redox chemistry to reduce the C2′-OH bond of ribonucleotides, forming dNTPs (Torrents, 2014). Zn^{2+} and Mn^{2+} dependent-deoxyribozymes such as 10MD9, 10MD1, 10MD14, and 10MD5 (Chandra, Sachdeva and Silverman, 2009), responsible for hydrolytic cleavage of the DNA sugar phosphate backbone during replication and repair processes *in vitro,* also make use of redox dependent reactions (Fekry and Gates, 2009). DNA primase, required for the synthesis of the RNA primer used at the replication of DNA daughter strand during DNA synthesis, operates via iron-dependent cluster co-factors to catalyse redox control over binding of the DNA template and synthesise the RNA primer, allowing DNA replication to take place (O'Brien *et al.*, 2018).

6.1.2. Oxidative Processes in the Response to DNA damage

The DNA damage response (DDR) pathway acts to detect and repair DNA from the constant barrage it faces in response to both endogenous sources of ROS (metabolic) and exogenous sources of ROS (UV radiation, xenobiotics) (Ciccia and Elledge, 2010). Several of the DDR pathways are redox active themselves, for example the base excision repair (BER) enzyme apurinic/apyrimidinic endonuclease 1 (APE1). APE1 is involved in both BER and redox regulation of transcription factors responsible for the expression of DDR genes, such as AP-1, NF-κB, CREB and p53 (Luo *et al.*, 2010). An overview of these DDR pathways, the damage they repair, and their mechanism of repair can be seen in Table 6.2.

DNA is subject to epigenetic modification via methylation of cytosine bases by DNA methyl transferases forming 5-methylcytosine (5-mC) which blocks the access of transcriptional machinery and is a repressive marker of transcription (Breiling and Lyko, 2015). Cytosine demethylation is catalysed by the iron (II) dependent ten-eleven translocation (TET) family

of dioxygenase enzymes (Zheng, Fu and He, 2014). TET enzymes convert 5-mC to 5-carboxycytosine (5-caC) via multiple oxidation steps and cytosine intermediates (for greater mechanistic details see Scourzic, Mouly and Bernard (2015). 5-caC is ultimately recognised by the BER system, reforming un-methylated cytosine (Kohli and Zhang, 2013).

Table 6.2-DDR pathways specific to DNA damage repair (adapted from Giglia-Mari, Zotter, & Vermeulen, 2011).

DNA Repair Pathway	Damage repaired	Mechanism
Nucleotide Excision Repair (NER)	Helix- distorting base lesions Intra-strand crosslinks	Excision of damaged base adducts by NER enzymes New bases added by DNA polymerase Ligation of new strand by DNA Ligase
Mismatch Repair (MMR)	Mismatches Insertion/deletion loops	Single strand scission of incorrect base Polymerisation new bases and ligation
Base Excision Repair (BER)	5mC 8-oxo-dG Deamination (C →U) Abasic sites SSB	Removal of damaged base by DNA glycosylases Abasic site repaired by polymerase Ligation of SSB by DNA Ligase
Non-Homologous End Joining (NHEJ)	DSB	Removal of single stranded tails at break by endonuclease Broken ends of DNA strand ligated by DNA Ligase Loss of nucleotides on damage strands
Homologous Recombination (HR)	DSB	Singe-stranded DNA generated at site of break Neighbouring complementary strand used as template for broken strands Regeneration of original strand

6.1.3. Oxidative processes in DNA damage

While controlled redox reactions play a critical role in nucleic acid homeostasis, pathological oxidation of nucleic acids (NA) can dramatically alter their structure and function. Oxidation of NA can promote mutagenic alterations to the genetic code and disrupt transcriptional and translational machinery by targeting RNA (Collins, 2009). As a result, oxidative damage of NA by ROS or RNS is considered to be central to various significant pathologies (e.g. cancer, Alzheimer's and Parkinson's disease (Gonzalez-Hunt, Wadhwa and Sanders, 2018)). However, not all species of ROS or RNS are capable of inducing significant damage to NA (*ibid*). Rather, they serve as intermediates leading to the generation of potent reactive species, such as free radicals including the hydroxyl ($OH^{\bullet}$) and peroxynitrite ($ONOO^{-}$) radicals (discussed in Chapter 1 section 1.2.5-1.2.10). The $OH^{\bullet}$ radical in particular is implicated in all known mechanisms of NA damage, as its oxidative potential is so high that it can react with both nucleotides and sugar phosphate backbone (Cadet *et al.*, 2012).

Multiple forms of DNA damage may occur including damage to the sugar phosphate backbone, nucleotide base oxidation and the formation of inter-strand cross links with the opposing DNA strand, and covalent crosslinking with associated histone proteins (Chatterjee and Walker, 2017). Each form of insult employs a specific mechanism to cause damage to DNA in response to different oxidants, resulting in mutagenic alterations or induction of regulated forms of cell death, such as apoptosis.

6.1.4. Attack on sugar phosphate backbone

The sugar moiety of the phosphodiester backbone of DNA is subject to oxidation by strong oxidising molecules, primarily the $OH^{\bullet}$ or hydroxyl-like radical produced by peroxynitrite. For example, iron has been seen to increase DNA damage and induce the DNA damage response

in endothelial cells, with damage attributed to production of $OH^{\bullet}$ or hydroxyl-like radicals (Mollet *et al.*, 2016). The sugar moiety of DNA is considered to be highly stable against hydrolysis under most physiological conditions, with an estimated half-life of 30 million years (Gates, 2009). However, $OH^{\bullet}$ radicals can react with the sugar moiety of DNA at near diffusion rates (10^{10} M^{-1} s^{-1}) (Kalyanaraman, 2013). Hydrogen abstraction from each sugar carbon results in the formation of five carbon-centred radicals which in turn undergo further complex oxidation reactions, leading to the loss of the phosphate group and complete hydrolysis of the sugar moiety. It is generally accepted that hydrogen abstraction at C3 and C5 is responsible for heterolytic cleavage and strand scission (reviewed Dizdaroglu & Jaruga, 2012). This will result in the formation of DNA strand breaks, abasic sites and consequently the release of unaltered DNA bases (Evans, Dizdaroglu, & Cooke, 2004). The specific carbon targeted by the $OH^{\bullet}$ for H abstraction is dictated by its steric accessibility, with steric accessibility following the trend of $H5' > H4' \gg H3' \approx H2' \approx H1'$ (Balasubramanian, Pogozelski and Tullius, 1998).

Single stranded (SSB) and double strand breaks (DSB) are the most serious forms of DNA damage (Zhdanov, 2016). While strand breaks do occur naturally as a consequence of topoisomerase activity, this occurs under tightly controlled conditions and such breaks are immediately repaired by the topoisomerases themselves (reviewed Povirk, 2012). Generation of SSB or DSB can result in serious consequences for the cell, primarily various rearrangements in the genome, deletions, and chromosomal translocations, fusions or breaks (Chakarov, Petkova, Russev, & Zhelev, 2014). When they occur at low frequency both SSB and DSB can be repaired by DDR enzymes, such as NER and BER for SSB (Abbotts and Wilson, 2017) and HR on NHEJ for DSB (Gursoy-Yuzugullu, House and Price, 2016). However, when breaks occur at a very high frequency, they can be difficult to repair, in

particular DSB. The inability to repair all of the strand breaks may result in the initiation of apoptotic signalling to remove the damaged cell (Mondal *et al.*, 2018).

6.2.Mechanisms of DNA Nucleotide oxidation

Oxidation of nucleotides can result in many different modifications and is dependent on the nucleotide base in which is targeted. This can happen at specific carbon or nitrogen sites within the base, resulting in either base modification or hydrolysis of the nucleotide/deoxyribose bond (Sachdeva *et al.*, 2014). The most characterised mechanistic examples are found the formation of abasic sites, deamination and methylation of cytosine, and the oxidation of guanine. These are discussed in detail below.

6.2.1. Formation of abasic sites

Oxidation of DNA bases can take the form of abasic sites, sites void of a nucleotide base but with an intact sugar phosphate backbone (Gates, 2009). The glycosidic bond between the nucleotide base and sugar phosphate backbone is more susceptible to hydrolytic cleavage and represent a weak point in the nucleic acid structure (*ibid*). The formation of abasic sites occurs as part of DNA repair mechanisms, where BER DNA glycosylases remove oxidised, damaged or mismatched nucleotides which are quickly replaced with the correct base (Krokan and Bjoras, 2013). Apurinic sites are one hundred times more likely to occur than apyrimidinic sites, as they are more susceptible to nucleophilic substitution and hydrolysis (reviewed Greenberg, 2014). While the sugar phosphate backbone remains intact following the formation of abasic sites, these sites are extremely reactive and sensitive as they are highly electrophilic and chemically unstable to further oxidation (e.g. by $OH^{\bullet}$) resulting in the formation of a SSB

(Sczepanski *et al.*, 2010). Abasic sites also block the normal processes of transcription and synthesis (Greenberg, 2014).

6.2.2. Deamination

Oxidation reactions centred on cytosine or 5-mC can result in the hydrolytic deamination (loss of amino group) and the formation of uracil or thymine, respectively (Yonekura *et al.*, 2009). Deamination may cause transition mutations, as DNA polymerase may base pair a corresponding adenine over a guanine during DNA replication, causing a C→T transition (Giglia-Mari, Zotter and Vermeulen, 2011). While targeted deamination plays significant roles in fostering immunologic processes such as antibody maturation, uncontrolled transitions following oxidative deamination can be deleterious (Nabel, Manning and Kohli, 2012). Such transitions are the most common forms of mutations seen in cancer and deamination is the most common accumulated mutational signature in cancer after aging (Greenman *et al.*, 2007; Alsøe *et al.*, 2017). The mispairing of G:U cause G:C to A:T transition mutations which if not repaired are pro-mutagenic. The presence of uracil over thymine is also a major source of endogenous abasic site formation through BER, further increasing damage susceptibility and mutagenic potential (Yonekura *et al.*, 2009).

As 5-mC is a regulatory epigenetic mark involved in gene silencing oxidative deamination has been implicated as a primary source of epigenetic-based alterations which disrupt normal regulation of the genome and therefore promote oncogenesis (Lewandowska and Bartoszek, 2011). Furthermore as 5-mC is deaminated into thymine it is generally not recognized as a DNA lesion and is therefore harder for repair enzymes to detect increasing its mutagenicity (Nabel, Manning and Kohli, 2012).

6.2.3. Oxidation of nucleotide bases

Guanine is the nucleotide with the highest oxidation potential and so is the primary nucleotide targeted by most forms of ROS ($OH^{\bullet}$, $ONOO^{-}$, $^{1}O_2$) (Niles, Wishnok and Tannenbaum, 2006; Agnez-Lima *et al.*, 2012; Hirakawa, 2018). The two main products of guanine oxidation in DNA are 8-hydroxydeoxyguanosine (8-oxodG) and 2,6-diamino-4-hydroxy-5-formamido-pyrimidine (FapyG) (Sova *et al.*, 2010). 8-oxodG is the most common form of DNA lesion resulting from oxidation by ROS and can be formed through the initial addition of $OH^{\bullet}$ to C8, generating 8-hydroxy-7,8-dihydroguan-8-yl radicals (Dizdaroglu and Jaruga, 2012; Xu *et al.*, 2019). In addition, 8-oxodG can base pair with adenine as well as cytosine causing transversion mutations of A:T to C:C or G:C to T:A (Kino *et al.*, 2017). Unlike larger DNA lesions, 8-oxodG nucleotides can be incorporated into the nascent DNA strand by DNA polymerase without significantly affecting DNA synthesis or transcription, further compromising the newly synthesised daughter strand with a mismatch mutation of G to T and C to A substitutions (Ishii *et al.*, 2018). 8-oxodG is used as a biomarker for oxidative stress and DNA damage (Malayappan *et al.*, 2007; Ock *et al.*, 2012).

FapyG is formed from the ring opening of 7-hydro-8-oxyguanine and, in similarity to 8-oxodG lesions, can also initiate mutations such as G to T conversions (Jena and Mishra, 2013). Unlike 8-oxodG however, FapyG does block DNA synthesis and transcriptional machinery and is therefore considered to be cytotoxic (Jena, 2012). Somewhat paradoxically, however, it is generally observed that -oxodG rather than FapyG is more likely to initiate mutagenic driven oncogenesis. This is because cytotoxic damage such as FapyG will be lost upon cell death, whereas 8-oxodG can continue after incorporation into daughter strands following DNA synthesis (Gates, 2009; Cadet and Wagner, 2013). RNS such as peroxynitrite may also lead to the formation of 8-nitroguanine (8-NO_2G) which has been reported to be highly cytotoxic.

Moreover it can result in the formation of G to A mutations or the generation of apurinic sites (for further details on 8-NO_2G see Niles, Wishnok, & Tannenbaum, 2006).

Although adenine can also undergo oxidation it possesses lower oxidation potential than the other nucleotide bases and is not as readily oxidised (Dizdaroglu and Jaruga, 2012). Oxidation of adenine leads to the formation of 8-oxo-7, 8-dihydroadenine (8-oxodA) and 4,6-diamino-5-formamidopyrimidine (Fapy-Ade), analogous to the guanine counterpart. Both 8-oxodA and Fapy-Ade have been shown to form tandem lesions and abasic sites (Cadet *et al.*, 2012). However, the low oxidative potential of adenine generally results in the transfer of radical species to neighbouring guanine bases, formation of clustered guanine lesions and the formation of guanine radical cations (Cadet and Wagner, 2013).

Finally, the oxidation of thymine can result in the production of thymine adducts with neighbouring bases, initiation of strand breaks by hydrogen abstraction by thymine radical intermediates or oxidation of thymines own methyl group forming the 5-(uracilyl) methyl radical (Robert and Wagner, 2019). This in turn can react with methyl groups on neighbouring cytosines forming intra- or inter-strand crosslinks.

6.2.4. Intra- and Inter Strand DNA crosslinks

Generation of DNA lesions can result in the formation of intra or inter-strand crosslinks, either between adjacent or complementary DNA strands or covalent binding with amino acid residues in associated histone, transcriptional, or DNA related proteins (Huang and Li, 2013). However, any protein in proximity with DNA has the potential to become cross-linked (Stingele, Bellelli and Boulton, 2017). Cross-linked DNA adducts are highly detrimental to cell viability as they are generally large and bulky in nature and will sterically hinder interaction of DNA with other

protein factors. This serves to stall normal chromatin-based processes involving DNA such as transcription, DNA unwinding and synthesis (Shoulkamy *et al.*, 2012). Many examples of DNA lesions susceptible to intra- and inter-strand crosslinks involve guanine. This is generally a result of either tandem lesions involving adjacent 8-oxodG at sites of multiple damage or between guanine and uracil produced by the deamination of cytosine (Jena, 2012). Other forms of crosslinks can arise from linking between oxidised purine bases, abasic sites, and between a nucleotide base and the sugar phosphate backbone, due to hydrogen extraction from ROS, such as $OH^{\bullet}$ (Huang and Li, 2013).

Similar to intra- and inter-strand DNA crosslinks, DNA-Protein crosslinks occur in response to various oxidising agents or UV radiation. The mechanism involves the addition of a DNA base radical to an aromatic amino acid of a nascent or nearby protein, or the addition of DNA base radical with an amino acid radical. Examples include thymine-tyrosine crosslink caused by exposure to formaldehyde, metal ions, H_2O_2, and carcinogenic compounds (Altman *et al.*, 1995; Evans, Dizdaroglu and Cooke, 2004), and crosslinking between 8-oxodG and lysine residues within the N-terminal tails of associated histone octamers (Johansen *et al.*, 2005).

The formation of DNA adducts and crosslinks has been a mechanism for chemotherapy directed cytotoxicity for many decades. Cisplatin, along with its carboplatin and oxaliplatin analogues induce the formation of DNA adducts and protein crosslinks with histones as one of its many mechanisms of action (Florea and Büsselberg, 2011). Indeed many other mainstream chemotherapy drugs such as the topoisomerase inhibitors doxorubicin and camptothecin, act via promoting covalent linkage between DNA topoisomerases and DNA (Stingele, Bellelli and Boulton, 2017).

6.2.5. RNA oxidation:

The oxidation of RNA and its effects within the cell has received relatively little attention compared DNA oxidation. However the role of RNA oxidation in the process of aging and neurodegenerative diseases has recently begun to demonstrate its significance as a chronic pathological process (Calabretta, Küpfer and Leumann, 2015). In diseases such as Alzheimer's disease, atherosclerosis and even cancer, RNA oxidation has been identified as a likely early event in disease progression, rather than as an indication of cellular decay (Küpfer and Leumann, 2014). Like DNA, the oxidation of RNA can result in scission of the sugar phosphate backbone causing strand breaks, modification of nucleobases or the formation of abasic sites, resulting in deleterious effects regarding transcription or translation (Li *et al.*, 2014).

However, RNA is far more vulnerable to oxidative damage than its DNA counterpart. As RNA is single stranded in structure, it is devoid of protective hydrogen bonding seen in double stranded DNA, potentially allowing greater access of oxidant species to alter nucleotide bases or cause strand scission (Kong *et al.*, 2008). RNA is further devoid of yet another layer of protection as a result of its lower association with cellular proteins, a protection offered to DNA by its tight association with, and protection by, highly condensed histone proteins. RNA is also four times more abundant by weight than DNA and is generally concentrated in the cytosol of the cell nearer to the mitochondria, where it may be more exposed to oxidant species, such as mitochondrial generated ROS (Fimognari, 2015). DNA being harboured in the nucleus, is offered yet another layer of protection from cellular oxidants (reviewed Yan & Zaher, 2019).

As noted above, DNA possesses multiple complex mechanisms dedicated to its repair which can remove oxidised nucleobases or repair SSB or DSB. As of yet no such mechanisms of RNA repair have been identified and much of the oxidised RNA is removed from the functional

RNA pool via degradation (Sugiyama *et al.*, 2019). It is thought that depletion of the functional RNA pool is a causative factor of cellular injury or death in response to RNA oxidation (Ishii *et al.*, 2018). It has been demonstrated by several studies that RNA can experience up 10-20 times more oxidative damage than DNA, and that treatments with oxidant generating drugs such as doxorubicin or H_2O_2 significantly damage RNA more than DNA (Hofer *et al.*, 2006). Certain classes of RNA have also displayed iron binding properties, with Ribosomal RNA (rRNA) having a higher affinity to iron over both transfer-RNA (tRNA) and messenger RNA (mRNA) (Fimognari, 2015). Iron Response Elements (IREs) within mRNA transcripts specific to iron regulatory genes have also been identified. In response to iron starvation, iron regulatory proteins bind IREs and post transcriptionally regulate mRNA expression either negatively through translational repression or positively through mRNA stabilisation (Campillos *et al.*, 2010). This affinity towards iron may increase the susceptibility of certain transcripts to oxidative damage through iron-catalysed $OH^{\bullet}$ production via Fenton and Haber Weiβ reactions (Poulsen *et al.*, 2012).

Similar to DNA, a significant biomarker of RNA oxidation is the oxidised form of guanine, known as 8-oxo-7, 8-dihydro-2'-deoxyguanosine (8-ox-dG) in DNA and 8-oxo-7,8-dihydroguanosine (8-oxo-rG) in RNA (Shan, Tashiro and Lin, 2003). As a result of RNAs abundance compared to DNA, 8-oxo-G is detected almost 20-fold more than 8-oxo-dG in DNA under normalised conditions (Fimognari, 2015). 8-oxo-G levels increase by 5-fold compared to base levels when mammalian cells are exposed to oxidative stress and are 10-25 times higher than 8-oxo-dG, implying that 8-oxo-G is a reliable biomarker of RNA oxidation (Calabretta, Küpfer and Leumann, 2015). However, while 8-ox-dG is considered to be highly mutagenic 8-oxo-rG can stall translation resulting in little to no protein miscoding (reviewed Yan and Zaher, 2019). Thus 8-oxo-rG is not seen to be as mutagenic as its deoxyribose counterpart (Simms *et*

al., 2014). Other oxidised RNA bases include 8-oxo-7,8-dihydroadenosine (8-oxo-rA), 5-hydroxyuridine (hm^5U) and 5-hydroxycytidine (hm^5C), all with much the same function to stall translation and cause RNA degradation (Küpfer and Leumann, 2014).

Overall, the main consequences of RNA oxidation appear to be i) ribosome dysfunction resulting in stalled translational machinery and when damage is sufficiently high, ER stress, ii) protein miscoding altering function and cell homeostasis, and iii) the alteration of the many regulatory signalling pathways of micro RNA further altering protein synthesis (Joazeiro, 2017; Nunomura *et al.*, 2017). The latter could cause the accumulation of inactive or unstable proteins, which could either prove fatal to the cell, or it could potentially allow an altered protein to continue and have detrimental effects on the functionality of long-living cells, such as neurons, potentially contributing to neurodegenerative diseases such as Alzheimer's or Parkinson's disease (Shan and Lin, 2006).

6.2.6. Investigation of nuclease mimetics

Compounds containing 1,10-Phen, or its derivatives, are well known to display nuclease mimetic activity (Butler *et al.*, 1969; Sigman *et al.*, 1979; Burkitt *et al.*, 1996). Chemical nuclease activity may be readily observed with standard agarose gel electrophoresis using appropriate substrates - purified plasmid DNA for the DNAse activity and total RNA for RNAse activity. Nuclease activity is revealed by characteristic changes in the pattern of bands as outlined below.

6.2.7. Agarose gel evaluation of nuclease activity *ex cellulo*

Purified plasmid DNA is generally found as a mixture of supercoiled and open circular forms. These structures may be observed as distinctive bands after separation by electrophoresis.

Cleavage of the DNA leads to the generation of nicks and/or cuts in the DNA, causing de-compaction of the supercoiled plasmid into a variety of potential forms including nicked/open circular plasmid, linear, or single stranded circular configurations (see Figure 6.1), each evident as a characteristic band on the DNA gel. Further DNA degradation is demonstrated by the formation of multiple bands with full degradation indicated by the presence of a smear of low molecular-weight fragments.

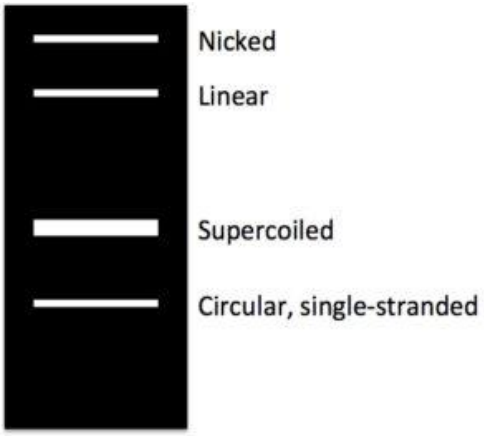

Figure 6.1-Various structural forms of plasmid DNA as they appear on an agarose gel (excluding low Mw smear) (Tirabassi, 2014).

Purified total RNA will appear as three distinct bands, denoted 28S, 18S and 5S RNA which represent ribosomal RNA (Figure 6.2). Breakdown of ribosomal RNA leads to the formation of a distinctive smear and loss of band intensity.

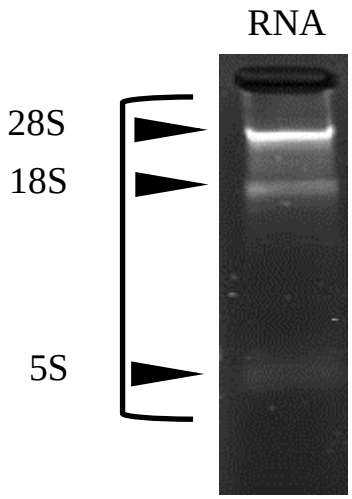

Figure 6.2-2% Agarose gel electrophoresis of total cellular RNA. The distinctive ribosomal 28S, 18S and 5S bands are indicated by arrows.

6.2.8. qPCR-based evaluation of nuclease activity *in cellulo*

To determine if RNAse mimetic activity could affect intracellular RNA, quantitative PCR based mRNA integrity assays may be used. The 3':5' assay is one such assay which has been added to the Minimum Information for Publication of Quantitative Real-Time PCR Experiments (MIQE) guidelines, as a form of method validation (Huggett *et al.*, 2013). This assay relies on the greater susceptibility of the 5' end of mRNA towards degradation than that of the 3' end with its poly adenylated tail (Swift, Peyton and MacDonald, 2000). This will result in a higher yield of 3' products over 5' products when amplified, with resulting in a 3':5' ratio greater than one (Padhi *et al.*, 2018). The principle of the assay is shown in Figure 6.3.

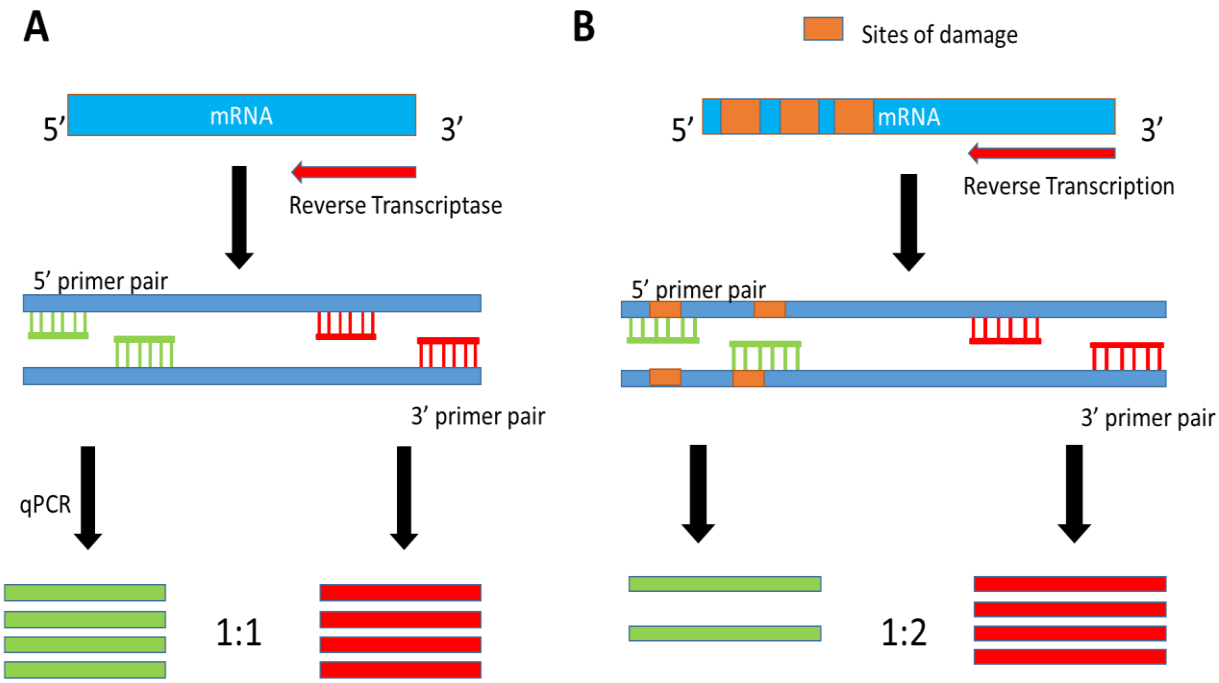

Figure 6.3-Principle of the 3':5' assay. A) Undamaged and intact mRNA template is reverse transcribed from the 3' end by Reverse Transcriptase (RT) generating a double stranded cDNA product of high integrity. A primer pair anchored towards the 5' end (green) and the 3' end (red) are employed to generate equal amounts of amplicon product following qPCR. B) A damaged mRNA strand is reverse transcribed by RT. However the more sensitive 5' end of the template is inefficiently transcribed and retains sites of damage. As such amplification during qPCR will favour the more integral 3' end generating a higher ratio of amplicon products. This figure was self-generated using Microsoft PowerPoint based on the current understanding of knowledge from a multitude of sources.

An alternative qPCR-based assay relies on the use of multiple primer pairs, each sharing a common 3' primer with the other primers designed to give rise to amplicons of differing lengths. If transcript degradation has occurred, reverse transcription will be interrupted and the amplicons closer to the 5' end will not be reverse transcribed efficiently, if at all. The result may be analysed in a similar manner to the 3':5' assay, where each amplicon is expressed relative to the smallest amplicon (Die *et al.*, 2011).

These PCR based assays have distinct advantages over other types of RNA integrity assays, such as the Agilent Bioanalyzer and qualitative agarose gel electrophoresis. Mainly, the 3':5' assay directly looks at the integrity of the mRNA template that is to be used during qPCR

experiments, whereas both the Agilent Bioanalyzer and qualitative electrophoresis detect the more abundant ribosomal RNA within an isolated sample. Measuring the integrity of ribosomal RNA will likely not reflect the integrity of mRNA. Multiple RNA targets can be probed in parallel, reducing the likelihood of false positive results. Finally, these assays can be much more cost effective than capillary electrophoretic assays and is available for high throughput screening (Die *et al.*, 2011).

6.3.Aims

It has been reported previously that analogous compounds lacking the ethereal oxygens (i.e. CMPD19 and CMPD22) possess the ability to cleave plasmid DNA (Kellett *et al.*, 2011). The primary aim of this Chapter is to define the capacity of CMPD73 and 74 to cleave nucleic acids under various in vitro conditions (*ex cellulo* and *in cellulo*). An additional aim is to investigate if any observed activity is dependent on the generation of ROS and, using a similar approach to that described in Chapter 4, to map the species of ROS involved in the nuclease mimetic activity.

6.4.Methods:

6.4.1. Agarose gel evaluation of nuclease activity *ex cellulo*

Plasmid degradation:

A 5.74 Kbp plasmid (pGlo) was used as the model for DNAse activity, as the exact nature of the DNA sequence was not considered critical for the activity. Plasmids were isolated from competent BL-21 bacterial cell colonies grown on L.B. agar (Cruinn) using a plasmid preparation kit (Sigma). The cleavage assay protocol used was adapted from Molphy *et al.*, (2015). 400ng of intact plasmid was incubated (in the dark at 37°C) in cleavage buffer (80 mM HEPES, 25 mM NaCl, pH 7.2) and with varying concentrations of novel metal-phen compounds for different time periods. Sodium-ascorbate was added to some incubations (final

concentration 1mM) to determine if compounds possessed self-cleaving capabilities or if an additional reductant was required to facilitate cleavage. Reactions were terminated by addition of 60mM EDTA. Samples were run on a 1.2% agarose gel containing ethidium bromide and DNA fluorescence was observed using standard image capture protocols.

RNA degradation:

RNA was isolated from A2780 ovarian cancer cells using Trizol reagent (Invitrogen) and the standard protocols. RNA cleavage was tested in the same manner as plasmid cleavage assays stated above but using 1µg of total RNA instead of 400ng plasmid DNA. Cleavage products were resolved using a 2% agarose gel, all in the presence of ascorbate. Isolated RNA was tested against both CMPD 73 and its constituent components, CMPD 74 and its constituent components and 1,10-Phen. Reactions were terminated by addition of 60mM EDTA Each assay was conducted in triplicate.

Inhibiting Ribonuclease activity using ROS/RNS specific scavengers:

Isolated RNA (1µg) was treated with both 1,10-Phen and novel copper (CMPD 74) and manganese (CMPD 73) compounds in the presence of scavengers for specific ROS and RNS in order to determine which reactive species were responsible for ribonuclease activity of test compounds. These assays were conducted in identical conditions as in similar RNA degradation reactions, with the addition of ROS/RNS scavengers. The names of the scavengers used, their ROS/RNS specific targets, and the working concentrations that were used can be seen in Table 6.3 (adapted from ThermoFisher Scientific, 2010). This method is a variation of similar methods used by Molphy *et al.*, (2015). The results presented are representative data of three independent biological replicates.

Table 6.3-ROS and RNS specific scavengers and their corresponding ROS/RNS targets and working concentrations.

Scavenger	Working Concentration	Target	Reference
Sodium Pyruvate (NaPy)	10mM	Hydrogen Peroxide (H_2O_2)	(Giandomenico *et al.*, 1997; Asmus, Mozziconacci and Schöneich, 2015)(Giandomenico *et al.*, 1997)
Sodium 4,5-dihydroxybenzene-1,3-disulfonate (Tiron)	10mM	Superoxide ($O_2^{\bullet-}$)	(Taiwo, 2008)
Dimethyl Sulfoxide (DMSO)	10%	Hydroxyl Radical ($OH^{\bullet}$)	(Rosenblum and El-Sabban, 1982; Macrides *et al.*, 1997)
Sozdium Azide (NaN_3)	10mM	Singlet Oxygen ($^1O_2$)	(Li *et al.*, 2001; Bancirova, 2011)
6-hydroxy-2,5,7,8-tetramethylchroman-2-carboxylic acid (Trolox)	100µM	Peroxyl Radical (ROO•)	(Watanabe *et al.*, 2012)
Carboxy-PTIO (CPTIO)	100µM	Nitric Oxide (NO)	(Franco, Panayiotidis and Cidlowski, 2007)
Uric Acid (UA)	100µM	Peroxynitrite anion ($ONOO^-$)	(Walford *et al.*, 2004)

6.4.2. RT-qPCR evaluation of nuclease activity *in cellulo*

A2780 cells were plated in duplicate wells of a 6 well plate and treated with IC_{10} and IC_{25} concentrations of CMPD 73, 74 or 1,10-Phen for 24hrs. Following exposure to the different agents, total RNA was extracted using Trizol reagent, as per the manufacturer's guidelines. 1µg of total RNA was reverse transcribed using the Takyon Reverse Transcriptase Core Kit (RT-RTCK-03, EuroGentec) as per the supplied protocol. For isolated RNA which was to be used to standard qPCR gene expression analysis random nonamer primers were used during the RT reaction. qPCR reactions were carried out using the Takyon SYBER 2X Master Mix (UF-LSMT-B0701, EuroGentec), using 100nM cDNA and primer concentrations, as per protocol using an Applied Biosystems 7500 Fast Thermocycler set to fast cycling. Cycling conditions are seen in Table 6.4. Significance testing for global transcriptional effects was conducted on raw Ct values using the Students T-Test.

Table 6.4-Cycling conditions for qPCR assays

Stage	Temperature (°C)	Time (seconds)
Holding	95	180
	Cycling (x40)	
Denaturing	95	3
Annealing	60	30
	Melt Curve (x2)	
Denaturing	95	15
Annealing	60	60

Reference Gene Stability:

To evaluate metal-phen nuclease activity in cellulo *GAPDH*, *PPIA*, *18S*, and *PGK1* reference genes were used to investigate whether stable expression patterns were held in response to treatment with metal-phen compounds. RNA was isolated and assayed as per protocol above using random nonamer primers for RT. The qPCR primer sets were generated using Primer3 and can be seen in Table 6.5. Preliminary data using the *18S* gene to investigate the effects of CMPD 74 on gene expression levels presented with low Ct values of 12-13 indicating a high

abundance of *18S* expression within the A2780 cell lines. The high abundance of *18S* expression could potentially mask any effects that the comparatively less potent CMPD 73 and 1,10-Phen would have on target gene expression. As such for experiments using both CMPD 73 and 1,10-Phen, dilutions of cDNA samples isolated from A2780 cells exposed to both compounds were made using RNase-free water into separate PCR tubes to give higher Ct values of ≈ 30 in attempt to make any effects on gene expression more apparent.

Experiments using 1,10-Phen as the compound of interest had a methanol (MeOH) vehicle control equivalent to the IC_{10} concentration of 1,10-Phen used in order to account for changes in gene expression resulting from the solvent used to dissolve 1,10-Phen. As such Ct values for gene expression in cells treated with 1,10-Phen were further normalised to MeOH vehicle control conditions following initial normalisation to non-treated control conditions.

Table 6.5-Forward and Reverse primers for HKGs

Gene	Forward primer	Reverse primer	Amplicon size (bp)
GAPDH	ACCCAGAAGACTGTGGATGG	AGTAGAGGCAGGGATGATG	84
PPIA	AGACAAGGTCCCAAAGAC	ACCACCCTGACACATAAA	118
18S	GCTTAATTTGACTCAACACGGGA	AGCTATCAATCTGTCAATCCTGC	200
PGK1	ACTTCTAGGGGCTGCATCAC	GTGCTCACATGGCTGACTTT	95

3’:5’ RT-qPCR Assay:

The 3’:5’ assay was adapted to human genes based on a report by Padhi *et al* (2018), which utilised the ubiquitously expressed phosphoglycerate kinase 1 (*Pgk1*, NM_000291.4) HKG in rat samples. Following treatment of cells as noted in section 6.1.4 above, cDNA was synthesised using oligo dT primers. Primers against the human *PGK1* gene (NM_000291.4) were designed using Primer3 and in accordance with the design principles for 3’:5’ assay primers, i.e. with approximately 1Kb between the 3’ and 5’ primer sites. The locations of the primers are shown in Figure 6.4 and the primer sequences are in Table 6.6.

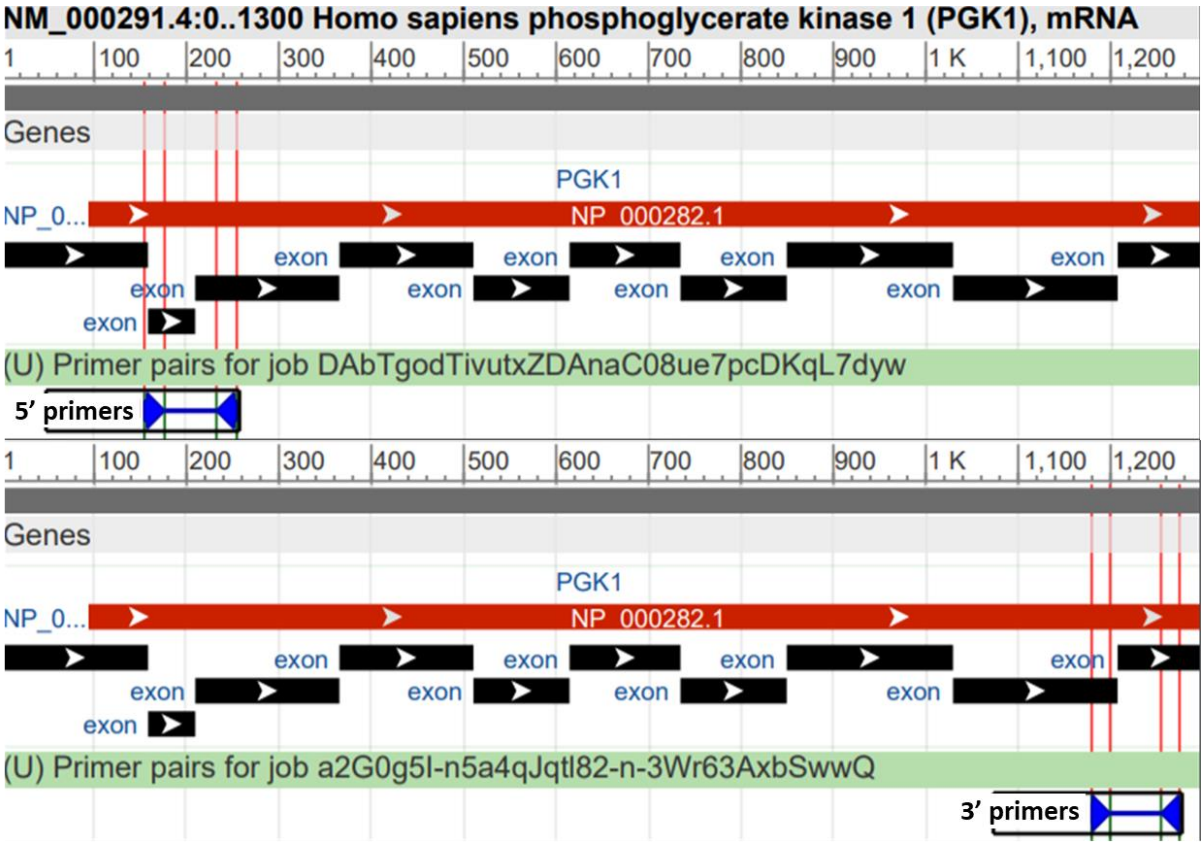

Figure 6.4-Location of primers for the 3’:5’ assay from Primer 3.

Table 6.6-Primer sequences used for the 3':5' assay

Primer set	Forward primer	Reverse primer	Amplicon size (bp)
5'	TGAGAGTCGACTTCAATGT	CCATTGTCCAAGCAGAATT	109
3'	ACTTCTAGGGGCTGCATCAC	GTGCTCACATGGCTGACTTT	95

Following qPCR, raw data was normalised to the negative control as follows:

$$\Delta C_t = C_t(Test) - C_t(Control).$$

Each ΔC_t was converted to relative cycles of difference using the following expression

$$Relative\ cycles\ of\ difference = 2^{-\Delta C_t}$$

The 3':5' ratio was then computed using these values and compared to a baseline ratio of 1, indicating no damage.

Differential amplicon size assay:

A differential amplicon assay was designed using the human *PGK1* sequence, to provide comparability with the 3':5' assay described above and was carried out on cDNA samples prepared as described above. A series of primers, each sharing a common reverse primer anchored at the 3' end of the gene, were designed to generate amplicons of 115, 292, 497 and 820 bp. The locations of the primers are shown in Figure 6.5 and the primer sequences are in Table 6.7.

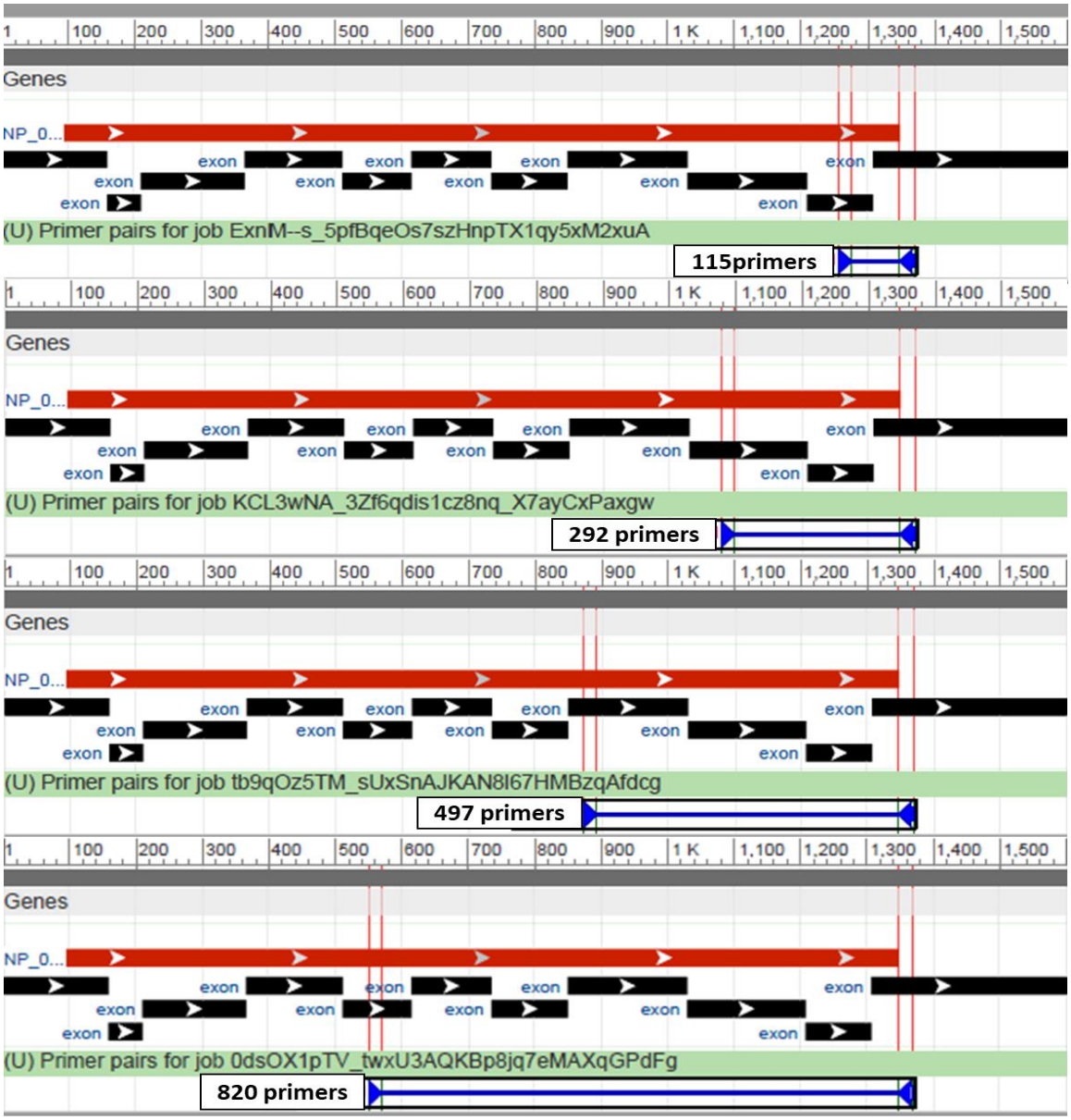

Figure 6.5- Primer locations for differential amplicon assay form Primer 3.

Table 6.7-Primer sets for differential amplicon assay

Primer	Sequence	Amplicon Size (bp)
Common 3' Reverse	GTGCTCACATGGCTGACTTT	
115bp Forward	AAAGTCAGCCATGTGAGCAC	115
292bp Forward	ACTCGGGCTAAGCAGATTGT	292
497bp Forward	AGAGGGAGCCAAGATTGTC	497
820bp Forward	TCACTTTCCAAGCTAGGGGA	820

Raw qPCR data was initially normalised to the negative control condition as follows:

$$\Delta C_t = C_t(Test) - C_t(Control).$$

Each ΔC_t was converted to relative cycles of difference using the following expression

$$Relative\ cycles\ of\ difference = 2^{-\Delta C_t}$$

Each value was then expressed relative to the value of the smallest amplicon, which was defined as the reference amplicon, to generate a crude transcript stability score. As above a ratio of 1 was taken to indicate no damage.

6.5.Results

6.5.1. Nuclease mimetic activity of CMPD73 and CMPD74

Initial nuclease activity was tested using both DNA and RNA as substrates. As shown in Figure 6.6, DNAse activity is observed for each compound tested. However, ascorbate is required for activity indicating that none of the compounds possessed self-cleavage activity and is demonstrated in Figure 6.7. A time-course revealed that CMPD74 appeared to be significantly more active than CMPD73 and can catalyse the almost complete breakdown of the plasmid DNA in 30 minutes (Figure 6.6, lane 3). In contrast a 24-hour incubation period with CMPD73 is required to degrade the plasmid substrate to a similar extent (Figure 6.6, lane 8) with a time course of degradation evident. These results highlight the modest nuclease activity of this compound.

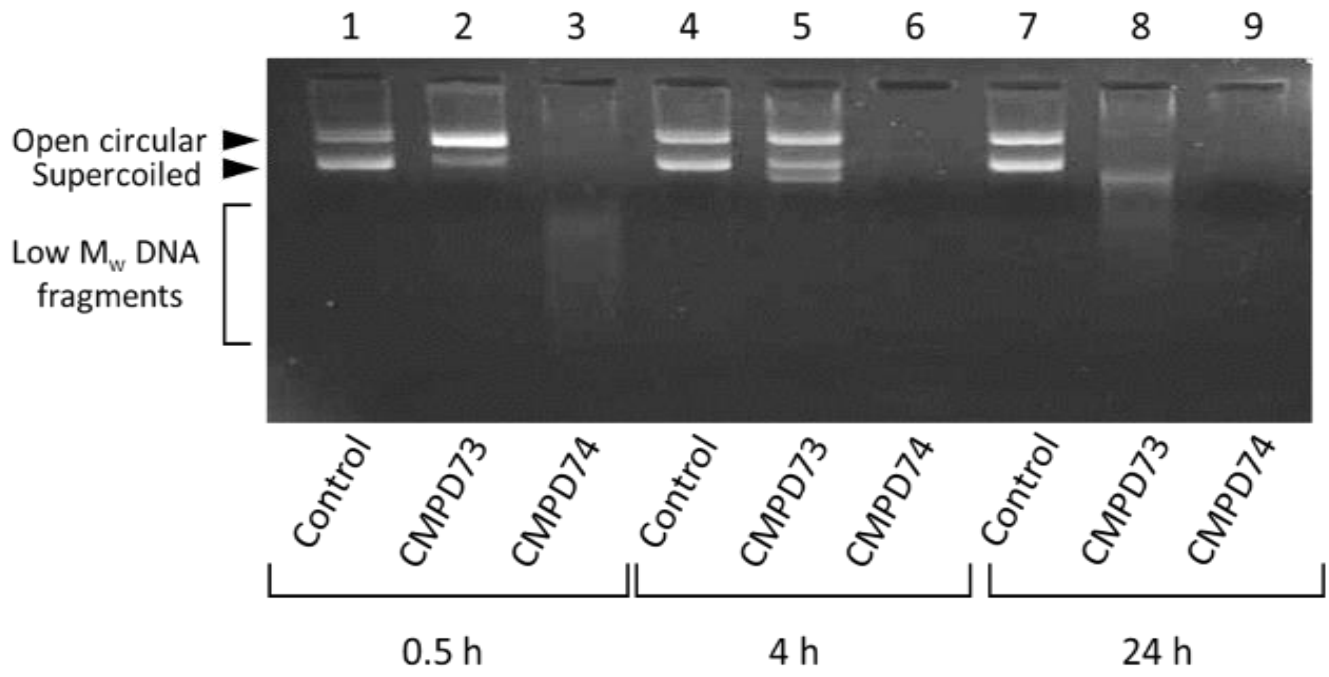

Figure 6.6- DNAse activity of CMPD73 and CMPD74 in the presence of added ascorbate as a reductant for 0.5, 4, and 24hrs at 100μM. CMPD74 is observed to be highly active as a nuclease, leading to the almost complete disappearance of the plasmid DNA with 30 minutes. CMPD73 is less

active and took up to 24 hours for significant cleavage to occur. An elevation of open circular DNA is observed at 0.5 hrs, with a band in the expected range for single stranded DNA appearing at 4 hrs.

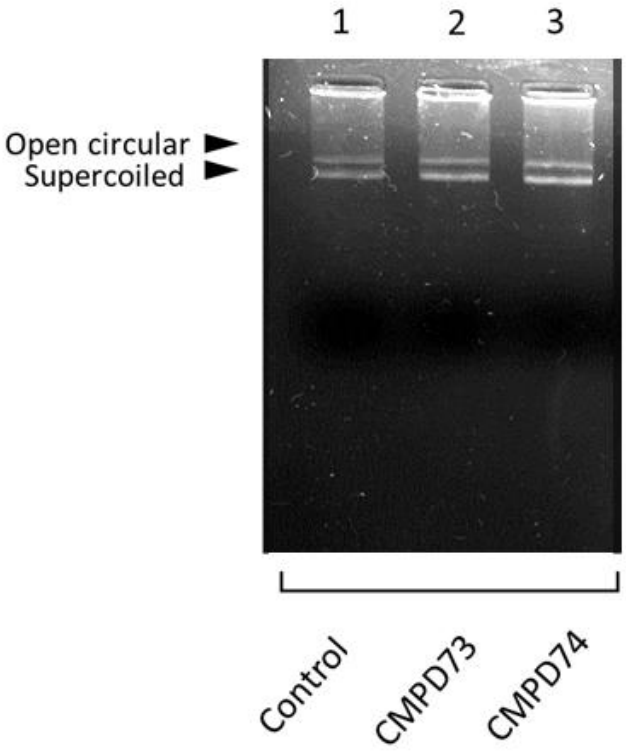

Figure 6.7-DNAse activity of CMPD73 and CMPD74 in the absence of added ascorbate as a reductant for 24hrs at 100μM. No nuclease activity is observed.

Analogous experiments using RNA as a substrate revealed that both CMPD73 and CMPD74 possessed significant RNAse mimetic activity (Figure 6.8 and Figure 6.9). The relative effectiveness of the nuclease mimetic activity was similar with both DNA and RNA substrates. In similarity with the results for plasmid DNA above, incubation with CMPD73 or its precursors for 0.5 or 1hr did not lead to observable RNA cleavage at concentrations ranging from 10nM to 1μM (data not shown). Following a 2hr incubation period cleavage reactions were observed at concentrations of 1μM, with no significant enhancement of RNA cleavage at concentrations up to 100 μM. There is no significant activity from any of the precursor

compounds tested (Figure 6.8, lanes 7-10). Hydrogen peroxide did not degrade RNA even at high concentrations of 100μM when used as a positive ROS control.

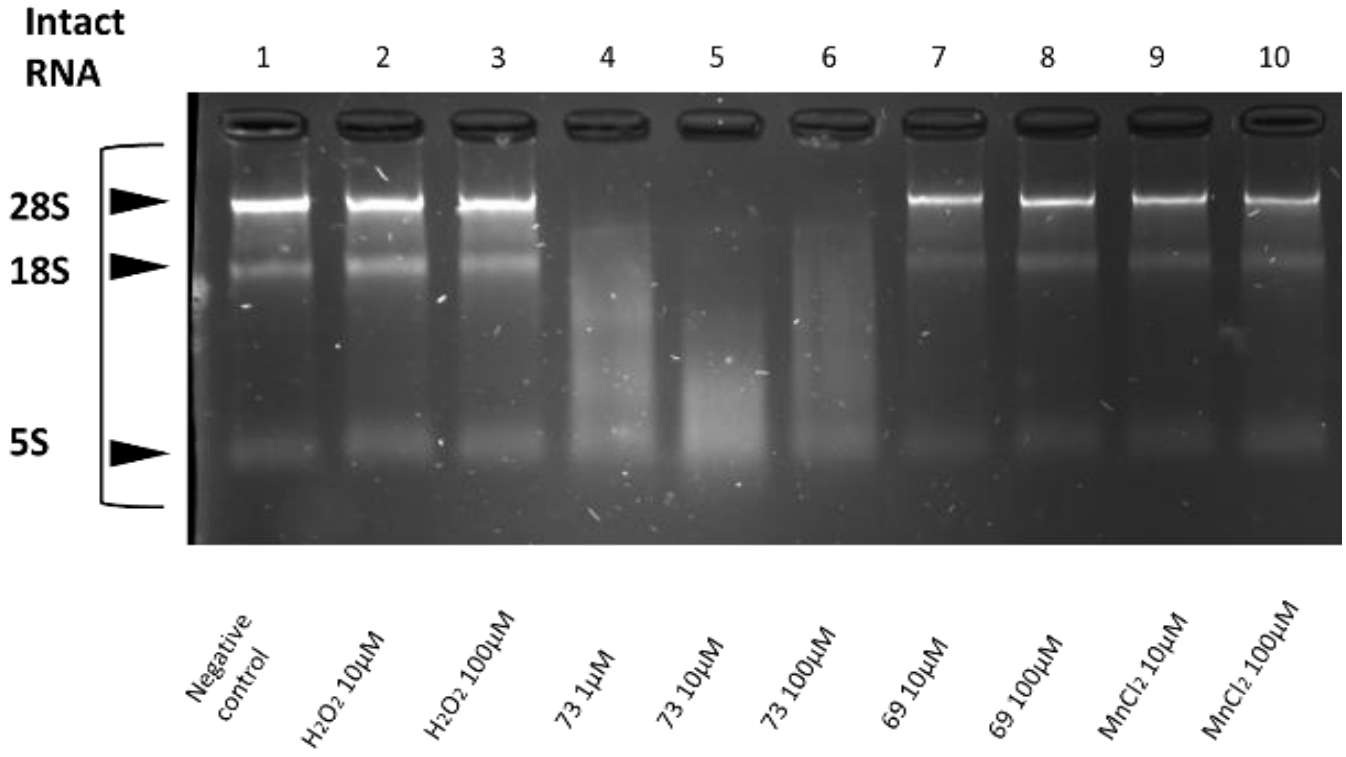

Figure 6.8 RNAse activity of CMPD73 and its precursors. Isolated RNA exposed to H_2O_2, CMPD 73, CMPD 69 precursor, and $MnCl_2$ for 2hr in the presence of ascorbate. CMPD73 displayed significant capacity to degrade RNA at concentrations as low as 1μM.

RNAse mimetic activity of CMPD74 is readily observable at 0.5 hours, a time point at which there is no observable activity for the manganese-containing CMPD73. In similarity with CMPD73, the RNAse activity of the constituent parts of CMPD74 were investigated (i.e. 1,10-Phen, the Cu-TDDA salt and $CuCl_2$). Unexpectedly, at sufficiently high concentrations, each component part appeared to be capable of causing some RNA degradation (Figure 6.9 lanes 7, 10 and 12 respectively). These data suggest that the RNAse activity of CMPD74 may be attributed to an additive effect between the copper and 1,10-Phen components of the compound.

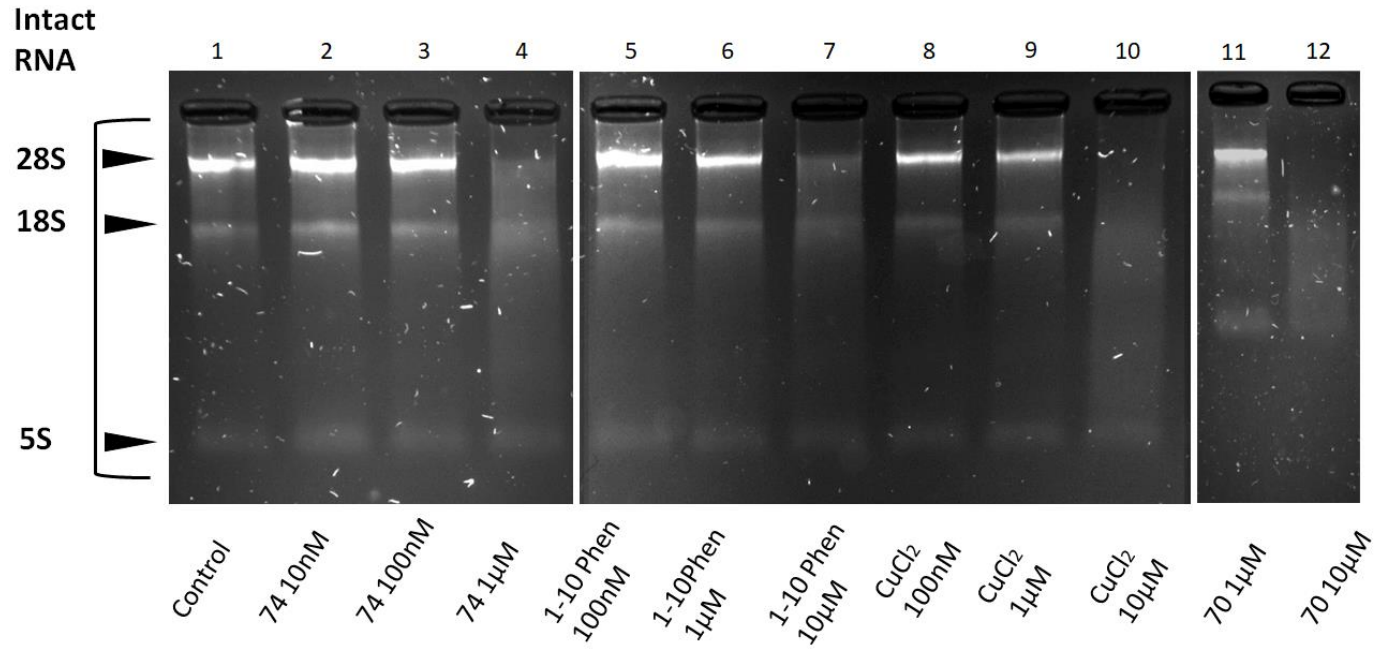

Figure 6.9 RNAse activity of CMPD74 and its precursors. Isolated RNA exposed to CMPD 74, 1,10-Phen, $CuCl_2$ and CMPD 70 precursor for 0.5hr in the presence of ascorbate. CMPD74 displayed significant capacity to degrade RNA at concentrations as low as 1µM, while 10µM concentrations of 1,10-Phen, CMPD70 or $CuCl_2$ all resulted in RNA breakdown.

The efficacy of CMPD74 and the finding that 1,10-phen also displayed RNAse activity prompted the investigation of the kinetics of RNA degradation in the presence of these compounds. CMPD74 (1µM) and 1,10-phen (10µM) were incubated with RNA for varying time intervals and breakdown products separated as above (Figure 6.10). Degradation of RNA by CMPD74 appeared to occurr very rapidly, with signs of degradation evident after only 15 minutes and total degradation following 20 minutes (Figure 6.10 compare lanes 6, 8 and 10). Degradation also proceeded in the presence of 1,10-phen alone, albeit with less efficacy and at a slower rate (Figure 6.10 compare lanes 7, 9 and 11).

The nuclease mimetic activity of 1,10-phen is generally attributed to its chelation of trace metals (e.g. iron, copper) in the reaction solution to form DNA/RNA degrading complexes. As such the addition of 1mM EDTA to the 1,10-phen reaction was conducted to confirm this

property of 1,10-Phen, which indeed resulted in a complete ablation of any RNA degradation activity (Figure 6.10, lane 12). This result supports the contention that 1,10-Phen is capable of indirect nuclease activity, due to the chelation of free catalytic ions. Direct ribonuclease activity would be expected to display degradation of RNA regardless of EDTA treatment. The addition of EDTA to reactions where CMPD 73 and 74 was also investigated giving identical results to 1. 10-Phen, whereby RNA degradation was totally inhibited (data not shown).

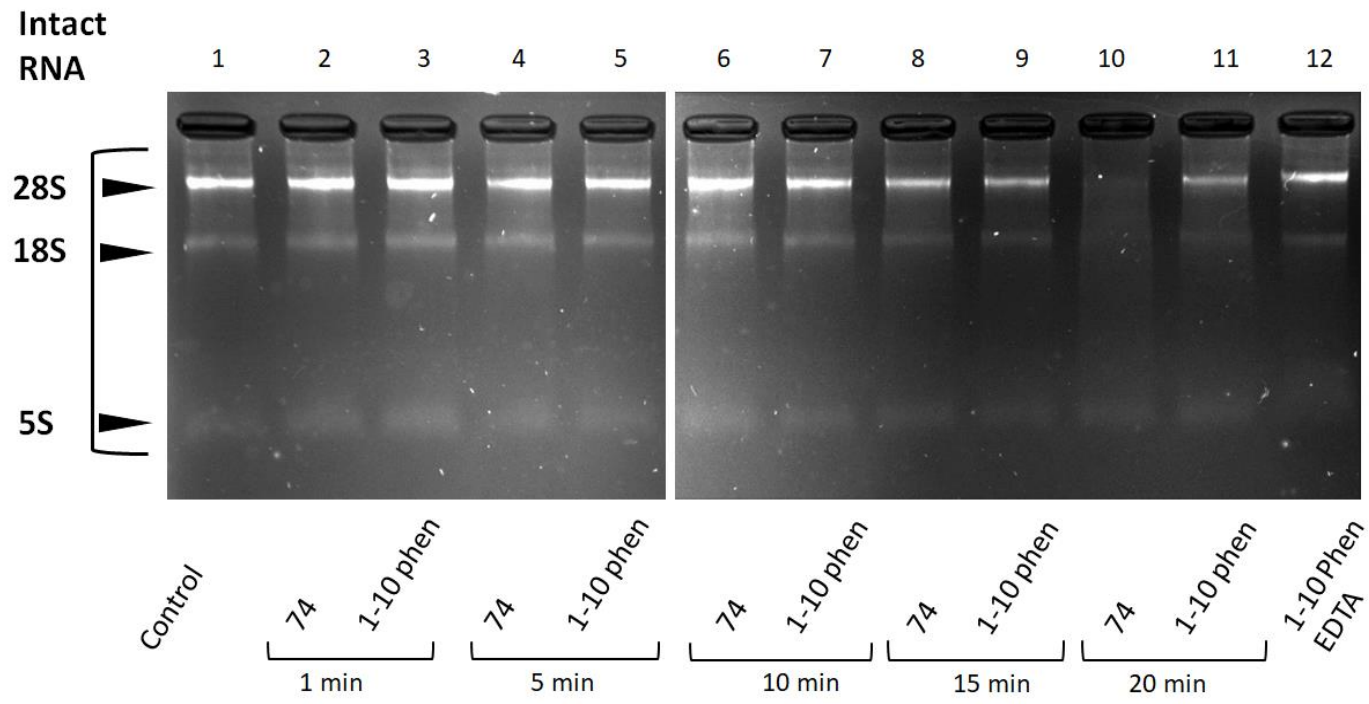

Figure 6.10 Kinetics of RNA degradation by 1μM CMPD74 and 10μM 1,10-Phen in the presence of ascorbate. Lane 1: negative control, Lanes 2-11: time dependent degradation in the presence of CMPD74 and 1,10-Phen, Lane 12: 1,10-Phen in the presence of 1mM EDTA.

6.5.2. Ribonuclease activity in response to ROS and RNS specific scavengers

It is generally accepted that the nuclease mimetic capabilities of metal-phen compounds likely depends on the generation of ROS by redox active copper and manganese (Kellett *et al.*, 2011; Molphy *et al.*, 2015). ROS specific scavengers may be used via an inhibitor profiling approach to identify the suspected ROS responsible for degradation of RNA. The principle is that if a specific ROS (e.g. $OH^{\bullet}$) is critical for RNA degradation then chemical blockage of that ROS

species will inhibit RNA breakdown and the distinctive RNA bands seen in Figure 6.2 would remain intact.

Figure 6.11 displays the effects on isolated RNA in response to scavengers of various forms of catalytic ROS potentially produced by metal-phen and phen compounds. Following two-hour incubation with CMPD 73 (Figure 6.11 A), a notable inhibition of RNA degradation was observed following treatment with scavengers of H_2O_2 and $O_2^{\bullet-}$ (lanes 4 and 6 compared with non-treated control in lane 1). There is a modest inhibition of CMPD 73 activity by both DMSO (lane 3) and sodium azide (lane 5), indicating possible production of both the hydroxyl radical and singlet oxygen. There was no obvious effect of Trolox, CarboPTO and uric acid (lanes 7-9) indicating that peroxyl radical, nitric oxide and peroxynitrite production are unlikely to be key mediators of the RNAse activity.

In similarity, CMPD 74 RNAse activity also appears to rely on the production of both H_2O_2 and $O_2^{\bullet-}$ as seen by strong inhibition of degraded bands in lanes 4 and 6 following 30-minute incubation (Figure 6.11 B). In contrast to CMPD 73, however, the production of the hydroxyl radical is seen to be essential for CMPD 74 activity as seen by strong inhibition of RNA degradation by DMSO (lane 3).

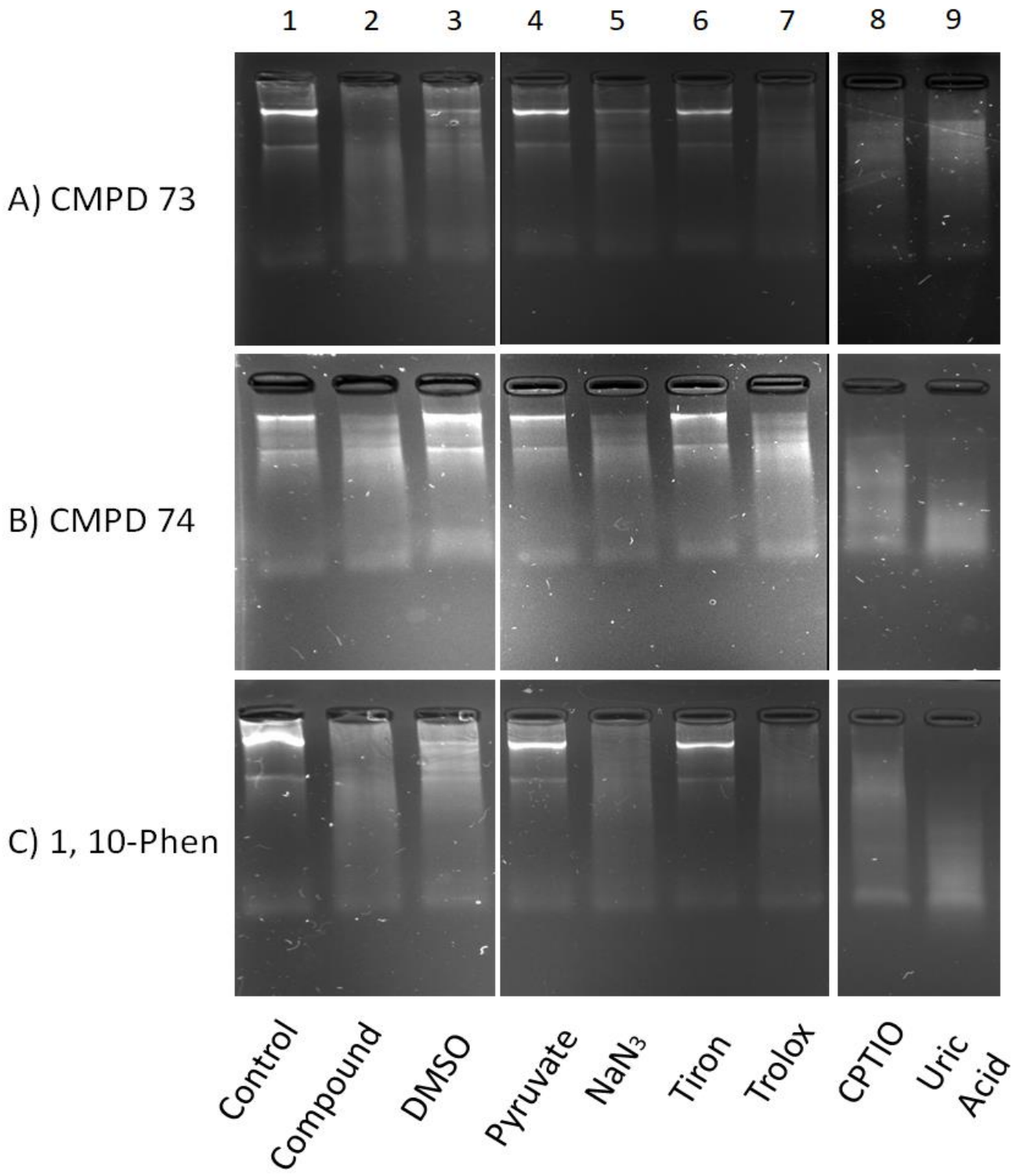

Figure 6.11- ROS inhibitor profiling of RNA degradation. Isolated RNA treated with A) 1µM CMPD 73 for 2hrs, B) 1µM CMPD 74 for 30 mins and C) 10µM 1,10-Phen for 30mins using scavengers of various ROS and RNS in the presence of ascorbate.

These data indicate that the copper containing CMPD 74 utilises Fenton-like chemistry to degrade RNA. Lanes 5 and 7-9 where sodium azide, Trolox, CarboPTO and uric acid were used to inhibit singlet oxygen, peroxyl radical, nitric oxide and peroxynitrite production respectively, demonstrated no inhibition.

The activity of 1,10-Phen in response to specific ROS scavengers followed a near identical profile to that of CMPD 73 following 30-minute incubation (Figure 6.11 C). The production of both H_2O_2 and $O_2^{\bullet-}$ appear to be critical for its ribonuclease mimetic activity (lanes 4 and 6) while hydroxyl radical generation is seen to be moderately involved (lane 3). However unlike the modest inhibition of CMPD 73 observed, inhibition of singlet oxygen by sodium azide did not appear to inhibit degradation (lane 5). Peroxyl radical, nitric oxide and peroxynitrite generation were similarly not detected as seen by an absence of inhibition and total RNA degradation in lanes7-9. It could be possible to further quantify the described data using densitometry to further analyse the degree of inhibition of test compounds in response to ROS inhibitors.

6.5.3. qPCR analysis of RNA damage

As an initial step to evaluate the impact of the novel compounds on RNA under *in cellulo* conditions we investigated the expression of a panel of four genes commonly used as endogenous controls in qPCR experiments (i.e. housekeeping genes, HKGs). Concentrations at the IC_{10} and IC_{25} were used to minimise any overt globalised toxic effects.

In general each compound resulted in a reduction in the expression of the four HKGs tested, although CMPD 74 was consistently more potent (Figure 6.12). However, some anomalies were noted, particularly in relation to the response for CMPD73 and the *18S* gene where an

elevation, rather than a reduction, in expression was noted at the IC_{25}. In further contrast to CMPD 73, CMPD 74 decreased the expression of *18S* in a concentration-dependent manner with IC_{10} ($P>0.05$) and significantly for IC_{25} concentrations. The significant decreases in *18S* expression despite high expression levels (control Ct 12) may highly suggest that CMPD 74 robustly interacts with and degrades ribosomal RNA within the cell, however further experiments to determine if these effects are transcriptional or post-transcriptional would be warranted.

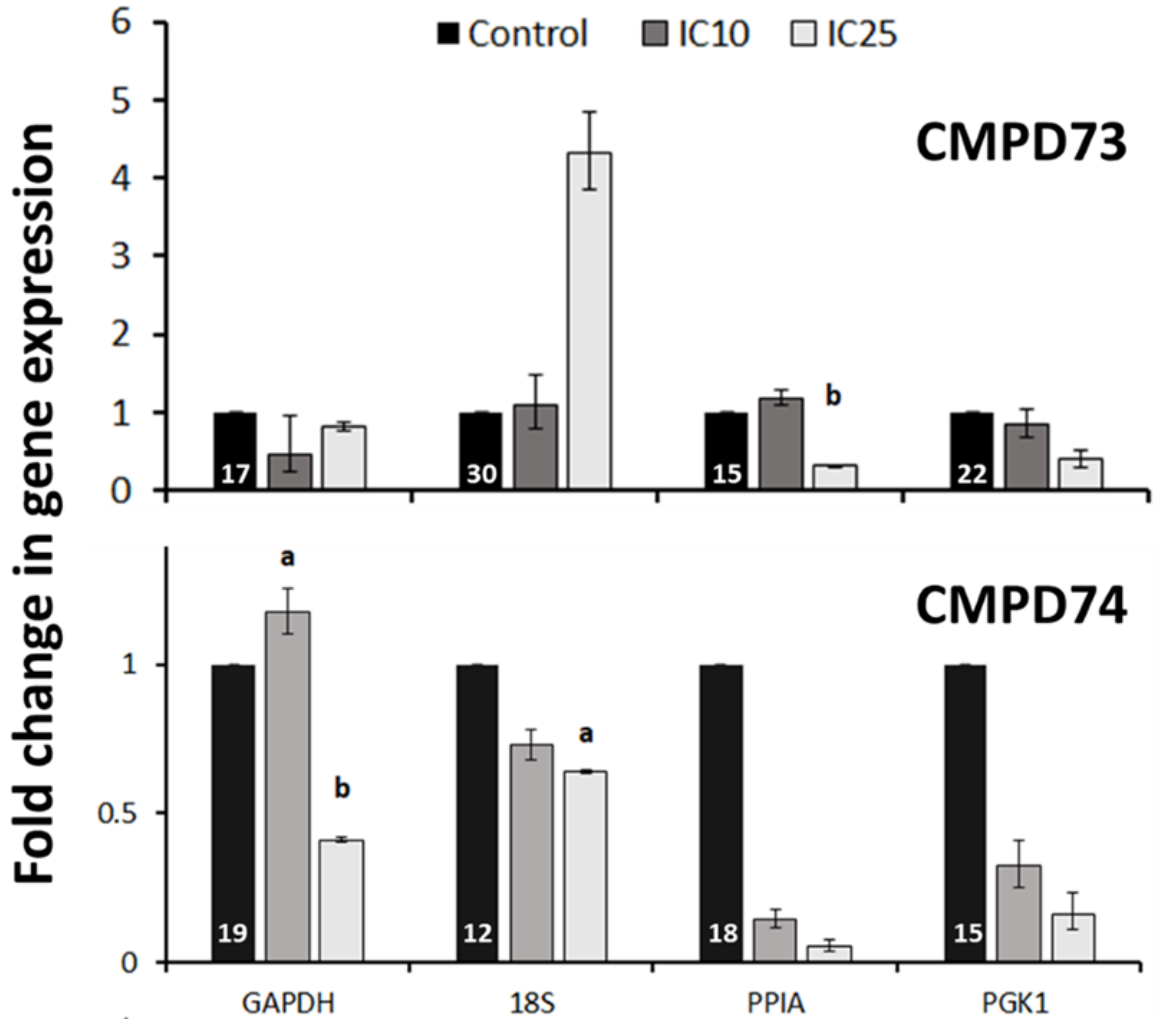

Figure 6.12- Gene expression analysis of *GAPDH*, *18S*, *PPIA* and *PGK1* HKGs isolated from A2780 cells, in response to treatment of IC_{10} and IC_{25} values of CMPD 73 for 24hrs. Mean control Ct values are present in each HKG. Results expressed as fold-change in gene expression relative to control conditions (± range of duplicate wells of duplicate biological replicates) (a= $P<0.05$ compared to control, b= $P<0.05$ compared to IC_{10} concentration).

PPIA is also observed to decrease in expression in a concentration-dependent manner regarding both CMPD 73 and 74. *PPIA* experiences an initial increase at IC_{10} CMPD 73; however a statistically significant decrease follows at IC_{25}. Neither concentration of CMPD 74 is seen to be statistically significant regarding decreases in *PPIA* expression ($P \approx 0.07$ for both concentrations); however the apparent biological significance cannot be ignored. Similarly *PGK1* expression is reduced in a concentration dependant manner following treatment with both compounds; however reduction by CMPD 74 is significantly more pronounced. Again, despite obvious biologically significant reduction of *PGK1* expression neither CMPD 73 ($P > 0.2$ both concentrations) nor CMPD 74 (IC_{10} $P<0.08$, IC_{25} $P<0.15$) is seen to be statistically significant. These data demonstrate that a high degree of caution must be applied to the interpretation of studies of these and related compounds unless great care has been given to demonstrate stability of HKGs used.

To characterise the impact of the parent 1,10-phen on HGK expression, parallel experiments were carried out with 1,10-phen (Figure 6.13). However, these were complicated by the requirement for relatively large amounts of methanol to enable solubilisation of the compound. On average the presence of methanol resulted in a 1.2 cycle increase in the expression of the HKGs. The elevation in *GAPDH* and *18S* expression is likely explainable by these changes. Expression of some of the genes, however, appeared to be reduced by 1,10-phen above the effects of the vehicle, suggesting that under the right conditions 1,10-phen may be able to degrade RNA in the cell. The impact of the vehicle precluded robust statistical interpretation.

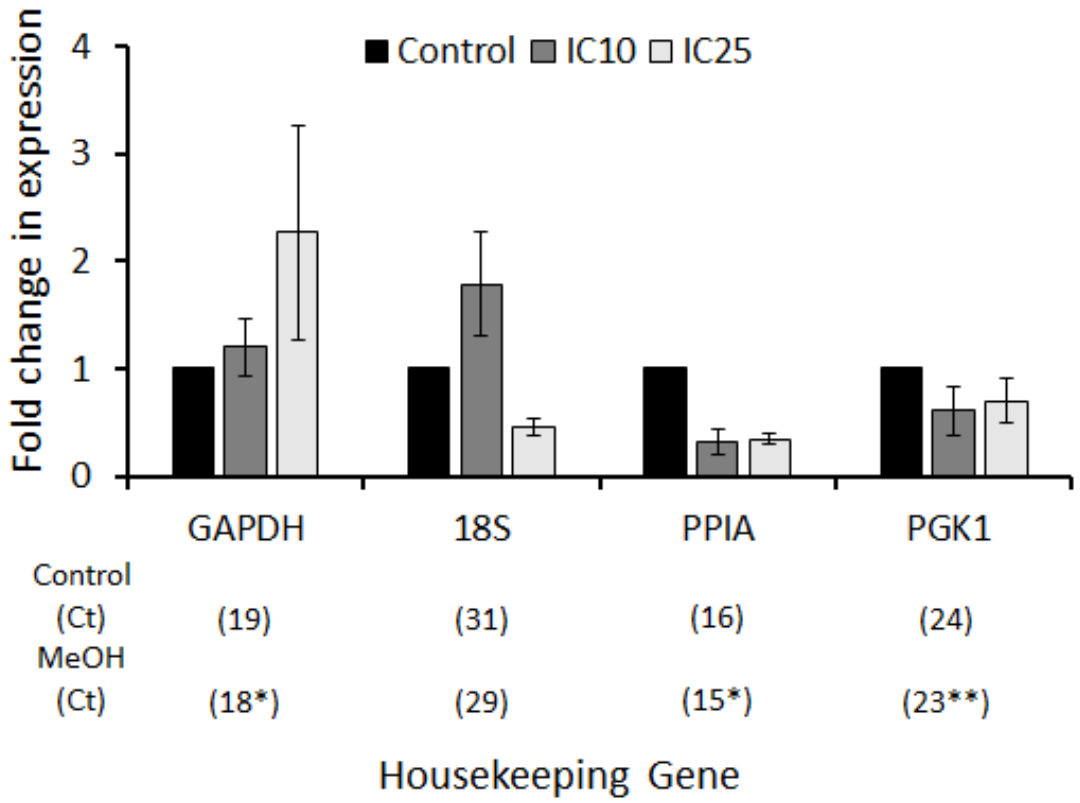

Figure 6.13- Gene expression analysis of *GAPDH, 18S, PPIA* and *PGK1* HKGs isolated from A2780 cells, in response to treatment of IC_{10} and IC_{25} values of 1,10-Phen for 24hrs. Mean Ct values for control and vehicle control are present beneath each HKG. Results expressed as fold-change in gene expression relative to vehicle control conditions (± range of duplicate wells of a duplicate biological replicates) (*P<0.05 compared to control Ct, **P<0.01 compared to control Ct).

6.5.4. 3':5' RT-qPCR assay

Figure 6.14 displays relative changes in the ratio of 3' amplicon compared to 5' amplicon following treatment of A2780 cells with CMPD 74 for 24hrs at IC_{10} and IC_{25} concentrations. CMPD 74 at both IC_{10} and IC_{25} concentrations appears to modestly increase the 3':5' ratio relative to control conditions, which is consistent with degree of RNA damage. The ratio at the IC_{25} dose appears to be slightly lower than IC_{10}'s ratio both concentrations are still observed to be above the threshold ratio of 1. Furthermore, as *PGK1* expression is significantly decreased at IC_{25} concentrations of CMPD 74 this could explain the slight reduction in ratio.

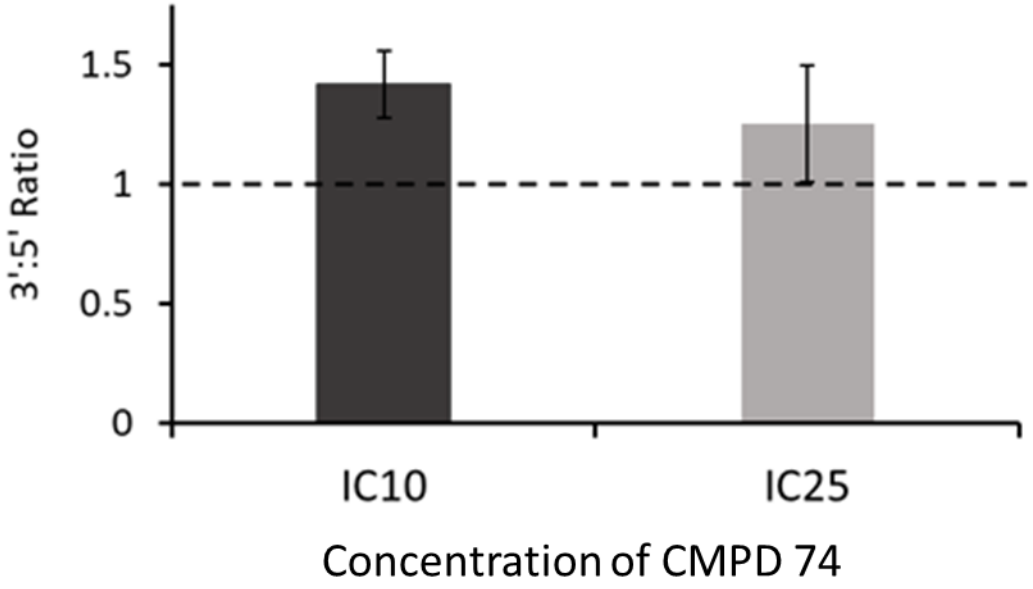

Figure 6.14- 3':5' ratio of *PGK1* HKG isolated from A2780 cells in response to treatment of IC_{10} and IC_{25} values of CMPD 74 for 24hrs. Results expressed as increase in relative 3' ratio compared to control conditions (dotted line) (± range of duplicate wells of an independent experiment)

6.5.5. Differential amplicon size assay

The principle of the differential amplicon size assay is that there should be less amplification of the larger amplicons from a given gene, due to degradation of the transcript and inability to maintain amplification during PCR. Thus, for a degraded sample the relative amount of the larger amplicon compared to the smallest (i.e. reference) amplicon, should increase resulting in an increase in the ratio of large: small. When cells are exposed to the IC_{25} concentration of CMPD74 there is a clear trend towards greater ratios with larger products, which is consistent with partial degradation of the larger transcripts (Figure 6.15 B). To further visualise this we plotted the size of the product as an indication of "distance from 3' end" (Figure 6.15 A). There is an approximate linear increase for the IC_{25} while no such effect is noted at the IC_{10}.

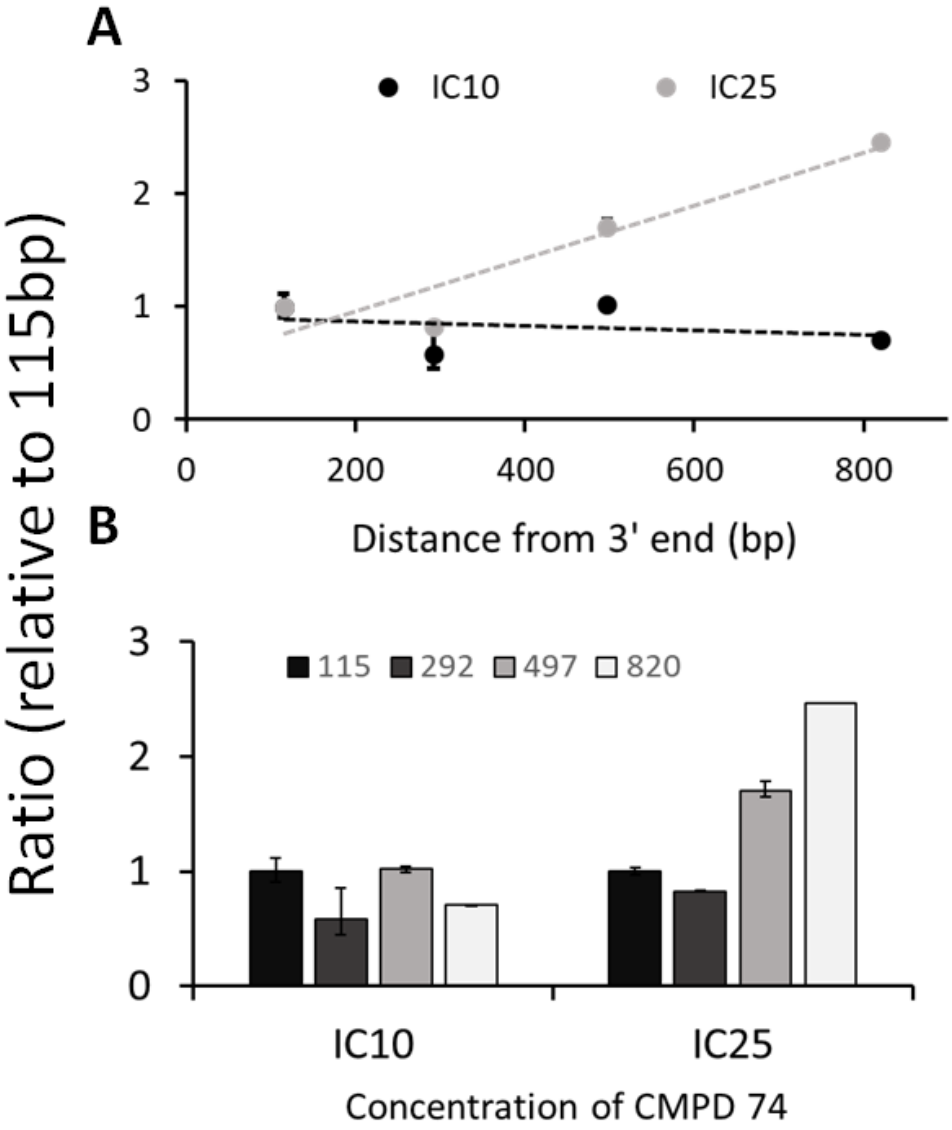

Figure 6.15- Differential amplicon size assay of *PGK1* HKG mRNA isolated from A2780 cells treated with of IC_{10} and IC_{25} concentrations of CMPD 74 for 24hrs. Both A and B are expressed as fold increase in the ratio of 115bp amplicon (± range of duplicate wells of an independent experiment).

6.6.Discussion:

The nuclease mimetic activity of novel CMPD 73 and 74 was assessed. It was determined that both compounds are potent nuclease mimetics against both plasmid DNA and isolated RNA, and that both tests compounds and 1, 10-Phen itself utilise ROS production to exert their mimetic activity. Using molecular based *in celluo* methods evidence of CMPD 74 mediated RNase mimetic activity was also seen in a cellular context.

Chemical nuclease activity is often observed in metal-phen coordination compounds. To evaluate the capacity of the current compounds to act as nuclease mimetics a series of incubations with RNA and DNA as nucleic acid substrates were completed. Previous data has shown that analogous compounds lacking the ethereal oxygens (i.e. CMPD19 and CMPD22) can act as chemical nucleases, with CMPD22 able to cleave plasmid DNA in the absence of ascorbate (Kellett *et al.*, 2011). The current data shows that both CMPD73 and CMPD74 can efficiently cleave and degrade plasmid DNA (Figure 6.6). CMPD74 is the more active of the two compounds tested and is able to almost completely degrade the plasmid DNA within 30 minutes, in contrast to the 24 hours required for CMPD73 for a similar extent of degradation. Comparison of these data to that of Kellett *et al* (2011) indicate that the current compounds are significantly more active as DNA nucleases, although an added reductant (i.e. ascorbate) is required to support activity (in contrast to the copper containing CMPD22) under *in vitro* conditions.

Given the strong DNA cleavage activity of these compounds it is considered of crucial interest to evaluate their potential to degrade RNA, the quantitatively dominating nucleic acid in cells. Both CMPD73 and CMPD74 were efficient RNAse mimetics and capable of significant

degradation of purified mammalian total RNA within two hours (Figure 6.8 and Figure 6.9). Interestingly, although requiring ten-fold greater concentration, $CuCl_2$, TDDA-Cu and 1,10-Phen (i.e. component moieties of the overall complex) were observed to promote the degradation RNA (Figure 6.9). Time-course experiments with CMPD74 and 1,10-Phen revealed a rapid impact of CMPD74 and a slower but significant RNAse mimetic activity of free 1,10-Phen. The activity associated with 1,10-Phen could be eliminated via addition of excess EDTA (Figure 6.10 lane 12) consistent with the observations that 1,10-Phen may be 'activated' via chelation of trace metals in solution (Burkitt *et al.*, 1996). These data support previous cytotoxicity results indicating an independent effect of 1,10-Phen, likely due to a similar mechanism to that uncovered here with regards to metal scavenging (Figure 2.13 page 90).

The potential to degrade RNA will have a profound effect on the biology of the cell – damage to ribosomal RNA would be expected to lead to deleterious effects on ribosome assembly, RNA splicing, silencing or translation, ultimately leading to impaired protein synthesis. In rapidly growing cells (such as tumours), this would lead to proteotoxic stress (Madden *et al.*, 2019). This effect would be exacerbated by direct effects on mRNA levels, further decreasing the ability of the cell to respond to the toxic insult mediated by the metal-phen compounds. The transcription factor Heat Shock Factor 1 (HSF1) has been shown to be a central regulator of the ribosomal stress response (Albert *et al.*, 2019). Intriguingly, previous work has shown (Nishimura and Dwyer, 1995) that 1,10-Phen can regulate the expression of selected heat shock mRNA and proteins, at least in rat cells.

The resulting degradation of intracellular RNA levels and its effects previously discussed (stalled ribosome function, RNA splicing, silencing or transcription) offer lucrative avenues

for target identification, e.g. via investigation of ER stress. Profiling of the importance of ROS for nuclease mimetic activity was investigated using an inhibitor approach, similar to that outlined previously in Chapter 4.

Speciation of suspected ROS produced by CMPD 74 was investigated, and results are shown in (Figure 6.11 B). The results of the inhibitor profiling approach indicate that under *in vitro* conditions CMPD74-mediated degradation of RNA occurs via Fenton-like chemistry utilising ascorbate as a redox catalyst. The total inhibition of CMPD 74 activity when scavengers against H_2O_2, superoxide and the hydroxyl radical were employed (Figure 6.11 B) supports this interpretation. It is likely that hydroxyl radical production is the predominant catalyst of RNA degradation, and that H_2O_2 and superoxide production are the vital intermediate steps involved.

Both H_2O_2 and superoxide are widely reported to be relatively inert as single agents against biomolecules such as nucleic acids, and so support the hypothesis that they drive hydroxyl radical formation to cause nucleic acid degradation rather than acting as single agents (Kalyanaraman, 2013; Santa-Gonzalez *et al.*, 2016). Indeed, we have noted that H_2O_2 alone is unable to induce any form of RNA degradation unless it is combined with $CuCl_2$ as an oxidising agent (data not shown).

The formula by which these Fenton reactions generate hydroxyl radicals utilising ascorbate as a reductant can be seen in Figure 6.16 formulas (1) to (5), adopted from Zhou, Zhang (*et al.*, 2016). Ascorbates ability to cycle Cu (II) to Cu (I) can provide copper in both its cupric and cuprous forms to generate both H_2O_2 and superoxide, allowing the production of the hydroxyl radical Figure 6.16 (5) (Uluata, McClements and Decker, 2015; Zhou, Zhang *et al.*, 2016).

$$Cu(I) + O_2 \rightarrow Cu(II) + O_2^{\bullet -} \; 0.48 \; M^{-1} \; s^{-1} \quad (1)$$

$$Cu(II) + O_2^{\bullet -} \rightarrow Cu(I) + O_2 \; 6.6 \times 10^8 \; M^{-1} \; s^{-1} \quad (2)$$

$$Cu(I) + O_2^{\bullet -} \xrightarrow{2H^+} Cu(II) + H_2O_2 \;\; 2.0 \times 10^9 \;\; M^{-1} \;\; s^{-1} \quad (3)$$

$$Cu(I) + H_2O_2 \xrightarrow{2H^+} Cu(II) + HO^{\bullet} + OH^- \;\; 4.7 \times 10^3 \;\; M^{-1} \;\; s^{-1} \quad (4)$$

$$Cu(II) + H_2O_2 \xrightarrow{-2H^+} Cu(I) + O_2^{\bullet -} \;\; 460 \;\; M^{-1} \;\; s^{-1} \quad (5)$$

Figure 6.16- Reduction of copper in the presence of AA and the generation of ROS (Zhou, Zhang *et al.*, 2016)

It is interesting to note the significant role that H_2O_2 played as a rate-limiting factor in the catalysis of RNA by CMPD 74. The use of pyruvate to scavenge H_2O_2 in a cellular setting did not yield any significant effects regarding the cytotoxic activity of CMPD 74 (Figure 4.24 page 153). It is therefore probable that H_2O_2 acts as a critical yet short lived intermediate essential for immediate catalytic activity, but not directly driving cytotoxicity. This hypothesis likely holds true regarding both CMPD 73 and 1,10-Phen. The role superoxide plays in CMPD 74 mimetic activity supports the previous observation that it is essential for total cytotoxicity within the cell.

In contrast to CMPD 74, both free 1,10-Phen and CMPD 73 were seen to have limited activity against RNA through production of the hydroxyl radical. These results are somewhat odd in that both H_2O_2 and superoxide are essential for the degradation of RNA by both compounds, suggesting that similar to CMPD 74, production of hydroxyl radical through Fenton-like chemistry would logically present itself as the direct catalytic mechanism of ribonuclease activity.

Watts, Sarasa, Loge, & Teel (2005) demonstrated that Mn could generate hydroxyl radicals from H_2O_2 through Fenton-like reactions, but these only occurred at much higher catalytic concentrations than its iron counterpart, and at a pH below biological relevance (at pH 6.8 no generation of hydroxyl radicals were detected). Mn has also been speculated to be less available to undergo Fenton reactions than copper or iron due to its higher reduction potential (Aguirre and Culotta, 2012). The limited impact of DMSO may be linked to formation of mixed subpopulations of 1,10-Phen following exchange of the metal centre with environmental ions such as copper or iron, before becoming active against the RNA. Since the RNA degrading activity of CMPD 73 appears to be slower acting than free 1,10-phen (2hrs for 73 and 0.5 hrs for 1,10-Phen) complex dissociation and capture of other ligand metals by 1,10-phen is a plausible explanation for the observed data.

This is in line with initial observations of kinetic replacement reactions of transition metals with 1,10-Phen. Hoyler and collaborators (1965) demonstrated that Cu-phen complexes possess relatively high formation rate constants higher than that of Mn-phen complexes. Cu(II) was also demonstrated to be a suitable decomposing ion for Mn-Phen complexes further supporting the notion that Mn-phen complexes require dissociation to become active (Holyer *et al*., 1965). Thus Mn-driven Fenton reactions is a less likely cause of RNA degradation.

Finally the variable nature at which DMSO appears to inhibit hydroxyl radical production by CMPD 73 and 1,10-Phen may be a result of experimental design. As is seen in Figure 10.3 in the appendix the inhibition of hydroxyl radical-mediated degradation of RNA by CMPD 74 is greatest following a 30-60min incubation period prior to compound exposure. Longer pre-incubation with DMSO before the addition of CMPD 73 or 1,10-Phen may serve to efficiently inhibit RNA degradation by the hydroxyl radical and demonstrate similar Fenton-like reactions

responsible for CMPD 74 activity. Due to government restrictions in light of the Coronavirus pandemic conducting this line of investigation was no longer possible.

Neither $MnCl_2$ nor the phen free precursor to CMPD 73 (Mn-TDDA) displayed RNA degradation capacity when tested (shown previously). As both free Phen and CMPD 73 display near identical ribonuclease profiles, these data support the hypothesis that the overall nuclease activity is a combination of free 1,10-Phen (liberated in the context of the experiment) and the intact compound. This is supported by data from cell cytotoxicity discussed previously in chapter 2.

The weak inhibition of RNA degradation seen in response to treatment with sodium azide (NaN_3) and CMPD 73 may indicate that the production of singlet oxygen ($^1O_2$) is a contributing factor in the degradation of RNA. While reactions utilising 1,10-Phen did not indicate $^1O_2$ inhibition as seen in Figure 6.11 (C) initial preliminary experiments did yield similar results to CMPD 73 regarding 1,10-Phen and NaN_3. This may be telling of the variable nature at which 1,10-Phen cycles catalytic ions to degrade RNA and further support the notion of a 1,10-Phen driven mechanisms for CMPD 73.

1,10-Phen is a Polycyclic Aromatic Hydrocarbon, which in some instances have been shown to react with oxygen to release $^1O_2$, indicating $^1O_2$ production could be plausible for 1,10-Phen containing compounds (Aubry *et al.*, 2003; You, 2018). However, while $^1O_2$ is a known free radical capable of oxidising nucleobases, it is not capable of causing breaks within the phosphate backbone of either DNA or RNA. It could be the case that $^1O_2$ is involved in a cyclic mechanism with superoxide and H_2O_2, whereby it is produced as a by-product of Fenton or Haber Weiβ chemistry, alongside the hydroxyl radical. $^1O_2$ may then be recycled back into

either H_2O_2 or superoxide to continue propagating the production of ROS capable of cleaving the sugar phosphate backbone. Indeed it has been shown by Kramarenko *et.al* (2006) that $^1O_2$ can react with ascorbate to generate H_2O_2. This can be further supported by Takeshita *et.al* (2000), who reported that $^1O_2$ can produce superoxide or H_2O_2 in the presence of certain biomolecules (Takeshita *et al.*, 2000). Therefore, scavenging of $^1O_2$ by NaN_3 may serve to dampen but not eliminate RNA degradation, as seen by the partial degradation in Figure 6.11 (C).

However, NaN_3 has been reported to possess some scavenger activity towards the hydroxyl radical (Girotti, 1998). As NaN_3 inhibition is very similar to inhibition in response to DMSO, it may be the production of the hydroxyl radical rather than $^1O_2$ that is being detected. As $^1O_2$ is incapable of sugar phosphate backbone scission and the hydroxyl radical is capable of such scission it may likely be the case. The fact that these small inhibitory bands were not seen in treatments using CMPD 74 may be a result of the high level of catalytic hydroxyl radical production in response to the copper element of CMPD 74. As it is speculated that CMPD 73 relies on 1,10-Phen for catalytic ribonuclease activity it is likely that the production of hydroxyl radicals would be at a slower rate as compound disassociation would be required for 1,10-Phen to become catalytically active. This could allow any potential scavenging by NaN_3.

At a practical level, RNA cleavage capabilities of both compounds will have downstream considerations regarding further experimental planning. As well as potential cellular targets, activity of these compounds against RNA (in particular mRNA) will have to be considered for any gene expression experiments (e.g. qPCR) that will likely be carried out in future, as part of a mechanistic approach to determine compound mode of action.

The effect that this ROS-mediated ribonuclease activity may have on gene expression studies was investigated. The 3':5' qPCR-based assay has been used as a tool to determine the quality of isolated mRNA that has been subject to treatment with cytotoxic compounds. It was therefore applied to determine whether the ribonuclease activity of metal phen compounds could significantly compromise the integrity of mRNA to be used in further gene expression studies. CMPD 74 was selected as the most likely candidate to test this hypothesis using both the 3':5' and the amplicon size assays owing to its rapid and potent ribonuclease mimetic activity.

Analysis of both methods yielded conflicting results as the standard 3':5' assay demonstrated both minimal increases in relative ratios and little difference in CMPD 74 concentration. Contrasting this the amplicon size assay to detect difference in expression level yielded little to no effect following treatment with IC_{10} concentrations yet observable changes in relative ratio following treatment at the IC_{25} concentration. The inability to observe a significant effect using the standard 3':5' assay may be a result of primer design with the 5' primer pair being too close in proximity to the 3' primer pair thereby creating a sensitivity issue in damage detection. It may also be related to the requirement to use a minimally toxic concentration to ensure that frank cytotoxic effects do not dominate, thus leading to a sensitivity issue. Regarding the amplicon size assay it would appear that expressing multiple amplicon products as a ratio of the smallest amplicon product may serve as an accurate measure of mRNA integrity in response to RNA damaging compounds e.g. metal-phen. However, it should be noted that CMPD 74 does have an impact on the expression of *PGK1* which is aligned with the findings of the 3':5' assay, i.e. damage to RNA and reduction in expression.

Further to the effects CMPD 74 had on *PGK1* expression observed following the 3':5' assays, multiple HKGs were analysed to determine which if any could be applicable to qPCR-based gene expression studies. Global alterations made to the expression of HKGs may also shed light on whether metal-phen compounds are affecting the transcription/translation processes as a result of nuclease mimetic activity. This would hold particularly true for changes to ribosomal *18S* expression as it would be a direct target of metal-phen compounds.

Interestingly CMPD 73 is observed to have varied effects on gene expression particularly regarding the expression of *18S*. While initially seen to reduce the expression of *GAPDH*, *PPIA* and *PGK1* CMPD 73 drastically increased *18S* expression at higher concentrations contradicting previous assumptions it would cause its degradation in a concentration-dependent manner. This may indicate that CMPD 73 is not targeting intracellular RNA as previously assumed and that reduced expression of the other three HKGs is a result of an alternate target over direct RNA degradation. Despite appearing to share many mechanistic properties CMPD 73 and 1,10-Phen did appear to diverge somewhat in the context of HKG expression. While 1,10-Phen did appear to reduce the expression of both *PPIA* and *PGK1* its effect was more pronounced than CMPD 73 and it is also seen to increase not decrease *GAPDH* expression. Interestingly 1,10-Phen also resulted in an increase in expression of the *18S* gene however in contrast to CMPD 73 this happened at IC_{10} concentrations rather than IC_{25} concentrations seen with CMPD 73. IC_{25} concentrations were then observed to significantly reduce *18S* expression again in contrast to CMPD 73. This somewhat paradoxical event may be explained by the inherent chelative properties possessed by 1,10-Phen.

Kloubert and Rink (2019) demonstrated that the stability of HKG expression can vary depending on the availability of zinc, while Yamagami *et al*., (2018) also demonstrated that weakly-chelated magnesium by amino acids aids in RNA stabilisation and folding. As such the

chelative properties of 1,10-Phen may in fact enhance RNA stability over RNA degradation at lower concentrations, with the ribonuclease-mimetic activity becoming prominent at higher concentrations. This could also likely explain the comparable effects seen regarding CMPD 73 and increased expression of *18S*. Similarly compound kinetics may explain these differences. CMPD 73 requires a longer incubation period to efficiently degrade RNA (2hrs) while 1,10-Phen can degrade RNA within 30mins but at concentrations one order of magnitude higher (1µM for CMPD 73 vs 10µM 1,10-Phen). Slower kinetic rates may allow the cell to counteract RNA degradation caused by the compounds resulting in significantly increased expression of RNA and in particular rRNA. However experimental error must not be excluded as a plausible explanation for these unexpected results.

Furthermore, the high concentration of MeOH required as a vehicle for both IC_{10} (1% v/v) and IC_{25} (2.5% v/v) concentrations of 1,10-Phen are seen to increase the expression of all HKGs investigated. The increases in expression observed regarding *GAPDH* and *18S* may be a result of vehicle effects rather than compound effects. This indicates certain limitations regarding compound delivery and solubility and further potential effects on experimental reproducibility. As such the significant effects MeOH as a vehicle for 1,10-Phen may also explain the HKG expression profiles observed with 1,10-Phen and difference with otherwise comparable CMPD 73. Furthermore IC_{10} and IC_{25} drug concentrations may not be the optimal concentrations at which to investigate these effects for any of the test compounds owing to cytotoxic induced variability. Optimising compound concentration and more robust experimental replicates may serve to overcome the limitations encountered in this study.

In contrast CMPD 74 is seen to cause significant reduction in gene expression of all four HKGs with significant reductions seen in *18S* expression despite inherently high expression levels (Ct

12). These data appear to support the hypothesis that CMPD 74 is capable of degrading intracellular RNA and that it may be a possible mechanism of cytotoxic action. CMPD 74s higher potency and rapid degradation of RNA may explain why it can reduce *18S* expression compared to CMPD 73 or 1,10-Phen. Further investigation using multiple alternate HKGs is warranted to ensure that these observations operate on a global level throughout the cell and are not limited to these specific HKGs. However the significant reductions in *18S* expression is suggestive of the presence of this effect. If altered expression levels in the larger panel of HKGs is detected this may be telling that the metal phen and phen compounds have global effects on mRNA expression. This would validate the original hypothesis that cellular RNA is a target of metal phen compounds, and that gene expression studies could be compromised as a result.

While certain limitations are noted regarding the data described using qPCR to investigate the *in cellulo* effects of these compounds, the combination of *in cellulo* and *ex cellulo* analysis do demonstrate that ROS-mediated RNase mimetic activity does persist within the cell in a biologically significant manner. This is further supported by the fact that ascorbate as an added reductant is not required for the effects measured *in cellulo* indicating that conditions required for RNAse mimetic activity are met within the cell.

As such the ribonuclease mimetic activity of these compounds should not be underestimated as a potential mechanism of action, particularly with regards to CMPD 74. While more experimentation is needed to fully determine the scope at which these compounds target RNA within the cell the data described thus far indicates that careful consideration must be taken when utilising gene expression and qPCR-based approaches to avoid artefactual and erroneous results.

7. Potential interactions between metal-based drugs and ER stress

7.1. Introduction

The processes of transcription and translation represent the canonical pathway for protein synthesis in the cell, with translation localised to ribosomes, either free or associated with the endoplasmic reticulum (ER) membrane, forming the rough ER (Jackson, Hellen and Pestova, 2010) (Wilson and Doudna Cate, 2012). Ribosomes are composed of a mixture of ribosomal RNA (rRNA) and associated proteins. During translation, transcribed mRNA is shuttled from the nucleus to the cytosol, where it becomes encapsulated by the small and large ribosomal subunits forming a single complex. Transfer RNAs (tRNA) also found in the cytosol are adaptor molecules which bind to free amino acids and become incorporated into the ribosome forming a polypeptide chain. As the polypeptide grows it is fed into the ER lumen, where it immediately begins to be folded and post-translationally modified to become a functional protein (reviewed Bravo et al., 2013). The lumen of the ER is rich in calcium which acts as a cofactor for many protein folding chaperons such as calreticulin and is both an energy and oxidant rich environment, to favour oxidation of cysteine residues required for disulphide bond formation (Carreras-Sureda, Pihán and Hetz, 2018).

The majority of polypeptide chains that enter the ER lumen are not successfully folded, and so are targeted for degradation through a process known as ER-associated degradation (ERAD) (reviewed Hetz & Papa, 2018). ERAD removes misfolded proteins by exporting them into the cytosol to undergo ubiquitin-mediated degradation and recycling in the proteasome. The clearance of misfolded proteins is an important process in order to maintain ER integrity and prevent the ER from experiencing secretory overload with misfolded and non-functional proteins (reviewed Ruggiano, Foresti and Carvalho, 2014). Incorporation of misfolded and non-functional proteins into cell structures and pathways could have detrimental effects to the

cell. This is seen in many diseases such as Alzheimer's, diabetes and cancer and underscores the need for an efficient mechanism of protein clearance (Scheper and Hoozemans, 2015).

When the cell experiences more severe forms of stress such as hypoxia, oxidative stress, starvation, or a loss of calcium homeostasis the resulting accumulation of misfolded proteins may overload the ER and induce ER stress. This initiates a separate process of protein clearance and is called the Unfolded Protein Response (UPR). The UPR is a dynamic intracellular signalling pathway that alleviates ER stress through two distinct mechanisms (reviewed Diehl, Fuchs and Koumenis, 2011). Firstly, the UPR causes global translational arrest to prevent further overloading of the ER with misfolded proteins, and also increases protein degradation through ERAD in order to clear the irregular proteins. Secondly, it initiates a transcriptional cascade of hundreds of genes involved in global proteostasis control, such as genes involved in maintaining ERAD function, ER chaperone and folding proteins, autophagy, and antioxidant defence genes (reviewed Tsai and Weissman, 2010). If the ER experiences prolonged stress and is unable to clear the accumulated misfolded proteins, the UPR is then capable of activating autophagic and apoptotic cell death to prevent incorporation of irregular proteins into the cell, compromising homeostasis. The UPR can therefore be seen as an intersection between adaptive and cytotoxic roles within the cell (Sano and Reed, 2013).

Misfolded proteins are typically recognised by a lack of post-translational modifications such as glycosylation. Misfolding will also result in the exposure of hydrophobic residues within the protein and unpaired cysteines, which are then recognised and bound by quality control proteins such as glucose-related protein 78/binding immunoglobulin protein (GRP78/BiP). GRP78/BiP is an important ER chaperone which binds misfolded proteins in an attempt to help rectify misfolding errors (reviewed Adams *et al.*, 2019). However GRP78/BiP is also the key

modulator of the three ER membrane-bound UPR sensory proteins, Inositol requiring enzyme 1 alpha (IRE1α), Protein kinase RNA-like endoplasmic reticulum kinase (PERK) and Activating transcription factor 6 (ATF6). These proteins are negatively regulated by GRP78/BiP, which binds their transmembrane receptors found within the ER lumen. Disassociation of GRP78/BiP in response to misfolded protein accumulation leads to the activation of all three proteins, either through homo/oligo dimerization or translocation from the ER (Bergmann and Molinari, 2018; Spaan *et al.*, 2019).

In response to the accumulation of misfolded proteins in the ER lumen, BiP/GRP78 disassociates from ATF6, IRE1α and PERK UPR regulatory proteins, facilitating activation (Casas, 2017). Activated ATF6 translocates from the ER membrane to the Golgi apparatus where it is cleaved at specific catalytic sites by serine proteases S1P and S2P releasing ATF6f. ATF6f translocates to the nucleus where it regulates the expression of genes involved in ERAD, autophagy and ER folding and chaperone proteins (Hillary and FitzGerald, 2018).

Activation of IRE1α results in receptor dimerization and auto trans-phosphorylation. Phosphorylated IRE1α dimer possess bi-functional kinase/ribonuclease. The ribonuclease domain is capable of alternatively splicing XBP1 mRNA present in the cytosol, removing its intron allowing for its translation (Chen and Brandizzi, 2013). The XBP1 protein then translocates to the nucleus where it regulates the expression of genes involved ERAD, autophagy, ER chaperones and redox homeostasis (Cubillos-Ruiz, Bettigole and Glimcher, 2016). The ribonuclease domain may also cause what is known as Regulated IRE1-Dependent Decay (RIDD) of specific mRNA, rRNA and miRNAs and serves to regulate many important biological functions such as UPR signalling itself, inflammation, translation and apoptosis (Maurel *et al.*, 2014). The kinase domain of IRE1α is capable of activating apoptotic protein

JNK. Sustained activation of JNK by IRE1α signals irreparable ER stress and signals apoptosis (Junjappa *et al.*, 2018). Thus JNK activation and RIDD serves as the link between UPR and apoptosis (Fribley, Zhang and Kaufman, 2009).

Activated PERK also dimerizes at the ER membrane where it phosphorylates and inhibits eukaryotic initiation factor 2 (eIF2α) causing global translational arrest. eIF2α inhibition allows for the translation of ATF4 which possesses an upstream open reading frame in its 5' region capable of bypassing translational arrest (McQuiston and Diehl, 2017). Translated ATF4 then translocates to the nucleus where it also regulates the expression or ERAD and redox associated genes as well as genes involved in autophagy and amino acid metabolism (Pitale, Gorbatyuk and Gorbatyuk, 2017). PERK activation has also been seen to promote Nrf2 phosphorylation further initiating the antioxidant response network (Cullinan *et al.*, 2003). ATF4 also regulates the expression of pro-apoptotic C/EBP Homologous Protein (CHOP). Therefore ATF4 acts in similar fashion to IRE1α which under sustained UPR signalling is capable of inducing apoptosis (Rozpedek *et al.*, 2016). A full visualisation of the UPR signalling cascade can be seen in Figure 7.1.

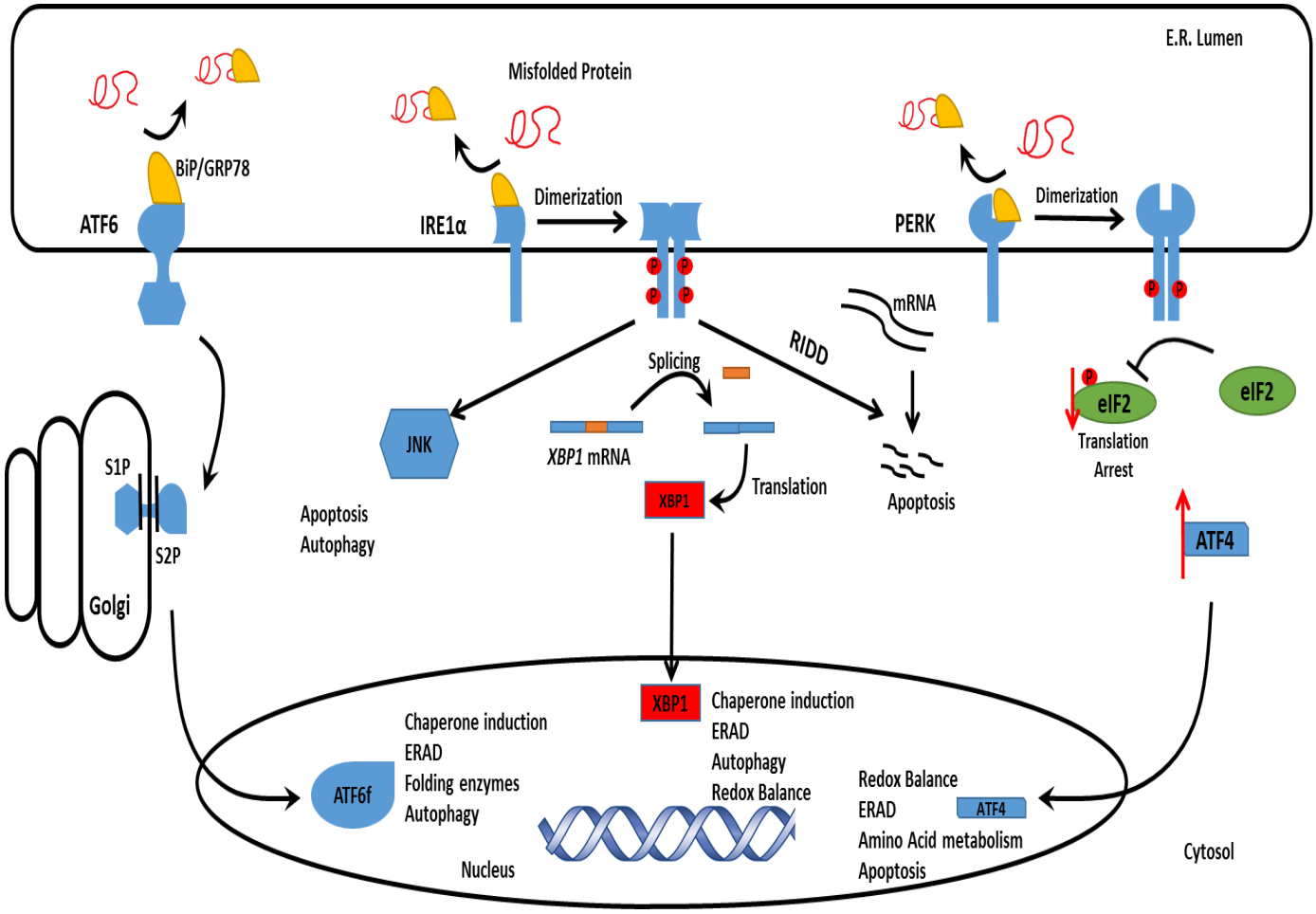

Figure 7.1-Activation of the UPR signalling pathway. Activation of the UPR signalling pathway. Accumulation of misfolded proteins causes BiP/GRP78 disassociation from transmembrane ATF6, IRE1α and PERK. Activation of all three UPR signalling pathways results in the increased expression of protein chaperones and folding enzymes, as well as autophagy, redox balance. Prolonged activation of the UPR pathway will result in IRE1α and PERK-mediated cell death signalling. Self-generated figure inspired by figures found in Walter and Ron, (2011); Ojha and Amaravadi (2017); Hetz and Papa, (2018).

Of the three UPR sensory proteins, IRE1α is the most conserved UPR sensor (Hetz and Papa, 2018). IRE1α is a ubiquitously expressed transmembrane, bi-functional kinase/ribonuclease responsible for the expression of the UPRs master regulatory protein, Xbox binding protein 1 (XBP-1) (Tsuru *et al.*, 2016).

Misfolded proteins in the ER are thought to be subjected to fruitless cycles of aberrant disulfide bond formation and reduction, increasing the production of Endoplasmic Reticulum Oxireductin-1 (ERO1)-derived H_2O_2, which would in turn exacerbate ER stress and activate UPR signalling. However, the source and nature of ER stress-derived ROS, and whether they are ERO1-derived, is not entirely clear (Redza-Dutordoir and Averill-Bates, 2016).

ER stress has been seen to play a dual role in cancer, whereby cancer cells have been seen to upregulate the UPR pathway to maintain tumorigenesis by increasing the protein folding capacity in response to high proliferative rates (Urra *et al.*, 2016). Cancer cells experience higher levels of cellular stress (hypoxia, nutrient depravation, genetic mutations) which can often lead to gross accumulation of misfolded and faulty proteins. Therefore cancer cells may depend on elevated UPR signalling in order to survive (Kim, Bhattacharya and Qi, 2015). Indeed increased UPR signalling and a dependence on PERK, IRE1α and ATF6 signalling has been comprehensively reviewed by Walczak *et al.* (2019).

Furthermore increased UPR signalling may also contribute to chemotherapy resistance by initiating cellular stress response and repair pathways clearing damaged proteins or organelles, such as the proteasomal or autophagic pathways (Madden *et al.*, 2019). However this state of prolonged UPR signalling may sensitise cancer cells overexpressing these pathways to targeted intervention/treatment (Ojha and Amaravadi, 2017).

Cu-Phen compounds have already been demonstrated to inhibit proteasome function (Zhang *et al.*, 2013, 2017), while Mn-Phen have been demonstrated to interact with the autophagic pathway (Slator *et al.*, 2017). Proteasome inhibition has been demonstrated to sensitise cancer cells to UPR mediated cell death (Amanso, Debbas and Laurindo, 2011), while prolonged activation of the autophagic pathway has been known to induce autophagic and apoptotic cell death. As such the inherent stress of proteasome inhibition by Cu-Phen compounds and induction of autophagy demonstrated by Mn-Phen may be linked by the ribonuclease mimetic activity of metal-phen compounds (as discussed in Chapter 6). UPR-mediated cell death may therefore be subject to a 'double hit' strategy by metal-phen compounds, whereby ribonuclease activity induces ribosomal stress and UPR signalling alongside concurrent induction of the UPR by proteasome inhibition and autophagic signalling, ultimately favouring UPR-mediated cell death (Figure 7.2).

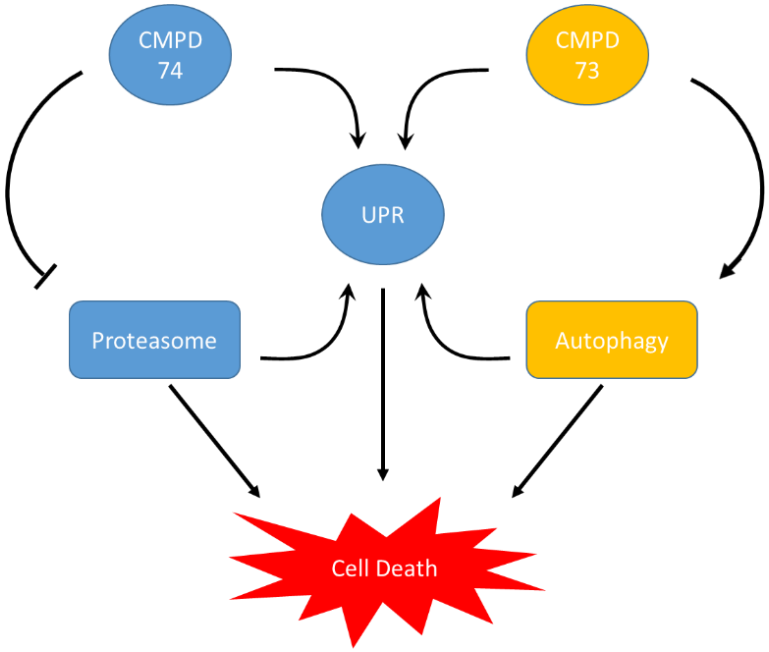

Figure 7.2-Potential crosstalk between UPR signalling and inherent metal-phen activity

The UPR pathway can be probed using two well established ER stress inducing agents, the antibiotics Anisomycin and Tunicamycin. Anisomycin has been shown to inhibit peptidyl

transferase the primary enzyme involved in protein translation which would stall protein biosynthesis and induce ER stress mechanisms (Croons *et al.*, 2009). As well as potent protein synthesis inhibition, anisomycin has been shown to induce apoptosis via activation of p38 mitogen-activated protein kinase pathway in macrophages (*ibid*).

Tunicamycin is an inhibitor of N-linked glycosylation via inhibition of N-acetylglucosamine-1 phosphotransferase (Guha *et al.*, 2017). As glycosylation is a major post translational modification and is critical for proper protein folding its inhibition will result in the accumulation of misfolded proteins in the ER and induction of ER stress. However the effects of inhibited glycosylation are not always exclusive to the ER and as such tunicamycin can effect multiple pathways reliant on glycoprotein signalling such as cell death (reviewed Lichtenstein and Rabinovich, 2013) or autophagic signalling (Wu *et al.*, 2018).

7.2.Aims

This chapter describes the results of experiments that were aimed at clarifying the downstream and intracellular effects of ribonuclease-mimetic CMPD 73, 74 and 1,10-Phen with the UPR as a possible mediator of cell death. This will be investigated using the compounds Anisomycin and Tunicamycin. while . Therefore both are well-known inducers of ER stress pathways and the UPR. The hypothesis is that if CMPDs 73 or 74 interact with the ER stress/UPR pathways an increase in cytotoxicity should be observed with combinatorial treatment.

7.3.Methods

7.3.1. Selective induction of the UPR pathway using UPR inducing compounds

A549 cells were seeded at a density of $5x10^3$ cells/well and A2780 cells were seeded at a density of $1x10^4$ cells/well in a black 96-well plate. For treatments using Anisomycin both A2780 and A549 cells were pre-treated for 24hrs with 100nM Anisomycin. Both cell lines were then exposed to concentrations of CMPD 73, 74 and 1,10-Phen for a further 24 hrs. Cells exposed to Tunicamycin were pre-treated with 5nM for 8hrs before being exposed to concentrations of CMPD 73, 74 and 1,10-Phen for 24 hrs. These treatment regimens can be seen in Figure 7.3. Both treatments were analysed using the Alamar Blue proliferation assay stated in Chapter 2 (section 2.5.1 page 68) and all pre-treatments and incubations were conducted at 37°C.

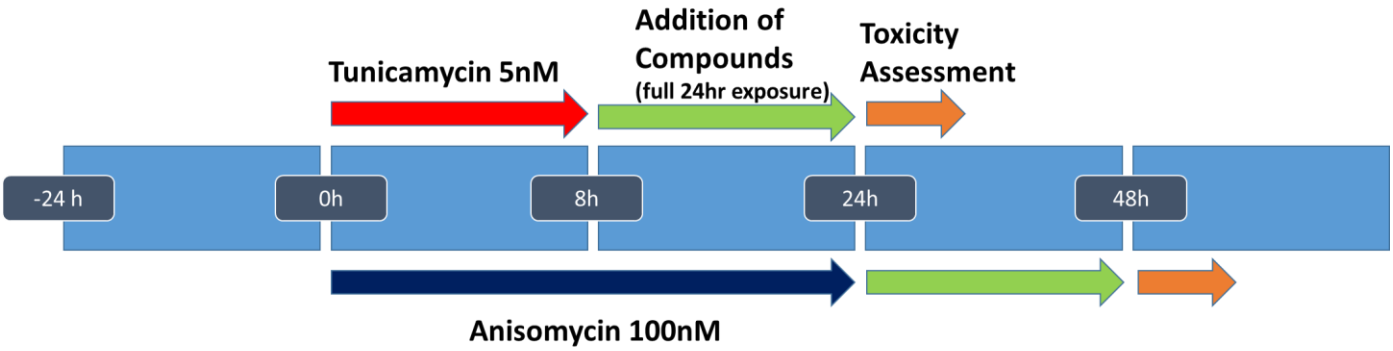

Figure 7.3-Timeline of Anisomycin and Tunicamycin incubation regimes.

7.3.2. Statistical analysis:

Data was analysed using Microsoft excel and graphs were generated using GraphPad Prism Version 5.00. Statistical analysis was conducted using Students T-Test and are expressed as a P Value < 0.05, 0.01, 0.001. for experiments where only one biological replicates were used, statistical analysis was conducted using technical replicates of control conditions against technical replicates of test conditions.

7.4.Results

Pre-treatment of A549 cells with 100nM Anisomycin for 24 hours followed by exposure to CMPD73 did not result in any additional cytotoxicity beyond that achieved by the metal-based compound alone (Figure 7.4). Anisomycin at a concentration of 100nM reduced A549 cell viability by 30%.

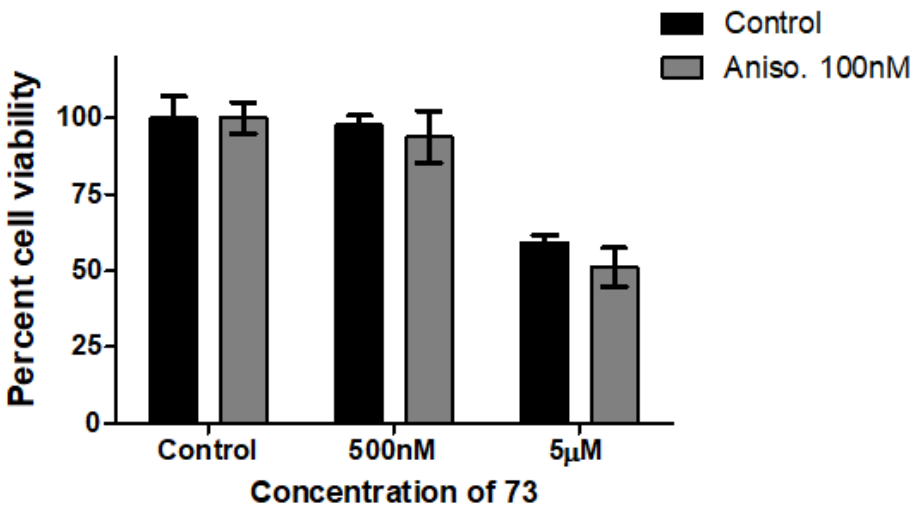

Figure 7.4-A549 cells pre-treated with 100nM Anisomycin for 24hrs followed by treatment with CMPD 73 for a further 24hrs. Results are expressed as mean percent viability ±1 Standard deviation of a single experiment. Anisomycin at a concentration of 100nM reduced A549 cell viability by 30%.

In contrast, however, a similar experiment with CMPD74, which has potent nuclease activity, revealed a significant impact of Anisomycin pre-treatment on cell viability in the high nano molar range of CMPD 74. No effect on cell viability is seen by the metal-phen compound without Anisomycin present (Figure 7.5).

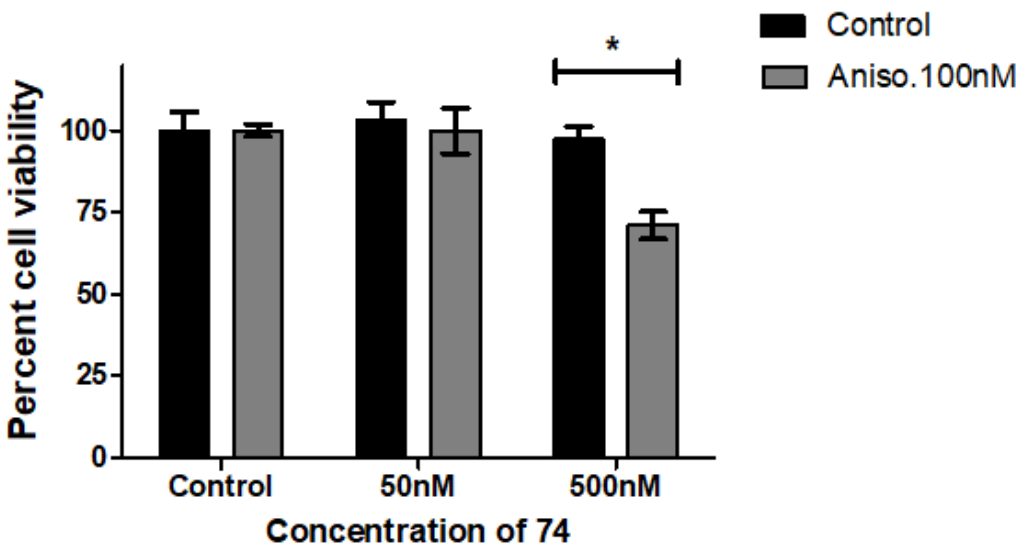

Figure 7.5-A549 cells pre-treated with 100nM Anisomycin for 24hrs followed by treatment with CMPD 74 for a further 24hrs. Results are expressed as mean percent viability ±1 Standard deviation of a single experiment (*P<0.05 compared to control). Anisomycin at a concentration of 100nM reduced A549 cell viability by 30%.

Parallel experiments with 1,10-Phen alone revealed a similar effect to that of CMPD74, albeit at much higher concentrations Figure 7.6) There is a significant increase in cytotoxicity of 50µM 1,10-phen in cells pre-treated with 100nM Anisomycin. An observable, but not statistically significant effect is noted at the lower 5µM concentration of 1,10-Phen.

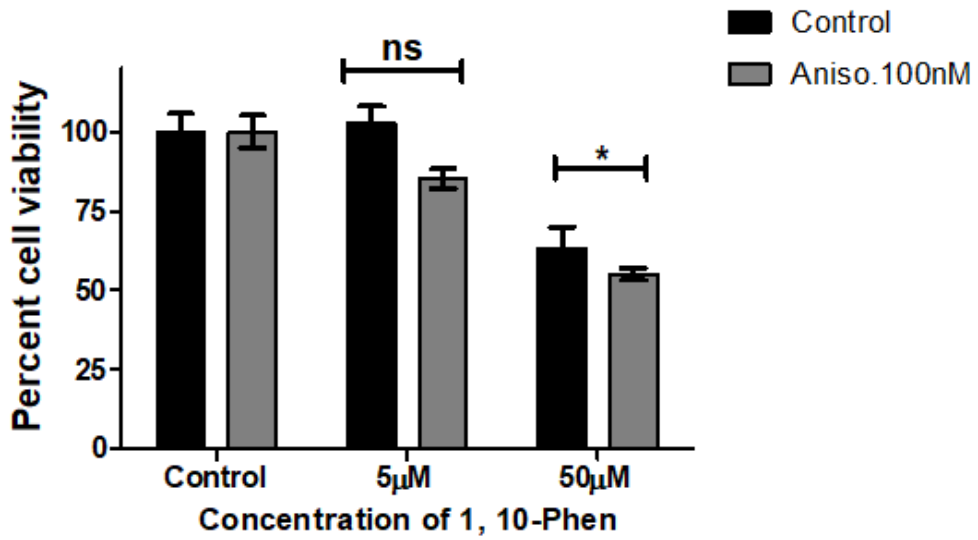

Figure 7.6-A549 cells pre-treated with 100nM Anisomycin for 24hrs followed by treatment with 1,10-Phen for a further 24hrs. Results are expressed as mean percent viability ±1 Standard deviation of two independent experiments. (*P<0.05 compared to control, ns=not significant compared to control). Anisomycin at a concentration of 100nM reduced A549 cell viability by 30%.

Similar experiments using A2780 cells revealed a modest yet highly significant increase in cytotoxicity when cells were treated with 500nM and 5μM CMPD73 (Figure 7.7). Anisomycin at 100nM reduced A2780 cell viability by 37%.

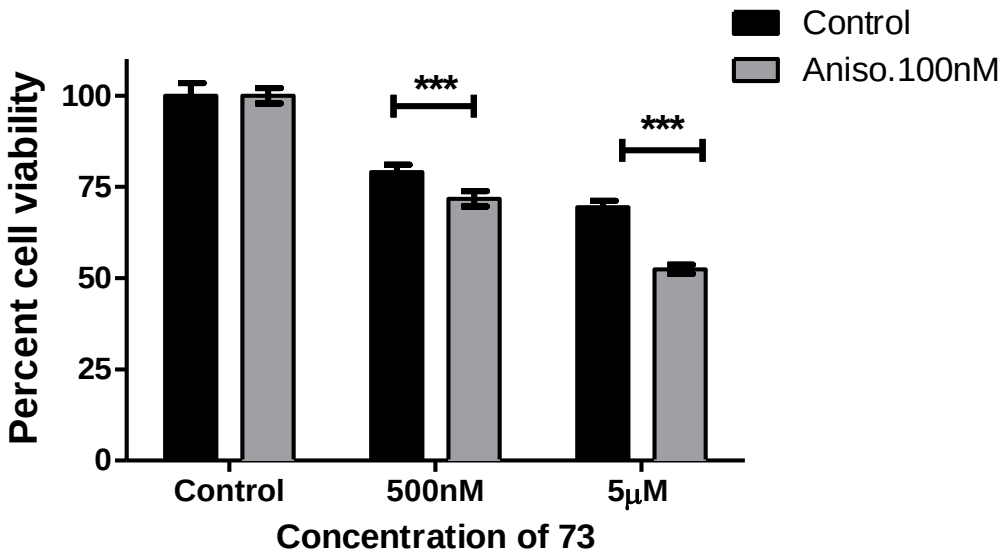

Figure 7.7-A2780 cells pre-treated with 100nM Anisomycin for 24hrs followed by treatment with CMPD 73 for a further 24hrs. Results are expressed as mean percent viability ±1 Standard deviation of a single experiment (***P<0.001 compared to control). Anisomycin at 100nM reduced A2780 cell viability by 37%.

CMDP 74 also demonstrated a modest yet significant increase in cytotoxicity at a concentration of 500nM (Figure 7.8). However a loss of effect is seen at the higher concentration of 5μM likely due to a generalised cytotoxic effect.

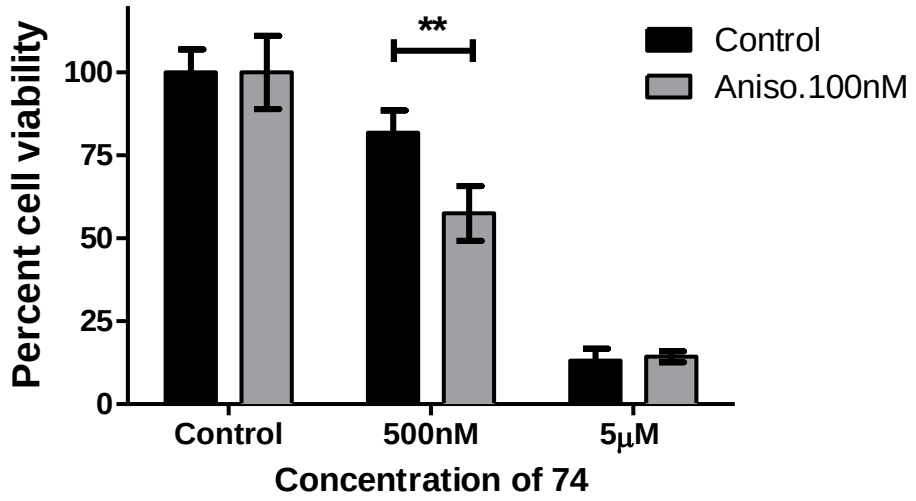

Figure 7.8-A2780 cells pre-treated with 100nM Anisomycin for 24hrs followed by treatment with CMPD 74 for a further 24hrs. Results are expressed as mean percent viability ±1 Standard deviation of a single experiment (**P<0.01 compared to control). Anisomycin at 100nM reduced A2780 cell viability by 37%.

A similar pattern is observed with A2780 cells using 1,10-Phen alone with that of CMPD 73 (Figure 7.9). Modest yet highly significant increases can be seen in both concentrations of 1,10-Phen used indicating a degree of interaction with UPR pathway.

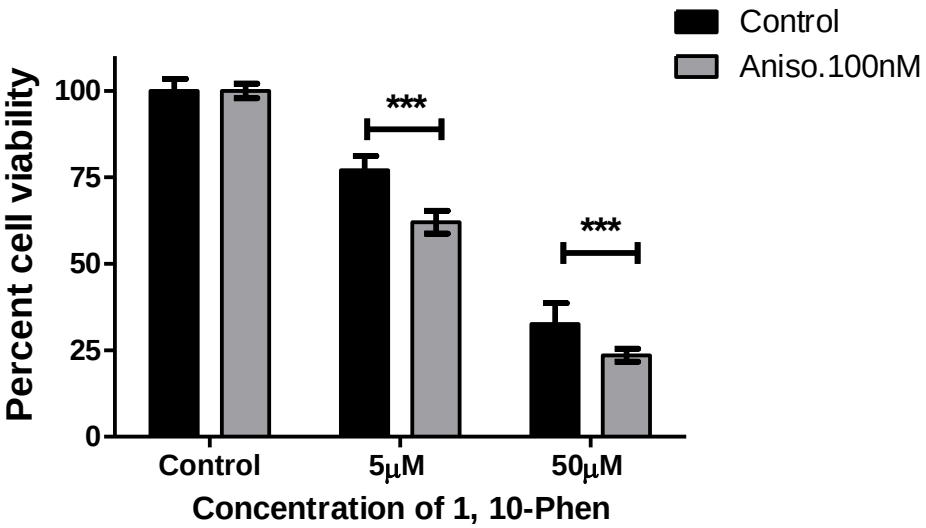

Figure 7.9-A2780 cells pre-treated with 100nM Anisomycin for 24hrs followed by treatment with 1,10-Phen for a further 24hrs. Results are expressed as mean percent viability ±1 Standard deviation of one experiment. (***P<0.001 compared to control). Anisomycin at 100nM reduced A2780 cell viability by 37%.

Pre-treatment of A549 and A2780 cells for 8hrs with 5nM Tunicamycin demonstrated similar results to Anisomycin pre-treatments. An unexpected increase in viability is observed in response to treatment with CMPD 73 indicating modest yet highly significant inhibition by Tunicamycin in A549 cells at both 500nM and 5µM (Figure 7.10). Tunicamycin at 5nM reduced A549 cell viability by 40%.

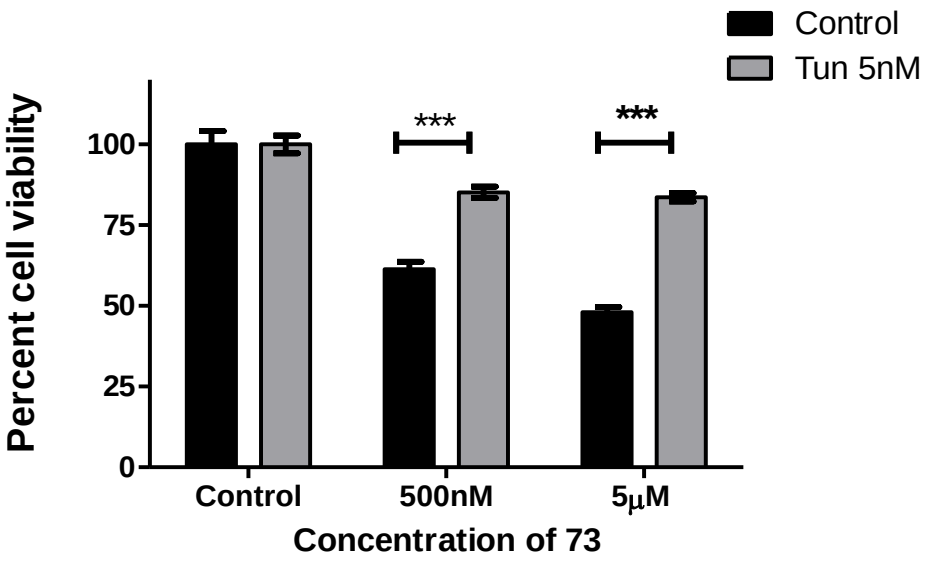

Figure 7.10-A549 cells pre-treated with 5nM Tunicamycin for 8hrs followed by treatment with CMPD 73 for a further 24hrs. Results are expressed as mean percent viability ±1 Standard deviation of two independent experiments. (*** P<0.001). Tunicamycin at 5nM reduced A549 cell viability by 40%.

CMPD 74 experienced a modest yet highly significant increase in cytotoxicity at a concentration of 500nM following pre-treatment with Tunicamycin in A549 cells (Figure 7.11). No change in cell viability is observed at 50nM.

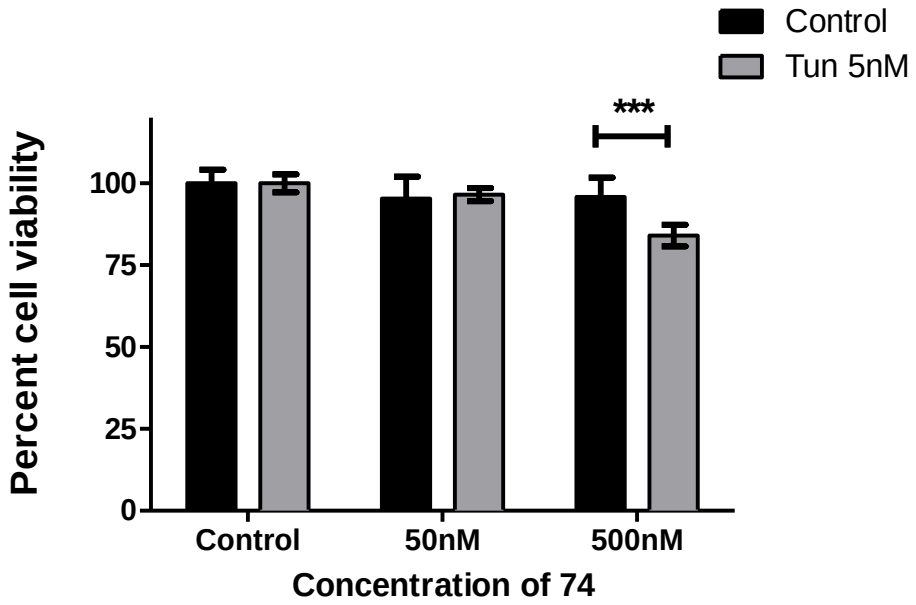

Figure 7.11-A549 cells pre-treated with 5nM Tunicamycin for 8hrs followed by treatment with CMPD 74 for a further 24hrs. Results are expressed as mean percent viability ±1 Standard deviation of two independent experiments (*** P<0.001). Tunicamycin at 5nM reduced A549 cell viability by 40%.

1,10-Phen experienced a similar significant inhibitory effect as CMPD 73 at both concentrations used (Figure 7.12).

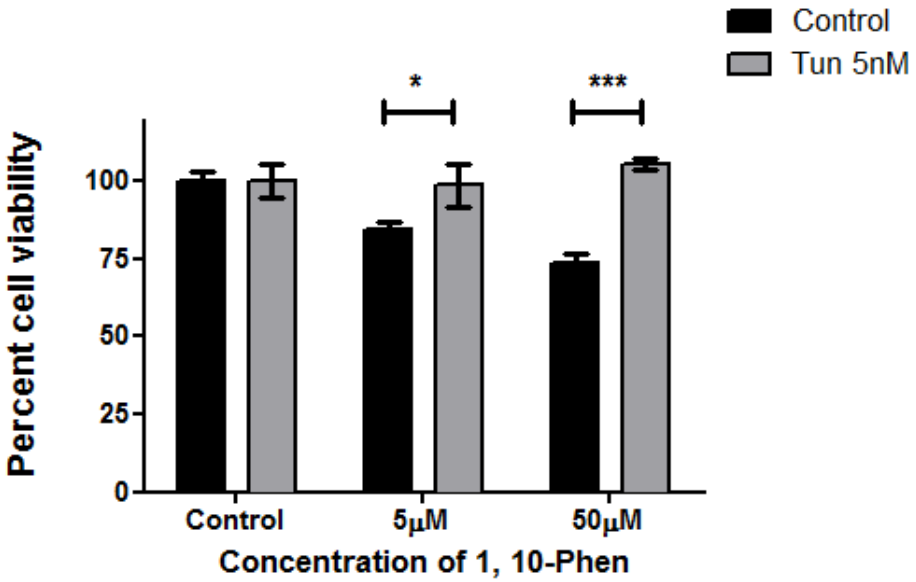

Figure 7.12- A549 cells pre-treated with 5nM Tunicamycin for 8hrs followed by treatment with 1,10-Phen for a further 24hrs. Results are expressed as mean percent viability ±1 Standard deviation of two independent experiments (*P<0.05, *** P<0.001). Tunicamycin at 5nM reduced A549 cell viability by 40%.

Parallel experiments using an 8-hour Tunicamycin pre-treatment and 24-hour exposure to the CMPD73 revealed a modest yet highly significant increase in cytotoxicity at the 500nM concentration in A2780 cells (Figure 7.13). No change in compound cytotoxicity can be seen at the 5µM concentration. This is in contrast to the results obtained using the A549 cell model. Tunicamycin at a concentration of 5nM reduced A2780 cell viability by 35%.

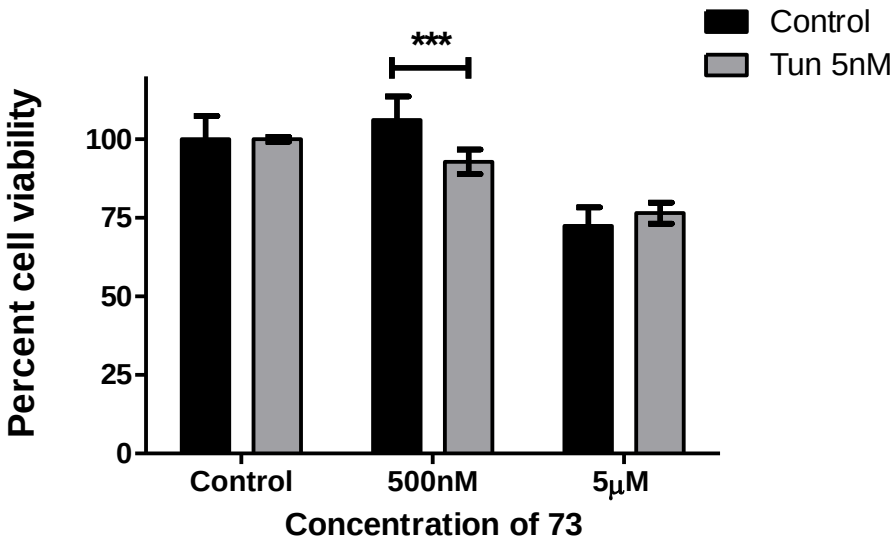

Figure 7.13-A2780 cells pre-treated with 5nM Tunicamycin for 8hrs followed by treatment with CMPD 73 for a further 24hrs. Results are expressed as mean percent viability ±1 Standard deviation of a single experiment. (*** P<0.001). Tunicamycin at a concentration of 5nM reduced A2780 cell viability by 35%.

Experiments using CMPD74 demonstrated a small but significant impact on cytotoxicity following treatment with 50nM of CMPD74 (Figure 7.14). The magnitude of this effect is similar to that of CMPD73. Unexpectedly, at higher concentrations of CMPD74 a significant decrease in cytotoxicity is observed in higher concentrations (500nM) of CMPD 74 in conjunction with Tunicamycin treatment.

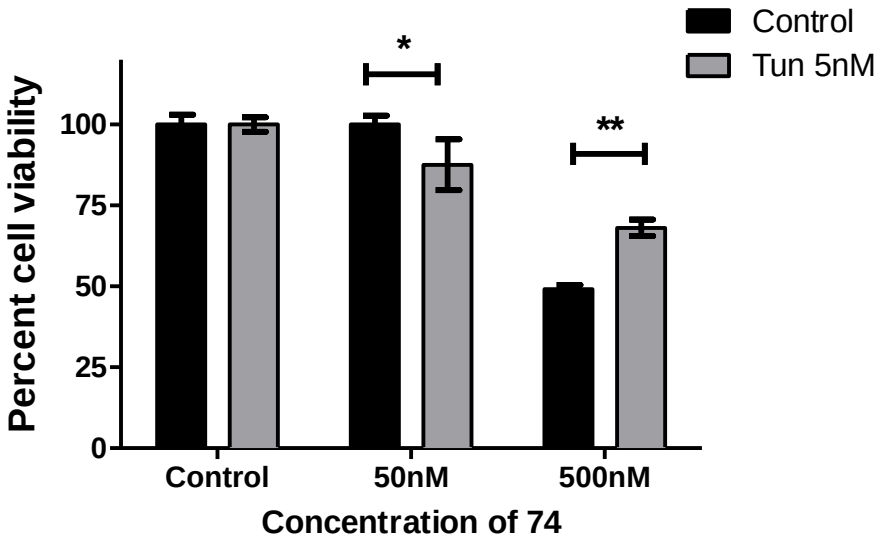

Figure 7.14-A2780 cells pre-treated with 5nM Tunicamycin for 8hrs followed by treatment with CMPD 74 for a further 24hrs. Results are expressed as mean percent viability ±1 Standard deviation of two independent experiments (*P<0.05, **P<0.01 compared to control). Tunicamycin at a concentration of 5nM reduced A2780 cell viability by 35%.

In similarity with the data described above, treatment with 1,10-Phen resulted in an increase in cytotoxicity at 50 µM concentrations (of 1,10-Phen) but not at 5µM (Figure 7.15).

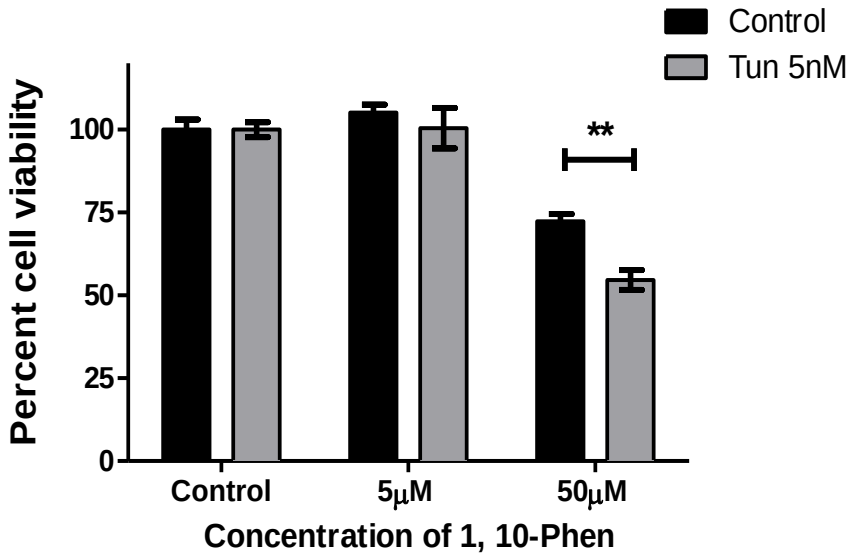

Figure 7.15-A2780 cells pre-treated with 5nM Tunicamycin for 8hrs followed by treatment with 1, 10-Phen for a further 24hrs. Results are expressed as mean percent viability ±1 Standard deviation of a single experiment (**P<0.01 compared to control). Tunicamycin at a concentration of 5nM reduced A2780 cell viability by 35%.

7.5.Discussion:

In a series of pilot experiments, the potential for metal-phen compounds to interact with the UPR pathway was assessed. The ability for metal-phen compounds to cause an increase in cell cytotoxicity in response to ER stress and UPR inducing drugs Anisomycin and Tunicamycin would implicate this stress response pathway as a target for metal-phen compounds. Overall these data indicate that CMPDs 73, 74 and 1,10-Phen interact with both UPR-inducing drugs to a modest degree and in a cell type-specific manner. While major changes in cytotoxicity were not seen, the modest yet significant enhancement of metal-phen compound efficacy suggests that the UPR may play a role in the mechanism of action of the metal-based compounds, although it may not be the primary mediator of cell death.

Moráň *et al.*, (2019) demonstrated that a mononuclear di-phenanthroline copper compound similar to CMPD 74 has reduced cytotoxic potential in the presence of an ER stress alleviating drug tauroursodeoxycholic acid (TUDCA). This data supports observations from this study that metal-phen compounds (particularly copper-phen) may be targeting the UPR in a significant manner and that biochemically targeting the UPR with ER-stress inducing or alleviating drugs is a valid experimental approach.

Both CMPD 73 and 1,10-Phen reacted with Anisomycin and Tunicamycin treatment in cell type-specific manners. In A549 cells the efficacy of 1,10-Phen is modestly yet significantly enhanced by Anisomycin with a similar trend observed in A2780 cells indicating that 1,10-Phen likely interacts with the UPR pathway albeit modestly. CMPD 73s interaction with the UPR inducing drugs is highly contextual in relation to the cell type analysed. CMPD 73 did not interact with Anisomycin in A549 cells yet experienced modest increases in cytotoxicity with a high degree of significance in A2780 cells following Anisomycin treatment.

Tunicamycin appeared to inhibit both CMPD 73 and 1,10-Phen activity in A549 cells while again modest yet highly significant increases in cytotoxicity were observed in A2780 cells. Collectively these data indicate that in similar fashion to 1,10-Phen, CMPD 73 does interact with the UPR pathway to a modest degree, however the somewhat contradictory results observed between A549 and A2780 cells regarding Tunicamycin pre-treatment is somewhat perplexing.

At the current state of knowledge, it is difficult to speculate about the mechanisms for this increase in viability. It may be a consequence of the experimental set-up with pre-treatment. One potential biological reason is that the treatment with a ribonuclease mimetic may reduce the flow of mRNA through the translational machinery, reducing the input of new proteins in the ER and thus limiting the scale of the UPR. An alternative approach is that the mechanism of action of CMPD73 is dependent on one or more glycoproteins, the concentration of which are reduced following Tunicamycin treatment in A549 cells but not A2780 cells. Glycans and glycoproteins are involved in the complex regulation of cell fate either promoting or inhibiting cell death in a context-dependent manner (reivewed by Lichtenstein and Rabinovich, 2013; Seyrek, Richter and Lavrik, 2019). As such alterations to glycosylation status of proteins involved in regulating cell death pathways by Tunicamycin could have unexpected effects regarding cytotoxic insult by metal-phen compounds. However the exact reasons for these effects are outside of the scope of the current work but is an avenue of investigation which should be followed in more detail.

CMPD 74 is seen to interact with Anisomycin and Tunicamycin in both cells lines and supports the notion that this compound interacts with the UPR stress pathway, possibly due to a combination of previously reported proteasome inhibition by copper-phen complexes (Zhang

et al., 2017) and (ribo) nuclease mimetic activity. Interestingly higher concentrations of CMPD 74 appeared to experience a cytoprotective effect similar to that of CMPD 73 following treatment with Tunicamycin. However, this inhibition is observed in A2780 cells regarding CMPD 74 yet CMPD 73 is inhibited only in A549 cells and is enhanced in A2780 cells following Tunicamycin treatment. Many of the reasons for these phenomena have already been speculated, and this specific instance of compound inhibition may be a combination of both cell type specific effects regarding not just Tunicamycin as previously thought but also cytotoxic mechanisms of the compounds in both cell lines.

To fully determine the extent the UPR plays in compound cytotoxicity the implementation of a multipronged approach would likely be required. Western blot analysis to detect translationally-activated XBP-1 protein would further validate the activation of the UPR pathway in response to treatment with metal-phen compounds. This would be further supported by the use of inhibitors targeting IRE1α and XBP-1 activity, which could determine whether their activity is detrimental to cell death signalling in response to treatment with metal-phen compounds.

Inhibitors of the autophagic process would also shed light on whether CMPD 73 shares similarities with CMPD 19, its analogous compound already shown to induce autophagic cell death (Slator *et al.*, 2017). Sequentially combining both UPR inhibitors with inhibitors of autophagy could also shed light on the degree of any potential crosstalk between the two pathways in relation to signalling cell death following treatment with CMPD 73. A change in cytotoxicity in response to one or both inhibitors would likely determine this. This could also apply in regard to CMPD 74 which has been demonstrated in Chapter 4 to be significantly

dependant of superoxide generation for cytotoxic effect, superoxide being the master regulator of autophagy.

Taken together these results, although preliminary, implicate the UPR pathway in mediating in part the effects of novel metal-based phen compounds albeit to a modest degree. Given the established ribonuclease mimetic activity, in particular that of CMPD74, the UPR remains a key avenue for investigation of the mechanistic aspects of these compounds.

8. Overall Discussion

Metal-based compounds remain a mainstay of many cancer therapies, even in an era of precision therapies (Ndagi, Mhlongo and Soliman, 2017). However, acquired resistance to such compounds and major toxicity issues have prompted the exploration of alternative metal-based compounds (*ibid*). 1,10-Phen has proved to be a versatile scaffold for the development of such compounds and a broad array of different compounds has been synthesised over the last few decades (Thederahn *et al.*, 1989; McCann *et al.*, 1997; Kellett *et al.*, 2011; Thornton *et al.*, 2016). The novel water-soluble 1,10-phenanthroline compounds incorporating trioxaundecanedioic acid and copper (CMPD74) or manganese (CMPD73) are the focus of this thesis (Figure 8.1).

The key findings of this thesis are that compound dissociation is likely prevalent among both compounds and contributes significantly towards the overall cytotoxicity of the compounds, with a more significant contribution of 1, 10-Phen mediated cytotoxicity also being highlighted. The identification of superoxide dependant cytotoxicity for both test compounds and 1, 10-Phen highlights both a more focused mechanisms of action and further supports 1, 10-Phens overall contribution towards compound cytotoxicity. Finally evidence of intracellular RNase activity highlights a novel mechanistic pathway for both compounds which can be further explored.

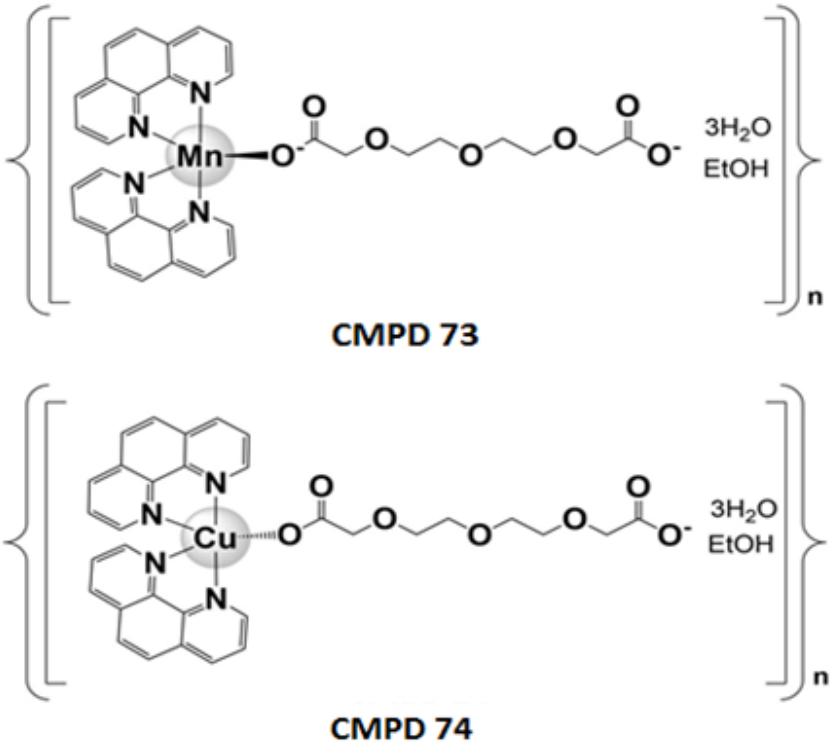

Figure 8.1- Chemical structures of CMPD 73 and 74

These novel compounds were synthesised as part of an existing programme of research to discover compounds with enhanced cytotoxic action. This thesis explored the efficacy and biological mechanisms of CMPD73 and CMPD74, gathering evidence that did not support initial hypotheses, identifying potential novel mechanisms of action and expanding our understanding of the biological effects of 1,10-Phen based compounds.

Experiments designed to evaluate the baseline cytotoxic action of these compounds uncovered evidence for compound dissociation and a resulting complex interplay of compound components (pages 77-78, 90). These data indicate that the effect observed *in cellulo* is likely to be due to the action of a few different compounds which together lead to the observed cytotoxic effect. Importantly, metal-free 1,10-phen generated a clear dose-dependent cytotoxic effect and indeed the presence of 1,10-phen was necessary and sufficient for activity (Figure

2.7and Figure 2.8 pages 74-76). This is consistent with the known capacity of 1,10-phen to chelate metal ions from aqueous environments which is well established as a key mechanism when used as a monotherapy (see McCann *et al.*, 2012 for a detailed review). Recent findings by Nunes *et al.*, (2020) further support this observation, where analogous copper-phen compound activity was determined to be a consequence of compound dissociation and formation of alternate metal-phen complexes were demonstrated to be an active part of the overall cytotoxic mechanism.

The mode of cell death was explored using tests for apoptosis, necrosis and, due to the metal-based nature of these compounds, the less well-studied ferroptosis. Data support apoptosis as a terminal mechanism for cell death and there was no indication that ferroptosis played any significant role in cell death (Chapter 5). In addition, a technical observation in relation to an LDH-based necrosis assay suggested that interaction with intermediate metabolism may potentially be involved in cell death, although it was outside the scope of the thesis work to explore this aspect.

These data thus support the view that dissociation of compounds leads to the generation of various bioactive entities, including 1,10-phen and diverse metal chelates of 1,10-phen with environmental metals. However, it should be noted that both CMPD73 and CMPD74 were more potent than the 1,10-phen, either alone or in combination with other compound components (Figure 2.7 and Figure 2.8). This activity was present in multiple cellular models, indicating a wide applicability. The observed effects are thus most likely an ‘ensemble effect’ of multiple chemical entities that may or may not have overlapping mechanisms of action. Despite these complexities, the efficacy of these compounds did not appear to be impaired in

cisplatin-resistant cell models. This is a significant advantage of these compounds, but additional studies (e.g. *in vivo*) would be required.

As the chemical nuclease activity of 1,10-phen-based compounds against DNA is well described (Kellett *et al.*, 2011; Molphy *et al.*, 2015), and also present in these novel compounds (Figure 6.6 page 213), an initial goal was to explore methods to enhance this activity (and hence cytotoxicity), mainly via supporting/promoting access of the compounds to the DNA substrate. The hypothesis was that if genomic DNA damage were the primary factor in cytotoxic action, then compounds that make DNA more accessible (e.g. HDACi) would enhance action of the compounds (Figure 8.2). Although the compounds demonstrated clear *in vitro* DNase mimetic activity, pre- and/or co-treatment with different chromatin modifying agents under different experimental conditions had minimal impact on observed cytotoxicity. This was in contrast to cisplatin, a known DNA damaging agent, where a significant increase of efficacy was noted, such that the resistant cells became sensitive to cisplatin (Table 3.6).

These data prompted the investigation of RNA as a substrate for the nuclease mimetic activity of the novel compounds. Surprisingly both CMPD73 and CMPD74 efficiently degraded RNA under *in vitro* conditions and, based on initial evidence presented in this thesis, in a cellular context. Gel-based degradation assays revealed that CMPD74 was capable of driving significant RNA degradation in as little as 20 minutes at 1μM concentration, making it significantly more active than CMPD73. Using a number of different RT-qPCR strategies, modest impact on RNA degradation *in cellulo* was evident. Previous studies, principally in yeast, have shown that 1,10-phen can cause transcriptional inhibition (Adams and Gross, 1991) at high concentrations (approximately 500 μM). However, the low concentrations used for cell experiments argues against this as a primary driver of our observations, although it is not

possible to rule out some contribution at the current state of knowledge. Although these experiments require further replication, taken together the available data from the 3':5' assay and differential amplicon size assay and the *in vitro* gel-based degradation assay indicate that RNA is a key substrate of nuclease-mimetic activity in the cell. In addition, a metal-dependent RNAse activity of 1,10-phen was also observed under *in vitro* conditions, although requiring higher concentrations than CMPD73 or CMPD74 but observably more rapid than CMPD 73. Notably, and in support of the idea that 1,10-phen's activity is dependent on the presence of metal ions, addition of EDTA efficiently abrogated the RNAse activity of 1,10-phen alone (Figure 6.10).

Numerous metal-based compounds can generate reactive oxygen species (ROS), including analogues of the novel compounds under investigation in this thesis. The generation of intracellular ROS and their role in the mechanism of action of the novel compounds was investigated using flow cytometry and plate-based assays. Each assay revealed an increase in total cellular ROS following treatment with CMPD73, CMPD74 and also with 1,10-phen. An inhibitor profiling approach, evaluating the impact of a panel of selective inhibitors/blockers of different ROS on cytotoxicity, revealed that superoxide was a key mediator of cell death, although some differences were observed between the compounds (Figure 4.23-Figure 4.25 pages 152-154).

This observation argues against significant intracellular superoxide dismutase mimetic-activity by CMPD73 or CMPD74, as this activity would degrade superoxide and form hydrogen peroxide. As there was a limited impact of sodium pyruvate, a well-established scavenger of hydrogen peroxide and 3-amino-1,2,4-triazol, an inhibitor of catalase, it is evident that any such intracellular activity is relatively minor. Parallel ROS scavenger studies of RNAse

mimetic activity again revealed the importance of ROS for the RNA degradation activity of the compounds. Scavengers of hydrogen peroxide and superoxide blocked RNAse mimetic-activity of both CMPD73 and CMPD74, while scavengers of the hydroxyl radical had a greater impact on the activity of CMPD74 compared to CMPD73. These data are consistent with that from Kellett *et al.* (2011) who studied the DNAse activity of analogous compounds lacking the ethereal groups.

Intriguingly, 1,10-phen was also demonstrated to possess RNAse mimetic activity under *in vitro* conditions. This activity was abolished by EDTA co-treatment indicating that the activity was dependent on the chelation of trace metal ions present in the reaction solutions. In addition, activity was also lost when ascorbate was not used in the experiments. Inhibitor profiling revealed a profile almost identical to that of CMPD73, although some minor differences were evident. These data again support the partial dissociation of the compound and the formation of novel metal-phenanthroline compounds in solution. While somewhat speculative at the current state of knowledge, the rate of action of 1,10-phen compared to that of CMPD73 (Figure 6.6 and Figure 6.10) suggests that a slow or partial dissociation of CMPD73 is followed by release of 1,10-phen and formation of new chelates which contributes to the observable RNAse activity. In contrast, the very rapid action of CMPD74 is consistent with direct activity as an intact molecular entity. This is in line with initial observations of kinetic replacement reactions of transition metals with 1,10-Phen. Hoyler and collaborators (1965) demonstrated that Cu-phen complexes possess relatively high formation rate constants, higher than that of Mn-phen complexes. Cu (II) was also demonstrated to be a suitable decomposing ion for Mn-Phen complexes further supporting the notion that Mn-phen complexes require dissociation to become active (Holyer *et al.*, 1965).

The lack of significant effect of chromatin modifying agents, despite demonstrable DNAse activity, requires exploration of other targets and mechanisms of action e.g. RNA driven. Importantly, the rank order of RNAse activity is consistent with the cytotoxic action – CMPD74 is more potent, by both of these measures, than CMPD73. Cytosolic RNA oxidation is thus a novel and viable mechanism which may represent one of the initiating factors in cell death, e.g. via promotion of ER stress and its sequelae, including autophagy which ER stress and oxidative stress are known to promote (Yan et al., 2015).

We carried out initial experiments to test this hypothesis by combining compound treatment with two known inducers of ER stress. There was a modest but significant impact on cell death with both CMPD73 and CMPD74, although the effects were cell-dependent. 1,10-phen dependent cell death was also impacted in these experiments, again indicating a potential role of free 1,10-phen in the effects of the compounds. It was not possible to carry out the reverse experiment, i.e. to test the effects of a known ER stress rescuer, tauroursodeoxycholic acid, on the efficacy of the novel compounds. Recent data from Moráň and collaborators (2019), however, demonstrated that tauroursodeoxycholic acid significantly reduced the cytotoxicity of a mononuclear, di-phenanthroline copper compound (similar to CMPD 74) (Moráň et al., 2019). It will be critical to evaluate the impact of tauroursodeoxycholic acid on the efficacy of CMPD73, CMPD74 and indeed 1,10-phen.

The action of the site-1 protease (S1P), an ER resident metalloprotease, is critical for the release of the membrane bound activating transcription factor 6 (ATF6), a key transducer of the unfolded protein response which regulates ER protein folding (Lebeau *et al.*, 2018). As 1,10-phen is a known metalloprotease inhibitor, inhibition of its activity by secondary to the intracellular dissociation of compounds may lead to additional indirect effects. Analogous

compounds have been shown to interact with downstream protein removal mechanisms, i.e. the proteasome (Zhang et al., 2013) and autophagy (Slator et al., 2017; Song et al., 2017). It is noteworthy that the proteasome regulatory particle lid subunit RPN11 is itself a metalloprotease and has been reported to be inhibited by 1,10-phen by several authors (Song *et al.*, 2016, 2017). These data again highlight the importance of (partial or full) dissociation of the compounds and generation of 1,10-phen within the cell. Indeed, in a recent thesis on the generation of metal-folate-phenanthroline complexes, evidence was presented that copper(II) phenanthroline, derived from the parent complex during cell treatment, was a specific proteasomal inhibitor (Crowley, 2019).

Taken together these data provide insight into the mechanism of action of these novel compounds, which add to the growing body of evidence that the overall effect of these compounds is a combination of a number of diverse effects (summarised in Figure 8.2). These results provide data for a plausible mechanistic model that unifies our observations, and those of others, and explains the mode of action of these compounds that is initiated by early RNA damage, triggering ER stress and ultimately apoptosis. In addition, the data provided here supports 'ensemble' modes of action with potentially diverse 1,10-phen based compounds influencing their targets with different efficacies, but which together give rise to the observed holistic cytotoxic effect. This may be advantageous in the context of therapeutic development as it may reduce the potential development of resistance and provide a rationale for future drug design. These data provide insights into the general mechanisms of 1,10-phen based compounds, opening up new avenues of research and potentially accelerating the translation of novel metal-based compounds to the clinic.

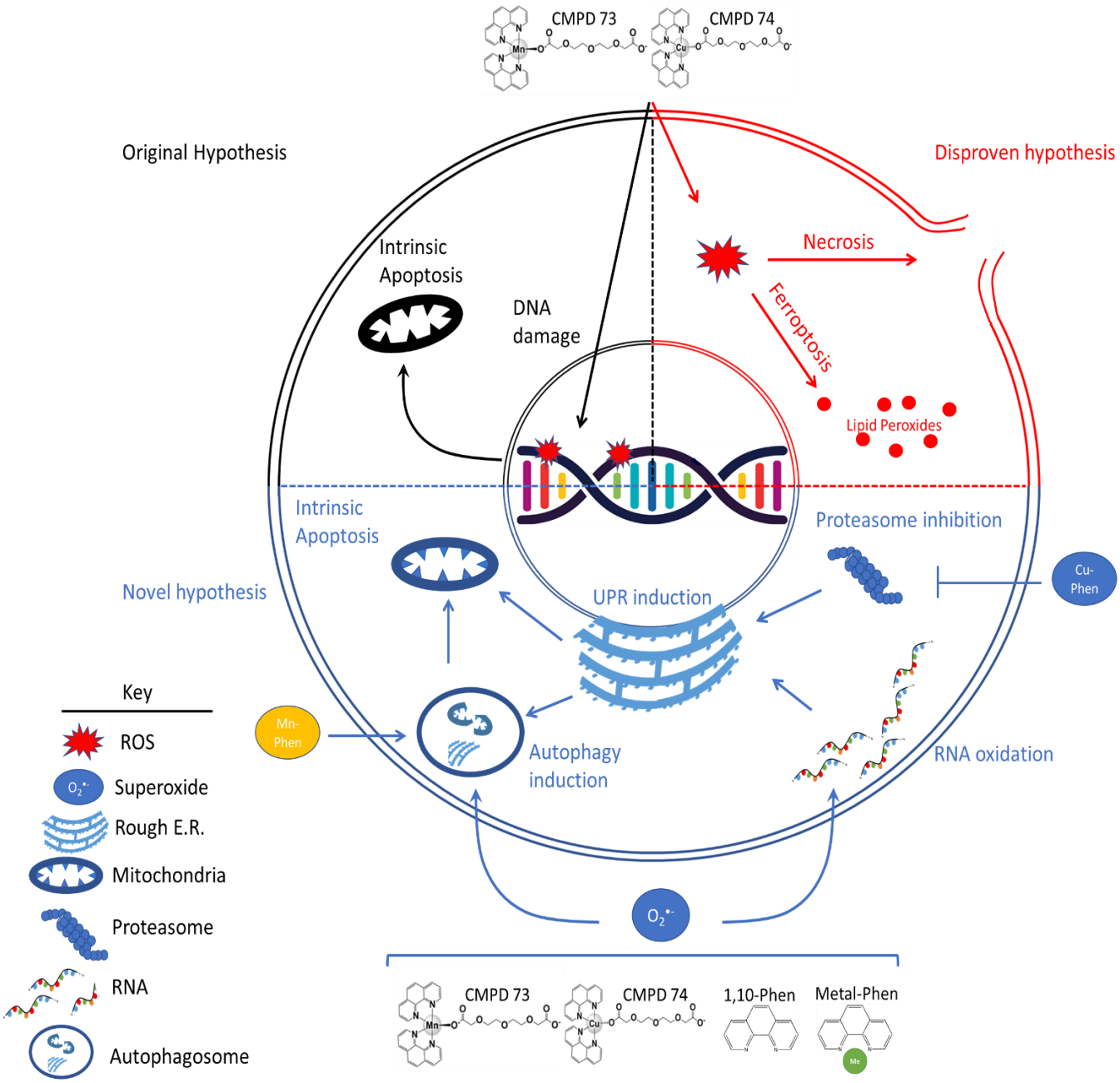

Figure 8.2- Model of forms of cell death associated with metal-phen compounds. Original cell death pathway (black section): CMPDs 73 and 74 were originally hypothesised to target genomic DNA initiating oxidative damage resulting in intrinsic apoptosis. Disproven cell death pathway (red section): CMPD 73 and 74 were investigated and shown not to interact with necrotic or ferroptotic pathways. Novel cell death pathway(s) (blue): both metal-phen compounds, 1,10-Phen and potential "alternate"-phen compounds hypothesised to target RNA and autophagy induction simultaneously using superoxide. RNA oxidation results in UPR induction which further stimulates autophagy and can include intrinsic apoptosis. Cu-Phen compound-mediated inhibition of the proteasome further increases UPR activation alongside Mn-Phen induction of autophagy further amplifying UPR-Autophagy apoptotic signalling.

9. Future perspectives

This study has explored a variety of different mechanisms through which the selected water-soluble metal-phen compounds are believed to exert their anti-cancer cytotoxicity while also highlighting novel mechanisms which require further examination.

To expand the current knowledge highlighted in this thesis elucidating the specific cellular targets of these compounds would further aid their potential clinical development. A comprehensive mapping using organelle specific, superoxide sensitive fluorescent probes, both chemical and genetically encoded sensors, would determine where in the cell the superoxide generated by these compounds taking greatest effect. Probing organelles such as the mitochondria (MitoSox-Red), the ER (ER-NACP, Xiao 2018) or the lysosome (HKSOX-2L, Lu, Jiao and Yang, 2016) would therefore be of critical importance to define a more focused model. A multi-pronged microscopy-based approach implementing multiple fluorophores simultaneously, and coupled with time-resolved mapping, would be an important tool to highlight both the sequence, site and molecular targets of ROS-mediated cytotoxic events.

The ability to circumvent chemotherapy resistance, in this case towards cisplatin, is demonstrated as a significant event regarding future compound development and indicates alternative mechanisms of action to that of cisplatin. However fully investigating these mechanisms is beyond the scope of this current investigation. Further expanding how these compounds escape resistant mechanisms would likely prove to be a fruitful avenue of investigation. Comparing gene/protein expression profiles of e.g. sensitive versus resistant cell lines would support understanding of the mechanism(s) of action and prompt other confirmatory experiments. However, as highlighted throughout this study some caution must be taken with regards to RNA-based gene expression analysis. Owing to the technical issues

described transcriptomic analysis would likely not be suitable with protein-based methods more appropriate. Candidates identified in this way could be confirmed via gain and loss of function studies using gene knockdowns and thus potentially identifying routes for synergistic treatment.

The implication of the ER stress response as a novel pathway involved in the activity of these compounds was an intriguing finding which opens up a completely new line of enquiry. Initial studies would evaluate the changes in UPR specific targets (such as activated XBP-1), ER stress reporter assays and gene knockdown studies using siRNA. Analogous approaches could be applied to autophagy and the proteasome to elucidate potential crosstalk between these pathways.

As the potential for mixed populations of metal-phen compounds following compound dissociation is highlighted in this study further investigation into the characterisation of these compounds will be essential. This will be challenging but it is an essential step in definitively proving the hypothesis of multiple compounds.

ICP-MS would be an essential tool for the investigation of these complexes. Studies conducted in parallel using sub-cellular fractionation coupled with mass spectrometry could further identify either intact, disassociated or alternate metal-phen complexes. An alternative approach would be to use direct imaging mass-spectrometry, which would provide information on both the localisation and identity of compounds. Use of isotope-labelled compounds (including individual components) would enable tracking of breakdown of the parent compound and formation of new compounds.

To further expand this line of inquiry the chelative effects that mixed populations of free 1,10-Phen or 1,10-Phen alone have on intracellular calcium concentrations could be investigated. Calcium is a key regulatory signal involved in multiple cell pathways such as ER homeostasis and apoptotic signalling in the mitochondria (reviewed Chernorudskiy and Zito, 2017). Calcium-based fluorescent probes capable of tracking calcium flux throughout the cell, particularly between the ER and mitochondria (a critical apoptotic event), may also be useful for determining intracellular signals contributing towards cell death.

To fully determine the degree to which the selected metal-phen complexes target genomic DNA if at all, assays detecting DNA damage such as the γH2AX or COMET assay would need to be implemented. However it must be ensured that direct DNA damage by the metal-phen compounds is detected as opposed to indirect DNA damage resulting from oxidative stress or induction of apoptosis. Time course analysis investigating the induction of DNA damage in the presence of apoptotic inhibitors would likely serve to determine direct vs indirect DNA damage, although interpretation of these effects is likely to be complex. Gene knockdown studies targeting DNA damage response pathways or experiments performed in cells deficient in damage repair genes (e.g. NER, SSBR and DSBR pathways) would also serve to determine how significant DNA as a target is for compound efficacy.

The ribonuclease activity of metal-phen and 1,10-Phen compounds is both a novel and lucrative target for these compounds. As such further expanding the research into cytosolic RNA as the primary target of compound ribonuclease mimetic activity would further support this observation. While qPCR analysis conducted in this study is suggestive of RNA degradation it is limited in that it lacks direct confirmation of damaged RNA. Directly detecting oxidised and

damaged bases would definitively determine RNA oxidation as a key mechanistic process of these compounds.

To investigate this an ELISA assay probing for 8-hydroxyguanosine (8-OHG), the oxidised form of guanosine in RNA would be useful to determine whether oxidation of cytosolic RNA is occurring in response to treatment with test compounds. To coincide with this further research into the effects of metal-phen compounds on have on reporter mRNA integrity required for qPCR analysis could shed further light on the reliability of using this assay to determine gene expression analysis in response to metal-phen compounds. Screening a larger sample of genes (e.g. via an array or NGS approach) would indicate whether qPCR analysis is applicable to studies involving metal-phen compounds and is a necessary first step to identify if there are any suitable endogenous control genes.

Furthermore the extent through which ribonuclease mimetic activity could impact on the vast number of other species of RNA is yet unknown. Owing to their short strand length and highly regulatory nature microRNAs (miRNAs) would be extremely sensitive to degradation by metal-phen compounds and degradation could have serious downstream effects regarding cell signalling and viability. As miRNAs have been seen to be dysregulated in a variety of cancers (Peng and Croce, 2016) investigating their role as a potential target may prove lucrative. However certain limitations may arise until qPCR techniques are validated for use with metal-phen complexes and as such ELISA based approaches similar to assays probing for 8-hydroxyguanosine (8-OHG) but specific for miRNAs would likely be required.

The future perspectives described herein will be fruitful avenues of investigation for years to come and likely contribute significantly to the development and understanding of metal-phen complexes as potential anti-cancer agents.

10. Appendix

Characterisation of CMPD 73:

{[Mn(3,6,9-tdda)(phen)2]3H2O.EtOH}n

Molecular Mass: 735.65 g/mol

Microanalysis (CHN):

% Calculated: C, 55.5; H, 5.5; N, 7.6

%Found: C, 52.7; H, 5.2; N, 7.4

Magnetic moment μ_{eff} = 6.0 B.M.

Infrared spectrum main peaks:

IR(KBr) Vmax: 3410, 2915, 1625, 1585, 1515, 1425, 1325, 1120, 1075, 845, 730, 635 cm^{-1}

Solubility: The complex was soluble in water, ethanol and methanol, and insoluble in ethyl acetate and acetone.

Characterisation of CMPD 74:

{[Cu(3,6,9-tdda)(phen)2].3H2O.EtOH}n

Molecular Mass: 744.26 g/mol

Microanalysis (CHN):

% Calculated: C: 54.87, H: 5.42, N: 7.53.

% Found: C: 54.65, H:5.63, N: 7.39

Magnetic moment μ_{eff} = 1.92 B.M.

Infrared spectrum main peaks:

IR (KBr) Vmax: 3982, 3415, 3041, 2901, 1989, 1752,

1618, 1587, 1513, 1421, 1320, 1252, 1221, 1121, 1090, 1077, 1011,

934, 893, 847, 770, 720, 704, 643, 619, 603, 573, 555, 507, 426 cm−1

Solubility: The complex was soluble in water, ethanol and methanol, and insoluble in ethyl acetate and acetone.

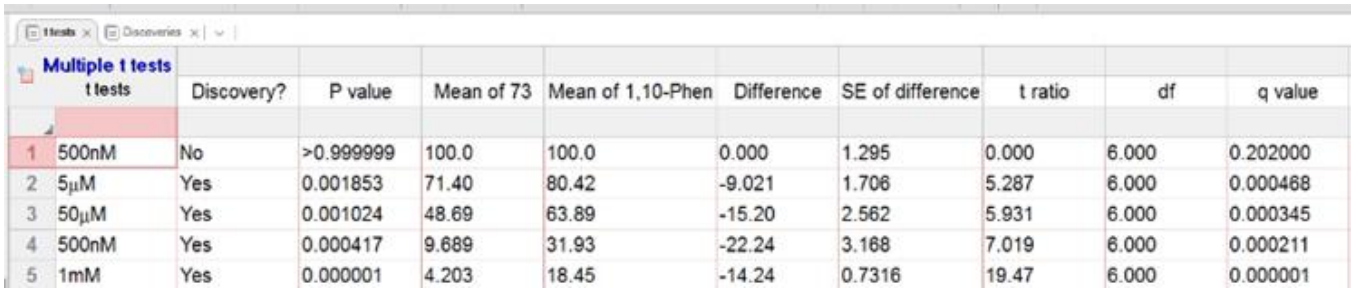

Multiple t tests — t tests

		Discovery?	P value	Mean of 73	Mean of 1,10-Phen	Difference	SE of difference	t ratio	df	q value
1	500nM	No	>0.999999	100.0	100.0	0.000	1.295	0.000	6.000	0.202000
2	5μM	Yes	0.001853	71.40	80.42	-9.021	1.706	5.287	6.000	0.000468
3	50μM	Yes	0.001024	48.69	63.89	-15.20	2.562	5.931	6.000	0.000345
4	500nM	Yes	0.000417	9.689	31.93	-22.24	3.168	7.019	6.000	0.000211
5	1mM	Yes	0.000001	4.203	18.45	-14.24	0.7316	19.47	6.000	0.000001

Figure 10.1- An example image of Multiple T-Test analysis from GraphPad Prism 8 testing statistical significance of each concentration of the intact CMPD 73 vs 1,10-Phen at the same concentration to generate a P value. Each combination of CMPD 73 component compounds were then analysed in identical fashion to 1,10-Phen to determine individual P values for each concentration tested compared to CMPD 73.

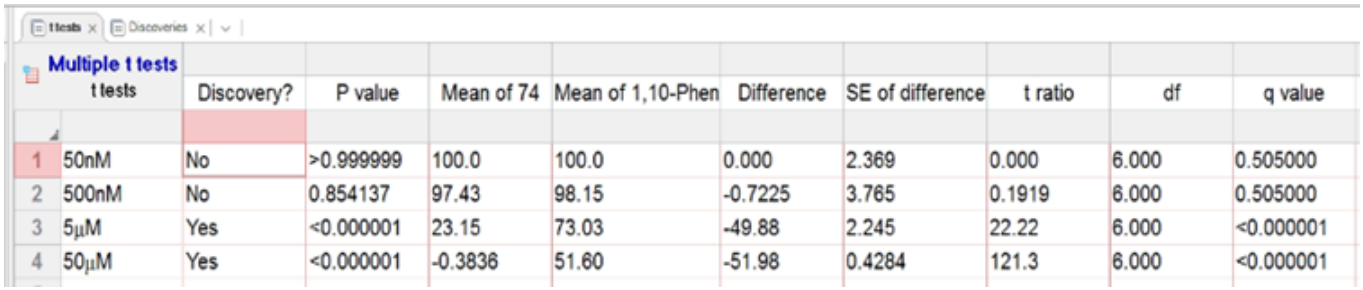

Multiple t tests — t tests

		Discovery?	P value	Mean of 74	Mean of 1,10-Phen	Difference	SE of difference	t ratio	df	q value
1	50nM	No	>0.999999	100.0	100.0	0.000	2.369	0.000	6.000	0.505000
2	500nM	No	0.854137	97.43	98.15	-0.7225	3.765	0.1919	6.000	0.505000
3	5μM	Yes	<0.000001	23.15	73.03	-49.88	2.245	22.22	6.000	<0.000001
4	50μM	Yes	<0.000001	-0.3836	51.60	-51.98	0.4284	121.3	6.000	<0.000001

Figure 10.2- An example image of Multiple T-Test analysis from GraphPad Prism 8 testing statistical significance of each concentration of the intact CMPD 7 vs 1,10-Phen at the same concentration to generate a P value. Each combination of CMPD 74 component compounds were then analysed in identical fashion to 1,10-Phen to determine individual P values for each concentration tested compared to CMPD 74.

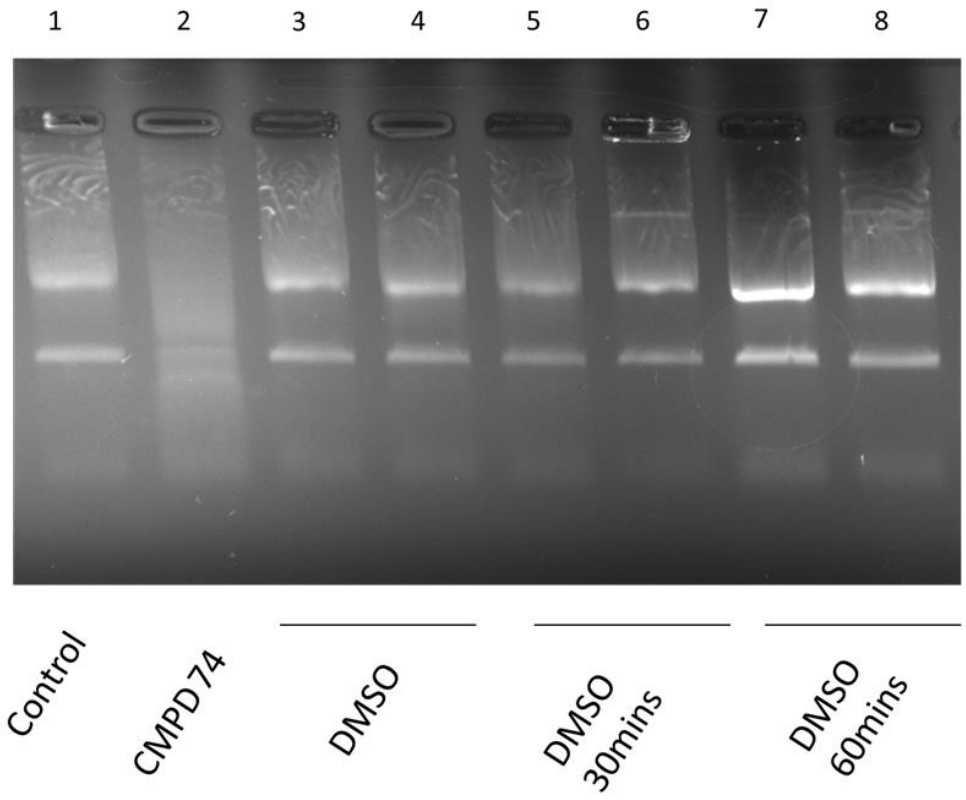

Figure 10.3- Isolated RNA exposed to CMPD 74 and DMSO at various pre-incubation times (Lanes 3-4 0min, lanes 5-6 30mins, lanes 7-8 60mins) in presence of ascorbate. Inhibition of CMPD 74 degradation of RNA is seen to be inhibited with greater efficacy following pre-treatment with DMSO.

11. References

Abbotts, R. and Wilson, D. M. (2017) 'Coordination of DNA single strand break repair', *Free Radical Biology and Medicine*, 107, pp. 228–244. doi: 10.1016/j.freeradbiomed.2016.11.039.

Abebe, A. *et al.* (2018) 'Synthesis of organic salts from 1,10-phenanthroline for biological applications', *Cogent Chemistry*, 4(1), pp. 1–10. doi: 10.1080/23312009.2018.1476077.

Accorsi, G. *et al.* (2009) '1,10-Phenanthrolines: versatile building blocks for luminescent molecules, materials and metal complexes', *Chemical Society Reviews*, 38(6), p. 1690. doi: 10.1039/b806408n.

Adams, C. C. and Gross, D. S. (1991) 'The yeast heat shock response is induced by conversion of cells to spheroplasts and by potent transcriptional inhibitors.', *Journal of Bacteriology*, 173(23), pp. 7429–7435. doi: 10.1128/JB.173.23.7429-7435.1991.

Adams, C. J. *et al.* (2019) 'Structure and Molecular Mechanism of ER Stress Signaling by the Unfolded Protein Response Signal Activator IRE1', *Frontiers in Molecular Biosciences*, 6(MAR), p. 11. doi: 10.3389/fmolb.2019.00011.

Adams, L., Franco, M. C. and Estevez, A. G. (2015) 'Reactive nitrogen species in cellular signaling', *Experimental Biology and Medicine*, 240(6), pp. 711–717. doi: 10.1177/1535370215581314.

Afaghi, A. *et al.* (2015) 'Study on genotoxicity, oxidative stress biomarkers and clinical symptoms in workers of an asbestoscement factory', *EXCLI Journal*, 14, pp. 1067–1077. doi: 10.17179/excli2015-469.

Afanas'ev, I. (2011) 'Reactive oxygen species signaling in cancer: Comparison with aging', *Aging and Disease*, 2(3), pp. 219–230.

Afanas'ev, I. (2015) 'Mechanisms of superoxide signaling in epigenetic processes: Relation to aging and cancer', *Aging and Disease*, 6(3), pp. 216–227. doi: 10.14336/AD.2014.0924.

Afghahi, A. *et al.* (2017) 'Tumor BRCA1 reversion mutation arising during neoadjuvant platinum-based chemotherapy in triple-negative breast cancer is associated with therapy resistance', *Clinical Cancer Research*, 23(13), pp. 3365–3370. doi: 10.1158/1078-0432.CCR-16-2174.

Agnez-Lima, L. F. *et al.* (2012) 'DNA damage by singlet oxygen and cellular protective mechanisms', *Mutation Research - Reviews in Mutation Research*, 751(1), pp. 15–28. doi: 10.1016/j.mrrev.2011.12.005.

Aguirre, J. D. and Culotta, V. C. (2012) 'Battles with iron: Manganese in oxidative stress protection', *Journal of Biological Chemistry*, 287(17), pp. 13541–13548. doi: 10.1074/jbc.R111.312181.

Aits, S. and Jäättelä, M. (2013) 'Lysosomal cell death at a glance', *Journal of Cell Science*, 126(9), pp. 1905–1912. doi: 10.1242/jcs.091181.

Al-Lazikani, B., Banerji, U. and Workman, P. (2012) 'Combinatorial drug therapy for cancer in the post-genomic era', *Nature Biotechnology*. Nature Publishing Group, pp. 679–692. doi: 10.1038/nbt.2284.

Alano, C. C. *et al.* (2010) 'NAD+ depletion is necessary and sufficient for poly(ADP-ribose) polymerase-1-mediated neuronal death', *Journal of Neuroscience*, 30(8), pp. 2967–2978. doi: 10.1523/JNEUROSCI.5552-09.2010.

Alavanja, M. C. R. and Bonner, M. R. (2012) 'Occupational pesticide exposures and cancer risk: A review', *Journal of Toxicology and Environmental Health - Part B: Critical Reviews*, pp. 238–263. doi: 10.1080/10937404.2012.632358.

Albert, B. *et al.* (2019) 'A ribosome assembly stress response regulates transcription to maintain proteome homeostasis', *eLife*, 8, pp. 1–24. doi: 10.7554/eLife.45002.

Allfrey, V. G., Faulkner, R. and Mirsky, A. E. (1964) 'Acetylation and Methylation of Histones and Their Possible Role in the Regulation of Rna Synthesis.', *Proceedings of the National*

Academy of Sciences of the United States of America, 51(1938), pp. 786–94. doi: 10.1073/pnas.51.5.786.

Allocati, N. *et al.* (2018) 'Glutathione transferases: Substrates, inihibitors and pro-drugs in cancer and neurodegenerative diseases', *Oncogenesis*, 7(1). doi: 10.1038/s41389-017-0025-3.

Alsøe, L. *et al.* (2017) 'Uracil Accumulation and Mutagenesis Dominated by Cytosine Deamination in CpG Dinucleotides in Mice Lacking UNG and SMUG', *Scientific Reports*, 7(1), pp. 1–14. doi: 10.1038/s41598-017-07314-5.

Altaf, M. *et al.* (2019) 'Potent in vitro and in vivo anticancer activity of new bipyridine and bipyrimidine gold (III) dithiocarbamate derivatives', *Cancers*, 11(4), pp. 1–14. doi: 10.3390/cancers11040474.

Altman, S. A. *et al.* (1995) 'Formation of DNA-protein cross-links in cultured mammalian cells upon treatment with iron ions', *Free Radical Biology and Medicine*, 19(6), pp. 897–902. doi: 10.1016/0891-5849(95)00095-F.

Amanso, A. M., Debbas, V. and Laurindo, F. R. M. (2011) 'Proteasome inhibition represses unfolded protein response and Nox4, sensitizing vascular cells to endoplasmic reticulum stress-induced death', *PLoS ONE*, 6(1), pp. 1–11. doi: 10.1371/journal.pone.0014591.

Anbu, S. *et al.* (2013) 'Effect of 1,10-phenanthroline on DNA binding, DNA cleavage, cytotoxic and lactate dehydrogenase inhibition properties of Robson type macrocyclic dicopper(II) complex', *Journal of Coordination Chemistry*, 66(1), p. 22. doi: 10.1080/00958972.2013.858136.

Andreini, C. *et al.* (2018) 'The human iron-proteome', *Metallomics*, 10(9), pp. 1223–1231. doi: 10.1039/c8mt00146d.

Arnold, R. S. *et al.* (2001) 'Hydrogen peroxide mediates the cell growth and transformation caused by the mitogenic oxidase Nox1', *Proceedings of the National Academy of Sciences of the United States of America*, 98(10), pp. 5550–5555. doi: 10.1073/pnas.101505898.

Ashworth, A. (2008) ‘Drug resistance caused by reversion mutation’, *Cancer Research*. American Association for Cancer Research, pp. 10021–10023. doi: 10.1158/0008-5472.CAN-08-2287.

Asmus, C., Mozziconacci, O. and Schöneich, C. (2015) ‘Low-Temperature NMR Characterization of Reaction of Sodium Pyruvate with Hydrogen Peroxide’, *The Journal of Physical Chemistry A*, 119(6), pp. 966–977. doi: 10.1021/jp511831b.

Assem, F. L., Holmes, P. and Levy, L. S. (2011) ‘The Mutagenicity and Carcinogenicity of Inorganic Manganese Compounds: A Synthesis of The Evidence’, *Journal of Toxicology and Environmental Health, Part B*, 14(8), pp. 537–570. doi: 10.1080/10937404.2011.615111.

Aubrey, B. J. *et al.* (2018) ‘How does p53 induce apoptosis and how does this relate to p53-mediated tumour suppression?’, *Cell Death & Differentiation*, 25(1), pp. 104–113. doi: 10.1038/cdd.2017.169.

Aubry, J.-M. *et al.* (2003) ‘Reversible Binding of Oxygen to Aromatic Compounds’, *Accounts of Chemical Research*, 36(9), pp. 668–675. doi: 10.1021/ar010086g.

Aunan, J. R., Cho, W. C. and Søreide, K. (2017) ‘The biology of aging and cancer: A brief overview of shared and divergent molecular hallmarks’, *Aging and Disease*. International Society on Aging and Disease, pp. 628–642. doi: 10.14336/AD.2017.0103.

Ayala, A., Muñoz, M. F. and Argüelles, S. (2014) ‘Lipid Peroxidation: Production, Metabolism, and Signaling Mechanisms of Malondialdehyde and 4-Hydroxy-2-Nonenal’, *Oxidative Medicine and Cellular Longevity*, 2014, pp. 1–31. doi: 10.1155/2014/360438.

Ayob, A. Z. and Ramasamy, T. S. (2018) ‘Cancer stem cells as key drivers of tumour progression’, *Journal of Biomedical Science*. BioMed Central Ltd., pp. 1–18. doi: 10.1186/s12929-018-0426-4.

Azadmanesh, J. and Borgstahl, G. (2018) ‘A Review of the Catalytic Mechanism of Human Manganese Superoxide Dismutase’, *Antioxidants*, 7(2), p. 25. doi: 10.3390/antiox7020025.

Azzi, S., Hebda, J. K. and Gavard, J. (2013) 'Vascular Permeability and Drug Delivery in Cancers', *Frontiers in Oncology*, 3. doi: 10.3389/fonc.2013.00211.

Baier, J. *et al.* (2007) 'Direct detection of singlet oxygen generated by UVA irradiation in human cells and skin', *Journal of Investigative Dermatology*, 127(6), pp. 1498–1506. doi: 10.1038/sj.jid.5700741.

Baines, C. P. (2010) 'Role of the mitochondrion in programmed necrosis', *Frontiers in Physiology*, 1 NOV(November), pp. 1–8. doi: 10.3389/fphys.2010.00156.

Balasubramanian, B., Pogozelski, W. K. and Tullius, T. D. (1998) 'DNA strand breaking by the hydroxyl radical is governed by the accessible surface areas of the hydrogen atoms of the DNA backbone', *Proceedings of the National Academy of Sciences of the United States of America*, 95(17), pp. 9738–9743. doi: 10.1073/pnas.95.17.9738.

Balkwill, F. R., Capasso, M. and Hagemann, T. (2012) 'The tumor microenvironment at a glance', *Journal of Cell Science*, 125(23), pp. 5591–5596. doi: 10.1242/jcs.116392.

Balvan, J. *et al.* (2015) 'Multimodal holographic microscopy: Distinction between apoptosis and oncosis', *PLoS ONE*, 10(3). doi: 10.1371/journal.pone.0121674.

Bancirova, M. (2011) 'Sodium azide as a specific quencher of singlet oxygen during chemiluminescent detection by luminol and Cypridina luciferin analogues', *Luminescence*, 26(6), pp. 685–688. doi: 10.1002/bio.1296.

Bansal, A. and Celeste Simon, M. (2018) 'Glutathione metabolism in cancer progression and treatment resistance', *Journal of Cell Biology*, 217(7), pp. 2291–2298. doi: 10.1083/jcb.201804161.

Barradas, M. *et al.* (2009) 'Histone demethylase JMJD3 contributes to epigenetic control of INK4a / ARF by oncogenic RAS', *Genes & Development*, pp. 1177–1182. doi: 10.1101/gad.511109.GENES.

Barrera, G. (2012) 'Oxidative stress and lipid peroxidation products in cancer progression and

therapy.', *ISRN oncology*, 2012, p. 137289. doi: 10.5402/2012/137289.

Bartos, Á., Hudecz, F. and Uray, K. (2009) 'A new water soluble 3,6,9-trioxaundecanedioic acid-based linker and biotinylating reagent', *Tetrahedron Letters*, 50, pp. 2661–2663. doi: 10.1016/j.tetlet.2009.03.112.

Basria S.M.N. Mydin, R. and Okekpa, S. I. (2019) 'Reactive Oxygen Species, Cellular Redox Homeostasis and Cancer', in *Homeostasis - An Integrated Vision*. IntechOpen. doi: 10.5772/intechopen.76096.

Baxevanis, C. N., Perez, S. A. and Papamichail, M. (2009) 'Combinatorial treatments including vaccines, chemotherapy and monoclonal antibodies for cancer therapy', *Cancer Immunology, Immunotherapy*. Springer, pp. 317–324. doi: 10.1007/s00262-008-0576-4.

Bayliak, M. *et al.* (2008) 'Inhibition of catalase by aminotriazole in vivo results in reduction of glucose-6-phosphate dehydrogenase activity in Saccharomyces cerevisiae cells', *Biochemistry (Moscow)*, 73(4), pp. 420–426. doi: 10.1134/S0006297908040068.

Bedford, D. C. and Brindle, P. K. (2012) 'Is histone acetylation the most important physiological function for CBP and p300?', *Aging*, 4(4), pp. 247–255. doi: 100453 [pii].

Bedford, M. R. *et al.* (2013) 'Iron Chelation in the Treatment of Cancer: A New Role for Deferasirox?', *The Journal of Clinical Pharmacology*, 53(9), pp. 885–891. doi: 10.1002/jcph.113.

Belli, C. *et al.* (2018) 'Targeting the microenvironment in solid tumors', *Cancer Treatment Reviews*, pp. 22–32. doi: 10.1016/j.ctrv.2018.02.004.

Bencini, A. and Lippolis, V. (2010) '1,10-Phenanthroline: A versatile building block for the construction of ligands for various purposes', *Coordination Chemistry Reviews*, 254(17–18), pp. 2096–2180. doi: 10.1016/j.ccr.2010.04.008.

Benedetti, S. *et al.* (2015) 'Reactive oxygen species a double-edged sword for mesothelioma.', *Oncotarget*, 6(19), pp. 16848–65. doi: 10.18632/oncotarget.4253.

van Bergen, L. A. H., Roos, G. and De Proft, F. (2014) 'From Thiol to Sulfonic Acid: Modeling the Oxidation Pathway of Protein Thiols by Hydrogen Peroxide', *The Journal of Physical Chemistry A*, 118(31), pp. 6078–6084. doi: 10.1021/jp5018339.

Berghe, T. Vanden *et al.* (2014) 'Regulated necrosis: The expanding network of non-apoptotic cell death pathways', *Nature Reviews Molecular Cell Biology*, pp. 135–147. doi: 10.1038/nrm3737.

Bergmann, T. J. and Molinari, M. (2018) 'Three branches to rule them all? UPR signalling in response to chemically versus misfolded proteins-induced ER stress', *Biology of the Cell*, 110(9), pp. 197–204. doi: 10.1111/boc.201800029.

Betteridge, D. J. (2000) 'What is oxidative stress?', in *Metabolism: Clinical and Experimental*. W.B. Saunders, pp. 3–8. doi: 10.1016/S0026-0495(00)80077-3.

Bianco, A. *et al.* (2018) 'Clinical diagnosis of malignant pleural mesothelioma', *Journal of Thoracic Disease*. AME Publishing Company, pp. S253–S261. doi: 10.21037/jtd.2017.10.09.

Bielenberg, D. R. and Zetter, B. R. (2015) 'The Contribution of Angiogenesis to the Process of Metastasis', *Cancer Journal (United States)*. Lippincott Williams and Wilkins, pp. 267–273. doi: 10.1097/PPO.0000000000000138.

Bienert, G. P., Schjoerring, J. K. and Jahn, T. P. (2006) 'Membrane transport of hydrogen peroxide', *Biochimica et Biophysica Acta - Biomembranes*, pp. 994–1003. doi: 10.1016/j.bbamem.2006.02.015.

Biswas, S. and Rao, C. M. (2017) 'Epigenetics in cancer: Fundamentals and Beyond', *Pharmacology and Therapeutics*, 173, pp. 118–134. doi: 10.1016/j.pharmthera.2017.02.011.

Blackadar, C. B. (2016) 'Historical review of the causes of cancer', *World Journal of Clinical Oncology*. Baishideng Publishing Group Co., Limited, pp. 54–86. doi: 10.5306/wjco.v7.i1.54.

Bonacorso, H. G. *et al.* (2015) 'Recent advances in the chemistry of 1,10-phenanthrolines and their metal complex derivatives: Synthesis and promising applications in medicine, technology,

and catalysis', *Targets in Heterocyclic Systems*, 19, pp. 1–27. doi: 10.17374/targets.2016.19.1.

Borovski, T. *et al.* (2011) 'Cancer Stem Cell Niche: The Place to Be', *Cancer Research*, 71(3), pp. 634–639. doi: 10.1158/0008-5472.CAN-10-3220.

Boyer, A. *et al.* (2018) 'Drug repurposing in malignant pleural mesothelioma: a breath of fresh air?', *European Respiratory Review*, 27(147), p. 170098. doi: 10.1183/16000617.0098-2017.

Bravo, R. *et al.* (2013) 'Endoplasmic Reticulum and the Unfolded Protein Response', in *International Review of Cell and Molecular Biology*, pp. 215–290. doi: 10.1016/B978-0-12-407704-1.00005-1.

Bray, F. *et al.* (2018) 'Global cancer statistics 2018: GLOBOCAN estimates of incidence and mortality worldwide for 36 cancers in 185 countries', *CA: A Cancer Journal for Clinicians*, 68(6), pp. 394–424. doi: 10.3322/caac.21492.

Breiling, A. and Lyko, F. (2015) 'Epigenetic regulatory functions of DNA modifications: 5-methylcytosine and beyond', *Epigenetics & Chromatin*, 8(1), p. 24. doi: 10.1186/s13072-015-0016-6.

Brewer, T. F. *et al.* (2015) 'Chemical Approaches to Discovery and Study of Sources and Targets of Hydrogen Peroxide Redox Signaling Through NADPH Oxidase Proteins', *Annual Review of Biochemistry*, 84(1), pp. 765–790. doi: 10.1146/annurev-biochem-060614-034018.

Brianti, P., De Flammineis, E. and Mercuri, S. R. (2017) 'Review of HPV-related diseases and cancers', *New Microbiologica*, pp. 80–85.

Brkljacic, J. and Grotewold, E. (2017) 'Combinatorial control of gene expression', *Biochimica et Biophysica Acta (BBA) - Gene Regulatory Mechanisms*, 1860(1), pp. 31–40. doi: 10.1016/j.bbagrm.2016.07.005.

Brodská, B. and Holoubek, A. (2011) 'Generation of Reactive Oxygen Species during Apoptosis Induced by DNA-Damaging Agents and/or Histone Deacetylase Inhibitors', *Oxidative Medicine and Cellular Longevity*, 2011, pp. 1–7. doi: 10.1155/2011/253529.

Brown, R. *et al.* (2014) 'Poised epigenetic states and acquired drug resistance in cancer', *Nature Reviews Cancer*, 14(11), pp. 747–753. doi: 10.1038/nrc3819.

Bu, S. *et al.* (2019) 'Epithelial ovarian cancer stem-like cells are resistant to the cellular lysis of cytokine-induced killer cells via HIF1A-mediated downregulation of ICAM-1', *International Journal of Oncology*, 55(1), pp. 179–190. doi: 10.3892/ijo.2019.4794.

Burke, J. R., Hura, G. L. and Rubin, S. M. (2012) 'Structures of inactive retinoblastoma protein reveal multiple mechanisms for cell cycle control', *Genes and Development*, 26(11), pp. 1156–1166. doi: 10.1101/gad.189837.112.

Burkitt, M. J. *et al.* (1996) '1,10-Phenanthroline stimulates internucleosomal DNA fragmentation in isolated rat-liver nuclei by promoting the redox activity of endogenous copper ions', *Biochemical Journal*, 313(1), pp. 163–169. doi: 10.1042/bj3130163.

Butler, H. M. *et al.* (1969) 'Bactericidal Action of Selected Phenanthroline Chelates and Related Compounds', *Aust J Exp Biol Med*, 47(5), pp. 541–552. doi: 10.1038/icb.1969.148.

Butow, P. *et al.* (2018) 'Fear of Cancer Recurrence: A Practical Guide for Clinicians', *Oncology (Williston Park, N.Y.)*, pp. 32–38.

Cabantchik, Z. I. (2014) 'Labile iron in cells and body fluids: Physiology, pathology, and pharmacology', *Frontiers in Pharmacology*, 5 MAR, p. 45. doi: 10.3389/fphar.2014.00045.

Cadet, J. *et al.* (2012) 'Biologically relevant oxidants and terminology, classification and nomenclature of oxidatively generated damage to nucleobases and 2-deoxyribose in nucleic acids', *Free Radical Research*, 46(4), pp. 367–381. doi: 10.3109/10715762.2012.659248.

Cadet, J. and Davies, K. J. A. (2017) 'Oxidative DNA damage & repair: An introduction', *Free Radical Biology and Medicine*, 106(March), pp. 100–110. doi: 10.1016/j.freeradbiomed.2017.02.017.

Cadet, J. and Wagner, J. R. (2013) 'DNA Base Damage by Reactive Oxygen Species ', *Cold Spring Harb Perspect Biol*, 5, pp. 1–18.

Calabretta, A., Küpfer, P. A. and Leumann, C. J. (2015) 'The effect of RNA base lesions on mRNA translation', *Nucleic Acids Research*, 43(9), pp. 4713–4720. doi: 10.1093/nar/gkv377.

Camara, A. K. S. *et al.* (2017) 'Mitochondrial VDAC1: A key gatekeeper as potential therapeutic target', *Frontiers in Physiology*. Frontiers Media S.A. doi: 10.3389/fphys.2017.00460.

Camaschella, C. and Pagani, A. (2018) 'Advances in understanding iron metabolism and its crosstalk with erythropoiesis', *British Journal of Haematology*, 182(4), pp. 481–494. doi: 10.1111/bjh.15403.

Campbell, K. J. and Tait, S. W. G. (2018) 'Targeting BCL-2 regulated apoptosis in cancer', *Open Biology*. Royal Society Publishing. doi: 10.1098/rsob.180002.

Campillos, M. *et al.* (2010) 'SIREs: searching for iron-responsive elements', *Nucleic Acids Research*, 38(Web Server), pp. W360–W367. doi: 10.1093/nar/gkq371.

Cancer statistics | Irish Cancer Society (2018). Available at: https://www.cancer.ie/cancer-information-and-support/cancer-information/about-cancer/cancer-statistics (Accessed: 5 February 2020).

Cao, J. Y. and Dixon, S. J. (2016) 'Mechanisms of ferroptosis', *Cellular and Molecular Life Sciences*, 73(11–12), pp. 2195–2209. doi: 10.1007/s00018-016-2194-1.

Carbone, M. and Yang, H. (2012) 'Molecular Pathways: Targeting Mechanisms of Asbestos and Erionite Carcinogenesis in Mesothelioma', *Clinical Cancer Research*, 18(3), pp. 598–604. doi: 10.1158/1078-0432.CCR-11-2259.

Carlsen, C. U., Møller, J. K. S. and Skibsted, L. H. (2005) 'Heme-iron in lipid oxidation', *Coordination Chemistry Reviews*, 249(3-4 SPEC. ISS.), pp. 485–498. doi: 10.1016/j.ccr.2004.08.028.

Carmeliet, P. (2005) 'VEGF as a key mediator of angiogenesis in cancer', *Oncology*, pp. 4–10. doi: 10.1159/000088478.

Carreras-Sureda, A., Pihán, P. and Hetz, C. (2018) 'Calcium signaling at the endoplasmic reticulum: fine-tuning stress responses', *Cell Calcium*, 70(April 2017), pp. 24–31. doi: 10.1016/j.ceca.2017.08.004.

Carter, S. K. (1984) 'Cisplatin — Past, Present and Future', in *Platinum Coordination Complexes in Cancer Chemotherapy*. Boston, MA: Springer US, pp. 359–376. doi: 10.1007/978-1-4613-2837-7_28.

Carver, J. A. *et al.* (1988) 'Inactivation of chicken liver pyruvate carboxylase by 1,10-phenanthroline', *Biochemical Journal*, 252(2), pp. 501–507. doi: 10.1042/bj2520501.

Casares, C. *et al.* (2012) 'Reactive oxygen species in apoptosis induced by cisplatin: Review of physiopathological mechanisms in animal models', *European Archives of Oto-Rhino-Laryngology*, pp. 2455–2459. doi: 10.1007/s00405-012-2029-0.

Casas, C. (2017) 'GRP78 at the Centre of the Stage in Cancer and Neuroprotection', *Frontiers in Neuroscience*, 11(APR), p. 177. doi: 10.3389/fnins.2017.00177.

Cavone, D. *et al.* (2019) 'Epidemiology of Mesothelioma', *Environments*, 6(7), p. 76. doi: 10.3390/environments6070076.

Chadwick, W. *et al.* (2011) 'Repetitive Peroxide Exposure Reveals Pleiotropic Mitogen-Activated Protein Kinase Signaling Mechanisms', *Journal of Signal Transduction*, 2011, pp. 1–15. doi: 10.1155/2011/636951.

Chan, C. K. *et al.* (2019) 'Human Papillomavirus Infection and Cervical Cancer: Epidemiology, Screening, and Vaccination—Review of Current Perspectives', *Journal of Oncology*, 2019, pp. 1–11. doi: 10.1155/2019/3257939.

Chan, F. K.-M., Moriwaki, K. and De Rosa, M. J. (2013) 'Detection of Necrosis by Release of Lactate Dehydrogenase (LDH) Activity', *Methods Mol Biol*, 979, pp. 1–12. doi: 10.1007/978-1-62703-290-2.

Chandra, M., Sachdeva, A. and Silverman, S. K. (2009) 'DNA-catalyzed sequence-specific

hydrolysis of DNA', *Nature Chemical Biology*, 5(10), pp. 718–720. doi: 10.1038/nchembio.201.

Chandrasekharan, J. A. and Sharma-Wali, N. (2015) 'Lipoxins: Nature's way to resolve inflammation', *Journal of Inflammation Research*, 8, pp. 181–192. doi: 10.2147/JIR.S90380.

Chatterjee, N. and Walker, G. C. (2017) 'Mechanisms of DNA damage, repair, and mutagenesis', *Environmental and Molecular Mutagenesis*, 58(5), pp. 235–263. doi: 10.1002/em.22087.

Chen, G. *et al.* (2019) 'Acetylation regulates ribonucleotide reductase activity and cancer cell growth', *Nature Communications*, 10(1). doi: 10.1038/s41467-019-11214-9.

Chen, K., Huang, Y. and Chen, J. (2013) 'Understanding and targeting cancer stem cells: therapeutic implications and challenges', *Acta Pharmacologica Sinica*, 34(6), pp. 732–740. doi: 10.1038/aps.2013.27.

Chen, L., Zeng, Y. and Zhou, S.-F. (2018) 'Role of Apoptosis in Cancer Resistance to Chemotherapy', in *Current Understanding of Apoptosis - Programmed Cell Death*. InTech. doi: 10.5772/intechopen.80056.

Chen, X., Qian, Y. and Wu, S. (2015) 'The Warburg effect: Evolving interpretations of an established concept', *Free Radical Biology and Medicine*, 79, pp. 253–263. doi: 10.1016/j.freeradbiomed.2014.08.027.

Chen, Y. *et al.* (2019) 'Tumor-associated macrophages: An accomplice in solid tumor progression', *Journal of Biomedical Science*. BioMed Central Ltd. doi: 10.1186/s12929-019-0568-z.

Chen, Y., Azad, M. B. and Gibson, S. B. (2009) 'Superoxide is the major reactive oxygen species regulating autophagy', *Cell Death and Differentiation*, 16(7), pp. 1040–1052. doi: 10.1038/cdd.2009.49.

Chen, Y. and Brandizzi, F. (2013) 'IRE1: ER stress sensor and cell fate executor', *Trends in*

Cell Biology, 23(11), pp. 547–555. doi: 10.1016/j.tcb.2013.06.005.

Chen, Z.-S. and Tiwari, A. K. (2011) 'Multidrug resistance proteins (MRPs/ABCCs) in cancer chemotherapy and genetic diseases', *FEBS Journal*, 278(18), pp. 3226–3245. doi: 10.1111/j.1742-4658.2011.08235.x.

Chiou, B. and Connor, J. R. (2018) 'Emerging and dynamic biomedical uses of ferritin', *Pharmaceuticals*, 11(4). doi: 10.3390/ph11040124.

Ciccia, A. and Elledge, S. J. (2010) 'The DNA Damage Response: Making It Safe to Play with Knives', *Molecular Cell*, 40(2), pp. 179–204. doi: 10.1016/j.molcel.2010.09.019.

Clément, M. V. and Pervaiz, S. (2001) 'Intracellular superoxide and hydrogen peroxide concentrations: A critical balance that determines survival or death', *Redox Report*, 6(4), pp. 211–214. doi: 10.1179/135100001101536346.

Cohen, I. *et al.* (2011) 'Histone Modifiers in Cancer: Friends or Foes?', *Genes & Cancer*, 2(6), pp. 631–647. doi: 10.1177/1947601911417176.

Collin, F. (2019) 'Chemical basis of reactive oxygen species reactivity and involvement in neurodegenerative diseases', *International Journal of Molecular Sciences*, 20(10). doi: 10.3390/ijms20102407.

Collins, A. R. (2009) 'Investigating oxidative DNA damage and its repair using the comet assay', *Mutation Research - Reviews in Mutation Research*, 681(1), pp. 24–32. doi: 10.1016/j.mrrev.2007.10.002.

Cominetti, M. R., Altei, W. F. and Selistre-De-araujo, H. S. (2019) 'Metastasis inhibition in breast cancer by targeting cancer cell extravasation', *Breast Cancer: Targets and Therapy*. Dove Medical Press Ltd., pp. 165–178. doi: 10.2147/BCTT.S166725.

Cortes-Dericks, L. *et al.* (2014) 'Cisplatin-resistant cells in malignant pleural mesothelioma cell lines show ALDHhighCD44+ phenotype and sphere-forming capacity', *BMC Cancer*, 14(1), p. 304. doi: 10.1186/1471-2407-14-304.

Cosgrove, M. S. and Wolberger, C. (2005) ‘How does the histone code work?’, *Biochemistry and Cell Biology*, 83(4), pp. 468–476. doi: 10.1139/o05-137.

Cox, J. and Weinman, S. (2016) ‘Mechanisms of doxorubicin resistance in hepatocellular carcinoma’, *Hepatic Oncology*, 3(1), pp. 57–59. doi: 10.2217/hep.15.41.

Croons, V. *et al.* (2009) ‘The protein synthesis inhibitor anisomycin induces macrophage apoptosis in rabbit atherosclerotic plaques through p38 mitogen-activated protein kinase’, *Journal of Pharmacology and Experimental Therapeutics*, 329(3), pp. 856–864. doi: 10.1124/jpet.108.149948.

Crowley, A. (2019) *The Generation of Novel Metal-Folate- Phenanthroline Complexes and Phenanthroline-Folate Conjugates with Potential as Chemotherapeutic Agents*. doi: 10.21427/232k-5777.

Csermely, P., Korcsmáros, T. and Nussinov, R. (2016) ‘Intracellular and intercellular signaling networks in cancer initiation, development and precision anti-cancer therapy’, *Seminars in Cell & Developmental Biology*, 58, pp. 55–59. doi: 10.1016/j.semcdb.2016.07.005.

Cubillos-Ruiz, J. R., Bettigole, S. E. and Glimcher, L. H. (2016) ‘Molecular Pathways: Immunosuppressive Roles of IRE1α-XBP1 Signaling in Dendritic Cells of the Tumor Microenvironment’, *Clinical Cancer Research*, 22(9), pp. 2121–2126. doi: 10.1158/1078-0432.CCR-15-1570.

Cullinan, S. B. *et al.* (2003) ‘Nrf2 Is a Direct PERK Substrate and Effector of PERK-Dependent Cell Survival’, *Molecular and Cellular Biology*, 23(20), pp. 7198–7209. doi: 10.1128/MCB.23.20.7198-7209.2003.

Czabotar, P. E. *et al.* (2013) ‘Control of apoptosis by the BCL-2 protein family: implications for physiology and therapy’, *Nature Reviews Molecular Cell Biology*, 15, p. 49. Available at: https://doi.org/10.1038/nrm3722.

D’Arcy, M. S. (2019) ‘Cell death: a review of the major forms of apoptosis, necrosis and

autophagy', *Cell Biology International*, 43(6), pp. 582–592. doi: 10.1002/cbin.11137.

Damiani, E. *et al.* (2019) 'How reliable are in vitro IC50 values? Values vary with cytotoxicity assays in human glioblastoma cells', *Toxicology Letters*, 302(December 2018), pp. 28–34. doi: 10.1016/j.toxlet.2018.12.004.

Dancy, B. M. and Cole, P. A. (2015) 'Protein lysine acetylation by p300/CBP', *Chemical Reviews*, 115(6), pp. 2419–2452. doi: 10.1021/cr500452k.

Dang, W. (2014) 'The controversial world of sirtuins', *Drug Discov Today Technol*, 70(4), pp. 646–656. doi: 10.1002/ana.22528.Toll-like.

Davalli, P. *et al.* (2018) 'Targeting Oxidatively Induced DNA Damage Response in Cancer: Opportunities for Novel Cancer Therapies', *Oxidative Medicine and Cellular Longevity*, 2018, pp. 1–21. doi: 10.1155/2018/2389523.

Dawson, M. a. and Kouzarides, T. (2012) 'Cancer epigenetics: From mechanism to therapy', *Cell*, 150(1), pp. 12–27. doi: 10.1016/j.cell.2012.06.013.

DeBerardinis, R. J. and Chandel, N. S. (2016) 'Fundamentals of cancer metabolism', *Science Advances*, 2(5), p. e1600200. doi: 10.1126/sciadv.1600200.

Deegan, C. *et al.* (2007) 'In vitro cancer chemotherapeutic activity of 1,10-phenanthroline (phen), [Ag2(phen)3(mal)] · 2H2O, [Cu(phen)2(mal)] · 2H2O and [Mn(phen)2(mal)] · 2H2O (malH2= malonic acid) using human cancer cells', *Cancer Letters*, 247(2), pp. 224–233. doi: 10.1016/j.canlet.2006.04.006.

Deepa, S. K. (2016) 'Impact of Western Lifestyle on Cancer Progression', *International Journal of Healthcare Sciences*, 4(1), pp. 305–310.

Dehne, N. *et al.* (2017) 'Cancer cell and macrophage cross-talk in the tumor microenvironment', *Current Opinion in Pharmacology*. Elsevier Ltd, pp. 12–19. doi: 10.1016/j.coph.2017.04.007.

Delcuve, G. P., Khan, D. H. and Davie, J. R. (2012) 'Roles of histone deacetylases in epigenetic

regulation: emerging paradigms from studies with inhibitors', *Clinical Epigenetics*, 4(1), p. 5. doi: 10.1186/1868-7083-4-5.

Denoyer, D. *et al.* (2015) 'Targeting copper in cancer therapy: "Copper That Cancer"', *Metallomics*, pp. 1459–76. doi: 10.1039/c5mt00149h.

Deo, K. *et al.* (2016) 'Transition Metal Intercalators as Anticancer Agents—Recent Advances', *International Journal of Molecular Sciences*, 17(11), p. 1818. doi: 10.3390/ijms17111818.

Depayras, S. *et al.* (2018) 'The Hidden Face of Nitrogen Oxides Species: From Toxic Effects to Potential Cure?', in *Emerging Pollutants - Some Strategies for the Quality Preservation of Our Environment*. InTech. doi: 10.5772/intechopen.75822.

Desoize, B. and Madoulet, C. (2002) 'Particular aspects of platinum compounds used at present in cancer treatment', *Critical Reviews in Oncology/Hematology*, 42(3), pp. 317–325. doi: 10.1016/S1040-8428(01)00219-0.

DeWitt, M. R., Chen, P. and Aschner, M. (2013) 'Manganese efflux in Parkinsonism: Insights from newly characterized SLC30A10 mutations', *Biochemical and Biophysical Research Communications*, 432(1), pp. 1–4. doi: 10.1016/j.bbrc.2013.01.058.

Dhuriya, Y. K. and Sharma, D. (2018) 'Necroptosis: A regulated inflammatory mode of cell death', *Journal of Neuroinflammation*. BioMed Central Ltd. doi: 10.1186/s12974-018-1235-0.

Dickinson, B. C., Lin, V. S. and Chang, C. J. (2013) 'Preparation and use of MitoPY1 for imaging hydrogen peroxide in mitochondria of live cells', *Nature Protocols*, 8(6), pp. 1249–1259. doi: 10.1038/nprot.2013.064.

Die, J. V. *et al.* (2011) 'Characterization of the 3′:5′ ratio for reliable determination of RNA quality', *Analytical Biochemistry*, 419(2), pp. 336–338. doi: 10.1016/j.ab.2011.08.012.

Diehl, J. A., Fuchs, S. Y. and Koumenis, C. (2011) 'The Cell Biology of the Unfolded Protein Response', *Gastroenterology*, 141(1), pp. 38-41.e2. doi: 10.1053/j.gastro.2011.05.018.

Digiuseppe, J. A. *et al.* (1999) 'Phenylbutyrate-induced G1 arrest and apoptosis in myeloid

leukemia cells: structure-function analysis', *Leukemia*, 13, pp. 1243–1253. Available at: http://www.stockton-press.co.uk/leu (Accessed: 28 April 2020).

Dixon, S. J. *et al.* (2012) 'Ferroptosis: An Iron-Dependent Form of Nonapoptotic Cell Death', *Cell*, 149(5), pp. 1060–1072. doi: 10.1016/j.cell.2012.03.042.

Dixon, S. J. *et al.* (2014) 'Pharmacological inhibition of cystine-glutamate exchange induces endoplasmic reticulum stress and ferroptosis', *eLife*, 2014(3), pp. 1–25. doi: 10.7554/eLife.02523.

Dixon, S. J. (2017) 'Ferroptosis: bug or feature?', *Immunological Reviews*. doi: 10.1111/imr.12533.

Diyabalanage, H. V. K., Granda, M. L. and Hooker, J. M. (2013) 'Combination therapy: Histone deacetylase inhibitors and platinum-based chemotherapeutics for cancer', *Cancer Letters*, pp. 1–8. doi: 10.1016/j.canlet.2012.09.018.

Dizdaroglu, M. and Jaruga, P. (2012) 'Mechanisms of free radical-induced damage to DNA', *Free Radical Research*, 46(4), pp. 382–419. doi: 10.3109/10715762.2011.653969.

Dobryszycka, W. and Owczarek, H. (1981) 'Effects of lead, copper, and zinc on the rat's lactate dehydrogenase in vivo and in vitro', *Archives of Toxicology*, 48(1), pp. 21–27. doi: 10.1007/BF00297072.

Dodson, M., Castro-Portuguez, R. and Zhang, D. D. (2019) 'NRF2 plays a critical role in mitigating lipid peroxidation and ferroptosis', *Redox Biology*, (November 2018), p. 101107. doi: 10.1016/j.redox.2019.101107.

Drummond, J. T. *et al.* (1996) 'Cisplatin and adriamycin resistance are associated with MutLα and mismatch repair deficiency in an ovarian tumor cell line', *Journal of Biological Chemistry*, 271(33), pp. 19645–19648. doi: 10.1074/jbc.271.33.19645.

Dwyer, F. *et al.* (1969) 'The Biological Actions of 1,10-Phenanthroline and 2,2′-Bipyridine Hydrichlorides, Quaternary Salts and Metla Chelates and Related Compounds', *Australian*

Journal of Experimental Biology and Medical Science, 47(2), pp. 203–218. doi: 10.1038/icb.1969.21.

Easwaran. Hariharan, H. T. B. B. (2014) 'Cancer epigenetics: Tumor Heterogeneity, Plasticity of Stem-like States, and Drug Resistance', *Mol Cell.*, 54(5), pp. 716–727. doi: 10.1038/jid.2014.371.

Einhorn, L. H. and Donohue, J. (1977) 'Cis-diamminedichloroplatinum, vinblastine, and bleomycin combination chemotherapy in disseminated testicular cancer', *Annals of Internal Medicine*, 87(3), pp. 293–298. doi: 10.7326/0003-4819-87-3-293.

Elmore, S. (2007) 'Apoptosis: A Review of Programmed Cell Death', *Toxicologic Pathology*, 35(4), pp. 495–516. doi: 10.1080/01926230701320337.

Epstein, T., Gatenby, R. A. and Brown, J. S. (2017) 'The Warburg effect as an adaptation of cancer cells to rapid fluctuations in energy demand', *PLOS ONE*. Edited by P. Dzeja, 12(9), p. e0185085. doi: 10.1371/journal.pone.0185085.

Eschke, R.-C. K.-R. *et al.* (2019) 'Impact of Physical Exercise on Growth and Progression of Cancer in Rodents—A Systematic Review and Meta-Analysis', *Frontiers in Oncology*, 9. doi: 10.3389/fonc.2019.00035.

Escobar, M. L., Echeverría, O. M. and Vázquez-Nin, G. H. (2015) 'Necrosis as Programmed Cell Death', in *Cell Death - Autophagy, Apoptosis and Necrosis*. InTech, p. 13. doi: 10.5772/61483.

Eskandari, A. and Suntharalingam, K. (2019) 'A reactive oxygen species-generating, cancer stem cell-potent manganese(ii) complex and its encapsulation into polymeric nanoparticles', *Chemical Science*, 10(33), pp. 7792–7800. doi: 10.1039/C9SC01275C.

European Commission (2018) *Cancer statistics-specific cancers Statistics Explained*. Available at: https://ec.europa.eu/eurostat/statisticsexplained/ (Accessed: 5 February 2020).

Evans, M. D., Dizdaroglu, M. and Cooke, M. S. (2004) *Oxidative DNA damage and disease:*

Induction, repair and significance, *Mutation Research - Reviews in Mutation Research*. doi: 10.1016/j.mrrev.2003.11.001.

Fahy, E. *et al.* (2011) 'Lipid classification, structures and tools', *Biochimica et Biophysica Acta (BBA) - Molecular and Cell Biology of Lipids*, 1811(11), pp. 637–647. doi: 10.1016/j.bbalip.2011.06.009.

Feinberg, A. P. (2005) 'Cancer epigenetics is no Mickey Mouse', *Cancer Cell*, 8(4), pp. 267–268. doi: 10.1016/j.ccr.2005.09.014.

Fekry, M. I. and Gates, K. S. (2009) 'DNA-catalyzed hydrolysis of DNA phosphodiesters', *Nature Chemical Biology*. Nature Publishing Group, pp. 710–711. doi: 10.1038/nchembio.224.

Feng, H. and Stockwell, B. R. (2018) 'Unsolved mysteries: How does lipid peroxidation cause ferroptosis?', *PLoS Biology*, 16(5), pp. 1–15. doi: 10.1371/journal.pbio.2006203.

Ferlay, J. *et al.* (2019) 'Estimating the global cancer incidence and mortality in 2018: GLOBOCAN sources and methods', *International Journal of Cancer*, 144(8), pp. 1941–1953. doi: 10.1002/ijc.31937.

Fernández-Medarde, A. and Santos, E. (2011) 'Ras in cancer and developmental diseases', *Genes and Cancer*. Impact Journals, LLC, pp. 344–358. doi: 10.1177/1947601911411084.

Ferreira, J. A. *et al.* (2016) 'Mechanisms of cisplatin resistance and targeting of cancer stem cells: Adding glycosylation to the equation', *Drug Resistance Updates*, 24, pp. 34–54. doi: 10.1016/j.drup.2015.11.003.

Festjens, N., Vanden Berghe, T. and Vandenabeele, P. (2006) 'Necrosis, a well-orchestrated form of cell demise: Signalling cascades, important mediators and concomitant immune response', *Biochimica et Biophysica Acta - Bioenergetics*, pp. 1371–1387. doi: 10.1016/j.bbabio.2006.06.014.

Fimognari, C. (2015) 'Role of Oxidative RNA Damage in Chronic-Degenerative Diseases', *Oxidative Medicine and Cellular Longevity*, 2015, pp. 1–8. doi: 10.1155/2015/358713.

Flanagan, D. J. *et al.* (2018) 'Wnt signalling in gastrointestinal epithelial stem cells', *Genes*. MDPI AG. doi: 10.3390/genes9040178.

Florea, A. M. and Büsselberg, D. (2011) 'Cisplatin as an anti-tumor drug: Cellular mechanisms of activity, drug resistance and induced side effects', *Cancers*, 3(1), pp. 1351–1371. doi: 10.3390/cancers3011351.

Förstermann, U. and Sessa, W. C. (2012) 'Nitric oxide synthases: Regulation and function', *European Heart Journal*. doi: 10.1093/eurheartj/ehr304.

Fouad, Y. A. and Aanei, C. (2017) 'Revisiting the hallmarks of cancer', *American Journal of Cancer Research*. E-Century Publishing Corporation, pp. 1016–1036.

Fraisl, P. *et al.* (2009) 'Regulation of Angiogenesis by Oxygen and Metabolism', *Developmental Cell*. Cell Press, pp. 167–179. doi: 10.1016/j.devcel.2009.01.003.

Franco, R., Panayiotidis, M. I. and Cidlowski, J. A. (2007) 'Glutathione depletion is necessary for apoptosis in lymphoid cells independent of reactive oxygen species formation', *Journal of Biological Chemistry*, 282(42), pp. 30452–30465. doi: 10.1074/jbc.M703091200.

Freinbichler, W. *et al.* (2011) 'Highly reactive oxygen species: Detection, formation, and possible functions', *Cellular and Molecular Life Sciences*, 68(12), pp. 2067–2079. doi: 10.1007/s00018-011-0682-x.

Fribley, A., Zhang, K. and Kaufman, R. J. (2009) 'Regulation of Apoptosis by the Unfolded Protein Response', in *Methods in molecular biology (Clifton, N.J.)*. NIH Public Access, pp. 191–204. doi: 10.1007/978-1-60327-017-5_14.

Friedmann Angeli, J. P., Krysko, D. V and Conrad, M. (2019) 'Ferroptosis at the crossroads of cancer-acquired drug resistance and immune evasion', *Nature Reviews Cancer*, 19(7), pp. 405–414. doi: 10.1038/s41568-019-0149-1.

Gaetke, L. M., Chow-Johnson, H. S. and Chow, C. K. (2014) 'Copper: toxicological relevance and mechanisms', *Archives of Toxicology*, pp. 1929–1938. doi: 10.1007/s00204-014-1355-y.

Galadari, S. *et al.* (2017) ‘Reactive oxygen species and cancer paradox: To promote or to suppress?’, *Free Radical Biology and Medicine*, 104(December 2016), pp. 144–164. doi: 10.1016/j.freeradbiomed.2017.01.004.

Galateau-Salle, F. *et al.* (2015) ‘The 2015 World Health Organization Classification of Tumors of the Pleura: Advances since the 2004 Classification’, *Journal of Thoracic Oncology*, 11, pp. 142–154. doi: 10.1016/j.jtho.2015.11.005.

Galluzzi, L. *et al.* (2014) ‘Systems biology of cisplatin resistance: past, present and future’, *Cell Death and Disease*, 5(5), p. e1257. doi: 10.1038/cddis.2013.428.

Galluzzi, L. *et al.* (2018) ‘Molecular mechanisms of cell death: Recommendations of the Nomenclature Committee on Cell Death 2018’, *Cell Death and Differentiation*, 25(3), pp. 486–541. doi: 10.1038/s41418-017-0012-4.

Gandra, R. M. *et al.* (2017) ‘Antifungal potential of copper(II), Manganese(II) and silver(I) 1,10-phenanthroline chelates against multidrug-resistant fungal species forming the Candida haemulonii Complex: Impact on the planktonic and biofilm lifestyles’, *Frontiers in Microbiology*, 8(JUL), pp. 1–11. doi: 10.3389/fmicb.2017.01257.

Gao, M. and Jiang, X. (2018) ‘To eat or not to eat — the metabolic flavor of ferroptosis’, *Current Opinion in Cell Biology*, 51, pp. 58–64. doi: 10.1016/j.ceb.2017.11.001.

Gao, Z. *et al.* (2014) ‘Cyclooxygenase-2-dependent oxidative stress mediates palmitate-induced impairment of endothelium-dependent relaxations in mouse arteries’, *Biochemical Pharmacology*, 91(4), pp. 474–482. doi: 10.1016/j.bcp.2014.08.009.

Garbutcheon-Singh, K. B. *et al.* (2011) ‘Transition Metal Based Anticancer Drugs’, *Current Topics in Medicinal Chemistry*, 11(5), pp. 521–542. doi: 10.2174/156802611794785226.

Gaschler, M. M. and Stockwell, B. R. (2017) ‘Lipid peroxidation in cell death’, *Biochemical and Biophysical Research Communications*, 482(3), pp. 419–425. doi: 10.1016/j.bbrc.2016.10.086.

Gates, K. S. (2009) ‘An Overview of Chemical Processes That Damage Cellular DNA: Spontaneous Hydrolysis, Alkylation, and Reactions with Radicals’, *Chemical Research in Toxicology*, 22(11), pp. 1747–1760. doi: 10.1021/tx900242k.

Gavrilescu, L. C. and Denkers, E. Y. (2003) ‘Apoptosis and the Balance of Homeostatic and Pathologic Responses to Protozoan Infection’, *Infection and Immunity*, 71(11), pp. 6109–6115. doi: 10.1128/IAI.71.11.6109-6115.2003.

Gerber, G. B., Léonard, A. and Hantson, P. (2002) ‘Carcinogenicity, mutagenicity and teratogenicity of manganese compounds’, *Critical Reviews in Oncology/Hematology*, pp. 25–34. doi: 10.1016/S1040-8428(01)00178-0.

Ghodke-Puranik, Y. *et al.* (2013) ‘Valproic acid pathway’, *Pharmacogenetics and Genomics*, 23(4), pp. 236–241. doi: 10.1097/FPC.0b013e32835ea0b2.

Ghosh, N. *et al.* (2018) ‘Reactive Oxygen Species, Oxidative Damage and Cell Death’, in *Immunity and Inflammation in Health and Disease*. Elsevier, pp. 45–55. doi: 10.1016/b978-0-12-805417-8.00004-4.

Ghosh, S. (2019) ‘Cisplatin: The first metal based anticancer drug’, *Bioorganic Chemistry*, 88, p. 102925. doi: 10.1016/j.bioorg.2019.102925.

Gialeli, C., Theocharis, A. D. and Karamanos, N. K. (2011) ‘Roles of matrix metalloproteinases in cancer progression and their pharmacological targeting’, *FEBS Journal*, pp. 16–27. doi: 10.1111/j.1742-4658.2010.07919.x.

Giandomenico, A. R. *et al.* (1997) ‘The Importance of Sodium Pyruvate in Assessing Damage Produced by Hydrogen Peroxide’, *Free Radical Biology and Medicine*, 23(3), pp. 426–434. doi: 10.1016/S0891-5849(97)00113-5.

Gibney, E. R. and Nolan, C. M. (2010) ‘Epigenetics and gene expression’, *Heredity*, 105(1), pp. 4–13. doi: 10.1038/hdy.2010.54.

Giglia-Mari, G., Zotter, A. and Vermeulen, W. (2011) ‘DNA damage response’, *Cold Spring*

Harbor Perspectives in Biology, 3(1), pp. 1–19. doi: 10.1101/cshperspect.a000745.

Gill, J. G., Piskounova, E. and Morrison, S. J. (2016) 'Cancer, oxidative stress, and metastasis', *Cold Spring Harbor Symposia on Quantitative Biology*, 81(1), pp. 163–175. doi: 10.1101/sqb.2016.81.030791.

Girotti, A. W. (1998) 'Lipid hydroperoxide generation, turnover, and effector action in biological systems.', *Journal of lipid research*, 39(8), pp. 1529–42. Available at: http://link.springer.com/10.1007/978-3-211-33303-7_2.

GLOBOCAN-WHO (2018a) *Cancer statistics Ireland*.

GLOBOCAN-WHO (2018b) *Europe Cancer Populations*.

Golstein, P. and Kroemer, G. (2007) 'Cell death by necrosis: towards a molecular definition', *Trends in Biochemical Sciences*, 32(1), pp. 37–43. doi: 10.1016/j.tibs.2006.11.001.

Gong, Y. *et al.* (2019) 'The role of necroptosis in cancer biology and therapy', *Molecular Cancer*, 18(1), p. 100. doi: 10.1186/s12943-019-1029-8.

Gonzalez-Hunt, C. P., Wadhwa, M. and Sanders, L. H. (2018) 'DNA damage by oxidative stress: Measurement strategies for two genomes', *Current Opinion in Toxicology*, 7, pp. 87–94. doi: 10.1016/j.cotox.2017.11.001.

González, M. *et al.* (1999) 'Intracellular determination of elements in mammalian cultured cells by total reflection X-ray fluorescence spectrometry', *J. Anal. At. Spectrom.*, 14(5), pp. 885–888. doi: 10.1039/A808748B.

Goodsell, D. S. (2006) 'The Molecular Perspective: Cisplatin', *The Oncologist*, 11(7), pp. 849–850. doi: 10.1634/theoncologist.11-7-849.

Gorodetska, I., Kozeretska, I. and Dubrovska, A. (2019) 'BRCA genes: The role in genome stability, cancer stemness and therapy resistance', *Journal of Cancer*. Ivyspring International Publisher, pp. 2109–2127. doi: 10.7150/jca.30410.

Goudarzi, F. *et al.* (2018) 'Hydrogen peroxide: a potent inducer of differentiation of human

adipose-derived stem cells into chondrocytes', *Free Radical Research*, 52(7), pp. 763–774. doi: 10.1080/10715762.2018.1466121.

Gough, D. R. and Cotter, T. G. (2011) 'Hydrogen peroxide: a Jekyll and Hyde signalling molecule.', *Cell death & disease*, 2, p. e213. doi: 10.1038/cddis.2011.96.

Govindaraju, M. *et al.* (2013) 'Copper interactions with DNA of chromatin and its role in neurodegenerative disorders', *Journal of Pharmaceutical Analysis*, 3(5), pp. 354–359. doi: 10.1016/j.jpha.2013.03.003.

Greenberg, M. M. (2014) 'Abasic and Oxidized Abasic Site Reactivity in DNA: Enzyme Inhibition, Cross-Linking, and Nucleosome Catalyzed Reactions', *Accounts of Chemical Research*, 47(2), pp. 646–655. doi: 10.1021/ar400229d.

Greenman, C. *et al.* (2007) 'Patterns of somatic mutation in human cancer genomes', *Nature*, 446(7132), pp. 153–158. doi: 10.1038/nature05610.

Grigull, J. *et al.* (2004) 'Genome-Wide Analysis of mRNA Stability Using Transcription Inhibitors and Microarrays Reveals Posttranscriptional Control of Ribosome Biogenesis Factors', *Molecular and Cellular Biology*, 24(12), pp. 5534–5547. doi: 10.1128/mcb.24.12.5534-5547.2004.

Guha, P. *et al.* (2017) 'Tunicamycin induced endoplasmic reticulum stress promotes apoptosis of prostate cancer cells by activating mTORC1', *Oncotarget*, 8(40), pp. 68191–68207. doi: 10.18632/oncotarget.19277.

Gulec, S. and Collins, J. F. (2014) 'Molecular Mediators Governing Iron-Copper Interactions', *Annual Review of Nutrition*, 34(1), pp. 95–116. doi: 10.1146/annurev-nutr-071812-161215.

Gunter, T. E. (2017) 'Manganese and Mitochondrial Function', in *Molecular, Genetic, and Nutritional Aspects of Major and Trace Minerals*. Elsevier, pp. 389–396. doi: 10.1016/B978-0-12-802168-2.00032-4.

Gursoy-Yuzugullu, O., House, N. and Price, B. D. (2016) 'Patching Broken DNA: Nucleosome

Dynamics and the Repair of DNA Breaks', *Journal of Molecular Biology*, 428(9), pp. 1846–1860. doi: 10.1016/j.jmb.2015.11.021.

Habib, S. and Ali, A. (2011) 'Biochemistry of nitric oxide', *Indian Journal of Clinical Biochemistry*, pp. 3–17. doi: 10.1007/s12291-011-0108-4.

Hamid, R. *et al.* (2004) 'Comparison of alamar blue and MTT assays for high through-put screening', *Toxicology in Vitro*, 18(5), pp. 703–710. doi: 10.1016/j.tiv.2004.03.012.

Hanahan, D. and Weinberg, R. A. (2011) 'Hallmarks of cancer: The next generation', *Cell*, pp. 646–674. doi: 10.1016/j.cell.2011.02.013.

Harischandra, D. S. *et al.* (2019) 'Manganese-induced neurotoxicity: New insights into the triad of protein misfolding, mitochondrial impairment, and neuroinflammation', *Frontiers in Neuroscience*. Frontiers Media S.A., p. 654. doi: 10.3389/fnins.2019.00654.

Hashimoto, T. and Shibasaki, F. (2015) 'Hypoxia-Inducible Factor as an Angiogenic Master Switch', *Frontiers in Pediatrics*, 3. doi: 10.3389/fped.2015.00033.

Hassan, M. *et al.* (2014) 'Apoptosis and Molecular Targeting Therapy in Cancer', *BioMed Research International*, 2014, pp. 1–23. doi: 10.1155/2014/150845.

Hasselbalch, H. C. (2013) 'Chronic inflammation as a promotor of mutagenesis in essential thrombocythemia, polycythemia vera and myelofibrosis. A human inflammation model for cancer development?', *Leukemia Research*, pp. 214–220. doi: 10.1016/j.leukres.2012.10.020.

Hattori, K. *et al.* (2009) 'The roles of ASK family proteins in stress responses and diseases', *Cell Communication and Signaling*, 7(1), p. 9. doi: 10.1186/1478-811X-7-9.

Hayyan, M., Hashim, M. A. and Alnashef, I. M. (2016) 'Superoxide Ion: Generation and Chemical Implications', *Chemical Reviews*, 116(5), pp. 3029–3085. doi: 10.1021/acs.chemrev.5b00407.

He, S. *et al.* (2009) 'Receptor Interacting Protein Kinase-3 Determines Cellular Necrotic Response to TNF-α', *Cell*, 137(6), pp. 1100–1111. doi: 10.1016/j.cell.2009.05.021.

He, Y. *et al.* (2016) 'The changing 50% inhibitory concentration (IC50) of cisplatin: a pilot study on the artifacts of the MTT assay and the precise measurement of density-dependent chemoresistance in ovarian cancer', *Oncotarget*, 7(43), pp. 70803–70821. doi: 10.18632/oncotarget.12223.

He, Z. and Simon, H.-U. (2013) 'A novel link between p53 and ROS', *Cell Cycle*, 12(2), pp. 201–201. doi: 10.4161/cc.23418.

Hegedűs, C. *et al.* (2018) 'Redox control of cancer cell destruction', *Redox Biology*, 16(December 2017), pp. 59–74. doi: 10.1016/j.redox.2018.01.015.

Helsel, M. E. and Franz, K. J. (2015) 'Pharmacological activity of metal binding agents that alter copper bioavailability', *Dalton Transactions*, 44(19), pp. 8760–8770. doi: 10.1039/c5dt00634a.

Hernroth, B. *et al.* (2018) 'Manganese Inhibits Viability of Prostate Cancer Cells', *Anticancer Research*, 38(1), pp. 137–145. doi: 10.21873/anticanres.12201.

Heron, P. *et al.* (2001) 'Paradoxical effects of copper and manganese on brain mitochondrial function', *Life Sciences*, 68(14), pp. 1575–1583. doi: 10.1016/S0024-3205(01)00948-1.

Hetz, C. and Papa, F. R. (2018) 'The Unfolded Protein Response and Cell Fate Control', *Molecular Cell*, 69(2), pp. 169–181. doi: 10.1016/j.molcel.2017.06.017.

Higby, D. J. *et al.* (1974) 'Diaminodichloroplatinum: A phase I study showing responses in testicular and other tumors', *Cancer*, 33(5), pp. 1219–1225. doi: 10.1002/1097-0142(197405)33:5<1219::AID-CNCR2820330505>3.0.CO;2-U.

Hillary, R. F. and FitzGerald, U. (2018) 'A lifetime of stress: ATF6 in development and homeostasis', *Journal of Biomedical Science*, 25(1), p. 48. doi: 10.1186/s12929-018-0453-1.

Hillegass, J. M. *et al.* (2010) 'Inflammation precedes the development of human malignant mesotheliomas in a SCID mouse xenograft model', *Annals of the New York Academy of Sciences*, 1203(1), pp. 7–14. doi: 10.1111/j.1749-6632.2010.05554.x.

Hilton, J. B. *et al.* (2018) 'The accumulation of enzymatically inactive cuproenzymes is a CNS-specific phenomenon of the SOD1 G37R mouse model of ALS and can be restored by overexpressing the human copper transporter hCTR1', *Experimental Neurology*, 307, pp. 118–128. doi: 10.1016/j.expneurol.2018.06.006.

Hinshaw, D. C. and Shevde, L. A. (2019) 'The tumor microenvironment innately modulates cancer progression', *Cancer Research*, pp. 4557–4567. doi: 10.1158/0008-5472.CAN-18-3962.

Hirakawa, K. (2018) 'Biomolecules Oxidation by Hydrogen Peroxide and Singlet Oxygen', *Reactive Oxygen Species (ROS) in Living Cells*. doi: 10.5772/intechopen.71465.

Höckendorf, U., Yabal, M. and Jost, P. J. (2017) 'Killing AML: RIPK3 leads the way', *Cell Cycle*. Taylor and Francis Inc., pp. 3–4. doi: 10.1080/15384101.2016.1232069.

Van Hoecke, L. *et al.* (2018) 'Treatment with mRNA coding for the necroptosis mediator MLKL induces antitumor immunity directed against neo-epitopes', *Nature Communications*, 9(1). doi: 10.1038/s41467-018-05979-8.

Hoesel, B. and Schmid, J. a (2013) 'The complexity of NF-κB signaling in inflammation and cancer.', *Molecular cancer*, 12(1), p. 86. doi: 10.1101/cshperspect.a000141.

Hofer, T. *et al.* (2006) 'A method to determine RNA and DNA oxidation simultaneously by HPLC-ECD: Greater RNA than DNA oxidation in rat liver after doxorubicin administration', *Biological Chemistry*, 387(1), pp. 103–111. doi: 10.1515/BC.2006.014.

Holohan, C. *et al.* (2013) 'Cancer drug resistance: An evolving paradigm', *Nature Reviews Cancer*, pp. 714–726. doi: 10.1038/nrc3599.

Hou, J. *et al.* (2019) 'Discovery of potent necroptosis inhibitors targeting RIPK1 kinase activity for the treatment of inflammatory disorder and cancer metastasis', *Cell Death and Disease*, 10(7). doi: 10.1038/s41419-019-1735-6.

Housman, G. *et al.* (2014) 'Drug resistance in cancer: An overview', *Cancers*, 6(3), pp. 1769–

1792. doi: 10.3390/cancers6031769.

HSE.ie (2018) *Cancer Incidence, Survival and Mortality Data - HSE.ie*. Available at: https://www.hse.ie/eng/services/list/5/cancer/pubs/intelligence/registrydata.html (Accessed: 5 February 2020).

Huang, R.-P. *et al.* (1999) 'Tumor promotion by hydrogen peroxide in rat liver epithelial cells', *Carcinogenesis*, 20(3), pp. 485–492. doi: 10.1093/carcin/20.3.485.

Huang, Y. and Li, L. (2013) 'DNA crosslinking damage and cancer - a tale of friend and foe.', *Translational cancer research*, 2(3), pp. 144–154. doi: 10.3978/j.issn.2218-676X.2013.03.01.

Huang, Z. *et al.* (2008) 'Inhibition of caspase-3 activity and activation by protein glutathionylation', *Biochemical Pharmacology*, 75(11), pp. 2234–2244. doi: 10.1016/j.bcp.2008.02.026.

Huggett, J. F. *et al.* (2013) 'The digital MIQE guidelines: Minimum information for publication of quantitative digital PCR experiments', *Clinical Chemistry*, 59(6), pp. 892–902. doi: 10.1373/clinchem.2013.206375.

Hylebos, M. *et al.* (2016) 'The genetic landscape of malignant pleural mesothelioma: Results from massively parallel sequencing', *Journal of Thoracic Oncology*. Lippincott Williams and Wilkins, pp. 1615–1626. doi: 10.1016/j.jtho.2016.05.020.

Ibrahim, M. A., Srivenugopal, K. S. and Rasul, K. I. (2013) 'Platinum resistance: the role of molecular, genetic and epigenetic factors', *J. Med. Sci*, pp. 160–168. doi: 10.3923/jms.2013.160.168.

Inoue, T. and Suzuki-Karasaki, Y. (2013) 'Mitochondrial superoxide mediates mitochondrial and endoplasmic reticulum dysfunctions in TRAIL-induced apoptosis in Jurkat cells', *Free Radical Biology and Medicine*, 61, pp. 273–284. doi: 10.1016/j.freeradbiomed.2013.04.020.

International Agency for Research on Cancer (2019) *Cancer Tomorrow*, *World Health Organization*. Available at: http://gco.iarc.fr/tomorrow/home (Accessed: 5 February 2020).

Ishii, T. *et al.* (2018) 'Specific binding of PCBP1 to heavily oxidized RNA to induce cell death', *Proceedings of the National Academy of Sciences of the United States of America*, 115(26), pp. 6715–6720. doi: 10.1073/pnas.1806912115.

Izeradjene, K. *et al.* (2005) 'Reactive oxygen species regulate caspase activation in tumor necrosis factor-related apoptosis-inducing ligand-resistant human colon carcinoma cell lines', *Cancer Research*, 65(16), pp. 7436–7445. doi: 10.1158/0008-5472.CAN-04-2628.

Jackson, R. J., Hellen, C. U. T. and Pestova, T. V. (2010) 'The mechanism of eukaryotic translation initiation and principles of its regulation', *Nature Reviews Molecular Cell Biology*, 11(2), pp. 113–127. doi: 10.1038/nrm2838.

Jafri, M. A. *et al.* (2016) 'Roles of telomeres and telomerase in cancer, and advances in telomerase-targeted therapies', *Genome Medicine*, 8(1), p. 69. doi: 10.1186/s13073-016-0324-x.

Jakubowska, K. *et al.* (2016) 'Reduced expression of caspase-8 and cleaved caspase-3 in pancreatic ductal adenocarcinoma cells', *Oncology Letters*, 11(3), pp. 1879–1884. doi: 10.3892/ol.2016.4125.

Jaramillo, M. C. and Zhang, D. D. (2013) 'The emerging role of the Nrf2-Keap1 signaling pathway in cancer', *Genes & Development*, 27(20), pp. 2179–2191. doi: 10.1101/gad.225680.113.

Jekimovs, C. *et al.* (2014) 'Chemotherapeutic compounds targeting the DNA double-strand break repair pathways: The good, the bad, and the promising', *Frontiers in Oncology*, 4 APR(April), pp. 1–18. doi: 10.3389/fonc.2014.00086.

Jena, N. R. (2012) 'DNA damage by reactive species: Mechanisms, mutation and repair', *Journal of Biosciences*, 37(3), pp. 503–507. doi: 10.1007/s12038-012-9218-2.

Jena, N. R. and Mishra, P. C. (2013) 'Is FapyG mutagenic?: Evidence from the DFT study', *ChemPhysChem*, 14(14), pp. 3263–3270. doi: 10.1002/cphc.201300535.

Jiang, L. *et al.* (2013) 'Knockdown of survivin contributes to antitumor activity in cisplatin-resistant ovarian cancer cells', *Molecular Medicine Reports*, 7(2), pp. 425–430. doi: 10.3892/mmr.2012.1216.

Joazeiro, C. A. P. (2017) 'Ribosomal Stalling During Translation: Providing Substrates for Ribosome-Associated Protein Quality Control', *Review in Advance*. doi: 10.1146/annurev-cellbio-111315.

Jog, N. R. and Caricchio, R. (2014) 'The role of necrotic cell death in the pathogenesis of immune mediated nephropathies', *Clinical Immunology*. Academic Press Inc., pp. 243–253. doi: 10.1016/j.clim.2014.05.002.

Johansen, M. E. *et al.* (2005) 'Oxidatively induced DNA-protein cross-linking between single-stranded binding protein and oligodeoxynucleotides containing 8-oxo-7,8-dihydro-2′-deoxyguanosine', *Biochemistry*, 44(15), pp. 5660–5671. doi: 10.1021/bi047580n.

Johnstone, T. C., Park, G. Y. and Lippard, S. J. (2014) 'Understanding and improving platinum anticancer drugs - Phenanthriplatin', in *Anticancer Research*, pp. 471–476.

Jung, M. *et al.* (2019) 'Iron as a Central Player and Promising Target in Cancer Progression', *International Journal of Molecular Sciences*, 20(2), p. 273. doi: 10.3390/ijms20020273.

Junjappa, R. P. *et al.* (2018) 'IRE1α Implications in Endoplasmic Reticulum Stress-Mediated Development and Pathogenesis of Autoimmune Diseases', *Frontiers in Immunology*, 9(JUN). doi: 10.3389/fimmu.2018.01289.

Kahlos, K. *et al.* (1998) 'Manganese superoxide dismutase in healthy human pleural mesothelium and in malignant pleural mesothelioma', *American Journal of Respiratory Cell and Molecular Biology*, 18(4), pp. 570–580. doi: 10.1165/ajrcmb.18.4.2943.

Kaiser, W. J. *et al.* (2013) 'Toll-like receptor 3-mediated necrosis via TRIF, RIP3, and MLKL', *Journal of Biological Chemistry*, 288(43), pp. 31268–31279. doi: 10.1074/jbc.M113.462341.

Kalkavan, H. and Green, D. R. (2018) 'MOMP, cell suicide as a BCL-2 family business', *Cell*

Death and Differentiation, 25(1), pp. 46–55. doi: 10.1038/cdd.2017.179.

Kalyanaraman, B. (2013) 'Teaching the basics of redox biology to medical and graduate students: Oxidants, antioxidants and disease mechanisms', *Redox Biology*, 1(1), pp. 244–257. doi: 10.1016/j.redox.2013.01.014.

Kansanen, E. *et al.* (2013) 'The Keap1-Nrf2 pathway: Mechanisms of activation and dysregulation in cancer', *Redox Biology*, 1(1), pp. 45–49. doi: 10.1016/j.redox.2012.10.001.

Kanti Das, T., Wati, M. R. and Fatima-Shad, K. (2014) 'Oxidative Stress Gated by Fenton and Haber Weiss Reactions and Its Association With Alzheimer's Disease', *Archives of Neuroscience*, 2(3). doi: 10.5812/archneurosci.20078.

Kanwal, R. and Gupta, S. (2012) 'Epigenetic modifications in cancer', *Clinical Genetics*, pp. 303–311. doi: 10.1111/j.1399-0004.2011.01809.x.

Karch, J. and Molkentin, J. D. (2015) 'Regulated necrotic cell death: The passive aggressive side of bax and bak', *Circulation Research*. Lippincott Williams and Wilkins, pp. 1800–1809. doi: 10.1161/CIRCRESAHA.116.305421.

Katayama, K., Noguchi, K. and Sugimoto, Y. (2014) 'Regulations of P-Glycoprotein/ABCB1/MDR1 in Human Cancer Cells', *New Journal of Science*, 2014, pp. 1–10. doi: 10.1155/2014/476974.

Kehrer, J. P. and Robertson, J. D. (2010) *.14 Free Radicals and Reactive Oxygen Species*.

Kelland, L. (2007) 'The resurgence of platinum-based cancer chemotherapy', *Nature Reviews Cancer*, 7(8), pp. 573–584. doi: 10.1038/nrc2167.

Kellett, A. *et al.* (2011) 'Water-soluble bis(1,10-phenanthroline) octanedioate Cu2+ and Mn2+ complexes with unprecedented nano and picomolar in vitro cytotoxicity: promising leads for chemotherapeutic drug development', *MedChemComm*, 2(7), p. 579. doi: 10.1039/c0md00266f.

Kendig, D. M. and Tarloff, J. B. (2007) 'Inactivation of lactate dehydrogenase by several

chemicals: Implications for in vitro toxicology studies', *Toxicology in Vitro*, 21(1), pp. 125–132. doi: 10.1016/j.tiv.2006.08.004.

Kennedy, L. J. *et al.* (1997) 'Quantitation of 8-Oxoguanine and Strand Breaks Produced by Four Oxidizing Agents', *Chemical Research in Toxicology*, 10(4), pp. 386–392. doi: 10.1021/tx960102w.

Kim, H.-J. and Bae, S.-C. (2011) 'Histone deacetylase inhibitors: molecular mechanisms of action and clinical trials as anti-cancer drugs.', *American journal of translational research*, 3(2), pp. 166–79. Available at: http://www.pubmedcentral.nih.gov/articlerender.fcgi?artid=3056563&tool=pmcentrez&rendertype=abstract (Accessed: 6 November 2015).

Kim, H., Bhattacharya, A. and Qi, L. (2015) 'Endoplasmic reticulum quality control in cancer: friend or foe', *Semin Cancer Biol.*, (33), pp. 25–33. doi: 10.1002/cncr.27633.Percutaneous.

Kim, M. S. *et al.* (2003) 'Inhibition of histone deacetylase increases cytotoxicity to anticancer drugs targeting DNA.', *Cancer research*, 63(21), pp. 7291–300. doi: 14612526.

Kino, K. *et al.* (2017) 'Generation, repair and replication of guanine oxidation products', *Genes and Environment*, 39(1), pp. 1–8. doi: 10.1186/s41021-017-0081-0.

Kitamura, H. and Motohashi, H. (2018) 'NRF2 addiction in cancer cells', *Cancer Science*, 109(4), pp. 900–911. doi: 10.1111/cas.13537.

Knak, A. *et al.* (2014) 'Exposure of vitamins to UVB and UVA radiation generates singlet oxygen', *Photochemical and Photobiological Sciences*, 13(5), pp. 820–829. doi: 10.1039/c3pp50413a.

Ko, A., Han, S. Y. and Song, J. (2016) 'Dynamics of ARF regulation that control senescence and cancer', *BMB Reports*. The Biochemical Society of the Republic of Korea, pp. 598–606. doi: 10.5483/BMBRep.2016.49.11.120.

Kobayashi, A. *et al.* (2004) 'Oxidative Stress Sensor Keap1 Functions as an Adaptor for Cul3-

Based E3 Ligase To Regulate Proteasomal Degradation of Nrf2', *Molecular and Cellular Biology*, 24(16), pp. 7130–7139. doi: 10.1128/MCB.24.16.7130-7139.2004.

Kohli, R. M. and Zhang, Y. (2013) 'TET enzymes, TDG and the dynamics of DNA demethylation', *Nature*, 502(5), pp. 213–223. doi: 10.1007/978-1-62703-673-3.

Kong, Q. *et al.* (2008) 'RNA oxidation: A contributing factor or an epiphenomenon in the process of neurodegeneration', *Free Radical Research*, 42(9), pp. 773–777. doi: 10.1080/10715760802311187.

Köpf-Maier, P., Köpf, H. and Neuse, E. W. (1984) 'Ferricenium complexes: A new type of water-soluble antitumor agent', *Journal of Cancer Research and Clinical Oncology*, 108(3), pp. 336–340. doi: 10.1007/BF00390468.

Koprinarova, M. *et al.* (2010) 'Sodium butyrate enhances the cytotoxic effect of cisplatin by abrogating the cisplatin imposed cell cycle arrest', *BMC Molecular Biology*, 11(1), p. 49. doi: 10.1186/1471-2199-11-49.

Kristinova, V. *et al.* (2014) 'The effect of dietary antioxidants on iron-mediated lipid peroxidation in marine emulsions studied by measurement of dissolved oxygen consumption', *European Journal of Lipid Science and Technology*, p. n/a-n/a. doi: 10.1002/ejlt.201400011.

Krock, B. L., Skuli, N. and Simon, M. C. (2011) 'Hypoxia-Induced Angiogenesis: Good and Evil', *Genes and Cancer*, 2(12), pp. 1117–1133. doi: 10.1177/1947601911423654.

Krokan, H. E. and Bjoras, M. (2013) 'Base Excision Repair', *Cold Spring Harbor Perspectives in Biology*, 5(4), pp. a012583–a012583. doi: 10.1101/cshperspect.a012583.

Küpfer, P. A. and Leumann, C. J. (2014) 'Oxidative Damage on RNA Nucleobases', in *Chemical Biology of Nucleic Acids*. Berlin, Heidelberg: Springer Berlin Heidelberg, pp. 75–94. doi: 10.1007/978-3-642-54452-1_5.

Kusaczuk, M. *et al.* (2016) 'Phenylbutyrate—a pan-HDAC inhibitor—suppresses proliferation of glioblastoma LN-229 cell line', *Tumor Biology*, 37(1), pp. 931–942. doi: 10.1007/s13277-

015-3781-8.

Kuwabara, M. *et al.* (1986) 'Nuclease activity of 1,10-phenanthroline-copper ion: reaction with CGCGAATTCGCG and its complexes with netropsin and EcoRI', *Biochemistry*, 25(23), pp. 7401–7408. doi: 10.1021/bi00371a023.

Lahtz, C. and Pfeifer, G. P. (2011) 'Epigenetic changes of DNA repair genes in cancer', *Journal of Molecular Cell Biology*, 3(1), pp. 51–58. doi: 10.1093/jmcb/mjq053.

Lambert, H. E. and Berry, R. J. (1985) 'High dose cisplatin compared with high dose cyclophosphamide in the management of advanced epithelial ovarian cancer (FIGO stages III and IV): report from the North Thames Cooperative Group.', *BMJ*, 290(6472), pp. 889–893. doi: 10.1136/bmj.290.6472.889.

Latunde-Dada, G. O. (2017) 'Ferroptosis: Role of lipid peroxidation, iron and ferritinophagy', *Biochimica et Biophysica Acta (BBA) - General Subjects*, 1861(8), pp. 1893–1900. doi: 10.1016/j.bbagen.2017.05.019.

Lebeau, P. *et al.* (2018) 'Pharmacologic inhibition of S1P attenuates ATF6 expression, causes ER stress and contributes to apoptotic cell death', *Toxicology and Applied Pharmacology*, 349, pp. 1–7. doi: 10.1016/j.taap.2018.04.020.

Lee, M. C. Il *et al.* (2014) 'Measurement and characterization of superoxide generation from xanthine dehydrogenase: A redox-regulated pathway of radical generation in ischemic tissues', *Biochemistry*, 53(41), pp. 6615–6623. doi: 10.1021/bi500582r.

Lee, T. I. and Young, R. A. (2013) 'Transcriptional regulation and its misregulation in disease', *Cell*. NIH Public Access, pp. 1237–1251. doi: 10.1016/j.cell.2013.02.014.

Lei, P., Bai, T. and Sun, Y. (2019) 'Mechanisms of Ferroptosis and Relations With Regulated Cell Death: A Review', *Frontiers in Physiology*, 10(FEB). doi: 10.3389/fphys.2019.00139.

Leone, K., Poggiana, C. and Zamarchi, R. (2018) 'The Interplay between Circulating Tumor Cells and the Immune System: From Immune Escape to Cancer Immunotherapy', *Diagnostics*,

8(3), p. 59. doi: 10.3390/diagnostics8030059.

Lewandowska, J. and Bartoszek, A. (2011) ‘DNA methylation in cancer development, diagnosis and therapy - Multiple opportunities for genotoxic agents to act as methylome disruptors or remediators’, *Mutagenesis*, 26(4), pp. 475–487. doi: 10.1093/mutage/ger019.

Li, L. and Yang, X. (2018) ‘The Essential Element Manganese, Oxidative Stress, and Metabolic Diseases: Links and Interactions’, *Oxidative Medicine and Cellular Longevity*, 2018, pp. 1–11. doi: 10.1155/2018/7580707.

Li, M. Y. *et al.* (2001) ‘Quenching of Singlet Molecular Oxygen (1O2) by Azide Anion in Solvent Mixtures¶’, *Photochemistry and Photobiology*, 74(6), p. 760. doi: 10.1562/0031-8655(2001)074<0760:QOSMOO>2.0.CO;2.

Li, X. *et al.* (2013) ‘Targeting mitochondrial reactive oxygen species as novel therapy for inflammatory diseases and cancers’, *Journal of Hematology and Oncology*. BioMed Central Ltd. doi: 10.1186/1756-8722-6-19.

Li, Z. *et al.* (2014) ‘Battle against RNA oxidation: molecular mechanisms for reducing oxidized RNA to protect cells’, *Wiley Interdisciplinary Reviews: RNA*, 5(3), pp. 335–346. doi: 10.1002/wrna.1214.

Liberti, M. V. and Locasale, J. W. (2016) ‘The Warburg Effect: How Does it Benefit Cancer Cells?’, *Trends in Biochemical Sciences*. Elsevier Ltd, pp. 211–218. doi: 10.1016/j.tibs.2015.12.001.

Lichtenstein, R. G. and Rabinovich, G. A. (2013) ‘Glycobiology of cell death: when glycans and lectins govern cell fate’, *Cell Death & Differentiation*, 20(8), pp. 976–986. doi: 10.1038/cdd.2013.50.

Liguori, I. *et al.* (2018) ‘Oxidative stress, aging, and diseases’, *Clinical Interventions in Aging*. Dove Medical Press Ltd., pp. 757–772. doi: 10.2147/CIA.S158513.

Lin, C. T. *et al.* (2008) ‘Valproic acid resensitizes cisplatin-resistant ovarian cancer cells’,

Cancer Science, 99(6), pp. 1218–1226. doi: 10.1111/j.1349-7006.2008.00793.x.

Lin, Y., Xu, J. and Lan, H. (2019) 'Tumor-associated macrophages in tumor metastasis: Biological roles and clinical therapeutic applications', *Journal of Hematology and Oncology*. BioMed Central Ltd., pp. 1–16. doi: 10.1186/s13045-019-0760-3.

Lipinski, B. (2011) 'Hydroxyl radical and its scavengers in health and disease', *Oxidative Medicine and Cellular Longevity*. doi: 10.1155/2011/809696.

Liu, F. *et al.* (2017) 'Release of free amino acids upon oxidation of peptides and proteins by hydroxyl radicals', *Analytical and Bioanalytical Chemistry*, 409(9), pp. 2411–2420. doi: 10.1007/s00216-017-0188-y.

Liu, J. and Wang, Z. (2015) 'Increased oxidative stress as a selective anticancer therapy', *Oxidative Medicine and Cellular Longevity*. Hindawi Publishing Corporation. doi: 10.1155/2015/294303.

Logue, S. E., Elgendy, M. and Martin, S. J. (2009) 'Expression, purification and use of recombinant annexin V for the detection of apoptotic cells', *Nature Protocols*, 4(9), pp. 1383–1395. doi: 10.1038/nprot.2009.143.

Lopes-Rodrigues, V. *et al.* (2017) 'Identification of the metabolic alterations associated with the multidrug resistant phenotype in cancer and their intercellular transfer mediated by extracellular vesicles', *Scientific Reports*, 7(1), pp. 1–17. doi: 10.1038/srep44541.

Lopez, J., Ramchandani, D. and Vahdat, L. (2019) 'Copper Depletion as a Therapeutic Strategy in Cancer', in Carver, P. L. (ed.) *Essential Metals in Medicine: Therapeutic Use and Toxicity of Metal Ions in the Clinic*. Berlin, Boston: De Gruyter, pp. 303–330. doi: 10.1515/9783110527872-012.

Loreto, C. *et al.* (2014) 'The role of intrinsic pathway in apoptosis activation and progression in Peyronie's disease', *BioMed Research International*, 2014. doi: 10.1155/2014/616149.

Lorusso, G. and Rüegg, C. (2012) 'New insights into the mechanisms of organ-specific breast

cancer metastasis', *Seminars in Cancer Biology*. Academic Press, pp. 226–233. doi: 10.1016/j.semcancer.2012.03.007.

Lozano, G. (2019) 'Restoring p53 in cancer: the promises and the challenges', *Journal of Molecular Cell Biology*, 11(7), pp. 615–619. doi: 10.1093/jmcb/mjz063.

Lu, B. *et al.* (2018) 'The role of ferroptosis in cancer development and treatment response', *Frontiers in Pharmacology*, 8(JAN), pp. 1–8. doi: 10.3389/fphar.2017.00992.

De Luca, A. *et al.* (2019) 'A structure-based mechanism of cisplatin resistance mediated by glutathione transferase P1-1', *Proceedings of the National Academy of Sciences of the United States of America*, 116(28), pp. 13943–13951. doi: 10.1073/pnas.1903297116.

Luo, M. *et al.* (2010) 'Redox regulation of DNA repair: Implications for human health and cancer therapeutic development', *Antioxidants and Redox Signaling*, 12(11), pp. 1247–1269. doi: 10.1089/ars.2009.2698.

Luque-Cabal, M. *et al.* (2016) 'Mechanisms behind the resistance to trastuzumab in HER2-amplified breast cancer and strategies to overcome It', *Clinical Medicine Insights: Oncology*, 10(Suppl 1), pp. 21–30. doi: 10.4137/CMO.S34537.

Lutsenko, S. (2010) 'Human copper homeostasis: a network of interconnected pathways', *Current Opinion in Chemical Biology*, 14(2), pp. 211–217. doi: 10.1016/j.cbpa.2010.01.003.

Lv, Y. *et al.* (2015) 'Hypoxia-inducible factor-1α induces multidrug resistance protein in colon cancer', *OncoTargets and Therapy*, 8, pp. 1941–1948. doi: 10.2147/OTT.S82835.

Ma, Q. and He, X. (2012) 'Molecular Basis of Electrophilic and Oxidative Defense: Promises and Perils of Nrf2', *Pharmacological Reviews*. Edited by D. R. Sibley, 64(4), pp. 1055–1081. doi: 10.1124/pr.110.004333.

Macrides, T. A. *et al.* (1997) 'A comparison of the hydroxyl radical scavenging properties of the shark bile steroid 5β-scymnol and plant pycnogenols', *Biochemistry and Molecular Biology International*, 42(6), pp. 1249–1260. doi: 10.1080/15216549700203721.

Madden, E. *et al.* (2019) 'The role of the unfolded protein response in cancer progression: From oncogenesis to chemoresistance', *Biology of the Cell*, 111(1), pp. 1–17. doi: 10.1111/boc.201800050.

Maeda, M. *et al.* (2010) 'Dysregulation of the immune system caused by silica and asbestos', *Journal of Immunotoxicology*, pp. 268–278. doi: 10.3109/1547691X.2010.512579.

Majumder, S. *et al.* (2009) 'The role of copper in drug-resistant murine and human tumors', *BioMetals*, 22(2), pp. 377–384. doi: 10.1007/s10534-008-9174-3.

Makovec, Tomaz and Makovec, Tomaž (2019) 'Cisplatin and beyond: molecular mechanisms of action and drug resistance development in cancer chemotherapy', *Slovenia | www.radioloncol.com Radiol Oncol*, 53(2), pp. 148–158. doi: 10.2478/raon-2019-0018.

Malayappan, B. *et al.* (2007) 'Urinary analysis of 8-oxoguanine, 8-oxoguanosine, fapy-guanine and 8-oxo-2′-deoxyguanosine by high-performance liquid chromatography-electrospray tandem mass spectrometry as a measure of oxidative stress', *Journal of Chromatography A*, 1167(1), pp. 54–62. doi: 10.1016/j.chroma.2007.08.024.

Mallini, P. *et al.* (2014) 'Epithelial-to-mesenchymal transition: What is the impact on breast cancer stem cells and drug resistance', *Cancer Treatment Reviews*, 40(3), pp. 341–348. doi: 10.1016/j.ctrv.2013.09.008.

Mani, M. *et al.* (2013) 'Activation of Nrf2-antioxidant response element mediated glutamate cysteine ligase expression in hepatoma cell line by homocysteine', *Hepatitis Monthly*, 13(5), pp. 1–7. doi: 10.5812/hepatmon.8394.

Mann, B. S. *et al.* (2007) 'FDA approval summary: vorinostat for treatment of advanced primary cutaneous T-cell lymphoma.', *Oncologist*, 12(10), pp. 1247–52. doi: 10.1634/theoncologist.12-10-1247.

Mansoori, B. *et al.* (2017) 'The different mechanisms of cancer drug resistance: A brief review', *Advanced Pharmaceutical Bulletin*, pp. 339–348. doi: 10.15171/apb.2017.041.

Mariño, G. *et al.* (2014) 'Self-consumption: The interplay of autophagy and apoptosis', *Nature Reviews Molecular Cell Biology*, pp. 81–94. doi: 10.1038/nrm3735.

Marnett, L. J. (1999) 'Lipid peroxidation—DNA damage by malondialdehyde', *Mutation Research/Fundamental and Molecular Mechanisms of Mutagenesis*, 424(1–2), pp. 83–95. doi: 10.1016/S0027-5107(99)00010-X.

Martin, S. J. and Henry, C. M. (2013) 'Distinguishing between apoptosis, necrosis, necroptosis and other cell death modalities', *Methods*, 61(2), pp. 87–89. doi: 10.1016/j.ymeth.2013.06.001.

Martinez-Finley, E. J. *et al.* (2013) 'Manganese neurotoxicity and the role of reactive oxygen species', *Free Radical Biology and Medicine*, pp. 65–75. doi: 10.1016/j.freeradbiomed.2013.01.032.

Mashima, R. and Okuyama, T. (2015) 'The role of lipoxygenases in pathophysiology; new insights and future perspectives', *Redox Biology*, 6, pp. 297–310. doi: 10.1016/j.redox.2015.08.006.

Matsuzaki, H. *et al.* (2012) 'Asbestos-Induced Cellular and Molecular Alteration of Immunocompetent Cells and Their Relationship with Chronic Inflammation and Carcinogenesis', *Journal of Biomedicine and Biotechnology*, 2012, pp. 1–9. doi: 10.1155/2012/492608.

Maurel, M. *et al.* (2014) 'Getting RIDD of RNA: IRE1 in cell fate regulation', *Trends in Biochemical Sciences*, 39(5), pp. 245–254. doi: 10.1016/j.tibs.2014.02.008.

McCann, M. *et al.* (2012) 'Deciphering the Antimicrobial Activity of Phenanthroline Chelators', *Current Medicinal Chemistry*, 19(17), pp. 2703–2714. doi: 10.2174/092986712800609733.

McCann, S. *et al.* (1997) 'Manganese(II) complexes of 3,6,9-trioxaundecanedioic acid (3,6,9-tddaH2): X-ray crystal structures of [Mn(3,6,9-tdda) (H2O)2]·2H2O and {[Mn(3,6,9-tdda)(phen)2·3H2O]·EtOH}n', *Polyhedron*, 16(24), pp. 4247–4252. doi: 10.1016/S0277-

5387(97)00233-7.

McGivern, T. J. P., Afsharpour, S. and Marmion, C. J. (2018) ‘Copper complexes as artificial DNA metallonucleases: From Sigman’s reagent to next generation anti-cancer agent?’, *Inorganica Chimica Acta*, 472, pp. 12–39. doi: 10.1016/j.ica.2017.08.043.

McIlwain, D. R., Berger, T. and Mak, T. W. (2013) ‘Caspase functions in cell death and disease’, *Cold Spring Harbor Perspectives in Biology*, 5(4), pp. 1–28. doi: 10.1101/cshperspect.a008656.

McKeage, M. J., Higgins, J. D. and Kelland, L. R. (1991) ‘Platinum and other metal coordination compounds in cancer chemotherapy. A commentary on the sixth international symposium: San Diego, California, 23-26th January 1991.’, *British journal of cancer*, 64(4), pp. 788–92. Available at: http://www.pubmedcentral.nih.gov/articlerender.fcgi?artid=1977702&tool=pmcentrez&rendertype=abstract (Accessed: 5 October 2015).

Mcnally, E. J., Luncsford, P. J. and Armanios, M. (2019) ‘Long telomeres and cancer risk: the price of cellular immortality’, *J Clin Invest*, 129(9), p. 3474. doi: 10.1172/JCI120851.

McQuiston, A. and Diehl, J. A. (2017) ‘Recent insights into PERK-dependent signaling from the stressed endoplasmic reticulum’, *F1000Research*, 6, p. 1897. doi: 10.12688/f1000research.12138.1.

Micelli, C. and Rastelli, G. (2015) ‘Histone deacetylases: Structural determinants of inhibitor selectivity’, *Drug Discovery Today*, 20(6), pp. 718–735. doi: 10.1016/j.drudis.2015.01.007.

Mittal, D. *et al.* (2014) ‘New insights into cancer immunoediting and its three component phases-elimination, equilibrium and escape’, *Current Opinion in Immunology*, pp. 16–25. doi: 10.1016/j.coi.2014.01.004.

Mollet, I. G. *et al.* (2016) ‘Low Dose Iron Treatments Induce a DNA Damage Response in Human Endothelial Cells within Minutes’, *PLOS ONE*. Edited by O. R. Bandapalli, 11(2), p.

e0147990. doi: 10.1371/journal.pone.0147990.

Moloney, J. N. and Cotter, T. G. (2018) 'ROS signalling in the biology of cancer', *Seminars in Cell and Developmental Biology*. Elsevier Ltd, pp. 50–64. doi: 10.1016/j.semcdb.2017.05.023.

Molphy, Z. *et al.* (2015) 'DNA oxidation profiles of copper phenanthrene chemical nucleases', *Frontiers in Chemistry*, 3(April), pp. 1–9. doi: 10.3389/fchem.2015.00028.

Mondal, T. *et al.* (2018) 'DNA double strand breaks, repair and apoptosis following 511 keV γ-rays exposure using 18 fluorine positron emitter: An in-vitro study', *Biomedical Physics and Engineering Express*, 4(6). doi: 10.1088/2057-1976/aae5b9.

Moráň, L. *et al.* (2019) 'Mixed copper (ii)–phenanthroline complexes induce cell death of ovarian cancer cells by evoking the unfolded protein response', *Metallomics*, 11(9), pp. 1481–1489. doi: 10.1039/C9MT00055K.

Moras, M., Lefevre, S. D. and Ostuni, M. A. (2017) 'From erythroblasts to mature red blood cells: Organelle clearance in mammals', *Frontiers in Physiology*, 8(DEC), pp. 1–9. doi: 10.3389/fphys.2017.01076.

Morera, L., Lübbert, M. and Jung, M. (2016) 'Targeting histone methyltransferases and demethylases in clinical trials for cancer therapy', *Clinical Epigenetics*, 8(1), p. 57. doi: 10.1186/s13148-016-0223-4.

Mou, Y. *et al.* (2019) 'Ferroptosis, a new form of cell death: Opportunities and challenges in cancer', *Journal of Hematology and Oncology*, 12(1), pp. 1–16. doi: 10.1186/s13045-019-0720-y.

Mukhopadhyay, P. *et al.* (2007) 'Simultaneous detection of apoptosis and mitochondrial superoxide production in live cells by flow cytometry and confocal microscopy', *Nature Protocols*, 2(9), pp. 2295–2301. doi: 10.1038/nprot.2007.327.

Murakawa, G. J. *et al.* (1989) 'Scission of RNA by the chemical nuclease of 1,10-

phenanthroline-eopper ion: Preference for single-stranded loops', *Nucleic Acids Research*, 17(13), pp. 5361–5376. doi: 10.1093/nar/17.13.5361.

Murphy, M. P. (2009) 'How mitochondria produce reactive oxygen species', *Biochemical Journal*, pp. 1–13. doi: 10.1042/BJ20081386.

Nabel, C. S., Manning, S. A. and Kohli, R. M. (2012) 'The Curious Chemical Biology of Cytosine: Deamination, Methylation,and Oxidation as Modulators of Genomic Potential', *ACS Chemical Biology*, 7(1), pp. 20–30. doi: 10.1021/cb2002895.

Nair, P. *et al.* (2014) 'Apoptosis initiation through the cell-extrinsic pathway', in *Methods in Enzymology*. Academic Press Inc., pp. 99–128. doi: 10.1016/B978-0-12-417158-9.00005-4.

Najafov, A., Chen, H. and Yuan, J. (2017) 'Necroptosis and Cancer', *Trends in Cancer*. Cell Press, pp. 294–301. doi: 10.1016/j.trecan.2017.03.002.

Narang, A. S. and Varia, S. (2011) 'Role of tumor vascular architecture in drug delivery', *Advanced Drug Delivery Reviews*. Elsevier, pp. 640–658. doi: 10.1016/j.addr.2011.04.002.

Narayanan, D. L., Saladi, R. N. and Fox, J. L. (2010) 'Ultraviolet radiation and skin cancer', *International Journal of Dermatology*, pp. 978–986. doi: 10.1111/j.1365-4632.2010.04474.x.

Natarajan, K. A. (2018) 'Experimental and Research Methods in Metals Biotechnology', in *Biotechnology of Metals*. Elsevier, pp. 433–468. doi: 10.1016/b978-0-12-804022-5.00014-1.

Ndagi, U., Mhlongo, N. and Soliman, M. (2017) 'Metal complexes in cancer therapy-an update from drug design perspective', *Drug Design, Development and Therapy*, 11, pp. 599–616. doi: 10.2147/DDDT.S119488.

Newcomer, M. E. and Brash, A. R. (2015) 'The structural basis for specificity in lipoxygenase catalysis', *Protein Science*, 24(3), pp. 298–309. doi: 10.1002/pro.2626.

Nguyen, T., Nioi, P. and Pickett, C. B. (2009) 'The Nrf2-Antioxidant Response Element Signaling Pathway and Its Activation by Oxidative Stress', *Journal of Biological Chemistry*, 284(20), pp. 13291–13295. doi: 10.1074/jbc.R900010200.

Nicolini, A. *et al.* (2018) ‘Tumour growth and immune evasion as targets for a new strategy in advanced cancer’, *Endocrine-related cancer*, 25(11). doi: 10.1530/ERC-18-0142.

Niki, E. (2015) ‘Evidence for beneficial effects of vitamin E’, *Korean Journal of Internal Medicine*. Korean Association of Internal Medicine, pp. 571–579. doi: 10.3904/kjim.2015.30.5.571.

Niles, J. C., Wishnok, J. S. and Tannenbaum, S. R. (2006) ‘Peroxynitrite-induced oxidation and nitration products of guanine and 8-oxoguanine: Structures and mechanisms of product formation’, *Nitric Oxide - Biology and Chemistry*, 14(2 SPEC. ISS.), pp. 109–121. doi: 10.1016/j.niox.2005.11.001.

Nishikawa, S. *et al.* (2014) ‘A molecular targeting against nuclear factor- κ B, as a chemotherapeutic approach for human malignant mesothelioma’, *Cancer Medicine*, 3(2), pp. 416–425. doi: 10.1002/cam4.202.

Nishimura, R. N. and Dwyer, B. E. (1995) ‘Pharmacological induction of heat shock protein 68 synthesis in cultured rat astrocytes’, *Journal of Biological Chemistry*, 270(50), pp. 29967–29970. doi: 10.1074/jbc.270.50.29967.

Nishimura, Y. *et al.* (2013) ‘Altered functions of alveolar macrophages and NK cells involved in asbestos-related diseases’, *Environmental Health and Preventive Medicine*, pp. 198–204. doi: 10.1007/s12199-013-0333-y.

Nishinaka, Y. *et al.* (2011) ‘Singlet oxygen is essential for neutrophil extracellular trap formation’, *Biochemical and Biophysical Research Communications*, 413(1), pp. 75–79. doi: 10.1016/j.bbrc.2011.08.052.

Norbet, C. *et al.* (2015) ‘Asbestos-Related Lung Disease: A Pictorial Review’, *Current Problems in Diagnostic Radiology*. Mosby Inc., pp. 371–382. doi: 10.1067/j.cpradiol.2014.10.002.

Nunes-Souza, V. *et al.* (2020) ‘3-Amino-1,2,4-Triazole Induces Quick and Strong Fat Loss in

Mice with High Fat-Induced Metabolic Syndrome', *Oxidative Medicine and Cellular Longevity*, 2020, pp. 1–14. doi: 10.1155/2020/3025361.

Nunes, P. *et al.* (2020) 'Copper Complexes with 1,10-Phenanthroline Derivatives: Underlying Factors Affecting Their Cytotoxicity', *Inorganic Chemistry*, 59(13), pp. 9116–9134. doi: 10.1021/acs.inorgchem.0c00925.

Nunomura, A. *et al.* (2017) 'Consequences of RNA oxidation on protein synthesis rate and fidelity: Implications for the pathophysiology of neuropsychiatric disorders', *Biochemical Society Transactions*. Portland Press Ltd, pp. 1053–1066. doi: 10.1042/BST20160433.

Nynäs, P. *et al.* (2017) 'Cancer Incidence in Asbestos-Exposed Workers: An Update on Four Finnish Cohorts', *Safety and Health at Work*, 8(2), pp. 169–174. doi: 10.1016/j.shaw.2016.11.003.

O'Brien, E. *et al.* (2018) 'Substrate Binding Regulates Redox Signaling in Human DNA Primase', *Journal of the American Chemical Society*, 140(49), pp. 17153–17162. doi: 10.1021/jacs.8b09914.

O'Brien, J. *et al.* (2000) 'Investigation of the Alamar Blue (resazurin) fluorescent dye for the assessment of mammalian cell cytotoxicity', *European Journal of Biochemistry*, 267(17), pp. 5421–5426. doi: 10.1046/j.1432-1327.2000.01606.x.

O'Keeffe, L. M. *et al.* (2018) 'Smoking as a risk factor for lung cancer in women and men: A systematic review and meta-analysis', *BMJ Open*. BMJ Publishing Group. doi: 10.1136/bmjopen-2018-021611.

O'Neal, S. L. and Zheng, W. (2015) 'Manganese Toxicity Upon Overexposure: a Decade in Review', *Current Environmental Health Reports*, 2(3), pp. 315–328. doi: 10.1007/s40572-015-0056-x.

Ock, C. Y. *et al.* (2012) '8-hydroxydeoxyguanosine: Not mere biomarker for oxidative stress, but remedy for oxidative stress-implicated gastrointestinal diseases', *World Journal of*

Gastroenterology, 18(4), pp. 302–308. doi: 10.3748/wjg.v18.i4.302.

Ogundele, O. M. *et al.* (2017) 'Differential oxidative stress thresholds distinguishes cellular response to vascular occlusion and chemotoxicity in vivo', *Drug and Chemical Toxicology*, 40(1), pp. 101–109. doi: 10.1080/01480545.2016.1188300.

Ohtani, N. *et al.* (2004) 'The p16INK4a-RB pathway: Molecular link between cellular senescence and tumor suppression', *Journal of Medical Investigation*, pp. 146–153. doi: 10.2152/jmi.51.146.

Oikonomou, E. and Pintzas, A. (2013) 'The TRAIL of oncogenes to apoptosis', *BioFactors*, 39(4), pp. 343–354. doi: 10.1002/biof.1112.

Ojha, R. and Amaravadi, R. K. (2017) 'Targeting the unfolded protein response in cancer', *Pharmacological Research*, 120, pp. 258–266. doi: 10.1016/j.phrs.2017.04.003.

Onyango, A. N. (2016) 'Endogenous generation of singlet oxygen and ozone in human and animal tissues: Mechanisms, biological significance, and influence of dietary components', *Oxidative Medicine and Cellular Longevity*, 2016. doi: 10.1155/2016/2398573.

Ortega, Á. L., Mena, S. and Estrela, J. M. (2010) 'Oxidative and Nitrosative Stress in the Metastatic Microenvironment', *Cancers*, 2, pp. 274–304. doi: 10.3390/cancers2020274.

Ostuni, R. *et al.* (2015) 'Macrophages and cancer: From mechanisms to therapeutic implications', *Trends in Immunology*. Elsevier Ltd, pp. 229–239. doi: 10.1016/j.it.2015.02.004.

Ozaki, T. and Nakagawara, A. (2011) 'Role of p53 in cell death and human cancers', *Cancers*, 3(1), pp. 994–1013. doi: 10.3390/cancers3010994.

Ozcan, A. and Ogun, M. (2015) 'Biochemistry of Reactive Oxygen and Nitrogen Species', in *Basic Principles and Clinical Significance of Oxidative Stress*. InTech, p. 13. doi: 10.5772/61193.

Pacheco-Yepez, J. *et al.* (2014) 'Peroxynitrite and peroxiredoxin in the pathogenesis of experimental amebic liver abscess', *BioMed Research International*. Hindawi Publishing

Corporation. doi: 10.1155/2014/324230.

Padhi, B. K. *et al.* (2018) 'A PCR-based quantitative assay for the evaluation of mRNA integrity in rat samples', *Biomolecular Detection and Quantification*, 15(December 2017), pp. 18–23. doi: 10.1016/j.bdq.2018.02.001.

Panday, A. *et al.* (2015) 'NADPH oxidases: An overview from structure to innate immunity-associated pathologies', *Cellular and Molecular Immunology*. Chinese Soc Immunology, pp. 5–23. doi: 10.1038/cmi.2014.89.

Pandey, A. N. (2014) 'Retinoblastoma: An overview', *Saudi Journal of Ophthalmology*. Elsevier, pp. 310–315. doi: 10.1016/j.sjopt.2013.11.001.

Pang, L. Y., Hurst, E. A. and Argyle, D. J. (2016) 'Cyclooxygenase-2: A Role in Cancer Stem Cell Survival and Repopulation of Cancer Cells during Therapy', *Stem Cells International*, 2016, pp. 1–11. doi: 10.1155/2016/2048731.

Panieri, E. and Saso, L. (2019) 'Potential applications of NRF2 inhibitors in cancer therapy', *Oxidative Medicine and Cellular Longevity*, 2019. doi: 10.1155/2019/8592348.

Papavassiliou, A. G. (1995) 'Chemical nucleases as probes for studying DNA-protein interactions', *Biochemical Journal*, 305(2), pp. 345–357. doi: 10.1042/bj3050345.

Parrish, A. B., Freel, C. D. and Kornbluth, S. (2013) 'Cellular mechanisms controlling caspase activation and function', *Cold Spring Harbor Perspectives in Biology*, 5(6). doi: 10.1101/cshperspect.a008672.

Parsa, N. (2012) 'Environmental factors inducing human cancers', *Iranian Journal of Public Health*. Iranian Journal of Public Health, pp. 1–9.

Patel, V. *et al.* (2015) 'Expression of executioner procaspases and their activation by a procaspase-activating compound in chronic lymphocytic leukemia cells', *Blood*, 125(7), pp. 1126–1136. doi: 10.1182/blood-2014-01-546796.

Pavlova, N. N. and Thompson, C. B. (2016) 'The Emerging Hallmarks of Cancer Metabolism',

Cell Metabolism, pp. 27–47. doi: 10.1016/j.cmet.2015.12.006.

Peltanova, B., Raudenska, M. and Masarik, M. (2019) 'Effect of tumor microenvironment on pathogenesis of the head and neck squamous cell carcinoma: A systematic review', *Molecular Cancer*. BioMed Central Ltd. doi: 10.1186/s12943-019-0983-5.

Percival, M. D. *et al.* (1992) 'Investigation of the mechanism of non-turnover-dependent inactivation of purified human 5-lipoxygenase. Inactivation by H2O2 and inhibition by metal ions', *European Journal of Biochemistry*, 210(1), pp. 109–117. doi: 10.1111/j.1432-1033.1992.tb17397.x.

Petruccelli, L. A. *et al.* (2011) 'Vorinostat Induces Reactive Oxygen Species and DNA Damage in Acute Myeloid Leukemia Cells', *PLoS ONE*. Edited by V. Cheriyath, 6(6), p. e20987. doi: 10.1371/journal.pone.0020987.

Peyrone, M. (1844) 'Ueber die Einwirkung des Ammoniaks auf Platinchlorür', *Annalen der Chemie und Pharmacie*, 51(1), pp. 1–29. doi: 10.1002/jlac.18440510102.

Pham, A. N. *et al.* (2013) 'Fenton-like copper redox chemistry revisited: Hydrogen peroxide and superoxide mediation of copper-catalyzed oxidant production', *Journal of Catalysis*, 301, pp. 54–64. doi: 10.1016/j.jcat.2013.01.025.

Phaniendra, A., Jestadi, D. B. and Periyasamy, L. (2015) 'Free Radicals: Properties, Sources, Targets, and Their Implication in Various Diseases', *Indian Journal of Clinical Biochemistry*, 30(1), pp. 11–26. doi: 10.1007/s12291-014-0446-0.

Pietsch, E. C. *et al.* (2008) 'The p53 family and programmed cell death', *Oncogene*, 27(50), pp. 6507–6521. doi: 10.1038/onc.2008.315.

Pilco-Ferreto, N. and Calaf, G. M. (2016) 'Influence of doxorubicin on apoptosis and oxidative stress in breast cancer cell lines', *International Journal of Oncology*, 49(2), pp. 753–762. doi: 10.3892/ijo.2016.3558.

Pinheiro, C. *et al.* (2015) 'Reprogramming energy metabolism and inducing angiogenesis: Co-

expression of monocarboxylate transporters with VEGF family members in cervical adenocarcinomas', *BMC Cancer*, 15(1). doi: 10.1186/s12885-015-1842-4.

Pitale, P. M., Gorbatyuk, O. and Gorbatyuk, M. (2017) 'Neurodegeneration: Keeping ATF4 on a Tight Leash', *Frontiers in Cellular Neuroscience*, 11, p. 410. doi: 10.3389/fncel.2017.00410.

Pitié, M., Boldron, C. and Pratviel, G. (2006) 'DNA Oxidation by Copper and Manganese Complexes', in, pp. 77–130. doi: 10.1016/S0898-8838(05)58003-6.

Pluta, P. *et al.* (2015) 'Expression of IAP family proteins and its clinical importance in breast cancer patients', *Neoplasma*, 62(4), pp. 666–673. doi: 10.4149/neo_2015_080.

Pobezinskaya, Y. L. and Liu, Z. (2012) 'The role of TRADD in death receptor signaling', *Cell Cycle*. Taylor and Francis Inc., pp. 871–876. doi: 10.4161/cc.11.5.19300.

Poulos, T. L. (2014) 'Heme Enzyme Structure and Function', *Chemical Reviews*, 114(7), pp. 3919–3962. doi: 10.1021/cr400415k.

Poulsen, H. E. *et al.* (2012) 'RNA modifications by oxidation: A novel disease mechanism?', *Free Radical Biology and Medicine*, 52(8), pp. 1353–1361. doi: 10.1016/j.freeradbiomed.2012.01.009.

Povirk, L. F. (2012) 'Processing of Damaged DNA Ends for Double-Strand Break Repair in Mammalian Cells', *ISRN Molecular Biology*, 2012, pp. 1–16. doi: 10.5402/2012/345805.

Prasad, S. B. *et al.* (2015) 'PI3K/AKT pathway-mediated regulation of p27Kip1 is associated with cell cycle arrest and apoptosis in cervical cancer', *Cellular Oncology*, 38(3), pp. 215–225. doi: 10.1007/s13402-015-0224-x.

Prisecaru, A. *et al.* (2012) 'Potent oxidative DNA cleavage by the di-copper cytotoxin: [Cu2(μ-terephthalate)(1,10-phen)4]2+', *Chemical Communications*, 48(55), p. 6906. doi: 10.1039/c2cc31023f.

Qin, X. *et al.* (2019) 'The role of necroptosis in cancer: A double-edged sword?', *Biochimica et Biophysica Acta (BBA) - Reviews on Cancer*, 1871(2), pp. 259–266. doi:

10.1016/j.bbcan.2019.01.006.

Radi, R. (2018) ‘Oxygen radicals, nitric oxide, and peroxynitrite: Redox pathways in molecular medicine’, *Proceedings of the National Academy of Sciences of the United States of America*, 115(23), pp. 5839–5848. doi: 10.1073/pnas.1804932115.

Rahman, K. (2007) ‘Studies on free radicals, antioxidants, and co-factors.’, *Clinical interventions in aging*, pp. 219–236.

Rajabi, M. and Mousa, S. A. (2017) ‘The role of angiogenesis in cancer treatment’, *Biomedicines*. MDPI AG. doi: 10.3390/biomedicines5020034.

Ramírez, A. *et al.* (2016) ‘Ion Channels and Oxidative Stress as a Potential Link for the Diagnosis or Treatment of Liver Diseases’, *Oxidative Medicine and Cellular Longevity*, 2016, pp. 1–17. doi: 10.1155/2016/3928714.

Ray Chaudhuri, A. and Nussenzweig, A. (2017) ‘The multifaceted roles of PARP1 in DNA repair and chromatin remodelling’, *Nature Reviews Molecular Cell Biology*, 18(10), pp. 610–621. doi: 10.1038/nrm.2017.53.

Ray, P. D., Huang, B. W. and Tsuji, Y. (2012) ‘Reactive oxygen species (ROS) homeostasis and redox regulation in cellular signaling’, *Cellular Signalling*, pp. 981–990. doi: 10.1016/j.cellsig.2012.01.008.

Redza-Dutordoir, M. and Averill-Bates, D. A. (2016) ‘Activation of apoptosis signalling pathways by reactive oxygen species’, *Biochimica et Biophysica Acta - Molecular Cell Research*, 1863(12), pp. 2977–2992. doi: 10.1016/j.bbamcr.2016.09.012.

Reed, S. M. and Quelle, D. E. (2014) ‘P53 acetylation: Regulation and consequences’, *Cancers*, 7(1), pp. 30–69. doi: 10.3390/cancers7010030.

Reinert, T. *et al.* (2013) ‘Bleomycin-Induced Lung Injury’, *Journal of Cancer Research*, 2013, pp. 1–9. doi: 10.1155/2013/480608.

Reuter, S. *et al.* (2010) ‘Oxidative stress, inflammation, and cancer: How are they linked?’,

Free Radical Biology and Medicine, 49(11), pp. 1603–1616. doi: 10.1016/j.freeradbiomed.2010.09.006.

Ribeiro Franco, P. I. *et al.* (2020) 'Tumor microenvironment components: Allies of cancer progression', *Pathology Research and Practice*. Elsevier GmbH. doi: 10.1016/j.prp.2019.152729.

Richon, V. M. (2006) 'Cancer biology: Mechanism of antitumour action of vorinostat (suberoylanilide hydroxamic acid), a novel histone deacetylase inhibitor', *British Journal of Cancer*, 95(SUPPL. 1), pp. 2–6. doi: 10.1038/sj.bjc.6603463.

Rivera, R. M. and Bennett, L. B. (2010) 'Epigenetics in humans: an overview', *Current Opinion in Endocrinology, Diabetes and Obesity*, 17(6), pp. 493–499. doi: 10.1097/MED.0b013e3283404f4b.

Rivlin, N. *et al.* (2011) 'Mutations in the p53 tumor suppressor gene: Important milestones at the various steps of tumorigenesis', *Genes and Cancer*, pp. 466–474. doi: 10.1177/1947601911408889.

Robert, G. and Wagner, J. R. (2019) 'Tandem Lesions Arising from 5-(Uracilyl)methyl Peroxyl Radical Addition to Guanine: Product Analysis and Mechanistic Studies', *Chemical Research in Toxicology*, p. acs.chemrestox.9b00407. doi: 10.1021/acs.chemrestox.9b00407.

Robinson, N. *et al.* (2019) 'Programmed necrotic cell death of macrophages: Focus on pyroptosis, necroptosis, and parthanatos', *Redox Biology*. Elsevier B.V. doi: 10.1016/j.redox.2019.101239.

Rocha, C. R. R. *et al.* (2014) 'Glutathione depletion sensitizes cisplatin- and temozolomide-resistant glioma cells in vitro and in vivo', *Cell Death and Disease*, 5(10), pp. 1–10. doi: 10.1038/cddis.2014.465.

Rocha, C. R. R. *et al.* (2018) 'DNA repair pathways and cisplatin resistance: An intimate relationship', *Clinics*, 73(8), pp. 1–10. doi: 10.6061/clinics/2018/e478s.

Rochford, G. (2018) *Investigating the mechanistic mode of action of novel Cu(II) complexes as potential chemotherapeutics drugs*.

Rodenhiser, D. and Mann, M. (2006) 'Epigenetics and human disease: Translating basic biology into clinical applications', *Cmaj*, 174(3), pp. 341–348. doi: 10.1503/cmaj.050774.

Røe, O. D. and Stella, G. M. (2015) 'Malignant pleural mesothelioma: History, controversy and future of a manmade epidemic', *European Respiratory Review*. European Respiratory Society, pp. 115–131. doi: 10.1183/09059180.00007014.

Rojo, A. I. *et al.* (2014) 'The PTEN/NRF2 axis promotes human carcinogenesis', *Antioxidants and Redox Signaling*, 21(18), pp. 2498–2514. doi: 10.1089/ars.2014.5843.

Rosenberg, B. *et al.* (1967) 'The inhibition of growth or cell division in Escherichia coli by different ionic species of platinum(IV) complexes.', *Journal of Biological Chemistry*, 242(6), pp. 1347–1352.

Rosenberg, B. *et al.* (1969) 'Platinum compounds: A new class of potent antitumour agents [24]', *Nature*. Nature Publishing Group, pp. 385–386. doi: 10.1038/222385a0.

Rosenberg, B. (1971) 'Some biological effects of platinum compounds', *Metalurgija/Metallurgy*, 15(2), pp. 42–51.

Rosenberg, B., Van Camp, L. and Krigas, T. (1965) 'Inhibition of cell division in Escherichia coli by electrolysis products from a platinum electrode', *Nature*. Nature Publishing Group, pp. 698–699. doi: 10.1038/205698a0.

Rosenblum, W. I. and El-Sabban, F. (1982) 'Dimethyl sulfoxide (dmso) and glycerol, hydroxyl radical scavengers, impair platelet aggregation within and eliminate the accompanying vasodilation of, injured mouse pial arterioles', *Stroke*, 13(1), pp. 35–39. doi: 10.1161/01.STR.13.1.35.

Rouault, T. A. (2012) 'Biogenesis of iron-sulfur clusters in mammalian cells: New insights and relevance to human disease', *DMM Disease Models and Mechanisms*, 5(2), pp. 155–164. doi:

10.1242/dmm.009019.

Rouault, T. A. (2016) ‘Mitochondrial iron overload: Causes and consequences’, *Current Opinion in Genetics and Development*. Elsevier Ltd, pp. 31–37. doi: 10.1016/j.gde.2016.02.004.

Roy, A. *et al.* (2012) ‘Sodium phenylbutyrate controls neuroinflammatory and antioxidant activities and protects dopaminergic neurons in mouse models of Parkinson’s disease’, *PLoS ONE*, 7(6). doi: 10.1371/journal.pone.0038113.

Roy, S. *et al.* (2008) ‘Phenanthroline derivatives with improved selectivity as DNA-targeting anticancer or antimicrobial drugs’, *ChemMedChem*, 3(9), pp. 1427–1434. doi: 10.1002/cmdc.200800097.

Rozpedek, W. *et al.* (2016) ‘The Role of the PERK/eIF2α/ATF4/CHOP Signaling Pathway in Tumor Progression During Endoplasmic Reticulum Stress’, *Current Molecular Medicine*, 16(6), pp. 533–544. doi: 10.2174/1566524016666160523143937.

Ruggiano, A., Foresti, O. and Carvalho, P. (2014) ‘ER-associated degradation: Protein quality control and beyond’, *The Journal of Cell Biology*, 204(6), pp. 869–879. doi: 10.1083/jcb.201312042.

Rupp, J. C. *et al.* (2017) ‘Host Cell Copper Transporters CTR1 and ATP7A are important for Influenza A virus replication’, *Virology Journal*, 14(1), pp. 1–12. doi: 10.1186/s12985-016-0671-7.

Sachdeva, M. *et al.* (2014) ‘Oxidants and Antioxidants in Complementary and Alternative Medicine: A Review’, *Spatula DD - Peer Reviewed Journal on Complementary Medicine and Drug Discovery*, 4(1), p. 1. doi: 10.5455/spatula.20140131074751.

Salehan, M. R. and Morse, H. R. (2013) ‘DNA damage repair and tolerance: A role in chemotherapeutic drug resistance’, *British Journal of Biomedical Science*. Step Publishing Ltd., pp. 31–40. doi: 10.1080/09674845.2013.11669927.

Salvador, J. M., Brown-Clay, J. D. and Fornace, A. J. (2013) 'Gadd45 in stress signaling, cell cycle control, and apoptosis', *Advances in Experimental Medicine and Biology*, 793, pp. 1–19. doi: 10.1007/978-1-4614-8289-5_1.

Sanchez-Vega, F. *et al.* (2018) 'Oncogenic Signaling Pathways in The Cancer Genome Atlas', *Cell*, 173(2), pp. 321-337.e10. doi: 10.1016/j.cell.2018.03.035.

Sangawa, A. *et al.* (2014) 'Phosphorylation status of Akt and caspase-9 in gastric and colorectal carcinomas', *International Journal of Clinical and Experimental Pathology*, 7(6), pp. 3312–3317. Available at: http://www.ncbi.nlm.nih.gov/pubmed/25031754 (Accessed: 25 January 2020).

Sano, R. and Reed, J. C. (2013) 'ER stress-induced cell death mechanisms', *Biochimica et Biophysica Acta - Molecular Cell Research*, 1833(12), pp. 3460–3470. doi: 10.1016/j.bbamcr.2013.06.028.

Santa-Gonzalez, G. A. *et al.* (2016) 'Distinctive adaptive response to repeated exposure to hydrogen peroxide associated with upregulation of DNA repair genes and cell cycle arrest', *Redox Biology*, 9, pp. 124–133. doi: 10.1016/j.redox.2016.07.004.

Saraste, A. (2000) 'Morphologic and biochemical hallmarks of apoptosis', *Cardiovascular Research*, 45(3), pp. 528–537. doi: 10.1016/S0008-6363(99)00384-3.

Sato, M. *et al.* (2018) 'The ferroptosis inducer erastin irreversibly inhibits system xc- and synergizes with cisplatin to increase cisplatin's cytotoxicity in cancer cells', *Scientific Reports*, 8(1), pp. 1–9. doi: 10.1038/s41598-018-19213-4.

Schell, M. J. *et al.* (2016) 'A multigene mutation classification of 468 colorectal cancers reveals a prognostic role for APC', *Nature Communications*, 7. doi: 10.1038/ncomms11743.

Scheper, W. and Hoozemans, J. J. M. (2015) 'The unfolded protein response in neurodegenerative diseases: a neuropathological perspective', *Acta Neuropathologica*, 130(3), pp. 315–331. doi: 10.1007/s00401-015-1462-8.

Schieber, M. and Chandel, N. S. (2014) ‘ROS function in redox signaling and oxidative stress’, *Current Biology*, 24(10), pp. R453–R462. doi: 10.1016/j.cub.2014.03.034.

Scourzic, L., Mouly, E. and Bernard, O. A. (2015) ‘TET proteins and the control of cytosine demethylation in cancer’, *Genome Medicine*, 7(1), p. 9. doi: 10.1186/s13073-015-0134-6.

Sczepanski, J. T. *et al.* (2010) ‘Rapid DNA-protein cross-linking and strand scission by an abasic site in a nucleosome core particle’, *Proceedings of the National Academy of Sciences of the United States of America*, 107(52), pp. 22475–22480. doi: 10.1073/pnas.1012860108.

Seibt, T. M., Proneth, B. and Conrad, M. (2019) ‘Role of GPX4 in ferroptosis and its pharmacological implication’, *Free Radical Biology and Medicine*, 133(September 2018), pp. 144–152. doi: 10.1016/j.freeradbiomed.2018.09.014.

Seifert, L. *et al.* (2016) ‘The necrosome promotes pancreatic oncogenesis via CXCL1 and Mincle-induced immune suppression’, *Nature*, 532(7598), pp. 245–249. doi: 10.1038/nature17403.

Seifert, L. and Miller, G. (2017) ‘Molecular pathways: The necrosome-A target for cancer therapy’, *Clinical Cancer Research*, 23(5), pp. 1132–1136. doi: 10.1158/1078-0432.CCR-16-0968.

Seija, M. *et al.* (2012) ‘Role of Peroxynitrite in Sepsis-Induced Acute Kidney injury in an experimental model of Sepsis Rats’, *Shock*, 38(4), pp. 403–410. doi: 10.1097/SHK.0b013e31826660f2.

Seo, Y. A., Li, Y. and Wessling-Resnick, M. (2013) ‘Iron depletion increases manganese uptake and potentiates apoptosis through ER stress’, *NeuroToxicology*, 38, pp. 67–73. doi: 10.1016/j.neuro.2013.06.002.

Seyfried, T. N. and Huysentruyt, L. C. (2013) ‘On the origin of cancer metastasis’, *Critical Reviews in Oncogenesis*, 18(1–2), pp. 43–73. doi: 10.1615/CritRevOncog.v18.i1-2.40.

Shahidi, F. and Zhong, Y. (2010) ‘Lipid oxidation and improving the oxidative stability’,

Chemical Society Reviews, 39(11), pp. 4067–4079. doi: 10.1039/b922183m.

Shakeri, R., Kheirollahi, A. and Davoodi, J. (2017) 'Apaf-1: Regulation and function in cell death', *Biochimie*. Elsevier B.V., pp. 111–125. doi: 10.1016/j.biochi.2017.02.001.

Shan, X. and Lin, C. G. (2006) 'Quantification of oxidized RNAs in Alzheimer's disease', *Neurobiology of Aging*, 27(5), pp. 657–662. doi: 10.1016/j.neurobiolaging.2005.03.022.

Shan, X., Tashiro, H. and Lin, C. G. (2003) 'The Identification and Characterization of Oxidized RNAs in Alzheimer ' s Disease mal processing of proteins occurred to the oxidized mRNAs . This may implicate the potential contribution of RNA oxidation in the', *The Journal of neuroscience*, 23(12), pp. 4913–4921.

Sharma, G. *et al.* (2010) 'CpG hypomethylation of MDR1 gene in tumor and serum of invasive ductal breast carcinoma patients', *Clinical Biochemistry*, 43(4–5), pp. 373–379. doi: 10.1016/j.clinbiochem.2009.10.009.

Sharma, P. *et al.* (2012) 'Reactive Oxygen Species, Oxidative Damage, and Antioxidative Defense Mechanism in Plants under Stressful Conditions', *Journal of Botany*, 2012, pp. 1–26. doi: 10.1155/2012/217037.

Sharma, S., Kelly, T. K. and Jones, P. a. (2009) 'Epigenetics in cancer', *Carcinogenesis*, 31(1), pp. 27–36. doi: 10.1093/carcin/bgp220.

Shechter, D. *et al.* (2007) 'Extraction, purification and analysis of histones', *Nat Protoc*, 2(6), pp. 1445–1457. doi: 10.1038/nprot.2007.202.

Shi, Y. (2004) 'Caspase activation, inhibition, and reactivation: A mechanistic view', *Protein Science*, 13(8), pp. 1979–1987. doi: 10.1110/ps.04789804.

Shi, Y. *et al.* (2014) 'ROS-dependent activation of JNK converts p53 into an efficient inhibitor of oncogenes leading to robust apoptosis', *Cell Death and Differentiation*, 21(4), pp. 612–623. doi: 10.1038/cdd.2013.186.

Shin, H.-J. *et al.* (2015) 'Doxorubicin-induced necrosis is mediated by poly-(ADP-ribose)

polymerase 1 (PARP1) but is independent of p53', *Scientific Reports*, 5(1), p. 15798. doi: 10.1038/srep15798.

Shintoku, R. *et al.* (2017) 'Lipoxygenase-mediated generation of lipid peroxides enhances ferroptosis induced by erastin and RSL3', *Cancer Science*, 108(11), pp. 2187–2194. doi: 10.1111/cas.13380.

Shiono, Y. *et al.* (2001) 'Iron accumulation in the liver of male patients with Wilson's disease', *The American Journal of Gastroenterology*, 96(11), pp. 3147–3151. doi: 10.1111/j.1572-0241.2001.05269.x.

Shirley, S., Morizot, A. and Micheau, O. (2011) 'Regulating TRAIL Receptor-Induced Cell Death at the Membrane: A Deadly Discussion', *Recent Patents on Anti-Cancer Drug Discovery*, 6(3), pp. 311–323. doi: 10.2174/157489211796957757.

Shogren-Knaak, M. *et al.* (2006) 'Histone H4-K16 acetylation controls chromatin structure and protein interactions.', *Science (New York, N.Y.)*, 311(5762), pp. 844–847. doi: 10.1126/science.1124000.

Shoulkamy, M. I. *et al.* (2012) 'Detection of DNA-protein crosslinks (DPCs) by novel direct fluorescence labeling methods: Distinct stabilities of aldehyde and radiation-induced DPCs', *Nucleic Acids Research*, 40(18). doi: 10.1093/nar/gks601.

Shukla, S. and Meeran, S. M. (2014) 'Epigenetics of cancer stem cells: Pathways and therapeutics', *Biochimica et Biophysica Acta - General Subjects*, 1840(12), pp. 3494–3502. doi: 10.1016/j.bbagen.2014.09.017.

Sies, H. (2017) 'Hydrogen peroxide as a central redox signaling molecule in physiological oxidative stress: Oxidative eustress', *Redox Biology*, 11, pp. 613–619. doi: 10.1016/j.redox.2016.12.035.

Sigman, D. S. *et al.* (1979) 'Oxygen-dependent Cleavage of DNA by the l,lO-Phenanthroline Cuprous complex', *Journal of Biological Chemistry*, 254(24), pp. 12269–12272.

Silva, B. and Faustino, P. (2015) 'An overview of molecular basis of iron metabolism regulation and the associated pathologies', *Biochimica et Biophysica Acta - Molecular Basis of Disease*, 1852(7), pp. 1347–1359. doi: 10.1016/j.bbadis.2015.03.011.

Simms, C. L. *et al.* (2014) 'An active role for the ribosome in determining the fate of oxidized mRNA', *Cell Reports*, 9(4), pp. 1256–1264. doi: 10.1038/mp.2011.182.doi.

Singh, R., Letai, A. and Sarosiek, K. (2019) 'Regulation of apoptosis in health and disease: the balancing act of BCL-2 family proteins', *Nature Reviews Molecular Cell Biology*, 20(3), pp. 175–193. doi: 10.1038/s41580-018-0089-8.

Skouta, R. *et al.* (2014) 'Ferrostatins inhibit oxidative lipid damage and cell death in diverse disease models', *Journal of the American Chemical Society*, 136(12), pp. 4551–4556. doi: 10.1021/ja411006a.

Slator, C. *et al.* (2017) 'Triggering autophagic cell death with a di-manganese(II) developmental therapeutic', *Redox Biology*, 12(October 2016), pp. 150–161. doi: 10.1016/j.redox.2017.01.024.

Slator, C. *et al.* (2018) 'Di-copper metallodrugs promote NCI-60 chemotherapy via singlet oxygen and superoxide production with tandem TA/TA and AT/AT oligonucleotide discrimination', *Nucleic Acids Research*, 46(6), pp. 1–18. doi: 10.1093/nar/gky105.

Smith, M. R. *et al.* (2017) 'Redox dynamics of manganese as a mitochondrial life-death switch', *Biochemical and Biophysical Research Communications*, 482(3), pp. 388–398. doi: 10.1016/j.bbrc.2016.10.126.

Sodani, K. *et al.* (2012) 'Multidrug resistance associated proteins in multindrung resistance', *Chinese Journal of Cancer*, 31(2), pp. 58–72. doi: 10.5732/cjc.011.10329.

Soga, M., Matsuzawa, A. and Ichijo, H. (2012) 'Oxidative Stress-Induced Diseases via the ASK1 Signaling Pathway', *International Journal of Cell Biology*, 2012, pp. 1–5. doi: 10.1155/2012/439587.

Son, B. *et al.* (2017) 'The role of tumor microenvironment in therapeutic resistance', *Oncotarget*, 8(3), pp. 3933–3945. doi: 10.18632/oncotarget.13907.

Song, Y. *et al.* (2016) 'Deubiquitylating Enzyme Rpn11/POH1/PSMD14 As Therapeutic Target in Multiple Myeloma', *Blood*, 128(22), pp. 4469–4469. doi: 10.1182/blood.v128.22.4469.4469.

Song, Y. *et al.* (2017) 'Blockade of deubiquitylating enzyme Rpn11 triggers apoptosis in multiple myeloma cells and overcomes bortezomib resistance', *Oncogene*, 36(40), pp. 5631–5638. doi: 10.1038/onc.2017.172.

Sosa, V. *et al.* (2013) 'Oxidative stress and cancer: An overview', *Ageing Research Reviews*, 12(1), pp. 376–390. doi: 10.1016/j.arr.2012.10.004.

Sova, H. *et al.* (2010) '8-Hydroxydeoxyguanosine: A new potential independent prognostic factor in breast cancer', *British Journal of Cancer*, 102(6), pp. 1018–1023. doi: 10.1038/sj.bjc.6605565.

Spaan, C. N. *et al.* (2019) 'Expression of UPR effector proteins ATF6 and XBP1 reduce colorectal cancer cell proliferation and stemness by activating PERK signaling', *Cell Death & Disease*, 10(7), p. 490. doi: 10.1038/s41419-019-1729-4.

Stayner, L., Welch, L. S. and Lemen, R. (2013) 'The Worldwide Pandemic of Asbestos-Related Diseases', *Annual Review of Public Health*, 34(1), pp. 205–216. doi: 10.1146/annurev-publhealth-031811-124704.

Stephenson, A. P. *et al.* (2013) 'Manganese-induced oxidative DNA damage in neuronal SH-SY5Y cells: Attenuation of thymine base lesions by glutathione and N-acetylcysteine', *Toxicology Letters*, 218(3), pp. 299–307. doi: 10.1016/j.toxlet.2012.12.024.

Stiborova, M. *et al.* (2012) 'The Synergistic Effects of DNA-Targeted Chemotherapeutics and Histone Deacetylase Inhibitors As Therapeutic Strategies for Cancer Treatment', *Current Medicinal Chemistry*, pp. 4218–4238. doi: 10.2174/092986712802884286.

Stingele, J., Bellelli, R. and Boulton, S. J. (2017) ‘Mechanisms of DNA-protein crosslink repair’, *Nature Reviews Molecular Cell Biology*, 18(9), pp. 563–573. doi: 10.1038/nrm.2017.56.

Stone, T. W., McPherson, M. and Gail Darlington, L. (2018) ‘Obesity and Cancer: Existing and New Hypotheses for a Causal Connection’, *EBioMedicine*. Elsevier B.V., pp. 14–28. doi: 10.1016/j.ebiom.2018.02.022.

Stoyanovsky, D. A. *et al.* (2019) ‘Iron catalysis of lipid peroxidation in ferroptosis: Regulated enzymatic or random free radical reaction?’, *Free Radical Biology and Medicine*, 133(September 2018), pp. 153–161. doi: 10.1016/j.freeradbiomed.2018.09.008.

Stratton, M., Campbell, P. and Futreal, P. (2009) ‘The cancer genome’, *Nature*, 458(7239), pp. 719–724. doi: 10.1038/nature07943.The.

Strilic, B. *et al.* (2016) ‘Tumour-cell-induced endothelial cell necroptosis via death receptor 6 promotes metastasis’, *Nature*, 536(7615), pp. 215–218. doi: 10.1038/nature19076.

Su, L.-J. *et al.* (2019) ‘Reactive Oxygen Species-Induced Lipid Peroxidation in Apoptosis, Autophagy, and Ferroptosis’, *Oxidative Medicine and Cellular Longevity*, 2019, pp. 1–13. doi: 10.1155/2019/5080843.

Sugiyama, T. *et al.* (2019) ‘Sequential Ubiquitination of Ribosomal Protein uS3 Triggers the Degradation of Non-functional 18S rRNA’, *Cell Reports*, 26(12), pp. 3400-3415.e7. doi: 10.1016/j.celrep.2019.02.067.

Suhaili, S. H. *et al.* (2017) ‘Mitochondrial outer membrane permeabilization: a focus on the role of mitochondrial membrane structural organization’, *Biophysical Reviews*. Springer Verlag, pp. 443–457. doi: 10.1007/s12551-017-0308-0.

Sun, L. *et al.* (2018) ‘Metabolic reprogramming for cancer cells and their microenvironment: Beyond the Warburg Effect’, *Biochimica et Biophysica Acta - Reviews on Cancer*, pp. 51–66. doi: 10.1016/j.bbcan.2018.06.005.

Sun, W. and Yang, J. (2010) 'Functional mechanisms for human tumor suppressors', *Journal of Cancer*, pp. 136–140. doi: 10.7150/jca.1.136.

Sun, Y.-E. *et al.* (2011) 'Autoxidation of Unsaturated Lipids in Food Emulsion', *Critical Reviews in Food Science and Nutrition*, 51(5), pp. 453–466. doi: 10.1080/10408391003672086.

Swann, J. B. and Smyth, M. J. (2007) 'Immune surveillance of tumors', *Journal of Clinical Investigation*. American Society for Clinical Investigation, pp. 1137–1146. doi: 10.1172/JCI31405.

Swift, G. H., Peyton, M. J. and MacDonald, R. J. (2000) 'Assessment of RNA quality by semi-quantitative RT-PCR of multiple regions of a long ubiquitous mRNA', *BioTechniques*, 28(3), pp. 524–531. doi: 10.2144/00283rr01.

Sznarkowska, A. *et al.* (2017) 'Inhibition of cancer antioxidant defense by natural compounds', *Oncotarget*, 8(9), pp. 15996–16016. doi: 10.18632/oncotarget.13723.

Tagde, A. *et al.* (2014) 'The glutathione synthesis inhibitor buthionine sulfoximine synergistically enhanced melphalan activity against preclinical models of multiple myeloma', *Blood Cancer Journal*, 4(7), pp. 1–13. doi: 10.1038/bcj.2014.45.

Taiwo, F. A. (2008) 'Mechanism of tiron as scavenger of superoxide ions and free electrons', *Spectroscopy*, 22, pp. 491–498. doi: 10.3233/SPE-2008-0362.

Takeda, K. *et al.* (2017) 'Hydroxyl radical generation with a high power ultraviolet light emitting diode (UV-LED) and application for determination of hydroxyl radical reaction rate constants', *Journal of Photochemistry and Photobiology A: Chemistry*, 340, pp. 8–14. doi: 10.1016/j.jphotochem.2017.02.020.

Takeshima, Kuroda and Yumura (2019) 'Cancer Chemotherapy and Chemiluminescence Detection of Reactive Oxygen Species in Human Semen', *Antioxidants*, 8(10), p. 449. doi: 10.3390/antiox8100449.

Takeshita, K. *et al.* (2000) 'Singlet Oxygen-Dependent Hydroxyl Radical Formation during Uroporphyrin-Mediated Photosensitization in the Presence of NADPH', *Antioxidants & Redox Signaling*, 2(2), pp. 355–362. doi: 10.1089/ars.2000.2.2-355.

Tan, S. J. *et al.* (2010) 'Copper, gold and silver compounds as potential new anti-tumor metallodrugs', *Future Medicinal Chemistry*, 2(10), pp. 1591–1608. doi: 10.4155/fmc.10.234.

Testino, G., Leone, S. and Borro, P. (2014) 'Alcohol and hepatocellular carcinoma: A review and a point of view', *World Journal of Gastroenterology*. WJG Press, pp. 15943–15954. doi: 10.3748/wjg.v20.i43.15943.

Thanikachalam, K. and Khan, G. (2019) 'Colorectal cancer and nutrition', *Nutrients*. MDPI AG. doi: 10.3390/nu11010164.

ThermoFisher Scientific (2010) 'Probes for Reactive Oxygen Species , Including Nitric Oxide Fluorophores', *The Molecular Probes ® Handbook*, p. Chapter 18.

Thomas, D. C. (2017) 'The phagocyte respiratory burst: Historical perspectives and recent advances', *Immunology Letters*. Elsevier B.V., pp. 88–96. doi: 10.1016/j.imlet.2017.08.016.

Thornton, L. *et al.* (2016) 'Water-soluble and photo-stable silver(I) dicarboxylate complexes containing 1,10-phenanthroline ligands: Antimicrobial and anticancer chemotherapeutic potential, DNA interactions and antioxidant activity', *Journal of Inorganic Biochemistry*, 159(I), pp. 120–132. doi: 10.1016/j.jinorgbio.2016.02.024.

Timucin, A. C., Basaga, H. and Kutuk, O. (2019) 'Selective targeting of antiapoptotic BCL-2 proteins in cancer', *Medicinal Research Reviews*. John Wiley and Sons Inc., pp. 146–175. doi: 10.1002/med.21516.

Tipu, S. A., Ahmed, I. and Ishtiaq, S. (2013) 'Malignant mesothelioma', *Pakistan Journal of Medical Sciences*, 29(6), pp. 261–280. doi: 10.12669/pjms.296.3938.

Tirabassi, R. (2014) 'How to identify supercoils, nicks and circles in plasmid preps', *BitesizeBio*, p. 1. Available at: https://bitesizebio.com/13524/how-to-identify-supercoils-

nicks-and-circles-in-plasmid-preps/ (Accessed: 31 July 2018).

Tiwari, A. K., Hasan, M. M. and Islam, M. (2013) 'An Overview of Oxidative Stress and Antioxidant Defensive System', *Transactions of the Canadian Society for Mechanical Engineering*, 37(4), pp. 1177–1188. doi: 10.4172/scientificreports.

Todoric, J., Antonucci, L. and Karin, M. (2016) 'Targeting Inflammation in Cancer Prevention and Therapy', *Cancer Prevention Research*, 9(12), pp. 895–905. doi: 10.1158/1940-6207.CAPR-16-0209.

Tomasson, K. *et al.* (2016) 'Malignant mesothelioma incidence by nation-wide cancer registry: a population-based study', *Journal of Occupational Medicine and Toxicology*, 11(1), p. 37. doi: 10.1186/s12995-016-0127-4.

Tonelli, C., Chio, I. I. C. and Tuveson, D. A. (2018) 'Transcriptional Regulation by Nrf2', *Antioxidants and Redox Signaling*, 29(17), pp. 1727–1745. doi: 10.1089/ars.2017.7342.

Tonnus, W. *et al.* (2019) 'The pathological features of regulated necrosis', *Journal of Pathology*. John Wiley and Sons Ltd, pp. 697–707. doi: 10.1002/path.5248.

Torrents, E. (2014) 'Ribonucleotide reductases: Essential enzymes for bacterial life', *Frontiers in Cellular and Infection Microbiology*, 4(APR), pp. 1–9. doi: 10.3389/fcimb.2014.00052.

Tran, T. Q., Lowman, X. H. and Kong, M. (2017) 'Molecular pathways: Metabolic control of histone methylation and gene expression in cancer', *Clinical Cancer Research*, 23(15), pp. 4004–4009. doi: 10.1158/1078-0432.CCR-16-2506.

Tsai, Y. C. and Weissman, A. M. (2010) 'The unfolded protein response, degradation from the endoplasmic reticulum, and cancer', *Genes and Cancer*, 1(7), pp. 764–778. doi: 10.1177/1947601910383011.

Tsuru, A. *et al.* (2016) 'Novel mechanism of enhancing IRE1α-XBP1 signalling via the PERK-ATF4 pathway', *Scientific Reports*, 6, pp. 1–8. doi: 10.1038/srep24217.

Tummers, B. and Green, D. R. (2017) 'Caspase-8: regulating life and death', *Immunological*

Reviews, 277(1), pp. 76–89. doi: 10.1111/imr.12541.

Uluata, S., McClements, D. J. and Decker, E. A. (2015) 'How the Multiple Antioxidant Properties of Ascorbic Acid Affect Lipid Oxidation in Oil-in-Water Emulsions', *Journal of Agricultural and Food Chemistry*, 63(6), pp. 1819–1824. doi: 10.1021/jf5053942.

Urra, H. *et al.* (2016) 'Endoplasmic Reticulum Stress and the Hallmarks of Cancer', *Trends in Cancer*, 2(5), pp. 252–262. doi: 10.1016/j.trecan.2016.03.007.

Valverde, M. *et al.* (2018) 'Hydrogen Peroxide-Induced DNA Damage and Repair through the Differentiation of Human Adipose-Derived Mesenchymal Stem Cells', *Stem Cells International*, 2018, pp. 1–10. doi: 10.1155/2018/1615497.

Vandermeers, F. *et al.* (2009) 'Valproate, in Combination with Pemetrexed and Cisplatin, Provides Additional Efficacy to the Treatment of Malignant Mesothelioma', *Clinical Cancer Research*, 15(8), pp. 2818–2828. doi: 10.1158/1078-0432.CCR-08-1579.

La Vecchia, C. *et al.* (2000) 'An age, period and cohort analysis of pleural cancer mortality in Europe', *European Journal of Cancer Prevention*, 9(3), pp. 179–184. doi: 10.1097/00008469-200006000-00006.

Verdone, L. (2006) 'Histone acetylation in gene regulation', *Briefings in Functional Genomics and Proteomics*, 5(3), pp. 209–221. doi: 10.1093/bfgp/ell028.

Viganor, L. *et al.* (2017) 'The Antibacterial Activity of Metal Complexes Containing 1,10-phenanthroline: Potential as Alternative Therapeutics in the Era of Antibiotic Resistance', *Current Topics in Medicinal Chemistry*, 17(11), pp. 1280–1302. doi: 10.2174/1568026616666161003143333.

Vilema-Enríquez, G. *et al.* (2016) 'Molecular and cellular effects of hydrogen peroxide on human lung cancer cells: Potential therapeutic implications', *Oxidative Medicine and Cellular Longevity*. Hindawi Limited. doi: 10.1155/2016/1908164.

Vinogradov, S., Wei, and X. and Thor (2013) 'Cancer stem cells and drug resistance: the

potential of nanomedicine', *Nanomedicine (Lond)*, 7(4), pp. 597–615. doi: 10.2217/nnm.12.22.Cancer.

Vogelzang, N. J. *et al.* (2003) 'Phase III study of pemetrexed in combination with cisplatin versus cisplatin alone in patients with malignant pleural mesothelioma', *Journal of Clinical Oncology*, 21(14), pp. 2636–2644. doi: 10.1200/JCO.2003.11.136.

Wajant, H. and Siegmund, D. (2019) 'TNFR1 and TNFR2 in the control of the life and death balance of macrophages', *Frontiers in Cell and Developmental Biology*. Frontiers Media S.A. doi: 10.3389/fcell.2019.00091.

Walczak, A. *et al.* (2019) 'The Role of the ER-Induced UPR Pathway and the Efficacy of Its Inhibitors and Inducers in the Inhibition of Tumor Progression', *Oxidative Medicine and Cellular Longevity*. Edited by G. Bartosz, 2019, pp. 1–15. doi: 10.1155/2019/5729710.

Waldhart, A. N. *et al.* (2017) 'Phosphorylation of TXNIP by AKT Mediates Acute Influx of Glucose in Response to Insulin', *CellReports*, 19, pp. 2005–2013. doi: 10.1016/j.celrep.2017.05.041.

Walford, G. A. *et al.* (2004) 'Hypoxia Potentiates Nitric Oxide-mediated Apoptosis in Endothelial Cells via Peroxynitrite-induced Activation of Mitochondria-dependent and -independent Pathways', *Journal of Biological Chemistry*, 279(6), pp. 4425–4432. doi: 10.1074/jbc.M310582200.

Walter, P. and Ron, D. (2011) 'The Unfolded Protein Response: From Stress Pathway to Homeostatic Regulation', *Science*, 334(6059), pp. 1081–1086. doi: 10.1126/science.1209038.

Wang, D. *et al.* (2018) 'The ferroptosis inducer erastin promotes proliferation and differentiation in human peripheral blood mononuclear cells', *Biochemical and Biophysical Research Communications*, 503(3), pp. 1689–1695. doi: 10.1016/j.bbrc.2018.07.100.

Wang, F. *et al.* (2010) 'Turning Tumor-Promoting Copper into an Anti-Cancer Weapon via High-Throughput Chemistry', *Current Medicinal Chemistry*, 17(25), pp. 2685–2698. doi:

10.2174/092986710791859315.

Wang, H., Jin, J. and Wang, J. (2014) 'Arctigenin Enhances Chemosensitivity to Cisplatin in Human Nonsmall Lung Cancer H460 Cells through Downregulation of Survivin Expression', *Journal of Biochemical and Molecular Toxicology*, 28(1), pp. 39–45. doi: 10.1002/jbt.21533.

Wang, J. *et al.* (2017) 'Novel strategies to prevent the development of multidrug resistance (MDR) in cancer', *Oncotarget*. Impact Journals LLC, pp. 84559–84571. doi: 10.18632/oncotarget.19187.

Wang, L. H. *et al.* (2019) 'Loss of tumor suppressor gene function in human cancer: An overview', *Cellular Physiology and Biochemistry*. S. Karger AG, pp. 2647–2693. doi: 10.1159/000495956.

Wang, M. and Su, P. (2018) 'The role of the Fas/FasL signaling pathway in environmental toxicant-induced testicular cell apoptosis: An update', *Systems Biology in Reproductive Medicine*, 64(2), pp. 93–102. doi: 10.1080/19396368.2017.1422046.

Wang, X., Zhang, H. and Chen, X. (2019) 'Drug resistance and combating drug resistance in cancer', *Cancer Drug Resistance*, 2, pp. 141–60. doi: 10.20517/cdr.2019.10.

Wang, Yafang *et al.* (2018) 'Iron Metabolism in Cancer', *International Journal of Molecular Sciences*, 20(1), p. 95. doi: 10.3390/ijms20010095.

Wang, Ying *et al.* (2018) 'Superoxide dismutases: Dual roles in controlling ROS damage and regulating ROS signaling', *Journal of Cell Biology*, 217(6), pp. 1915–1928. doi: 10.1083/jcb.201708007.

Wani, W. A. *et al.* (2016) 'Recent advances in iron complexes as potential anticancer agents', *New Journal of Chemistry*, 40(2), pp. 1063–1090. doi: 10.1039/C5NJ01449B.

Wapenaar, H. and Dekker, F. J. (2016) 'Histone acetyltransferases: challenges in targeting bi-substrate enzymes', *Clinical Epigenetics*, 8(1), p. 59. doi: 10.1186/s13148-016-0225-2.

Watanabe, J. *et al.* (2012) 'Method validation by interlaboratory studies of improved

hydrophilic oxygen radical absorbance capacity methods for the determination of antioxidant capacities of antioxidant solutions and food extracts', *Analytical Sciences*, 28(2), pp. 159–166. doi: 10.2116/analsci.28.159.

Watnick, R. S. (2012) 'The Role of the Tumor Microenvironment in Regulating Angiogenesis', *Cold Spring Harbor Perspectives in Medicine*, 2(12). doi: 10.1101/cshperspect.a006676.

Watts, R. J. *et al.* (2005) 'Oxidative and reductive pathways in manganese-catalyzed Fenton's reactions', *Journal of Environmental Engineering*, 131(1), pp. 158–164. doi: 10.1061/(ASCE)0733-9372(2005)131:1(158).

Weerasinghe, P. and Buja, L. M. (2012) 'Oncosis: An important non-apoptotic mode of cell death', *Experimental and Molecular Pathology*, 93(3), pp. 302–308. doi: 10.1016/j.yexmp.2012.09.018.

Westover, D. and Li, F. (2015) 'New trends for overcoming ABCG2/BCRP-mediated resistance to cancer therapies', *Journal of Experimental and Clinical Cancer Research*. BioMed Central Ltd., pp. 1–9. doi: 10.1186/s13046-015-0275-x.

WHO (2018) *Latest global cancer data*, *International Agency for Research on Cancer*. Available at: http://gco.iarc.fr/, (Accessed: 5 February 2020).

Wilson, D. N. and Doudna Cate, J. H. (2012) 'The Structure and Function of the Eukaryotic Ribosome', *Cold Spring Harbor Perspectives in Biology*, 4(5), pp. a011536–a011536. doi: 10.1101/cshperspect.a011536.

Wilson, S. M. *et al.* (2008) 'mTOR mediates survival signals in malignant mesothelioma grown as tumor fragment spheroids', *American Journal of Respiratory Cell and Molecular Biology*, 39(5), pp. 576–583. doi: 10.1165/rcmb.2007-0460OC.

Wisastra, R. and Dekker, F. J. (2014) 'Inflammation, cancer and oxidative lipoxygenase activity are intimately linked', *Cancers*, 6(3), pp. 1500–1521. doi: 10.3390/cancers6031500.

Wittmann, C. *et al.* (2012) 'Hydrogen peroxide in inflammation: Messenger, guide, and

assassin', *Advances in Hematology*. doi: 10.1155/2012/541471.

Witzig, T. E. *et al.* (2000) 'Induction of apoptosis in malignant B cells by phenylbutyrate or phenylacetate in combination with chemotherapeutic agents', *Clinical Cancer Research*, 6(2), pp. 681–692.

Wong, C. C., Qian, Y. and Yu, J. (2017) 'Interplay between epigenetics and metabolism in oncogenesis: Mechanisms and therapeutic approaches', *Oncogene*. Nature Publishing Group, pp. 3359–3374. doi: 10.1038/onc.2016.485.

Wong, D. L. and Stillman, M. J. (2018) 'Capturing platinum in cisplatin: Kinetic reactions with recombinant human apo-metallothionein 1a', *Metallomics*, 10(5), pp. 713–721. doi: 10.1039/c8mt00029h.

Wong, R. S. (2011) 'Apoptosis in cancer: from pathogenesis to treatment', *Journal of Experimental & Clinical Cancer Research*, 30(1), p. 87. doi: 10.1186/1756-9966-30-87.

Wroblewski, L. E., Peek, R. M. and Wilson, K. T. (2010) 'Helicobacter pylori and Gastric Cancer: Factors That Modulate Disease Risk', *Clinical Microbiology Reviews*, 23(4), pp. 713–739. doi: 10.1128/CMR.00011-10.

Wu, C. C. and Bratton, S. B. (2013) 'Regulation of the intrinsic apoptosis pathway by reactive oxygen species', *Antioxidants and Redox Signaling*, 19(6), pp. 546–558. doi: 10.1089/ars.2012.4905.

Wu, J. *et al.* (2018) 'Tunicamycin specifically aggravates ER stress and overcomes chemoresistance in multidrug-resistant gastric cancer cells by inhibiting N-glycosylation', *Journal of Experimental & Clinical Cancer Research*, 37(1), p. 272. doi: 10.1186/s13046-018-0935-8.

Wu, Y., Dong, G. and Sheng, C. (2020) 'Targeting necroptosis in anticancer therapy: mechanisms and modulators', *Acta Pharmaceutica Sinica B*. doi: 10.1016/j.apsb.2020.01.007.

Xie, Y. *et al.* (2016) 'Ferroptosis: Process and function', *Cell Death and Differentiation*, 23(3),

pp. 369–379. doi: 10.1038/cdd.2015.158.

Xu, J. *et al.* (2018) 'Vorinostat: a histone deacetylases (HDAC) inhibitor ameliorates traumatic brain injury by inducing iNOS/Nrf2/ARE pathway', *Folia Neuropathologica*, 56(3), pp. 179–186. doi: 10.5114/fn.2018.78697.

Xu, T. *et al.* (2019) 'Molecular mechanisms of ferroptosis and its role in cancer therapy', *Journal of Cellular and Molecular Medicine*, 23(8), pp. 4900–4912. doi: 10.1111/jcmm.14511.

Xu, W., Trepel, J. and Neckers, L. (2011) 'Ras, ROS and proteotoxic stress: A delicate balance', *Cancer Cell*, pp. 281–282. doi: 10.1016/j.ccr.2011.08.020.

Xue, J. J. *et al.* (2014) 'Synthesis, cytotoxicity for mimics of catalase: Inhibitors of lactate dehydrogenase and hypoxia inducible factor', *European Journal of Medicinal Chemistry*, 80, pp. 1–7. doi: 10.1016/j.ejmech.2014.04.035.

Yamaguchi, T. *et al.* (2010) 'Histone deacetylases 1 and 2 act in concert to promote the G1-to-S progression', *Genes and Development*, 24(5), pp. 455–469. doi: 10.1101/gad.552310.

Yan, L. L. and Zaher, H. S. (2019) 'How do cells cope with RNA damage and its consequences?', *Journal of Biological Chemistry*, 294(41), pp. 15158–15171. doi: 10.1074/jbc.REV119.006513.

Yang, H. *et al.* (2018) 'The role of cellular reactive oxygen species in cancer chemotherapy', *Journal of Experimental and Clinical Cancer Research*, 37(1), pp. 1–10. doi: 10.1186/s13046-018-0909-x.

Yang, J. K. (2015) 'Death effecter domain for the assembly of death-inducing signaling complex', *Apoptosis*, 20(2), pp. 235–239. doi: 10.1007/s10495-014-1060-6.

Yang, J., Yan, J. and Liu, B. (2018) 'Targeting VEGF/VEGFR to modulate antitumor immunity', *Frontiers in Immunology*. Frontiers Media S.A. doi: 10.3389/fimmu.2018.00978.

Yang, S. *et al.* (2017) 'AKT2 blocks nucleus translocation of apoptosis-inducing factor (AIF) and endonuclease G (EndoG) while promoting caspase activation during cardiac ischemia',

International Journal of Molecular Sciences, 18(3). doi: 10.3390/ijms18030565.

Yang, W. S. and Stockwell, B. R. (2016) 'Ferroptosis: Death by Lipid Peroxidation', *Trends in Cell Biology*, 26(3), pp. 165–176. doi: 10.1016/j.tcb.2015.10.014.

Yatabe, Y., Tavare, S. and Shibata, D. (2001) 'Investigating stem cells in human colon by using methylation patterns', *Proc Natl Acad Sci U S A*, 98(19), pp. 10839–10844. doi: 10.1073/pnas.191225998\r191225998 [pii].

Yimit, A. *et al.* (2019) 'Differential damage and repair of DNA-adducts induced by anti-cancer drug cisplatin across mouse organs', *Nature Communications*, 10(1), pp. 1–11. doi: 10.1038/s41467-019-08290-2.

Yixuan, L. and Seto, E. (2016) 'HDACs and HDAC Inhibitors in Cancer Development and Therapy', *Cold Spring Harb Perspect Med*, 3(September 2016), pp. 37–41. doi: 10.4161/epi.3.1.5736.

Yonekura, S.-I. *et al.* (2009) 'Generation, Biological Consequences and Repair Mechanisms of Cytosine Deamination in DNA', *Journal of Radiation Research*, 50(1), pp. 19–26. doi: 10.1269/jrr.08080.

Yoon, S.-O. *et al.* (2002) 'Sustained Production of H 2 O 2 Activates Pro-matrix Metalloproteinase-2 through Receptor Tyrosine Kinases/Phosphatidylinositol 3-Kinase/NF-κB Pathway', *Journal of Biological Chemistry*, 277(33), pp. 30271–30282. doi: 10.1074/jbc.M202647200.

You, Y. (2018) 'Chemical tools for the generation and detection of singlet oxygen', *Organic and Biomolecular Chemistry*, 16(22), pp. 4044–4060. doi: 10.1039/c8ob00504d.

Yuste, J. E. *et al.* (2015) 'Implications of glial nitric oxide in neurodegenerative diseases', *Frontiers in Cellular Neuroscience*, 9(AUGUST). doi: 10.3389/fncel.2015.00322.

Zahreddine, H. and Borden, K. L. B. (2013) 'Mechanisms and insights into drug resistance in cancer', *Frontiers in Pharmacology*, 4 MAR(March), pp. 1–8. doi: 10.3389/fphar.2013.00028.

Zenonos, K. (2013) ‘RAS signaling pathways, mutations and their role in colorectal cancer’, *World Journal of Gastrointestinal Oncology*, 5(5), p. 97. doi: 10.4251/wjgo.v5.i5.97.

Zhang, F. *et al.* (2019) ‘Genetic programming of macrophages to perform anti-tumor functions using targeted mRNA nanocarriers’, *Nature Communications*, 10(1). doi: 10.1038/s41467-019-11911-5.

Zhang, H. *et al.* (2008) ‘Mitochondrial autophagy is an HIF-1-dependent adaptive metabolic response to hypoxia’, *Journal of Biological Chemistry*, 283(16), pp. 10892–10903. doi: 10.1074/jbc.M800102200.

Zhang, L. and Shay, J. W. (2017) ‘Multiple Roles of APC and its Therapeutic Implications in Colorectal Cancer’, *JNCI: Journal of the National Cancer Institute*, 109(8). doi: 10.1093/jnci/djw332.

Zhang, Q. *et al.* (2014) ‘Study on the relationship between manganese concentrations in rural drinking water and incidence and mortality caused by cancer in Huai’an City’, *BioMed Research International*, 2014. doi: 10.1155/2014/645056.

Zhang, Z. *et al.* (2013) ‘1,10-phenanthroline promotes copper complexes into tumor cells and induces apoptosis by inhibiting the proteasome activity’, *J Biol Inorg Chem*, 17(8), pp. 1257–1267. doi: 10.1007/s00775-012-0940-x.1.

Zhang, Z. *et al.* (2017) ‘Novel copper complexes as potential proteasome inhibitors for cancer treatment (Review)’, *Molecular Medicine Reports*, 15(1), pp. 3–11. doi: 10.3892/mmr.2016.6022.

Zhao, X. *et al.* (2017) ‘Prognostic significance of tumor-associated macrophages in breast cancer: A meta-analysis of the literature’, *Oncotarget*. Impact Journals LLC, pp. 30576–30586. doi: 10.18632/oncotarget.15736.

Zhdanov, V. P. (2016) ‘Kinetic aspects of enzyme-mediated repair of DNA single-strand breaks’, *BioSystems*, 150, pp. 194–199. doi: 10.1016/j.biosystems.2016.09.007.

Zheng, G., Fu, Y. and He, C. (2014) 'Nucleic acid oxidation in DNA damage repair and epigenetics', *Chemical Reviews*, 114(8), pp. 4602–4620. doi: 10.1021/cr400432d.

Zhou, Zhang, J. *et al.* (2016) 'Generation of hydrogen peroxide and hydroxyl radical resulting from oxygen-dependent oxidation of l-ascorbic acid via copper redox-catalyzed reactions', *RSC Advances*, 6(45), pp. 38541–38547. doi: 10.1039/c6ra02843h.

Zhou, S. *et al.* (2014) 'Multipoint targeting of the PI3K/mTOR pathway in mesothelioma', *British Journal of Cancer*, 110(10), pp. 2479–2488. doi: 10.1038/bjc.2014.220.

Zilka, O. *et al.* (2017) 'On the Mechanism of Cytoprotection by Ferrostatin-1 and Liproxstatin-1 and the Role of Lipid Peroxidation in Ferroptotic Cell Death', *ACS Central Science*, 3(3), pp. 232–243. doi: 10.1021/acscentsci.7b00028.

Zimta, A. A. *et al.* (2019) 'The role of Nrf2 activity in cancer development and progression', *Cancers*, 11(11), pp. 1–26. doi: 10.3390/cancers11111755.

Zou, Y. *et al.* (2019) 'A GPX4-dependent cancer cell state underlies the clear-cell morphology and confers sensitivity to ferroptosis', *Nature Communications*, 10(1). doi: 10.1038/s41467-019-09277-9.

Zuo, L. *et al.* (2004) 'Lipoxygenase-dependent superoxide release in skeletal muscle', *Journal of Applied Physiology*, 97(2), pp. 661–668. doi: 10.1152/japplphysiol.00096.2004.

Zupkovitz, G. *et al.* (2010) 'The Cyclin-Dependent Kinase Inhibitor p21 Is a Crucial Target for Histone Deacetylase 1 as a Regulator of Cellular Proliferation', *Molecular and Cellular Biology*, 30(5), pp. 1171–1181. doi: 10.1128/MCB.01500-09.